P-WAVE REFLECTIVITY OF THE CRUST AND UPPER MANTLE BENEATH THE CENTRAL AND EASTERN U.S.: IMPLICATIONS FOR SUPPORT OF MOUNTAIN TOPOGRAPHY AND A NEW CRITERION FOR MAPPING THE BASE OF THE CONTINENTAL LITHOSPHERE

by

LAURA HANAWALT

(Under the Direction of ROBERT HAWMAN)

ABSTRACT

P-wave reflections generated by earthquakes and recorded by the Transportable Array across the eastern US image subsurface structures ranging from coastal plain sediments to layering within the asthenosphere. Reflections from the Moho increase in two-way travel time from 10-11 s in the east to 14-18 s beneath the highest elevations of the Appalachian Highlands, where they also increase in complexity before decreasing in time somewhat before leveling off or deepening further to the west. A new criterion for identifying the base of the lithosphere (LAB) based on a downward increase in horizontal reflectivity determined objectively using waveform coherence suggests a westward increase in LAB depth from 32-38 s (115-140 km) along the east coast to 40 s (150 km) beneath the continental interior. This transition in reflection density is interpreted as layering caused by horizontal strain in the lowermost lithosphere and drag-induced flow in the asthenosphere.

INDEX WORDS: P-wave reflectivity, Moho, lithosphere-asthenosphere boundary, reflection density, drag-induced flow, lithosphere, asthenospheric layering

P-WAVE REFLECTIVITY OF THE CRUST AND UPPER MANTLE BENEATH THE CENTRAL AND EASTERN U.S.: IMPLICATIONS FOR SUPPORT OF MOUNTAIN TOPOGRAPHY AND A NEW CRITERION FOR MAPPING THE BASE OF THE CONTINENTAL LITHOSPHERE

by

LAURA HANAWALT

BS, UNIVERSITY OF GEORGIA, 2020

A Thesis Submitted to the Graduate Faculty of The University of Georgia in Partial Fulfillment of the Requirements for the Degree

MASTER OF SCIENCE

ATHENS, GEORGIA

2023

© 2023

Laura Hanawalt

All Rights Reserved

P-WAVE REFLECTIVITY OF THE CRUST AND UPPER MANTLE BENEATH THE CENTRAL AND EASTERN U.S.: IMPLICATIONS FOR SUPPORT OF MOUNTAIN TOPOGRAPHY AND A NEW CRITERION FOR MAPPING THE BASE OF THE CONTINENTAL LITHOSPHERE

by

LAURA HANAWALT

Major Professor:	Robert Hawman
Committee:	Doug Crowe
	Christian Klimczak

Electronic Version Approved:

Ron Walcott
Vice Provost for Graduate Education and Dean of the Graduate School
The University of Georgia
May 2023

DEDICATION

This thesis is dedicated to my family and friends, who always inspire me and push me to do my best. They allow me to persevere. My mom and dad have always supported me, and I will forever be so thankful to have such loving and supportive parents. My sister and brother have inspired me and always welcome me with open arms for anything and everything. My families support and love is precious to me. My best friends Madeline and Jake are always a phone call away and have my back through the smallest and biggest things. My friends Sarah, Tricia, and Taylor, Josh, Elham, and Meghan have allowed me to be myself and helped me through undergrad and grad school. Because of them, I will always feel like someone has my back and that is invaluable. I would also like to dedicate this to Madison, for being extremely supportive, kind, and always being there to listen.

ACKNOWLEDGEMENTS

First and foremost, I would like to give immense thanks to my advisor, Dr. Rob Hawman. He has allowed me to grow and learn. His fascination and knowledge of geology and geophysics inspires me, and his patience and trust are truly one of a kind. I would also like to give thanks to my committee members, Dr. Doug Crowe, and Dr. Christian Klimczak- for their trust, knowledge, and humor. Thanks to them I felt like I could push myself harder, answer the tough questions, and give myself just the right amount of pressure and credit where it was due. I would also like to thank Dr. Steve Holland for being immensely supportive and always advocating for me and every graduate student in the department. The UGA Geology department as a whole deserves my thanks and acknowledgement. This department has served me through my undergraduate and graduate coursework, allowed me to grow, shaped who I am, and allowed me to meet the most amazing people along the way. Every professor in this department has taught me and believed in me in a way that made me feel immensely supported and given me the drive and confidence to believe in myself. I would also love to thank the field school program, as both a student and a teaching assistant- this program truly changed me in a way that I am proud of. I would like to thank my friends and fellow graduate students in the department- everyone is incredibly welcoming and lovely, to me this place feels like a home. In particular, I want to thank Alex Bonham and Cade Orchard for being there with me through my best and worst times and allowing me to be myself openly and proudly! My family and friends deserve immense thanks and kudos

for always sticking by me and helping me through everything I could ever need. Lastly, and certainly not least, I want to thank the National Science Foundation and the grants (EAR-0844154 & EAR-1830182) that allowed me to be here!

TABLE OF CONTENTS

Page

ACKNOWLEDGEMENTS ..... iv-vi

LIST OF TABLES ix

LIST OF FIGURES ..... x-xii

CHAPTER

1 INTRODUCTION 1-14

BACKGROUND 1

STUDY AREA 3

GEOLOGIC HISTORY 5

2 PART ONE 15-54

THE MOHOROVIČIĆ DISCONTINUITY 15

MID-LITHOSPHERIC DISCONTINUITIES 17

COASTAL PLAIN SEDIMENTS 18

MISSISSIPPI EMBAYMENT 19

METHODOLOGY 20

RESULTS 22

DISCUSSION 28

3 PART TWO 55-95

THE LITHOSPHERE-ASTHENOSPHERE BOUNDARY 55

METHODOLOGY 57

RESULTS 63

DISCUSSION 70

4 CONCLUSIONS 96-97

REFERENCES 98-107

APPENDICES

A EARTHQUAKE DATA 108-113

B STUDY AREA 114

C METHODOLOGY 115-162

D SIGNFILTER FIGURES 163-176

E COMPARISON FIGURES 177-183

F TALLYRUN 184-195

G TA STATIONS 196-221

H STATION COVERAGE 222-227

I CODING 228-361

LIST OF TABLES

Page

Table 1: Level calculation for the sign test.....73

Table 2: Power calculation for the sign test.....74

LIST OF FIGURES

Page

Figure 1: Study area on Transportable Array map....6

Figure 2: Study area on physiographic province map....7

Figure 3: Study area on USGS geologic map....8

Figure 4: Study area on Precambrian basement map....9

Figure 5: Precambrian basement map....10

Figure 6: Study area on <250 km wavelength Bouguer gravity map....11

Figure 7: Study area on <1000 km wavelength Bouguer gravity map....12

Figure 8: Study area on >250 km wavelength Bouguer gravity map....13

Figure 9: Station coverage for Line T....14

Figure 10: Mississippi Embayment map....31

Figure 11: PKIKP phase in the earth....32

Figure 12: PKIKP phase and polarity reversals....33

Figure 13: Earthquakes used for analysis....34

Figure 14: Line T single earthquake plot....35

Figure 15: Line U single earthquake plot....36

Figure 16: Line T conventional stacked plot....37

Figure 17: Line T color plot....38

Figure 18: Line U conventional stacked plot....39

Figure 19: Line U color plot....40

Figure 20: Line V conventional stacked plot 41
Figure 21: Line V color plot 42
Figure 22: Line W color plot 43
Figure 23: Line X conventional stacked plot 44
Figure 24: Line X color plot 45
Figure 25: Line Y conventional stacked plot 46
Figure 26: Line Y color plot 47
Figure 27: Line Z conventional stacked plot 48
Figure 28: Line Z color plot 49
Figure 29: Composite Mississippi Embayment figure with color plots 50
Figure 30: Schmandt et al., 2015 and Line U comparison 51
Figure 31: Composite Moho figure Lines T-V 52
Figure 32: Composite Moho figure Lines X-Z 53
Figure 33: Bouguer gravity anomaly and elevation comparison 54
Figure 34a: Sign test procedure 75
Figure 34b: Line V window length 7 signfilter plot 76
Figure 35: Line V window length 9 signfilter plot 77
Figure 36: Line V window length 5 tallyrun avgabs plot 78
Figure 37: Line V window length 7 tallyrun avgabs plot 79
Figure 38: Line V window length 9 tallyrun avgabs plot 80
Figure 39: Line V window length 11 tallyrun avgabs plot 81
Figure 40: Line N smoothed signfilter plot 82
Figure 41: Line T smoothed signfilter plot 83

Figure 42: Line O smoothed signfilter composite plot 84

Figure 43: Reflectivity categories 85

Figure 44a: Composite signfilter plot for Lines L-S 86

Figure 44b: Composite signfilter plot for Lines T-Z 87

Figure 45: Chen et al., 2018 receiver function and Line O signfilter overlay plot 88

Figure 46: Chen et al., 2018 receiver function and Line Q signfilter overlay plot 89

Figure 47: Chen et al., 2018 receiver function and Line S signfilter overlay plot 90

Figure 48: Chen et al., 2018 shear-wave and Line Q signfilter overlay plot 91

Figure 49: Chen et al., 2018 shear-wave and Line U signfilter overlay plot 92

Figure 50: Chen et al., 2018 shear-wave and Line V signfilter overlay plot 93

Figure 51: Summary of models for the LAB 94

Figure 52: Models for drag-induced flow 95

CHAPTER ONE

INTRODUCTION

BACKGROUND

The Transportable Array (TA) has provided new insight related to the structure of the crust and upper mantle beneath North America. The TA, as the name implies, was a temporary and transportable set of 400 broadband seismographs that were placed at regular intervals (~70 km) across the conterminous U.S. from the west coast to the east coast from 2004 to 2013. These seismographs remained at one location for about two years and were then moved to a new location; nearly 2000 locations were occupied with the TA in total. Because of its regular station spacing and its ability to detect small earthquakes, the TA provided an important database for imaging the structure of the lithosphere and asthenosphere beneath North America. The TA was funded by the National Science Foundation and is a part of the bigger USArray initiative which is administered by the Incorporated Research Institutions for Seismology (IRIS). Much of the research involving the TA has been based on studies of surface waves (Chen et al., 2018), mode-converted body waves (Abt et al., 2010; Fischer et al., 2020), ambient noise (Savage et al., 2017), and shear-wave splitting (Long et al., 2016). These studies and numerous others have provided important information regarding the structure of the crust, the subcrustal lithosphere, and the lithosphere-asthenosphere boundary (LAB).

However, most of these studies have focused on long-wavelength features with relatively poor spatial resolution. Vertically incident, P-wave reflection studies using the global phase PKPdf as a virtual seismic source have been successful at mapping much finer-scale structure (Ruigrok & Wapenaar, 2012; Kennett, 2015). Recent studies using P-wave reflections recorded by the SESAME array in the southern Appalachians have imaged the subsurface over a wide range of scales, from unconsolidated sediments of the Atlantic Coastal Plain, to the base of the crust beneath the Appalachian Highlands, to layering within the asthenosphere (Verellen et al., 2020). Studies that have focused on P-wave velocity typically utilize a body-wave tomography method or utilize velocity and anisotropy rather than the methodology outlined in this study (Abt at al., 2010; Schmandt at al., 2014; Biryol et al., 2016; Buehler et al, 2016; Long et al., 2016; Yang et al., 2017). Studies that have used this exact methodology were limited to a smaller study area using the Southeastern Suture of the Appalachian Margin Experiment (SESAME) array (Verellen et al., 2020). So, using P-wave reflectivity in this capacity and at this large of a scale is significant- structures in the lithosphere that have already been imaged should show improved resolution and structures that have been difficult or impossible to resolve in the past should resolve with this method. This study is also significant as it involves using a new criterion for determining where the LAB is based on patterns in reflectivity using a new methodology.

The overall goal of the present study was to use stations of the TA to extend high-resolution imaging of structure northward along the Appalachians and westward across neighboring provinces of the continental interior.

Specific goals included the following:

- investigate the relationship between topography, gravity, and crustal thickness to place constraints on processes that support mountain topography
- evaluate the potential of the PKPdf method for imaging fine-scale structure within sedimentary basins
- use reflections identified objectively using the sign test statistic to establish a new criterion for mapping the base of the lithosphere based on P-wave reflectivity. In particular, test the hypothesis that the LAB (as identified by independent geophysical data) is marked by an abrupt downward increase in horizontal reflectivity, consistent with models for drag-induced flow in the asthenosphere.

STUDY AREA

This study is presented in two parts.

Part 1 focuses on the crust. Specific objectives include a better understanding of:

- Structure within the uppermost crust beneath the Mississippi Embayment
- The relationship between elevation and crustal thickness, with the long-term goal of testing models for isostatic compensation of mountain topography

Part 2 focuses on the nature of the boundary between the lithosphere and asthenosphere (the LAB) beneath continents, as observed across the transition from the Appalachian orogen to the stable continental interior. Given current models for drag-induced flow within the asthenosphere, we test the hypothesis that the LAB is marked by an abrupt

downward increase in horizontal reflectivity. Reflections are identified objectively using the sign test statistic (Hansen et al., 1988). The results then are compared with estimates for lithospheric thickness based on lower-resolution models of shear-wave velocity structure derived by tomographic inversion of surface waves (Chen et al., 2018).

For Part 1, earthquake data recorded by the TA from Line T through Line Z from stations 32 or 33 in the mid-continent through the east coast were used to create multiple W-E profiles to image the crust and upper mantle (Figure 1). A total of 205 stations were utilized in this part of the study (Appendix, Table G1). This study area encompasses a wide range of geologic provinces, geologic units, Precambrian basement regions, and Bouguer gravity anomalies (Figures 2-8).

For Part 2, Lines L through S were analyzed alongside Lines T through Z. These lines included 254 more stations in the northern part of the Appalachian Mountain chain to give a more complete analysis (Figure 1b; Appendix F, Table G2).

Using a P-wave reflectivity approach that will be further covered in the methodology section, 16 previously researched earthquakes from SESAME were used in this study (Verellen et al., 2020) (Appendix A, Table A1 and A2). These particular earthquakes were utilized because they generate PKPdf (PKIKP) arrivals, which arrive at the TA stations at a nearly vertical angle and are ideal for seismically imaging features in the earth's interior. The station coverage for these earthquakes advanced from west to east as the TA was redeployed (Figure 9; Appendix Figures H1-H6). The idea of using P-wave reflectivity rather than S-waves, as done previously, is to increase the resolution of

laterally continuous structures of the uppermost mantle (Verellen et al., 2020). Preliminary results indicate that this approach can be effective for imaging structure beneath more coarsely sampled arrays such as the TA (Hanawalt et al., 2021; Hanawalt et al., 2022).

GEOLOGIC HISTORY

The study area covers the Appalachian Mountains and westward towards the interior craton. The Appalachians are a diachronous product of at least four different orogenic events and at least one full Wilson cycle (Hatcher, 1989; Duff & Kellogg, 2017).

The geologic history of the area can be summarized very succinctly into a few steps (Spotila & Prince, 2022):

- The Grenville orogeny, involving continental collision to form the supercontinent Rodinia (1.3-1.1 Ga)
- Rifting and formation of the Iapetus Ocean (760 Ma)
- Taconic (early Ordovician ~485 Ma) and Acadian (Devonian ~375 Ma) orogenies involving terrane accretion
- Alleghanian orogeny involving the collision of Gondwana and Laurentia (330-260 Ma)
- Subsequent rifting due to the breakup of Pangea and initiation of Atlantic seafloor spreading (220-180 Ma), resulting in the present day passive margin along the eastern coast of the United States

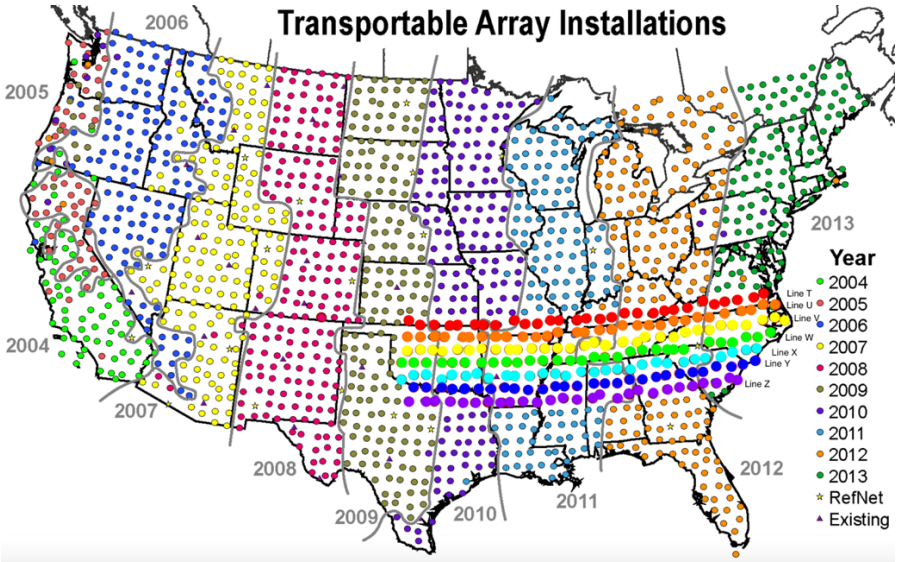


Figure 1a. The Transportable Array Installation map with the extent of the study area shown in red dots by line. The northernmost line is Line T, while the southernmost line is Line Z. The base map comes from the IRIS website about the Transportable Array.

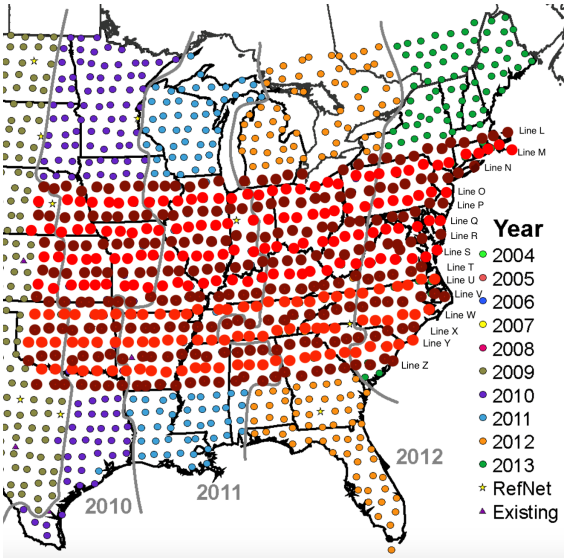


Figure 1b. Stations of Lines L-Z of the TA used to study the transition for lithosphere to asthenosphere.

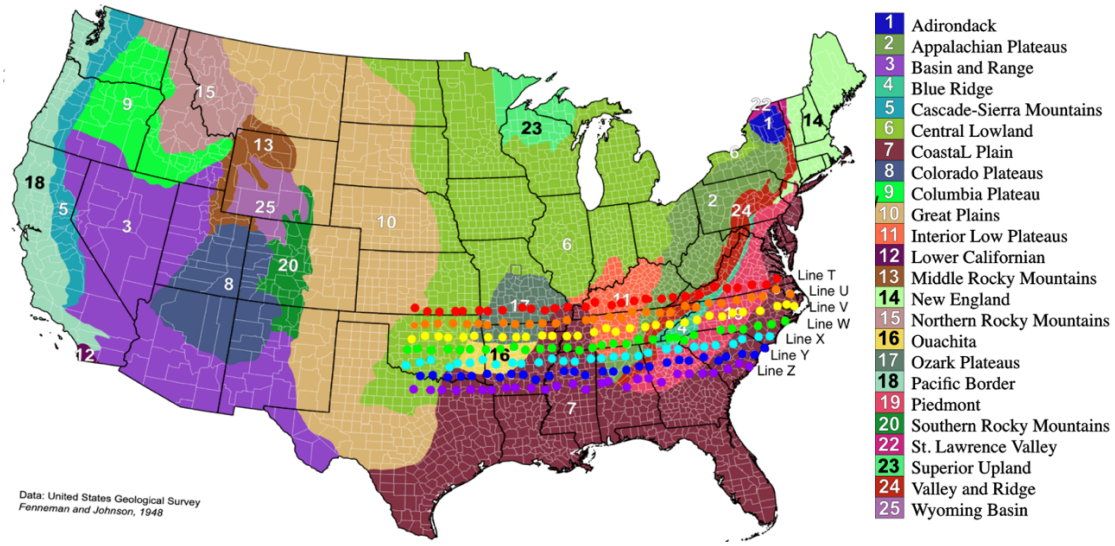


Figure 2. TA stations of Lines T-Z superimposed on a map of physiographic provinces (Fenneman & Johnson, 1943).

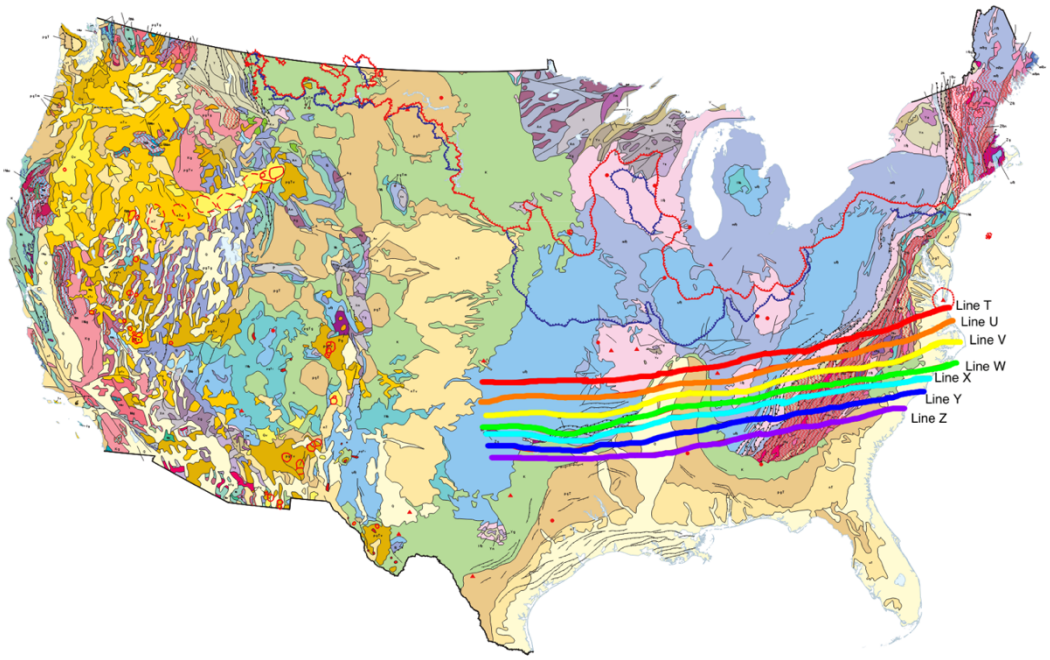


Figure 3. TA stations of Lines T-Z superimposed on a USGS (USGS Department of the Interior) generalized geologic map of the US.

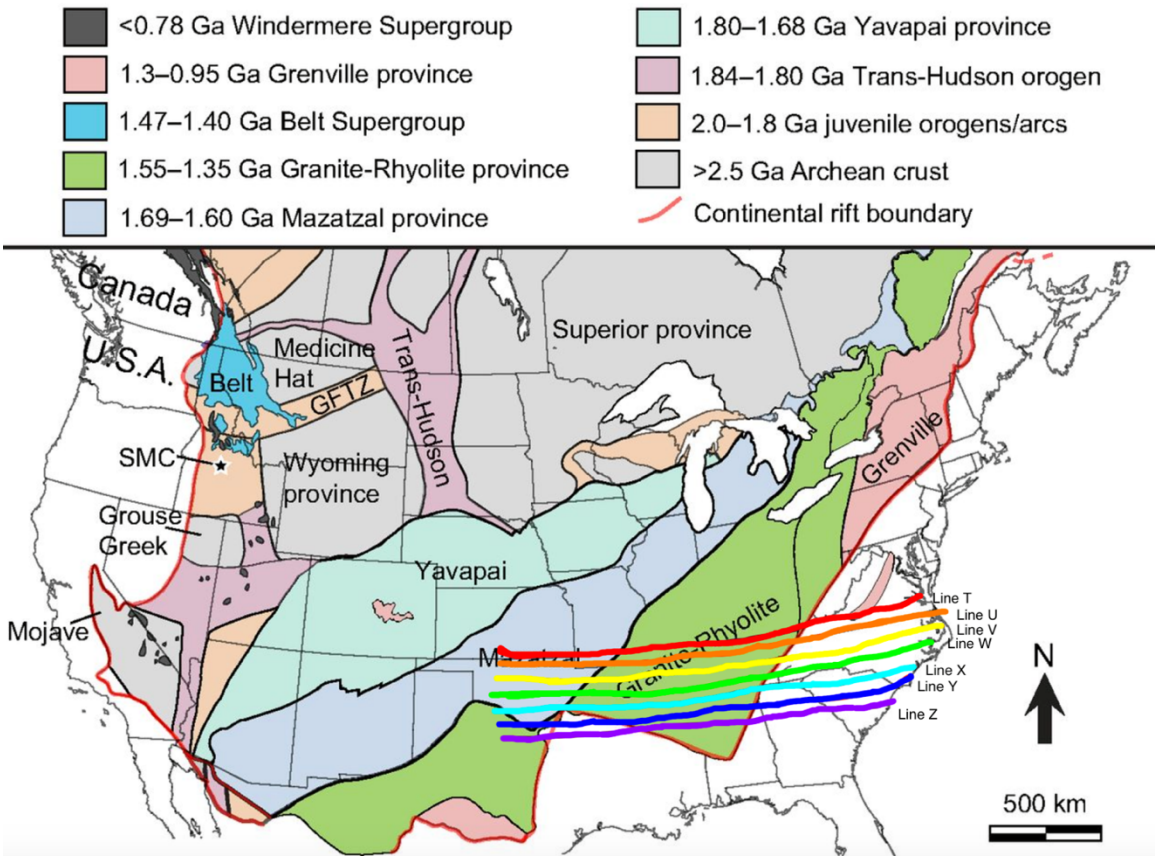


Figure 4. TA stations of Lines T-Z superimposed on a map of Precambrian basement (Ma et al., 2016).

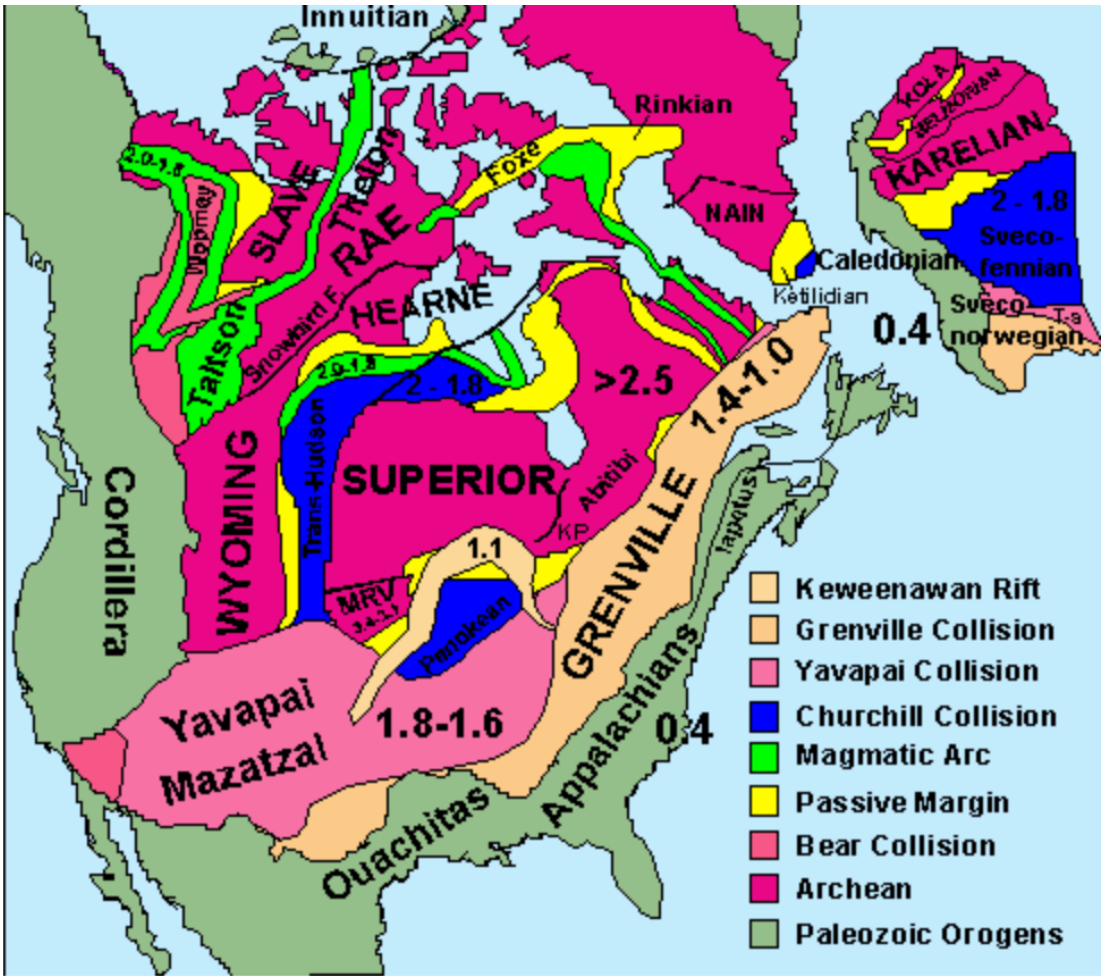


Figure 5. This map may more accurately shows the extent of the Grenville Front and Grenville basement than Figure 4 (USGS).

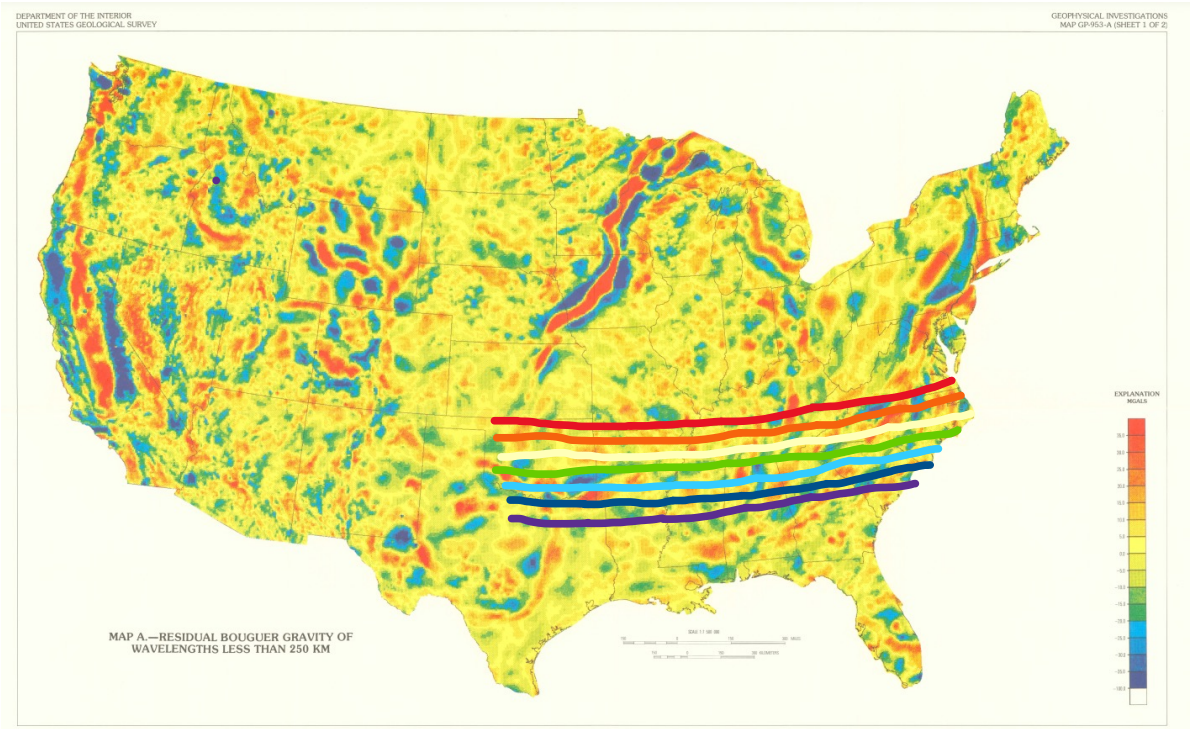


Figure 6. TA stations of Lines T-Z superimposed on a regional Bouguer gravity map filtered to show wavelengths less than 250 km (USGS Department of the Interior).

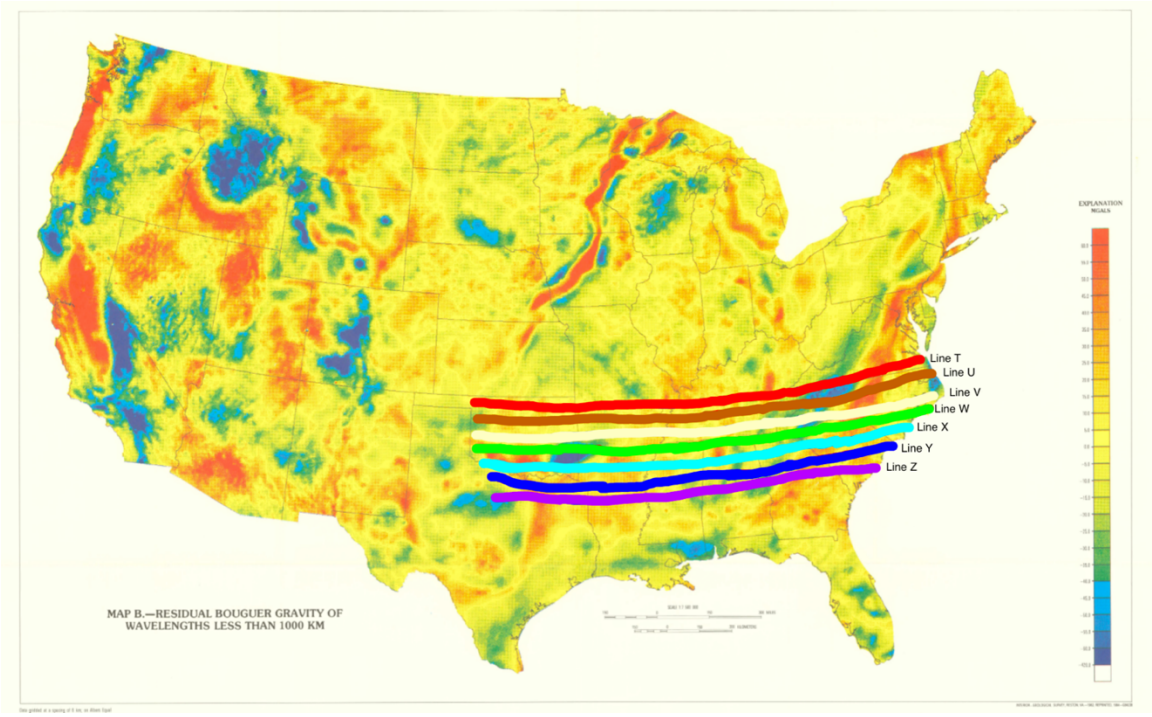


Figure 7. TA stations of Lines T-Z superimposed on a regional Bouguer gravity map filtered to show wavelengths less than 1000 km (USGS Department of the Interior).

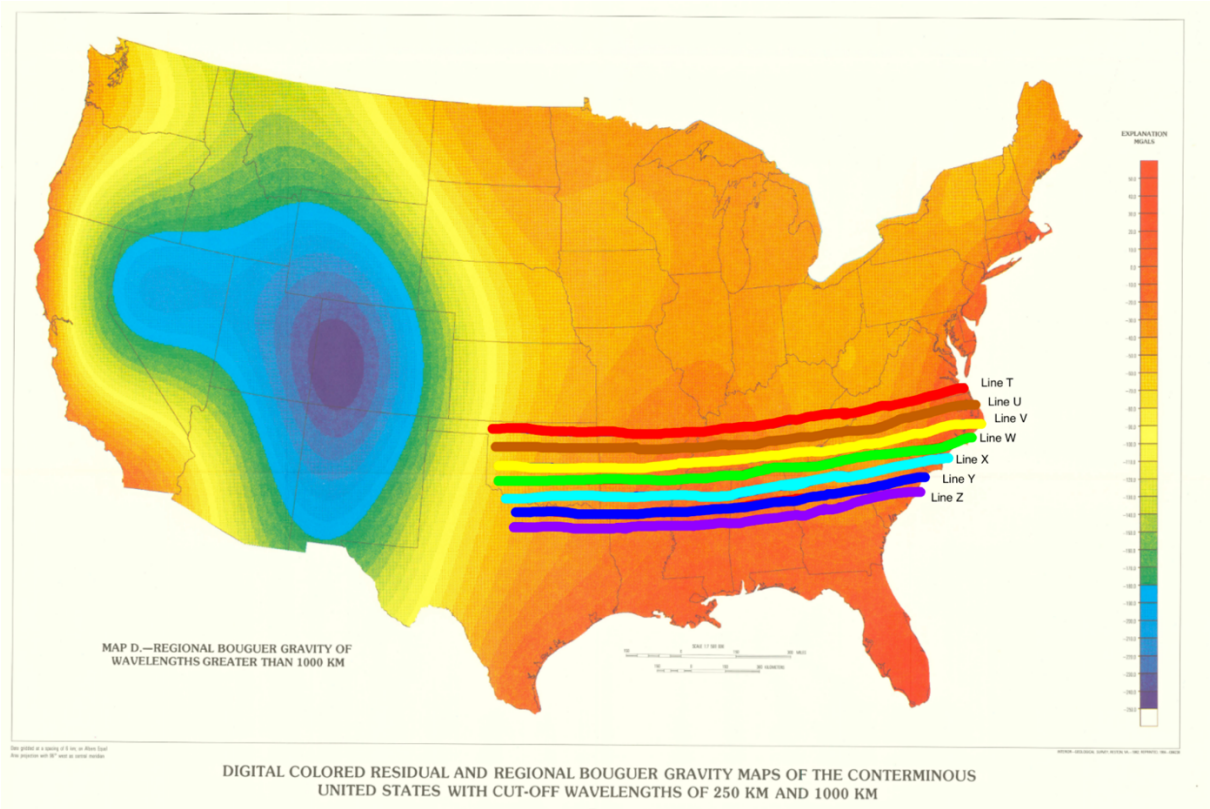


Figure 8. TA stations of Lines T-Z superimposed on a regional Bouguer gravity map filtered to show wavelengths greater than 1000 km (USGS Department of the Interior).

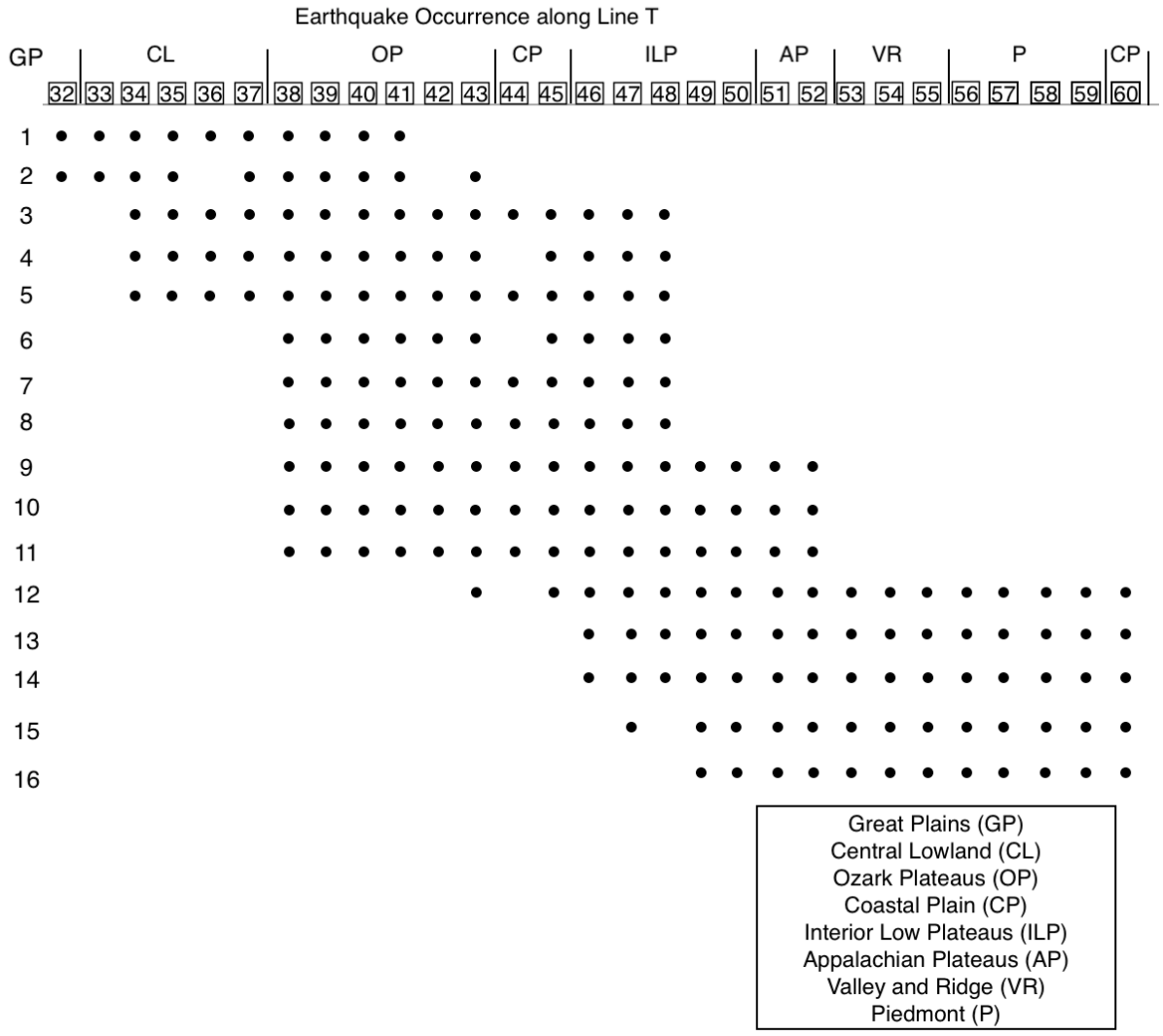


Figure 9. Station coverage for Line T for each of the 16 earthquakes analyzed. The coverage shows the gradual eastward migration of the TA.

CHAPTER TWO

PART ONE

THE MOHOROVIČIĆ DISCONTINUITY

The Moho, or the crust-mantle boundary, is the boundary separating earth's crust and upper mantle. The discovery of the Moho in 1910 using body waves from earthquakes, led to a greater understanding of the interior of the earth itself (Braile & Chiang, 1986). Despite the simple definition, the actual Moho is yet to be entirely understood and can be highly complex. The Moho represents a change in mineral composition, seismic wave velocity, and density (Jarchow & Thompson, 1989). Originally, the Moho was modeled as a first-order discontinuity in which seismic velocity increases from 6.8-7.2 km/s to 7.8-8.4 km/s (Braile & Chiang, 1986). However, studies using a combination of near-vertical and wide-angle seismic reflections suggested that the Moho consists of a 0-5 km thick, layered transition zone (Braile & Chiang, 1986).

Oceanic Moho is thought to be a layered mafic and ultramafic complex transition zone at a depth of about 5-8 km that is underlain by peridotite (Jarchow & Thompson, 1989). Continental Moho is deepest (40-50 km) underneath cratons that have little tectonic activity, and is thinner, but still thicker than oceanic Moho, beneath more tectonically active continental crust (Jarchow & Thompson, 1989).

In some regions, the Moho may be a dynamic boundary, as suggested by multicyclic reflections observed in Consortium for Continental Reflection Profiling (COCORP) profiles across the Atlantic Coastal Plain. Here, it is suggested that the present-day Moho

formed during a regional thermal event related to initial rifting of the Atlantic (McBride & Nelson, 1991).

In recent P-wave reflectivity analysis across the Southern Appalachians, SESAME data imaged the Moho at a two-way time (TWT) of about 11.2-12.0 s (~34 to 39 km) beneath the Atlantic Coastal Plain. Multicyclic reflections may represent crustal layering and support the idea of a crust-mantle transition zone, rather than a first-order discontinuity (Verellen et al., 2020). Reprocessing of COCORP data has found a prominent reflection Moho around 13 s beneath the Inner Piedmont which rises to around 11 s eastward (Cook & Vasudevan, 2006).

Crustal thickness increases northwestward to 50-56 km beneath the Blue Ridge Mountains, which is consistent with local isostatic compensation of topography (French et al., 2009; Hawman et al., 2012, Parker et al., 2013; Schmandt et al., 2015). Using SESAME and TA data, isostatic balance is suggested by receiver functions that indicate a crustal root (~55 km) beneath the highest elevations of the Blue Ridge Mountains and it is hypothesized that this root is a remnant of a larger region of thickened crust due to Alleghanian thrusting (Parker et al., 2013). A similar trend is seen for P-wave reflections observed beneath the SESAME lines (Verellen et al., 2020), supporting the correlation between elevation and crustal thickness.

However, ratios of surface elevation to root thickness are lower in the Appalachian orogen compared to younger mountain chains (Hawman et al., 2012; Schmandt et al., 2015). This is consistent with observations from other Paleozoic orogens that suggest a loss of buoyancy of the crustal root with age (Fischer, 2002).

Buoyancy of crustal roots is hypothesized to support mountain topography in cases of continental collision and in turn, surface uplift. Erosion of mountains is accompanied by uplift of their crustal roots, however, because of loss of crustal root buoyancy for older mountain chains, exhumation of the root is reduced. The loss of buoyancy might be due retrograde metamorphism of granulite-facies to denser garnet-rich eclogite-facies rocks (Fischer, 2002).

One factor contributing to the high relief seen for the Appalachian Mountains may be enhanced erosion in valleys which creates an increase in relief and absolute elevation of mountain peaks due to isostatic rebound (England & Molnar, 1990; Parker et al., 2016). We return to this topic in the Discussion for Part 1.

MID-LITHOSPHERIC DISCONTINUITES

The term mid-lithospheric discontinuity describes a discontinuity occurring within the sub-crustal lithosphere, especially beneath more stable cratons, that does not coincide with the LAB (Yuan & Levin, 2014). At depths around 80 to 100 km in the continental lithosphere, S-wave receiver functions show negative phases corresponding to a decrease in seismic velocity. These phases are interpreted as the LAB in areas with thinner lithosphere such as tectonically active areas. However, in stable cratons with thicker lithosphere, this feature occurs within the continental lithospheric mantle and is labeled as an MLD (Selway et al., 2015).

MLD's are still not entirely understood; possible explanations include contrasts in anisotropy, refertilized depleted mantle, partial melt, and elastically accommodated grain-boundary sliding (Abt et al., 2010; Yuan & Levin, 2014; Karato et al., 2015; Calo et al., 2016; Verellen et al., 2020). Studies utilizing S-wave receiver functions hypothesize that MLD's are unlikely to be caused by partial melt and more likely to be due to a layer of a low-velocity mineral (mostly amphibole) or changes in anisotropy (Selway et al., 2015).

Anisotropy in the crust and upper mantle can be constrained via converted seismic waves. One study interpretates multiple MLD's in the Granite-Rhyolite Province of the central US. A north to northwest orientation of anisotropy in this region may be due to craton formation via stacking oceanic plates during subduction cycles and/or underthrusting (Wirth & Long, 2014).

COASTAL PLAIN SEDIMENTS

Seismic analysis on this scale is mostly used for imaging deep, continuous structure in the interior of the earth. However, earthquakes can be used to image shallow structure as well. In Georgia, Alabama, and Mississippi, coastal plain deposits of Upper Cretaceous and Cenozoic age include nonmarine, marine margin, and marine siliciclastic and carbonate sediments up to 2000 m thick (Manicini et al., 1996; Parker et al., 2016). In Georgia, the oldest deposit in contact with crystalline basement is the Tuscaloosa formation (Cooke, 1943). Analysis of SESAME data has resolved the base of Cretaceous deposits at TWT of 0.2 to 1.4 s (Verellen et al., 2020).

MISSISSIPPI EMBAYMENT

Similarly to coastal plain sediments, the Mississippi Embayment is an example of shallow structure that can be resolved using P-wave reflectivity analysis. The Mississippi Embayment is an extremely large (around 100,000 sq mi) wedge-shaped region that extends from Illinois to parts of Alabama, Arkansas, Kentucky, Louisiana, Mississippi, Missouri, Tennessee, and Texas (Cushing et al.,1964; Nyamwandha et al., 2016).

The lateral extent and thickness of sediments are constrained by electrical well logs and oil test holes (Cushing et al., 1964). The embayment is described as a syncline plunging south and striking parallel to the Mississippi River that is filled with sedimentary rocks and unconsolidated sediments from Jurassic to Quaternary in age (Cushing et al., 1964; Cox & Van Arsdale, 2002). Furthermore, it is reported that Paleozoic basement rock is what forms the embayment's synclinal structure, and this basement rock is overlain by Cretaceous deposits (Cushing et al., 1964). The geologic units comprising the embayment include water-bearing strata that are ideal for forming vast aquifers (Cushing et al., 1964).

The initial collapsing of the synclinal structure of the embayment is thought to be the result from the uplift of the Appalachian Mountains at the end of the Paleozoic. The dominant portion of the subsidence is likely through subcrustal movement and sedimentary loading and the compaction of sediments due to weathering of uplifted areas of the Ozark uplift and Ouachita mountains in the Mesozoic (Cushing et al., 1964). Other studies have suggested that the Mississippi Embayment may have been formed by the Bermuda hotspot forcing uplift that then eroded and refilled with sediments (Morgan,

1983). The embayment contains close to 1.5 km of Cretaceous and Cenozoic sediments underlain by a fault complex (Cox & Van Arsdale, 2002).

A study involving upper mantle P and S wave velocity models determined that extensional features, like rifts, including the Reelfoot Rift, developed in this area during the breakup of Rodinia and a rift complex coinciding with the Mississippi Embayment is referred to as the Mississippi Valley Graben (MVG) (Hao et al., 2015; Nyamwandha et al., 2016). The Mississippi Embayment is also spatially correlated with the New Madrid Seismic Zone (NMSZ), and it is suggested that earthquake occurrence in this region is linked to tectonic processes that created the embayment (Nyamwandha et al., 2016) (Figure 10).

METHODOLOGY

To complete this exploratory work, the global seismic phase PKIKP (PKPdf) was used to generate P-wave reflections in the lithosphere beneath the study area. The PKIKP phase represents a P-wave that passes through the mantle, outer core, and inner core and then returns to the surface at almost vertical incidence (Figure 11). When this phase is reflected at the earth's surface, a polarity reversal occurs and the reflection travels back into the earth's interior to reflect at discontinuities in the subsurface (Figure 12). Because of this, reflections that have a positive impedance contrast (a lower velocity layer over a higher velocity layer) will have a negative polarity (e.g. the Moho) and vice versa. The methods used in this work are adapted from the global phase seismic interferometry

method that uses PKPdf phases as a virtual source for P-wave reflections (Ruigrok & Wapenaar, 2012).

This study used earthquakes that occurred in the Western Pacific around 112°-135° from the study area, as this is the ideal distance range to obtain nearly vertical incidence and to avoid other seismic phases that might interfere with the PKIKP signal (Figure 13).

Preliminary processing of the data followed the approach described by Verellen et al. (2020). The recordings were processed to deconvolve (remove) the effect of the extended source-time function for each earthquake. The deconvolved trace gathers for individual earthquakes then were stacked (summed) together to suppress noise and enhance signals. Details of the methods as applied to the present data can be found in Appendix C.

Resolving Power

Different measures are used for quantifying resolving power in the vertical and horizontal directions. Vertical resolution for this dataset ranges from 1–1.5 km in the crust (Vp = 3.5-6.5 km/s) to 3-8 km in the upper mantle (Vp = 8.1 km/s), corresponding to dominant periods of 1-4 s, based on the quarter wavelength criterion. Horizontal resolution, defined as the radius of the first Fresnel zone for plane waves, ranges from 3-15 km in the crust to 20-70 km within the upper mantle. Lateral resolving power is also controlled by station spacing, which varies from 39.8-145.1 km for the TA lines.

RESULTS

Stacked sections for lines T through Z of the TA are displayed here in both conventional (wiggle-trace) format and in color. For color plots, each sample is displayed with a color determined by its amplitude. Positive-polarity samples with the largest amplitudes are plotted in dark blue, grading into green for samples with near-zero amplitudes, and finally through yellow, orange, and red for negative-polarity samples with the largest absolute amplitudes.

Also shown here are several examples of trace gathers for individual earthquakes, plotted in wiggle-trace format.

Single Earthquakes

Sections for single earthquakes are very useful for analyzing smaller scale subsurface structures as well as comparing structures with stacks to determine how continuous a structure is. As analyzing single earthquakes is not the overall goal of this research, this section is brief.

For Line T, the results for the April 06, 2013 (m7.0) earthquake (Appendix Table A1) deconvolved with a Gaussian parameter of α=2.0 show laterally continuous signals (Figure 14). The feature highlighted with red arrows at 10 s is consistent with the TWT for signals interpreted as Moho reflections on COCORP lines (Cook & Vasudevan, 2006). The feature beginning at 18 s in the west to 15 s towards the east could also be related to the Moho, or an MLD. The signal at roughly 56 s could be related to

asthenosphere layering or related to the Lehmann discontinuity (See Part 2 for further discussion).

For Line U, seismograms for the July 07, 2013 (m7.3) earthquake deconvolved with a Gaussian parameter of α=2.0 show a prominent signal increasing in TWT from 36 s in the east to 40 s in the west (Figure 15). As discussed further in Part 2, these times are consistent with a westward thickening of the lithosphere beneath the stable craton.

Stacks and Color Plots

While single earthquakes proved to be more informative than originally anticipated, earthquake stacks are more useful as they enhance signal-to-noise ratio. Creating stacks also generates a more complete section along a profile because a given earthquake was recorded over only a portion of each line. Ideally, traces from all available earthquakes would be included in the stacks, but given the relatively small number of earthquakes analyzed, those with strong noise can degrade rather than enhance the results. Therefore, multiple stacks were generated for each line depending on a "grade" ("A" being the best) given to a particular earthquake. Earthquakes with higher signal-to-noise ratios were graded more favorably and in turn stacks with better graded earthquakes are easier and more useful to analyze. These stacks were created for each profile line.

The original stacks are shown with their corresponding color plots in tandem to highlight important features in multiple ways.

The color plots show physiographic provinces (based on the map in Figure 2) and elevation profiles along the top of the displays. The physiographic provinces come from Figure 2, where stations are shown above provinces. The elevation profiles were made in ArcGIS using a Digital Elevation Model (DEM) and smoothing the elevations using Focal Statistics to create profiles along each line (Danielson et al., 2011). The DEM used was taken from a report by the USGS for Global Multi-Resolution Terrain Elevation Data that provided elevation data for the world (Danielson et al., 2011), this was then smoothed using an ArcGIS program called Focal Statistics that averaged the elevation of one point (or cell) by a 30-cell radius surrounding it, which equates to roughly 7.5 km. Two-way time was also converted to depth in kilometers using a model that represents a global average for continents (Kennett, 2015).

To begin, earthquakes with a grade A and B were stacked together for Line T to create a stack with strong signals. The original stacked plot and color plot of the same stack with a Gaussian parameter of α=2.0 are shown together (Figures 16 and 17). Both figures showcase a signal that increases in TWT from 10 s in the east to 15 s in the west that is interpreted as a signal from the Moho.

Similarly, grade A and earthquakes with better shallow signals were stacked for Line U with a Gaussian parameter of α=2.0 (Figures 18 and 19). Both the conventional and color plots indicate a signal that starts around 10 s in the east and increases to about 14 s in the middle of the section corresponding to higher elevations. The original stacked plot shows the Moho continuing to increase in TWT to 17 s towards the mid-continent.

For Line V, grade A and good earthquakes showing shallow signals were used for stacking. In particular, the original with a Gaussian parameter of α=4.0 and color plot with a Gaussian parameter of α=2.0 were the most useful to interpret for this particular line (Figures 20 and 21). Both plots show a very interesting signal towards the west with a very shallow TWT of 1-2.5 s. This signal is almost certainly related to the Mississippi embayment and Line V is the first line that shows prominent signals from this structure. This will be looked at in more detail. The plot also shows a shallow 0.5-1 s TWT signal at the end of the line to the east, probably related to coastal plain sediments. The color plot also indicates a signal at 10 s in the east that is consistent with the TWT for signals interpreted as Moho reflections on COCORP lines (Cook & Vasudevan, 2006).

For Line W, stacks were made using all 16 earthquakes (Figure 22). A signal that starts at 11 s in the east, increases to 15-18 s in the central part of the section, and decreases again to 10-12 s in the west is interpreted as reflections from the Moho.

For Line X, earthquakes that received a grade A were utilized for stacking. Both the original and color plot with a Gaussian parameter of α=2.0 show strong signals (Figures 23 and 24). Both plots show a signal very prominently around 1-2 s that is related to the Mississippi Embayment. Both plots also show a signal interpreted as the reflection from the Moho starting at approximately 10 s in the east and increasing to 14-15 s in the middle and to the west. This reflection increases in TWT and becomes multicyclic beneath the highest elevations, suggesting a more complex crust-mantle transition

beneath this portion of the Appalachians. A similar effect has been observed for the Blue Ridge mountains in Georgia and North Carolina (Rice, 2019).

For Line Y, earthquakes with grades of A through C were utilized for stacking. For this analysis, the original stack as well as the color plot with a Gaussian parameter of α=2.0 were used (Figures 25 and 26). Both plots show prominent signals relating to the Mississippi Embayment from 1-2.5 s towards the westward end of the stack, as well as coastal plain sediments at the same TWT on the far east side of the stack for the original stack. Both plots also show a signal interpreted as a reflection from the Moho on both the east and west ends of the section at around 10 s. The color plot more clearly shows the same signal increasing in TWT to around 13 s towards the middle of the section, relating to the highest elevations in the mountain chain.

Lastly, the stacked plots for Line Z include all earthquakes with a grade A through C. The plots with a Gaussian parameter of α=2.0 yield the clearest signals for this profile. Signals from around 1-4 s in the western side of the stacks that likely represent the Mississippi Embayment as well as signals from 0.5-1 s in the east relating to coastal plain sediments can be seen on the original plot. In the color plot, a signal starting at 10 s in the east increases in TWT to around 15-17 s and becomes more complex beneath higher elevations (Figures 27 and 28).

Analyzing these stacks in a progressive order highlights the signals that represent the Mississippi Embayment (Figure 29). Portions of the lines showing signals associated with

this feature progressively widen and migrate westward to the south, in agreement with the mapped extent of the embayment. The reflection response changes from a thin zone of high-amplitude signals in the north to a gradually thickening sequence to the south; in Line Z, the southernmost line, the concave-upward shape of the basin is clearly resolved. Maximum thickness of the sediments, assuming a velocity of 2100 m/s, is approximately 4.2 km.

As noted above, several of the TA profiles, notably Lines V, Y, and Z, show signals at 0.5-1 s TWT that are interpreted as the base of unconsolidated and poorly consolidated sediments in the Atlantic Coastal Plain. Assuming a velocity of 2100 m/s places these reflections at depths of approximately 1-2 km, in agreement with recent studies (Verellen et al., 2020).

Comparisons with Previous Work

Here, the results from this study are compared with results of previous analyses of data from the same TA stations but derived using different methods. For example, Figure 30 shows structures imaged by P-wave reflections in the stack for Line U that are in close agreement with features imaged using Ps (P to S wave converted) receiver functions (Schmandt et al., 2015).

Signals that can be seen on both figures, for example the prominent blue signal interpreted as the Moho, east of -80°, are better resolved in the Line U profile. The signal interpreted as a Ps conversion at the Moho in the Schmandt et al., 2015 figure increases

in depth from 37± 3 to 50± 3 km moving westward, while the Line U profile shows the Moho increasing in depth from 33± 2 to 49± 2 km over the same distance. These differences are within the uncertainties of the estimates and could be related to the slight differences in latitudes between compared profiles, or to the differences in average velocity used to convert time to depth. Overall, the match of related signals across similar latitudes is remarkable and gives an indication that the methodology outlined in this study is providing signal, and perhaps even resolving signals better than before.

DISCUSSION

Moho

Signals identified as reflections from the Moho are prominent in most of the profiles (Figures 31 and 32).

The general trend that the Moho shows throughout original stacked plots, color plots, and signfilter plots in Lines T-Z, starts with shallower signals towards the eastern ends of the sections beneath the coastal plain, typically around 10-11 s TWT (~30-35 km) in agreement with COCORP and SESAME profiles (Cook & Vasudevan, 2006; Parker et al., 2016; Verellen et al., 2020). The Moho then tends to deepen and sometimes even show more complexity moving westward towards the highest elevations of the Blue Ridge Mountains in each line. Typically, the Moho increases in TWT to 14-18 s (~45-55 km). Line X shows a particularly interesting increase in depth and complexity of the Moho underneath highest elevations (Figure 30). However, other lines, such as Line T, U, W, and Z show this as well (Figures 23, 25, 28, and 34). This is highlighted further in

composite Moho figures (Figures 31 and 32). This noticeable thickening of the crust beneath the highest elevations provides at least part of the support for mountain topography (Hawman, 2008; French et al., 2009; Hawman et al., 2012; Parker et al., 2013; Verellen et al., 2020). Additional support may come from lateral variations in density within the upper mantle (MacDougall et al., 2015; Yang et al., 2021). Overall, most of the TA lines then show the Moho either leveling off or deepening somewhat (15-17 s; 49-53 km) towards the west. Results based on much denser arrays across the southern Appalachians suggest that the root is localized beneath the highest elevations, with crustal thickness decreasing somewhat along the northwest flank before increasing again towards the continental interior (Hawman et al., 2012; Parker et al., 2013). This detail is not resolved by the TA but is interesting because it is consistent with a local rather than regional mechanism for isostatic compensation.

Factors responsible for the occurrence of high relief in the Appalachians have generated much debate (Spotila & Prince, 2022). In addition to isostatic uplift fed by the substantial crustal root, changes in buoyancy due to convection and other processes in the upper mantle may also play a role. For example, uplift due to delamination of the dense lowermost lithosphere has been proposed based on lateral variations in velocity beneath portions of the central Appalachians (Biryol et al., 2016; Wagner et al., 2018; Long et al., 2021) but these anomalies do not extend along the full distance spanned by high topography.

The effect of isostatic uplift may be enhanced by variations in erosion rates. Globally, average erosion rates for drainage basins are up to an order of magnitude greater than

those for ridges/summits; the difference appears to be controlled by greater rates of chemical weathering for soil-covered terrain versus bare rock (Portenga & Bierman, 2011). Erosion rates of 6 m/my for summits versus 30-100 m/my in river valleys have been documented in the central Appalachians (Hancock & Kirwan, 2007), with smaller differences reported for the Blue Ridge Mountains of the southern Appalachians (McKeon et al., 2014). The net result can be an increase in both relief and absolute elevation of individual peaks due to isostatic uplift (England & Molnar, 1990). Changes in base level due to changes in climate can accelerate these processes (Molnar, 2004).

Another method of analyzing isostasy is to compare elevations with Bouguer gravity anomalies. Bouguer gravity anomalies are variations in gravity in a certain location, typically on land, that "remove" (account for) the mass effect of the mountains themselves, or the attraction of terrain. This means Bouguer gravity anomalies show the effect of lateral variations in density beneath the earth's surface, and this includes mountain roots. Mountain roots create Bouguer gravity lows beneath mountain peaks. A comparison of the elevation and gravity data suggests that Bouguer anomaly lows directly correlate with the highest elevations of the Appalachian Mountains. Lines T, U, V, and W show this particularly well (Figure 33). The correlation of elevation with gravity and Moho depth is consistent with the idea that support for mountain topography is provided by variations in crustal thickness but does not rule out the possibility that variations in thickness and composition of the lithosphere may also play a role (Lamb et al., 2020).

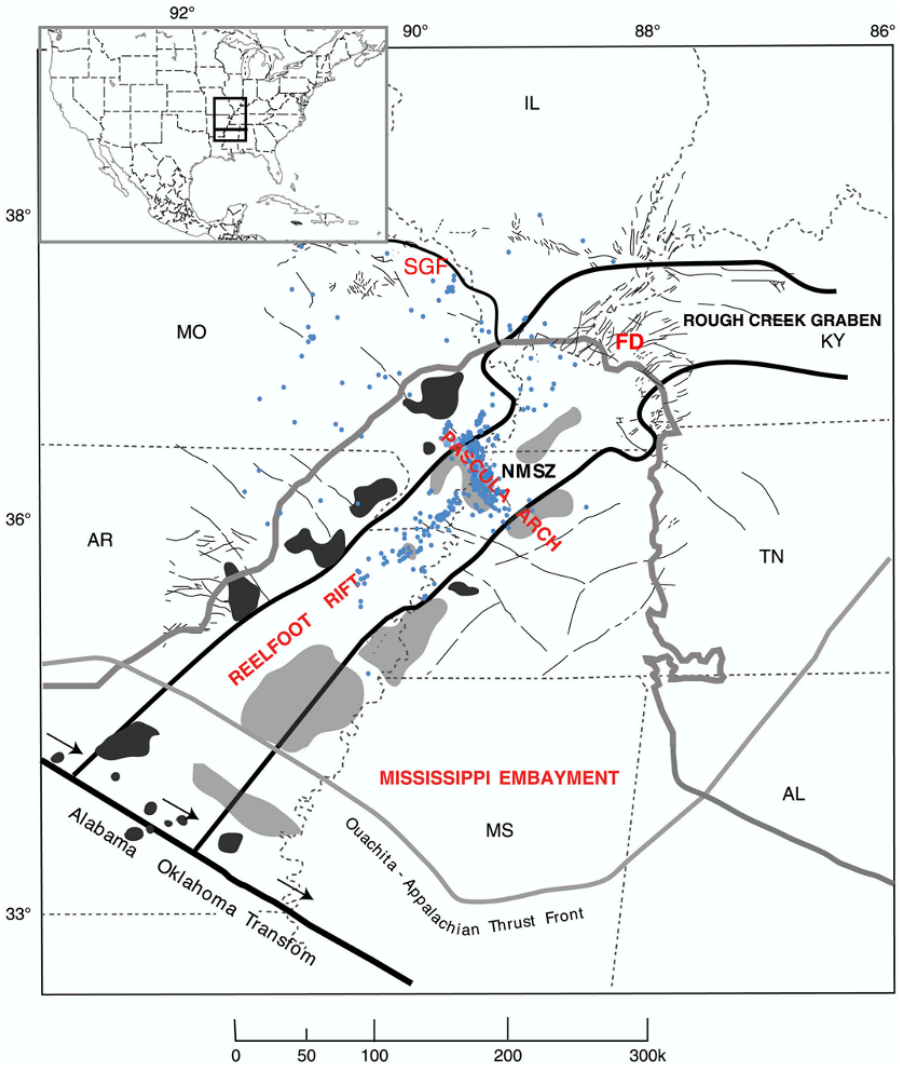


Figure 10. The extent of the Mississippi Emabyment, the Reelfoot Rift, and the New Madrid Seismic Zone (NMSZ) (Nyamwandha et al., 2016). These areas are in the central, southern part of the study area.

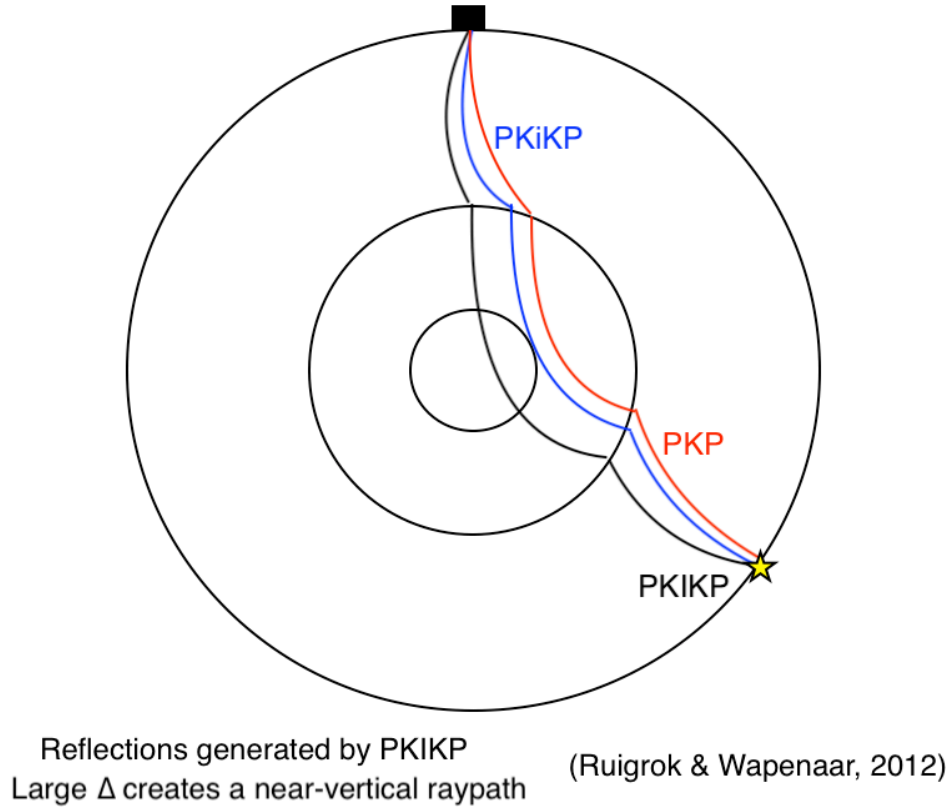


Figure 11. The PKIKP (PKPdf) phase travelling through the mantle, outer core, and inner core of the earth. It is pictured with the PKiKP and PKP phases, which arrive at similar times to PKIKP arrivals.

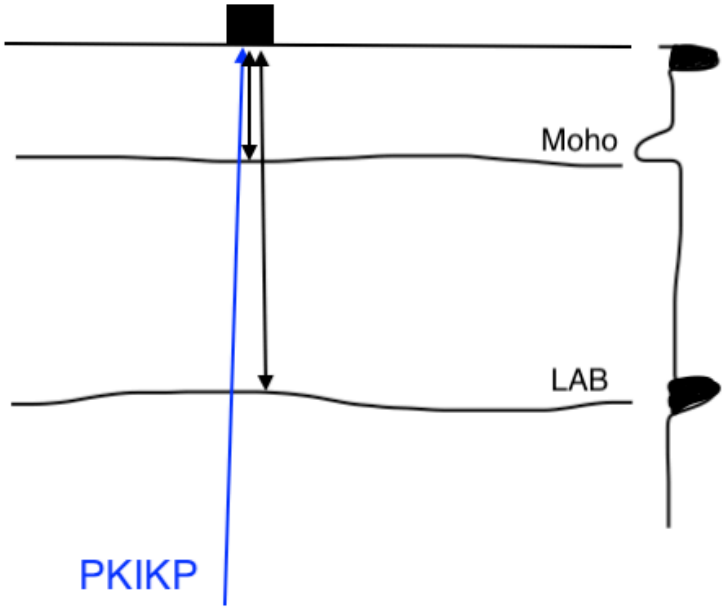


Figure 12. A closer view of the PKIKP phase, where it is reflected at the earth's surface, is reversed in polarity, travels downward, and is reflected by discontinuities in the crust and upper mantle.

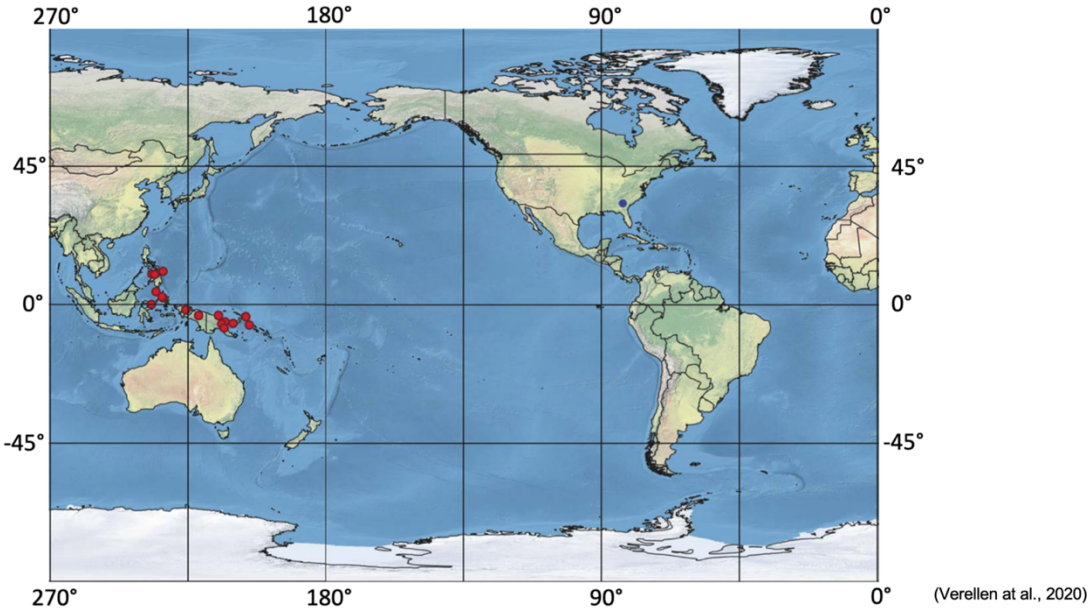


Figure 13. The epicenters of the 16 earthquakes, in red, utilized in this study (after Verellen et al., 2020).

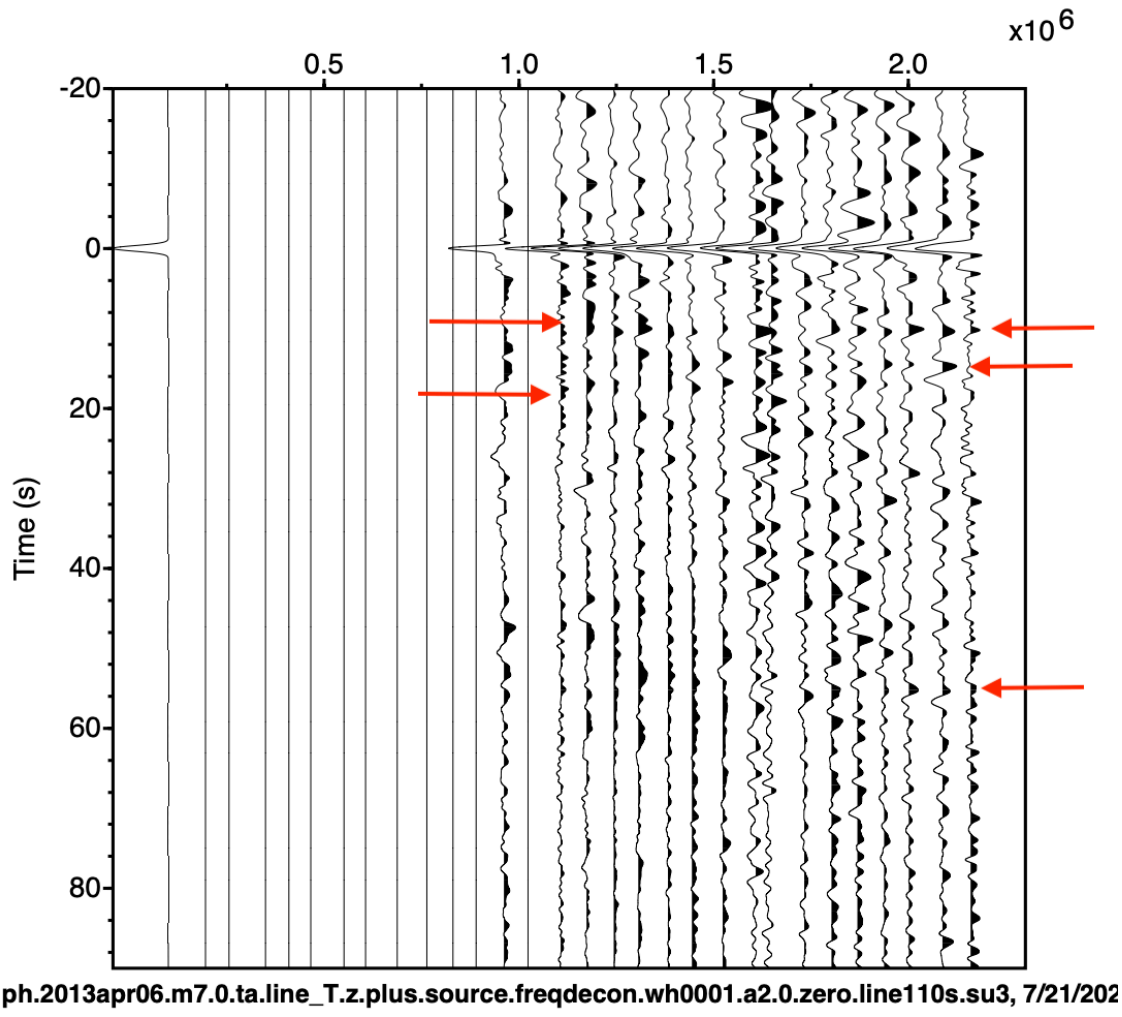


Figure 14. Example of a single earthquake (April 06, 2013) recorded along Line T plotted with a negative polarity and with a Gaussian parameter of α=2.0. This plot highlights major structures with red arrows. The topmost arrows point to the Moho, the middle arrows point to an MLD and the bottommost arrow points to a feature that is either related to layering in the asthenosphere or the Lehmann discontinuity.

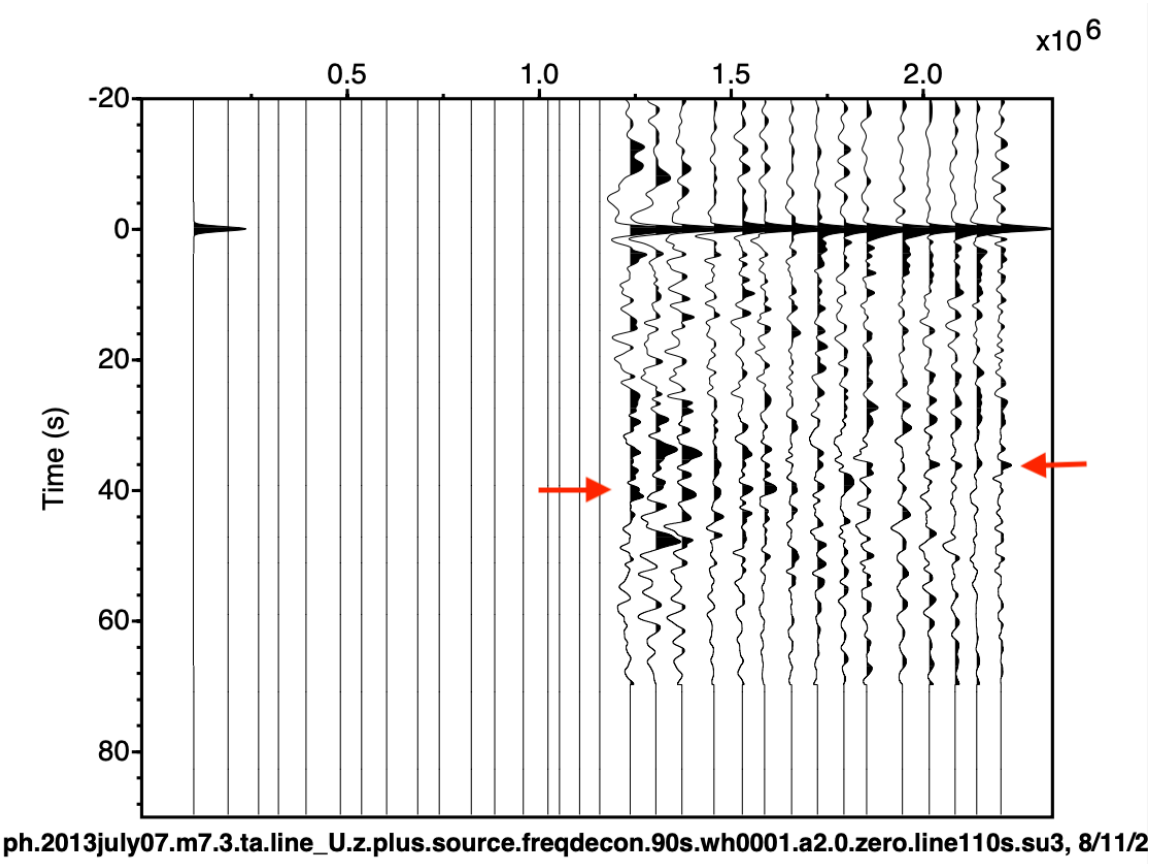


Figure 15. Example of a single earthquake (July 07, 2013, m 7.3) recorded along Line U plotted with a positive polarity and with a Gaussian parameter of α=2.0. This plot highlights major structures with red arrows. The arrows here point to a westward dipping LAB.

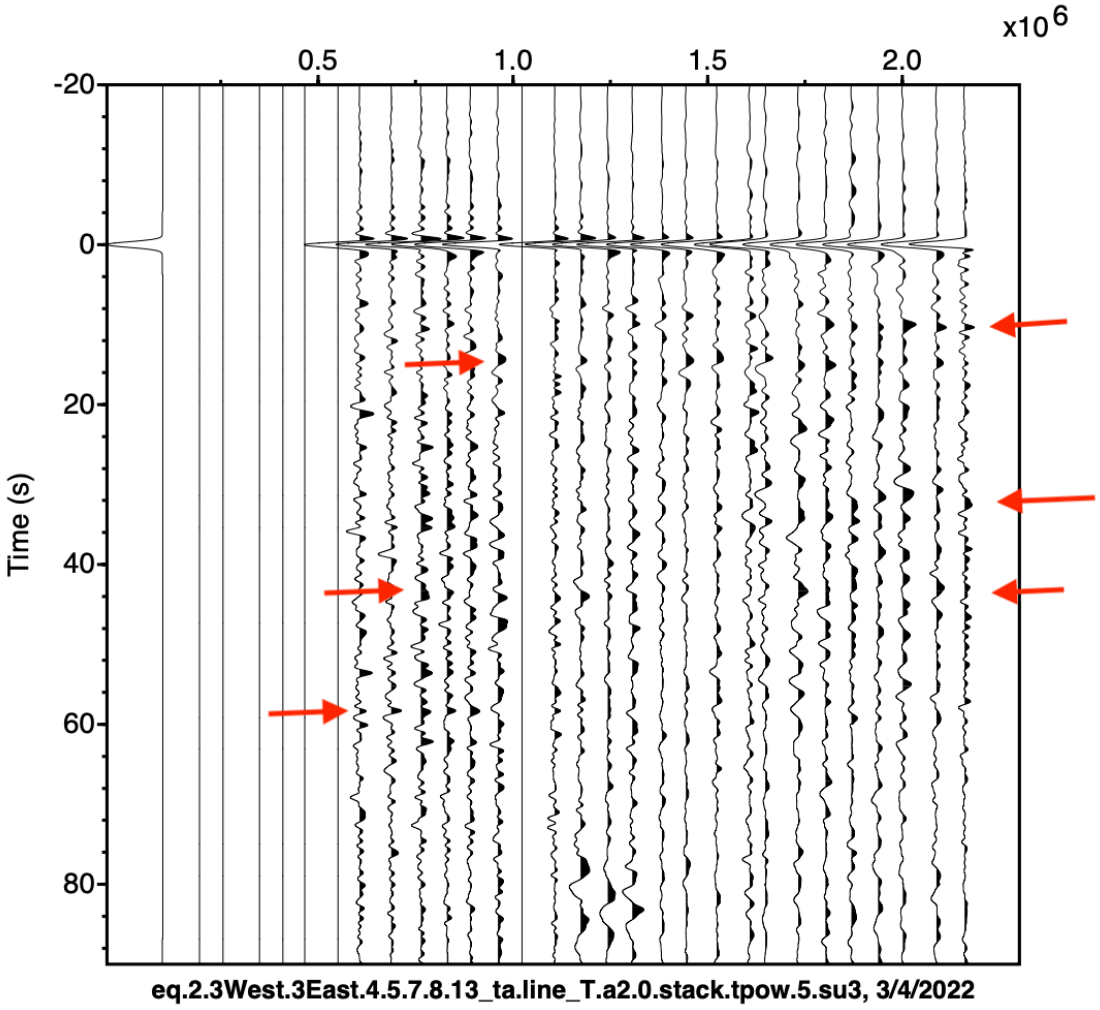


Figure 16. Example of a stacked earthquake plot for Line T with a negative polarity and with a Gaussian parameter of α=2.0. This plot highlights major structures with red arrows. The topmost arrows point to the Moho, the middle arrows point to a multicyclic LAB, and the bottommost arrow points to a feature that is related to layering in the asthenosphere.

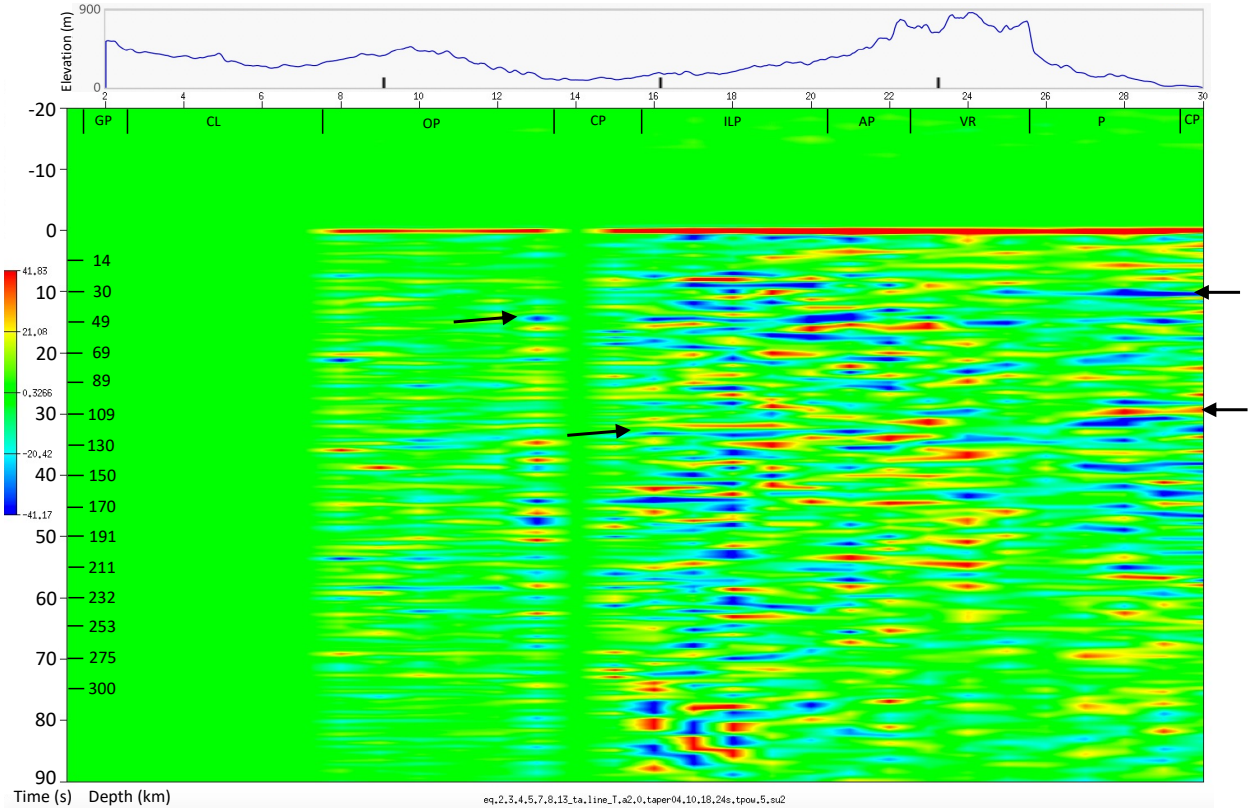


Figure 17. Example of a stacked earthquake color plot for Line T with a Gaussian parameter of α=2.0. Physiographic provinces (Figure 2) and elevations are shown at the top. This plot highlights major structures with black arrows. The topmost arrows point to the Moho, the bottommost arrows point to a westward dipping LAB.

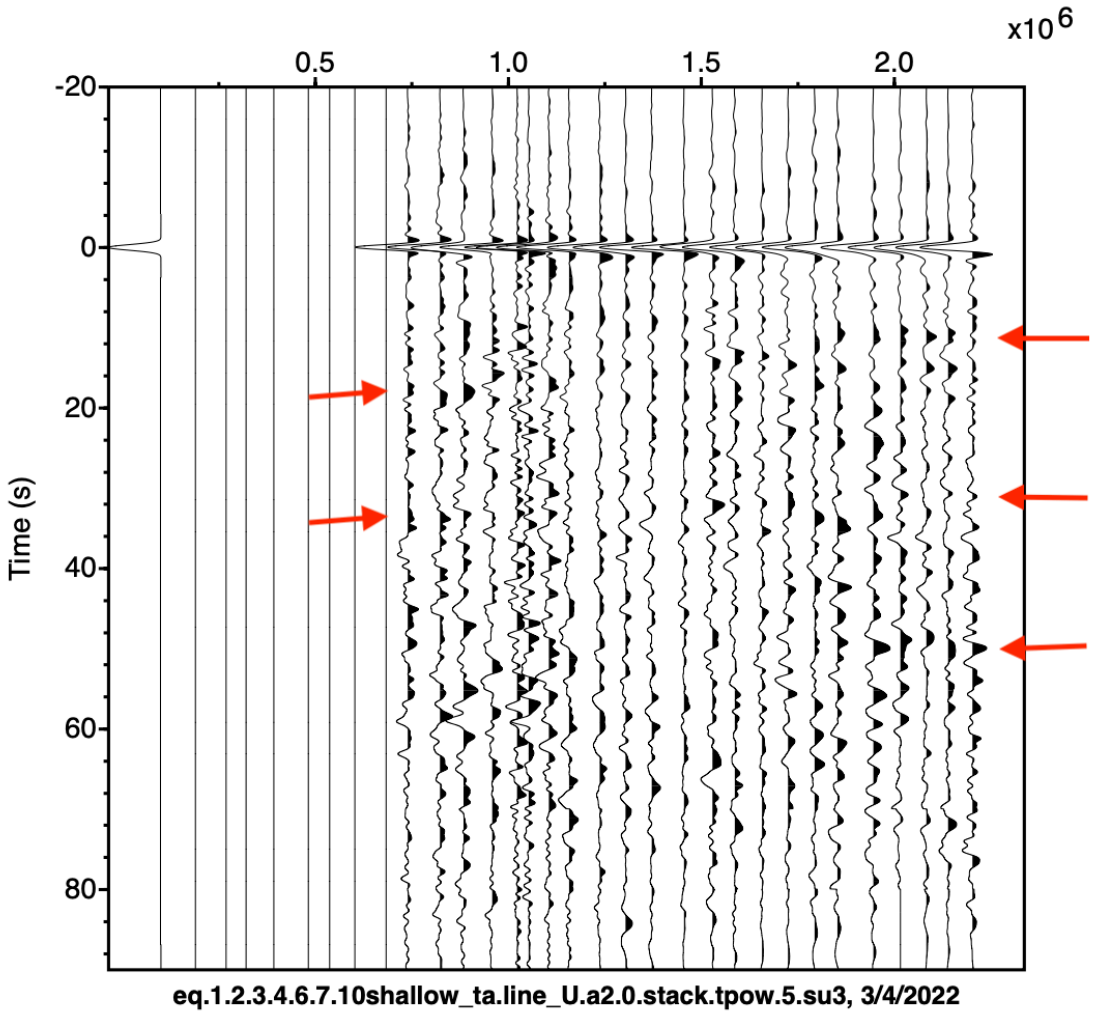


Figure 18. Example of a stacked earthquake plot for Line U with a negative polarity and with a Gaussian parameter of α=2.0. This plot highlights major structures with red arrows. The topmost arrows point to the Moho, the middle arrows point to a westward dipping LAB, and the bottommost arrow points to a feature that is related to layering in the asthenosphere.

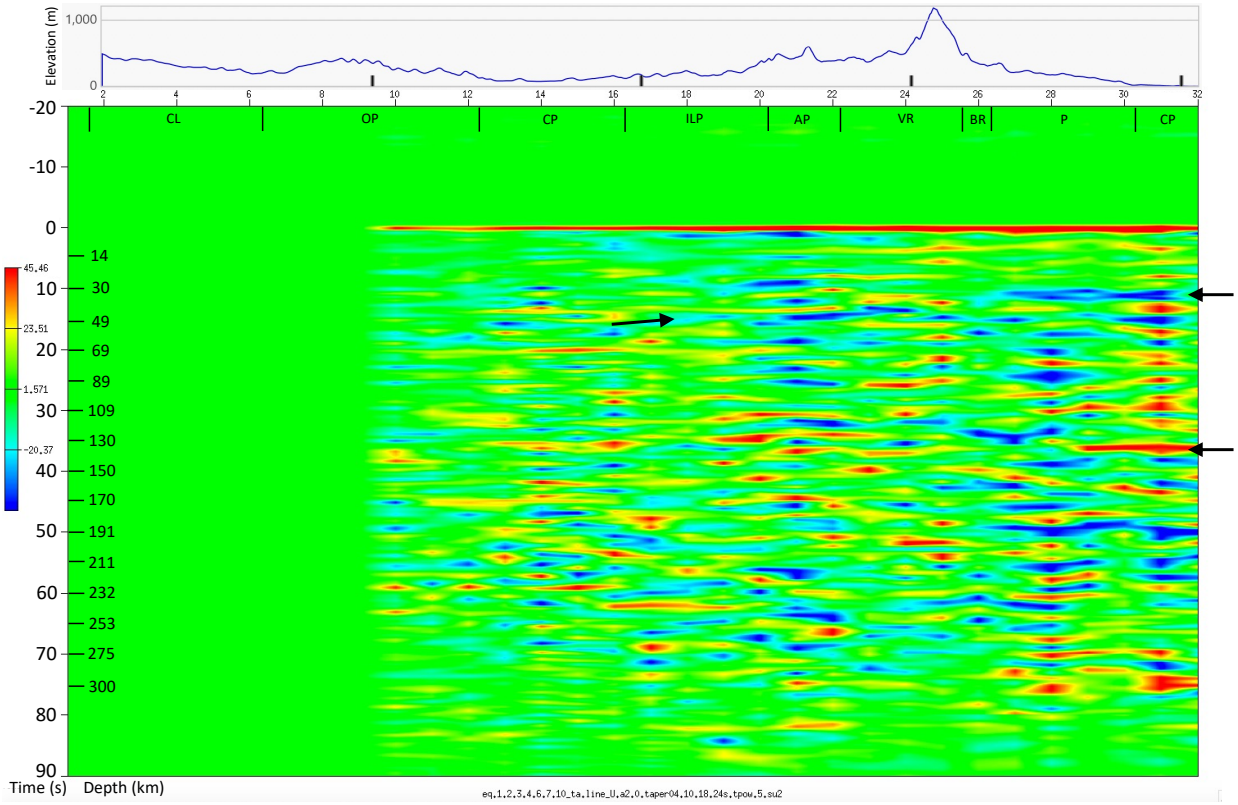


Figure 19. Example of a stacked earthquake color plot for Line U with a Gaussian parameter of α=2.0. This plot highlights major structures with black arrows. The topmost arrows point to the Moho, and the bottommost arrow points to the LAB.

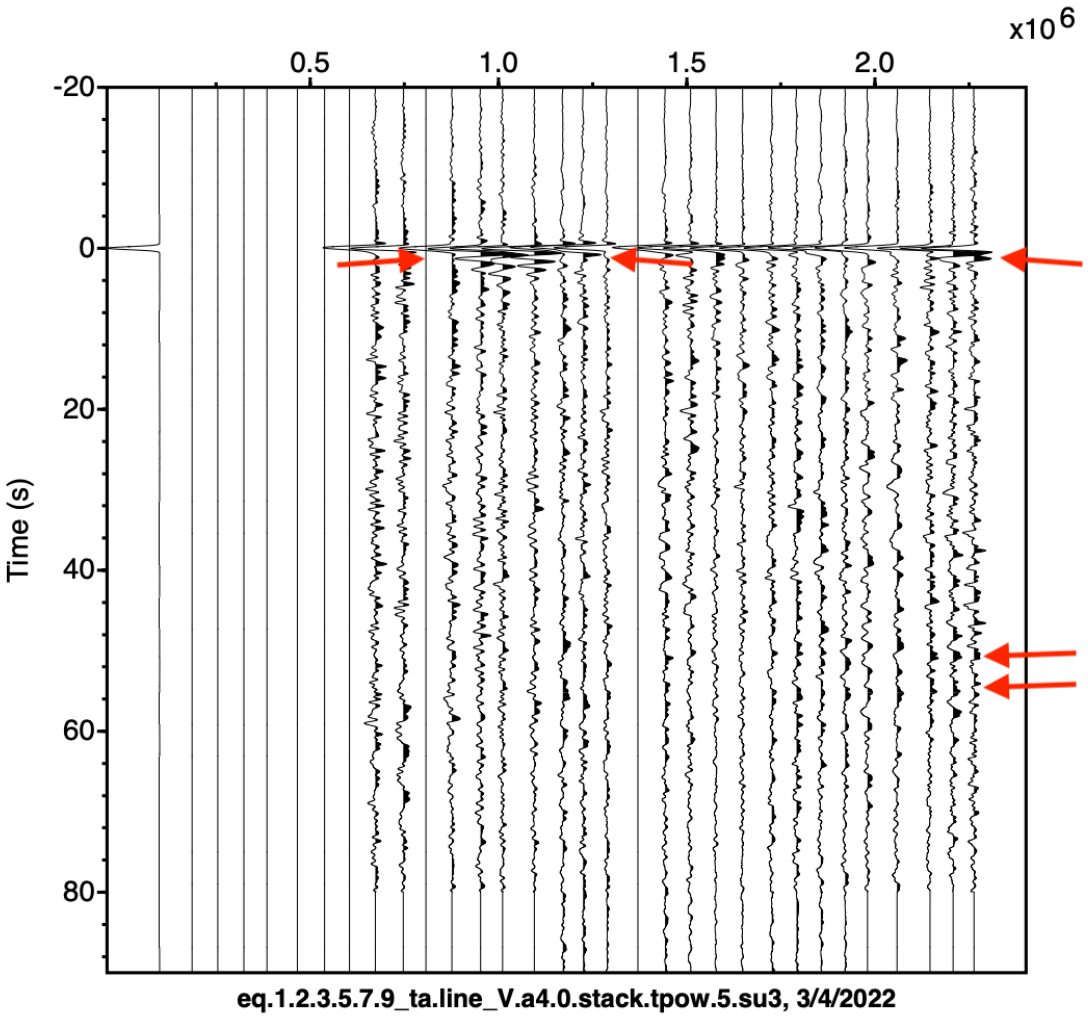


Figure 20. Eample of a stacked earthquake plot for Line V with a negative polarity and with a Gaussian parameter of α=4.0. This plot highlights major structures with red arrows. The topmost arrows in the middle of the section point to the Mississippi Embayment, while the arrow in the top east points to coastal plain sediments. The bottom two stacked arrows point to signals related to layering in the asthenosphere.

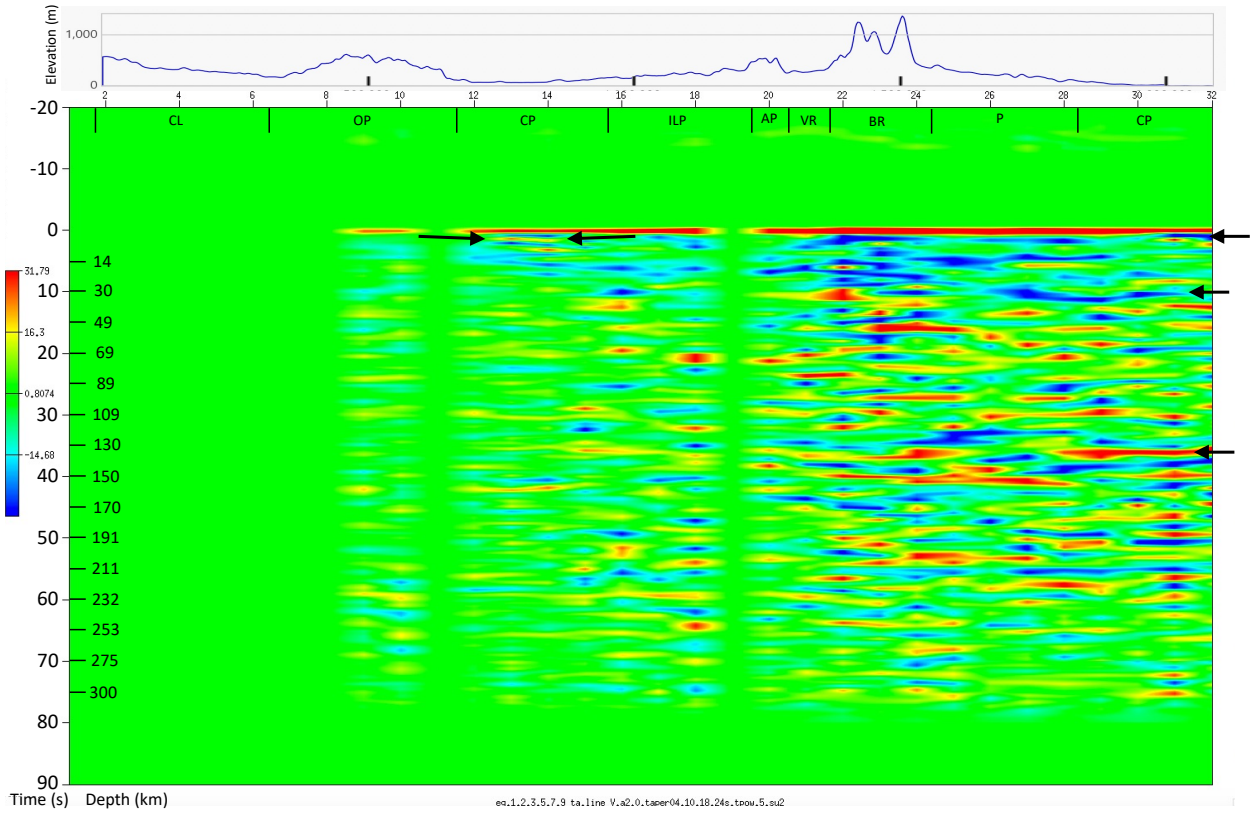


Figure 21. Example of a stacked earthquake color plot for Line V with a Gaussian parameter of α=2.0. This plot highlights major structures with black arrows. The topmost arrows in the middle of the section point to the Mississippi Embayment, while the arrow in the top east points to coastal plain sediments. The middle arrow points to the Moho. The bottommost arrow points to layering in the asthenosphere.

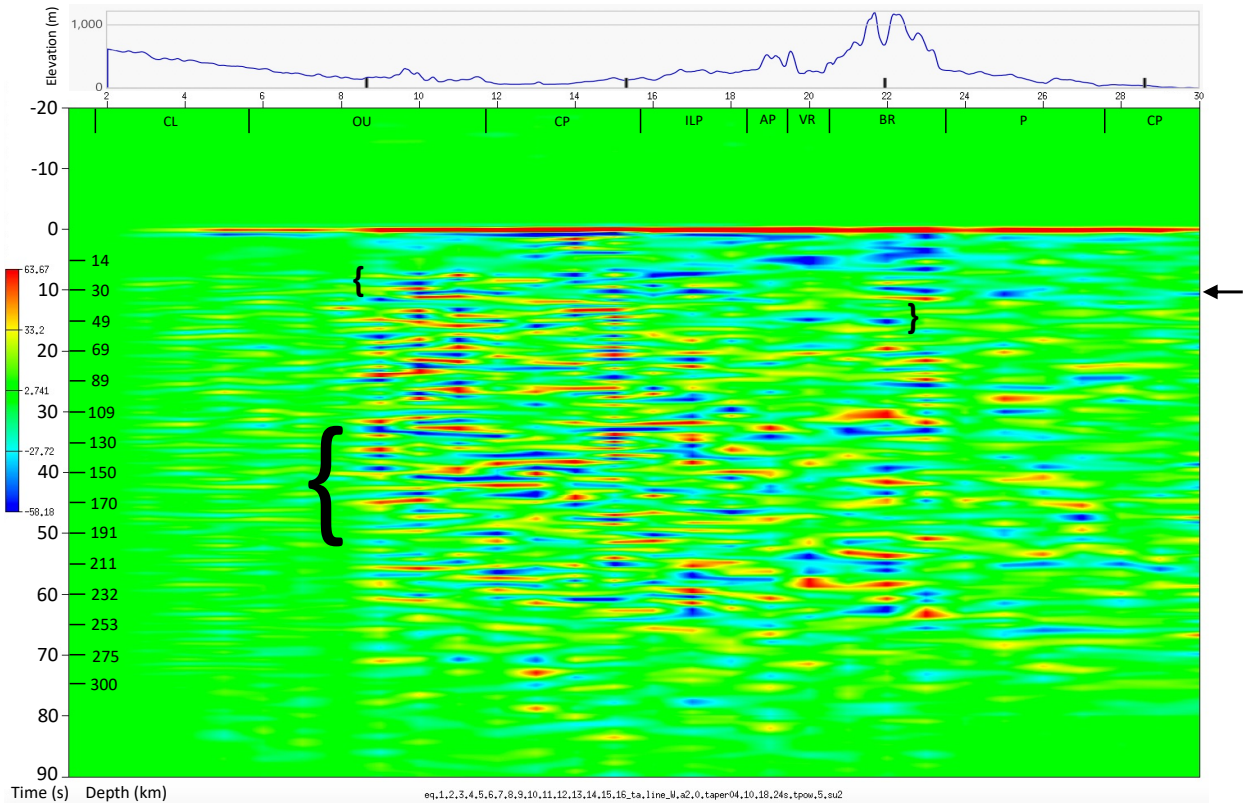


Figure 22. Example of a stacked earthquake color plot for Line W with a Gaussian parameter of α=1.0. This plot highlights major structures with black arrows. The top arrows and small brackets point out the Moho while the large bracket points out an increase in reflectivity.

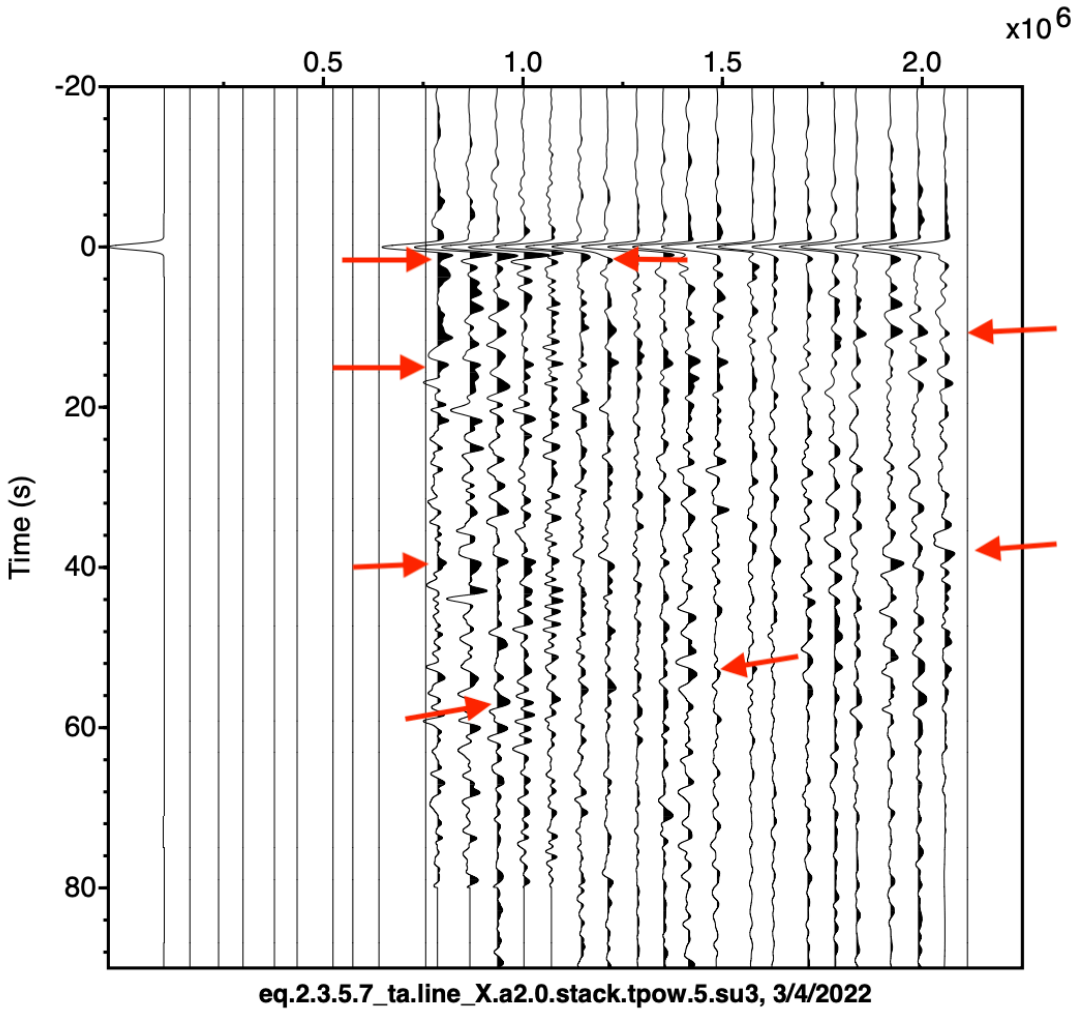


Figure 23. Example of a stacked earthquake plot for Line X with a negative polarity and with a Gaussian parameter of α=2.0. This plot highlights major structures with red arrows. The topmost arrows point to signals relating to the Mississippi Embayment. The middle arrows underneath that point out the Moho and the arrows under the Moho point out the LAB. The bottommost arrows are likely related to layering in the asthenosphere.

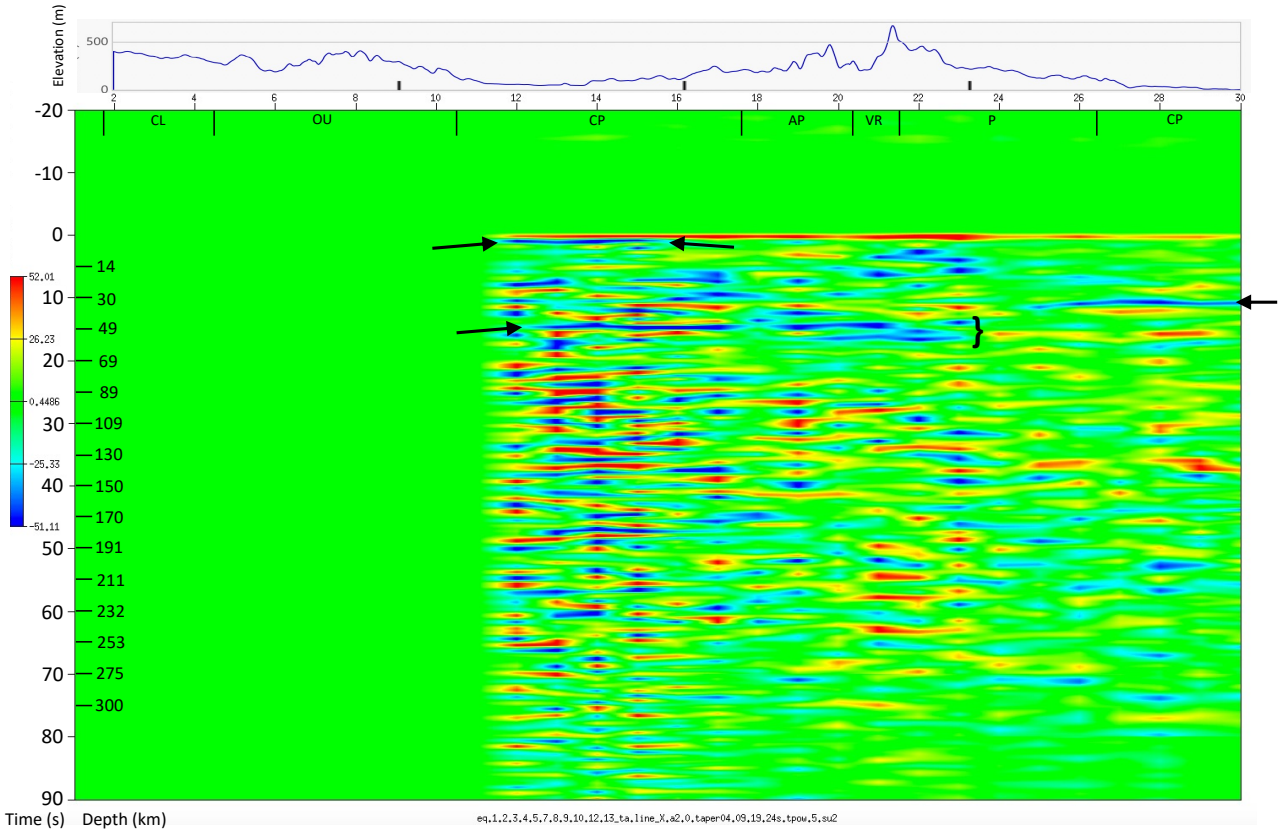


Figure 24. Example of a stacked earthquake color plot for Line X with a Gaussian parameter of α=2.0. This plot highlights major structures with black arrows. The topmost arrows point to signals relating to the Mississippi Embayment and the bottommost arrows and bracket point out the Moho.

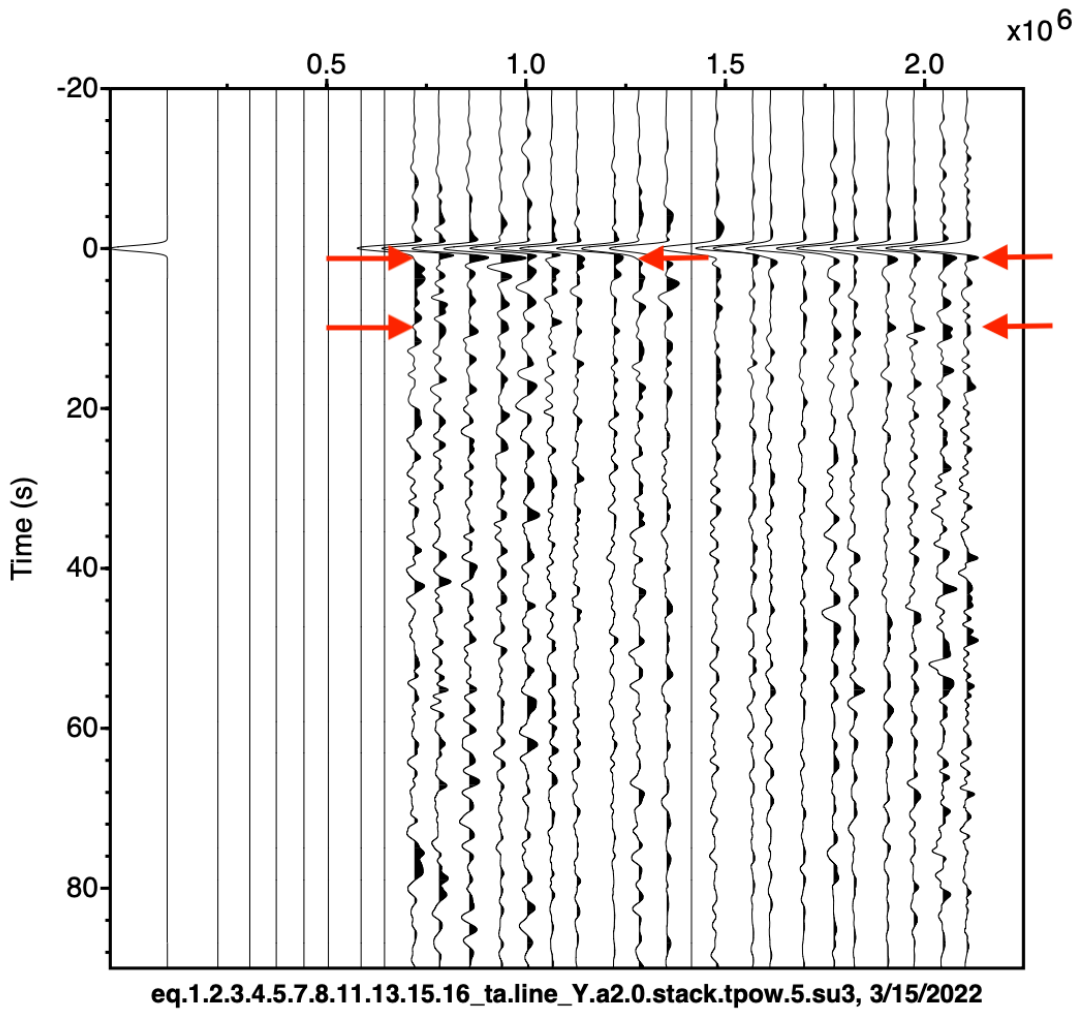


Figure 25. Example of a stacked earthquake plot for Line Y with a negative polarity and with a Gaussian parameter of α=2.0. This plot highlights major structures with red arrows. The topmost arrows in the middle of the section point to signals relating to the Mississippi Embayment, while the top east arrow points out coastal plain sediments. The bottommost arrows point out the Moho.

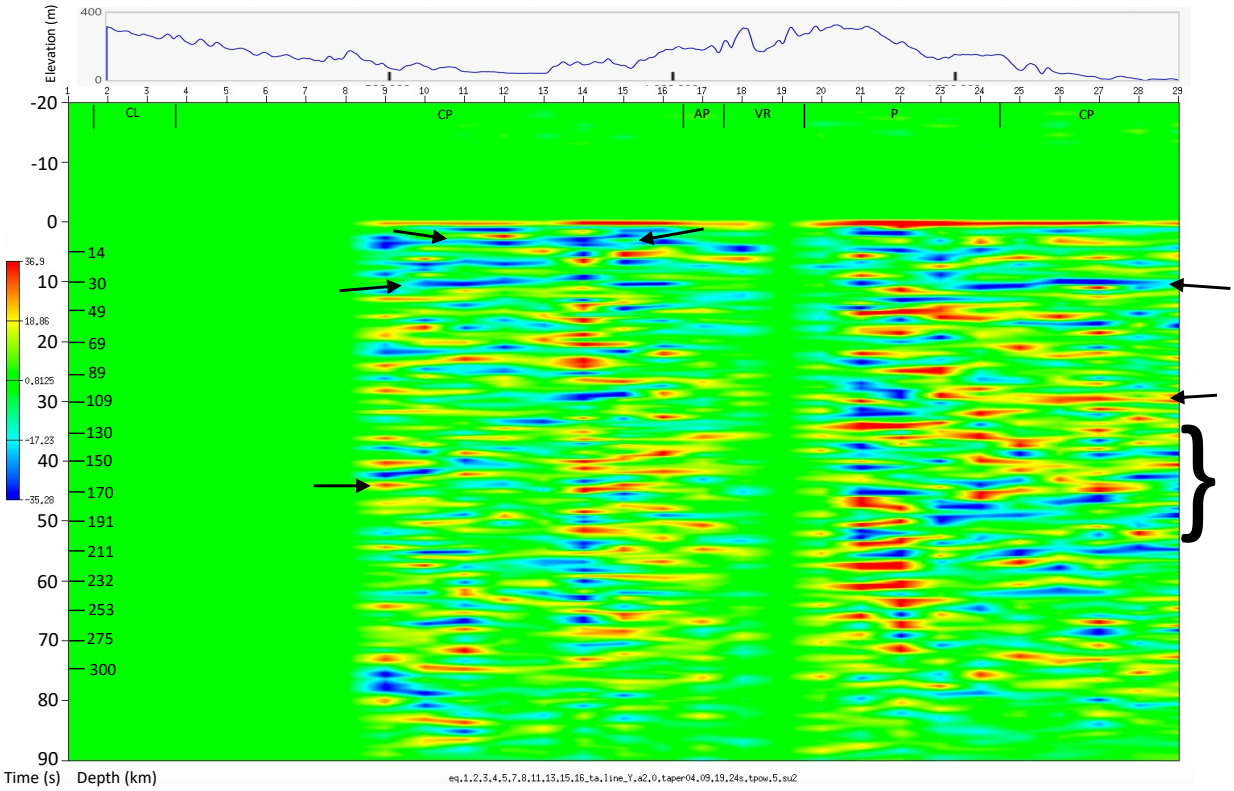


Figure 26. Example of a stacked earthquake color plot for Line Y with a Gaussian parameter of α=2.0. This plot highlights major structures with black arrows. The topmost arrows in point to signals relating to the Mississippi Embayment. The middle arrows point out the Moho. The arrows below that point to a westward dipping LAB and the bracket highlights an increase in reflectivity.

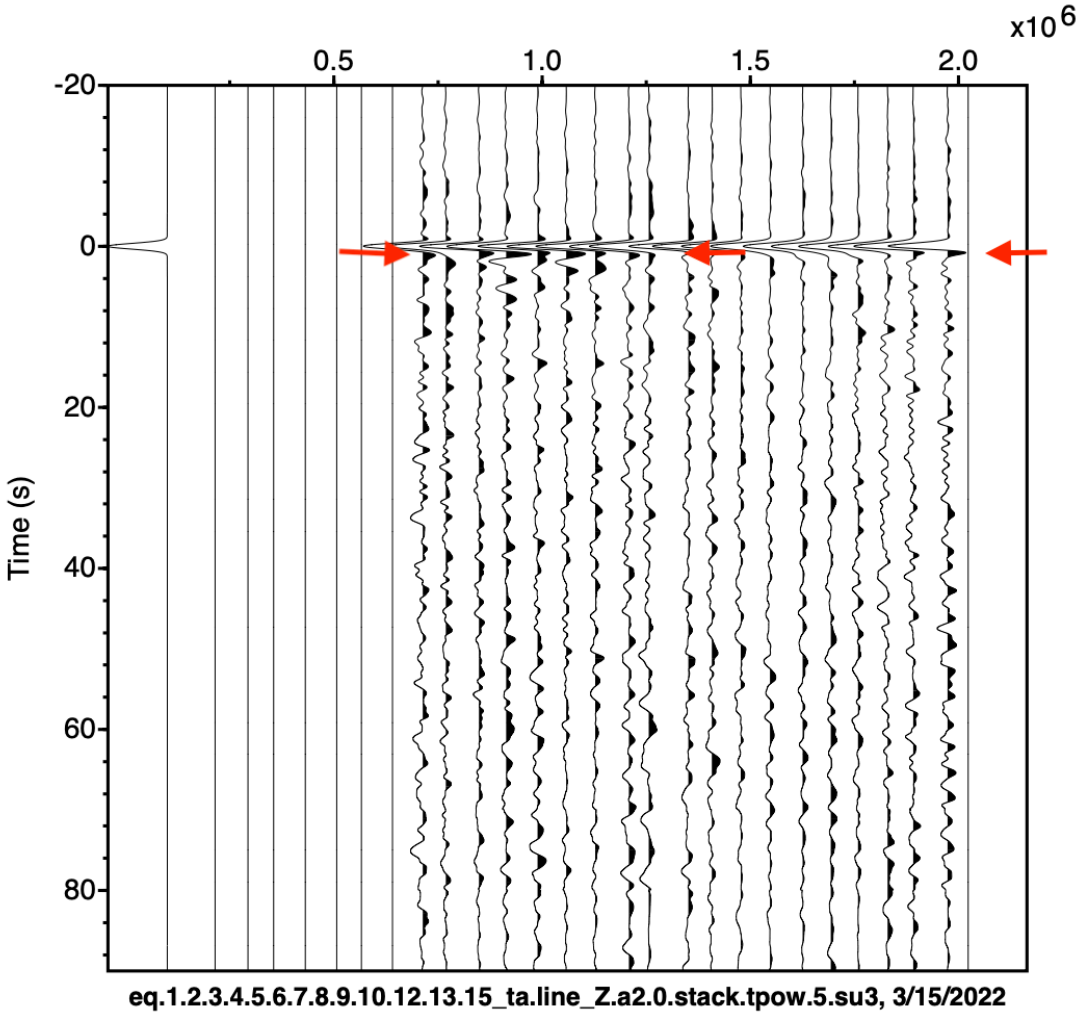


Figure 27. Example of a stacked earthquake plot for Line Z with a negative polarity and with a Gaussian parameter of α=2.0. This plot highlights major structures with red arrows. The arrows in the middle of the section point to signals relating to the Mississippi Embayment, while the arrow in the east points out coastal plain sediments.

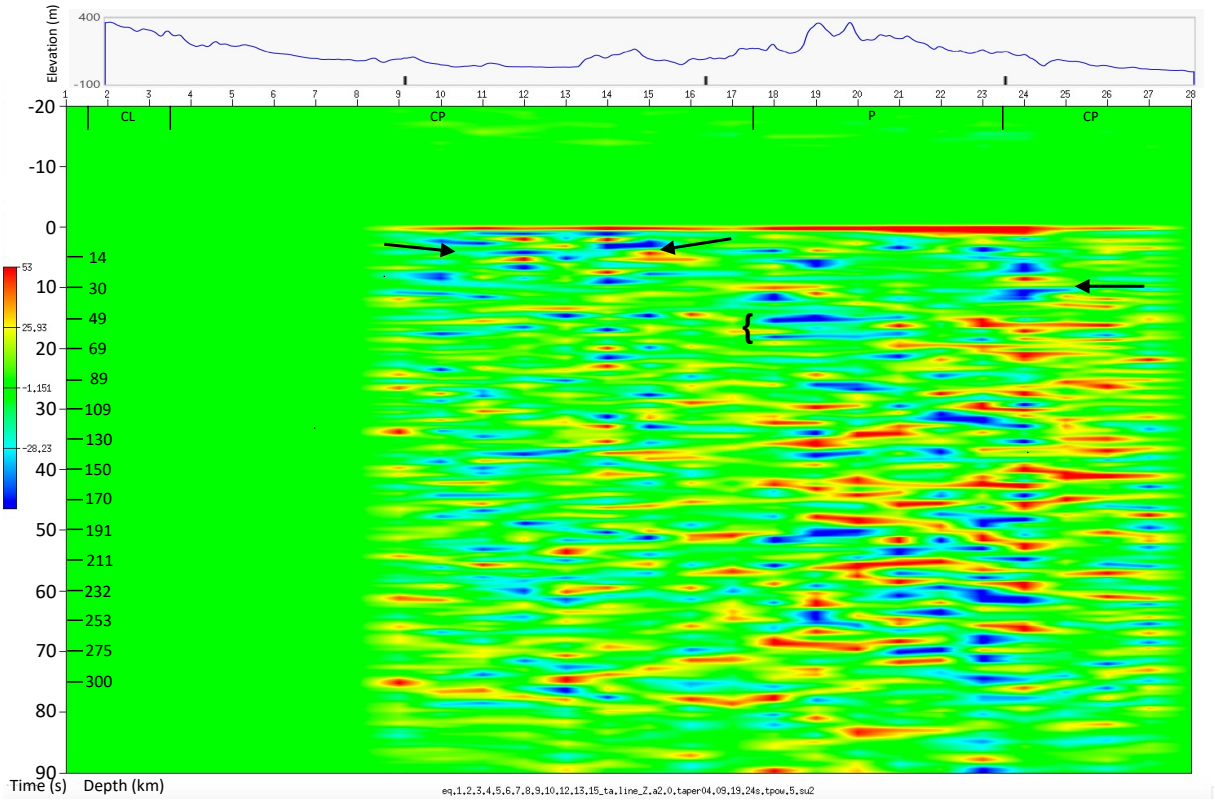


Figure 28. Example of a stacked earthquake color plot for Line Z with a Gaussian parameter of α=2.0. This plot highlights major structures with black arrows. The topmost arrows in the middle of the section point to signals relating to the Mississippi Embayment. The arrow and bracket beneath that point out the Moho.

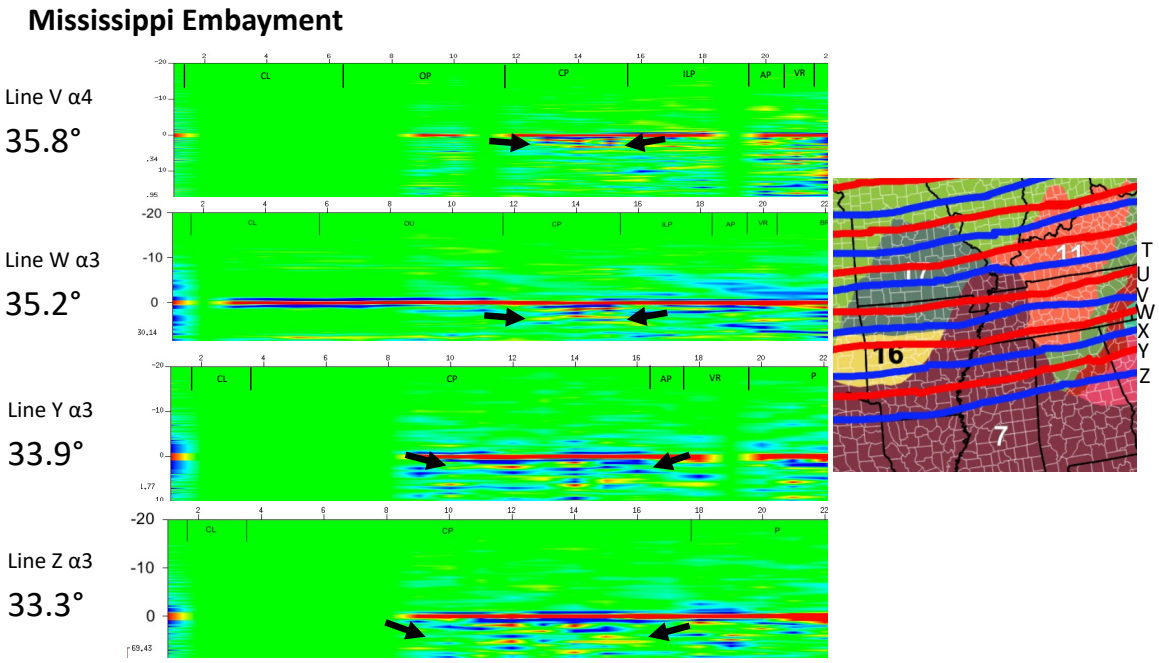


Figure 29. A composite image showing Lines V, W, Y, and Z correlated to the physiographic province map to highlight sediments of the Mississippi Embayment.

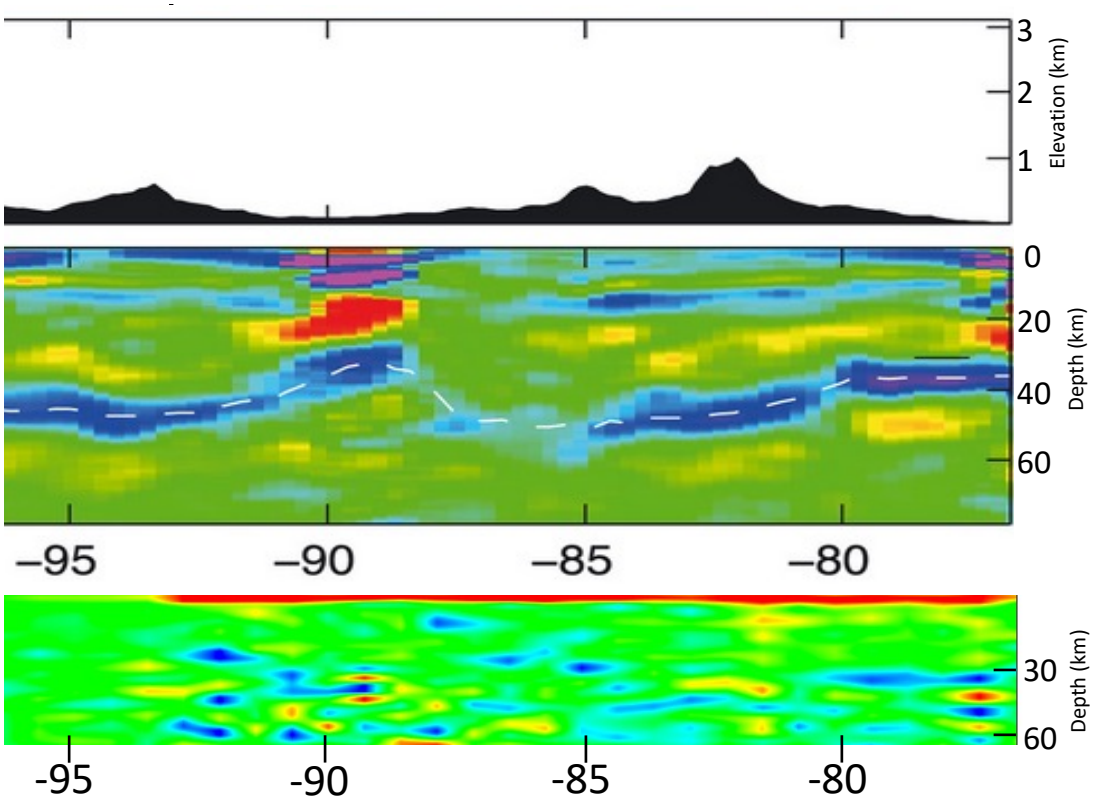


Figure 30. A comparison between a profile (36°) from Schmandt et al., 2015 (top) (from Figure 2b) and the Line U profile (36.4°) from this study (bottom). Note the similarity of the blue signals interpreted as the Ps conversion (top, with white dashed line) and P-wave reflection (bottom) at the Moho east of -85°.

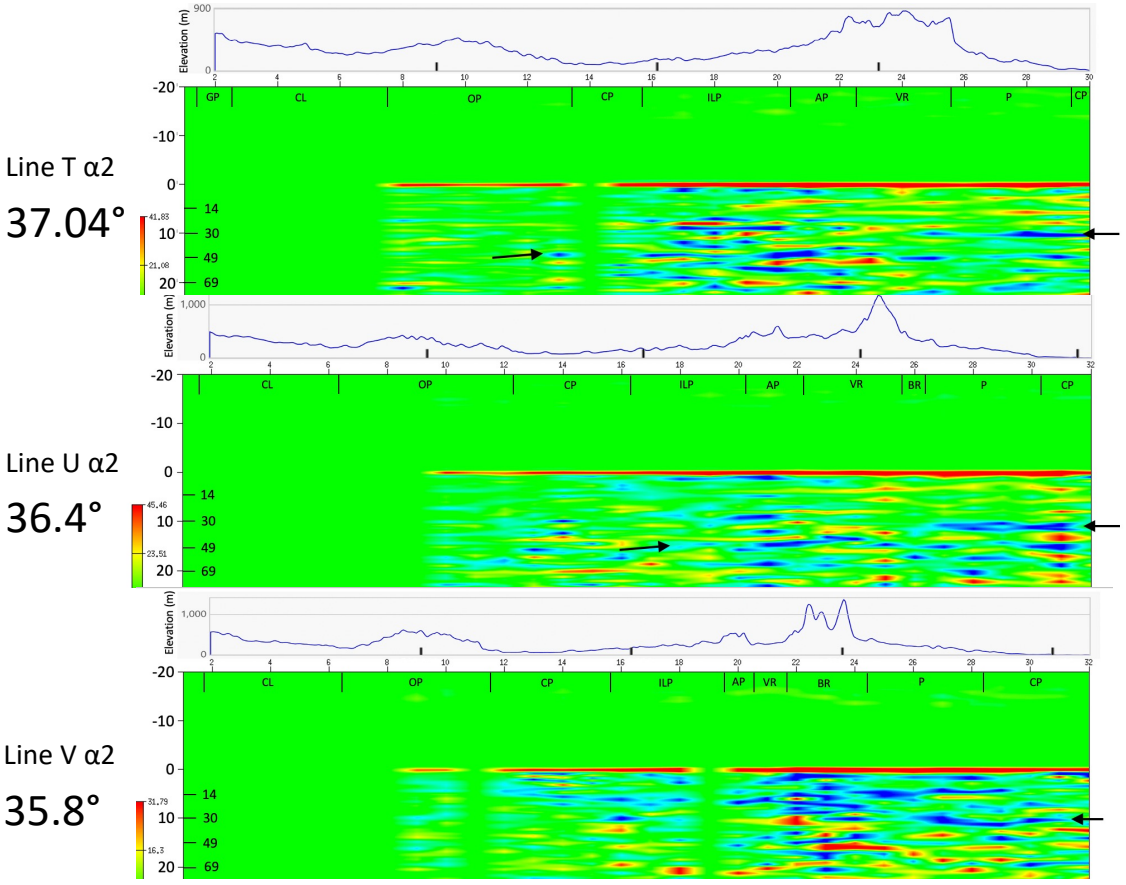


Figure 31. A composite showing interpreted Moho reflections (black arrows) from Lines T-V.

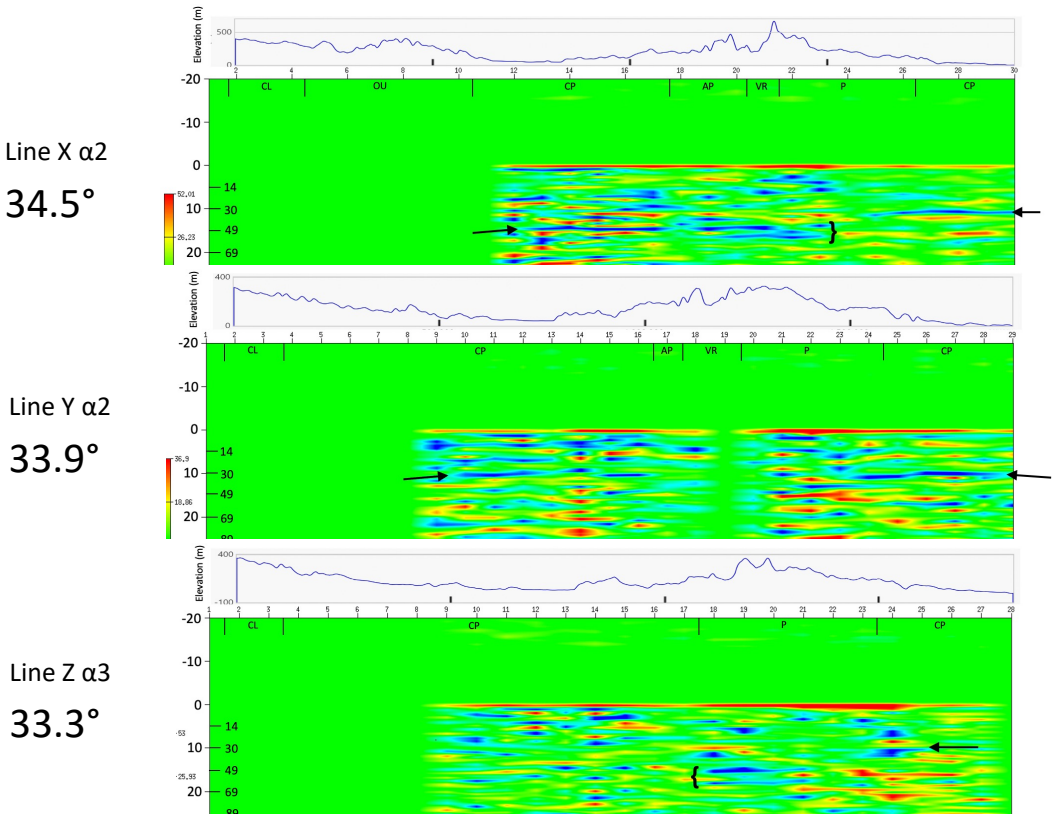


Figure 32. A composite showing interpreted Moho reflections (black arrows and brackets) from Lines X-Z.

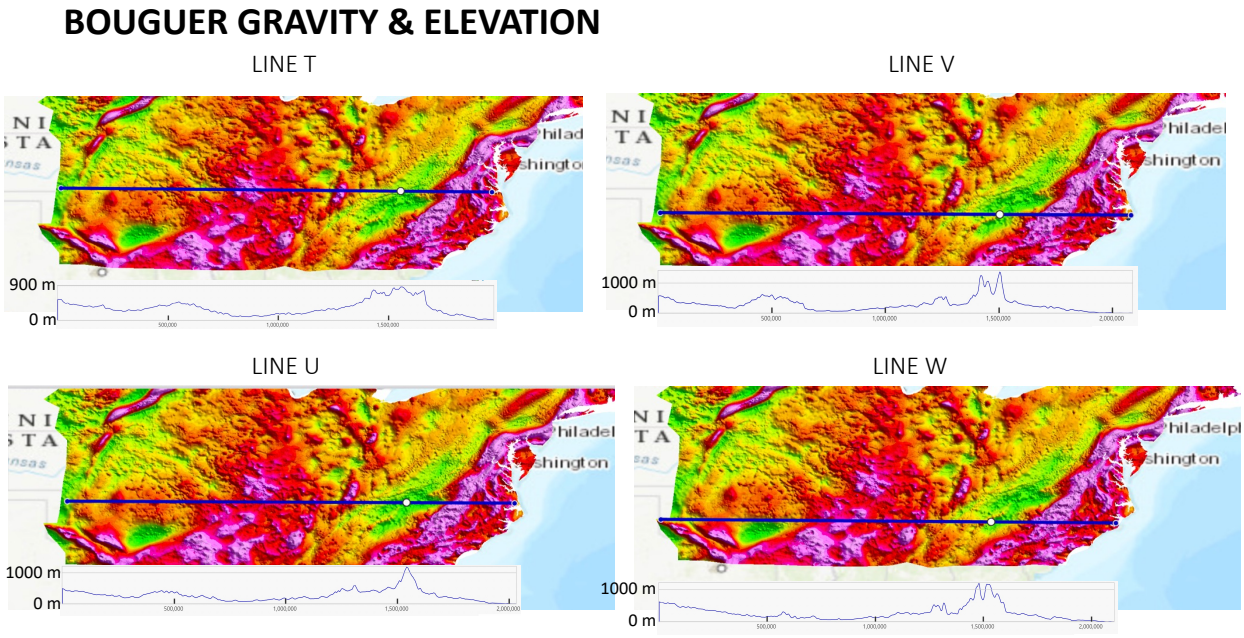


Figure 33. Correlation of Bouguer gravity anomalies with elevations along Lines T, U, V and W. The white dots show that the lowest Bouguer gravity anomaly is directly related to the highest elevation along these lines. The map shows the lowest Bouguer gravity anomaly values in green and the highest in pinks and reds.

CHAPTER THREE

PART TWO

THE LITHOSPHERE-ASTHENOSPHERE BOUNDARY

The LAB represents the boundary between the brittle crust and uppermost solid mantle (the lithosphere) and the less resistant, weak part of the upper mantle that flows and convects (the asthenosphere) (Eaton et al., 2009). The lithosphere and asthenosphere are contrasted by their seismic velocities, heat flow, electrical conductivity, and density (Fischer et al, 2010). The lithosphere is thought to be a compositionally distinct layer due to melt depletion during crust formation. However, a consistent set of criteria for defining the base of the lithosphere has not yet been widely accepted; definitions have been based on a variety of parameters, including temperature, viscosity, and strain rate (Fischer et al., 2020; Garel & Thoraval, 2021).

According to the definition based on temperature, the LAB represents a thermal boundary layer between the asthenosphere, where heat is transferred by convection, and the overlying lithosphere, where heat is transferred by conduction (Fischer et al., 2010). Other definitions involve the mechanical LAB and the electrical LAB. One study suggests that a mechanical LAB (difference in mechanical properties) can be interpreted based on azimuthal anisotropy and that the electrical LAB is characterized by a large reduction in electrical resistivity across the transition from the lithosphere to the asthenosphere (Eaton et al., 2009).

Ps and Sp converted seismic phase data indicates that the LAB in the eastern U.S. is too sharp to be explained by a thermal gradient alone (Abt et al., 2010). The thermal gradient might be combined with a contrast in chemical depletion, partial melt in the asthenosphere, and vertical variations in anisotropy (Fischer et al., 2010). An asthenosphere with a small amount of partial melt would also reduce its seismic wave velocity compared to a mostly melt-free lithosphere (Fischer et al., 2020). This partial melt may be due to the presence of volatiles (Rychert et al., 2020). It has also been hypothesized that contrasts in conductivity across cratons can be explained in terms of a dry lithosphere overlying a hydrated asthenosphere (Fischer et al., 2010).

In regions of thicker lithosphere (~130 km), including portions of the Phanerozoic Appalachian orogen, the LAB is characterized by a gradient zone 60-80 km thick that may be purely thermal in origin (Fischer et al., 2020). These results suggest that the LAB is more gradual in regions of thicker lithosphere than in regions with thinner lithosphere (Abt et al., 2010). Lithospheric thickening with age is observed towards continental interiors, which indicates that temperature plays a very important role in lithospheric thickness, and in turn, LAB depth (Rychert et al., 2020). However, in recent SESAME research, the results indicate that the frequency content of the LAB indicates much smaller wavelength variations in velocity than expected for a purely thermal boundary, at least in the Southern Appalachians (Verellen et al., 2020).

Recent observations of P-wave reflectivity suggest that multicyclic reflections at 32 to 36 s (120-135 km) correspond to the LAB (Verellen et al., 2020). Research involving shear wave velocities show the LAB as the steepest negative velocity gradient, or the sharpest

transition from fast to slow velocities, typically ranging from 100-150 km (Kennett et al., 2017; Chen et al., 2018).

P-wave reflections observed at TWT from 44 to 58 s (167-224 km) might be reflections due to drag-induced flow that causes asthenospheric layering (Eaton et al., 2009; Fischer et al., 2010; Long et al., 2016; Verellen et al., 2020). However, a discontinuity called the Lehmann discontinuity (~200 km and greater), which may correspond to around 58 s, could also explain some of these reflections. This discontinuity is thought to represent a chemical boundary under continental cratons that is distinct in its petrology or a "sharp base of the asthenospheric low velocity zone" (Eaton et al., 2009; Calo et al., 2016; Verellen et al., 2020). More recent research has found that the "translating block," or the lithosphere is not fully rigid and that reflections seen around the LAB may also be the deformed part of the base of the lithospheric plate (Garel & Thoraval, 2021).

METHODOLOGY

A major objective of this study was understanding the reflection response of the lithosphere versus the asthenosphere and what that information can provide about strain in the uppermost mantle. Reflectivity was evaluated in two stages. In the first stage, we applied a coherency filter based on polarities (Hansen et al., 1988) to automate the process of identifying reflections and estimate its reliability. In the second stage, we evaluated the significance of contrasts in reflectivity for various time windows (work in progress).

Reflection coherence was evaluated by applying a filter designed to pass waveforms with matching polarities across adjacent stations. We followed the approach outlined in Hansen et al. (1988), in which the "sign test statistic", an adaptation of the Wilcoxon rank-sum test (Lehmann, 1975), is used to extract coherent signals embedded in noise. The statistic is non-parametric, i.e., knowledge about the specific distribution of noise is not required (Hansen et al.,1988).

This statistic is defined as:

$$S(X) = s_1 + s_2 + s_3 + \ldots s_w$$

where

$$s_i = 1 \text{ if } x_i > 0$$

$$s_i = 0 \text{ if } x_i \leq 0$$

and x_i are the amplitudes of waveforms sampled along a linear trajectory across traces of a seismic section.

The test is governed by two parameters, the window length, w, and the threshold for significance, t, where w is the number of samples in a given spatial window (one sample per trace) and t is the minimum number of positive amplitudes within a window signifying the presence of signal.

The null hypothesis, H_0, is that a given window contains only noise. The alternative hypothesis, H_1, is that the window contains signal. For $S(X) \geq t$, the null hypothesis is rejected and all the samples in the window are identified as signal.

The sign filter itself consists of an array with the same dimensions as the seismic section. Each element of the array has a value of zero or one; initially, all values are set to zero. Upon rejection of the null hypothesis, the elements of all samples in the filter corresponding to a given window are assigned a value of one.

The final step of the process is multiplication of the seismic section by the filter; this zeroes out those waveforms identified as noise.

The test is repeated after reversing the polarity of waveforms to identify coherent signals with negative polarity.

Under the assumption that the noise is random with a symmetric distribution about a mean value of zero, one can compute the "level" of the sign test for a single window. The level is a measure of the probability of a "type 1" error, i.e., the probability that H_0 will be rejected when H_0 is true (when the window contains only noise). In other words, it is the probability of erroneously identifying noise as signal. The level, α, is defined as:

$$\alpha = \frac{1}{2^w} \sum_{k=t}^{w} \binom{w}{k} = \frac{1}{2^w} \sum_{k=t}^{w} \frac{w!}{k!\,(w-k!)} \qquad (1)$$

which reduces to $1/2^w$ for t=w. The expected number of "false alarms" (noise windows erroneously identified as signal) then is given by Nα, where N is the total number of windows of width w in the seismic section.

Values of α for a range of values for w and t are summarized in Table 1.

Given more specific information about the distribution of noise, one can also compute the "power", 1 – β, of the test, defined as the probability that H_0 will be rejected when H_1 is true (that is, the probability of correctly identifying signal).

For noise with a Gaussian distribution, the power is given by:

$$1 - \beta_{w,t}(z) = \sum_{k=t}^{w} \binom{w}{k} [\Phi(z)]^k [1 - \Phi(z)]^{w-k} \qquad (2)$$

where

$$z = \frac{peak\ signal\ amplitude - mean\ amplitude}{rms\ noise\ level} = \frac{peak\ signal\ level - 0}{rms\ noise\ level}$$

where the peak signal amplitude is assumed to be uniform within the window and the noise has a mean value of zero,

$\Phi(z)$ = the cumulative probability for the standardized normal distribution,

and where

β = probability of a "type 2" error or a "miss", i.e., the probability of characterizing signal as noise

A "perfect" test will be characterized by alpha=0 and power $1 - \beta = 1$; in practice, the optimum choice of filter parameters will be determined by the tradeoff between the two.

Values of the power for a range of signal amplitudes and values of w and t are summarized in Table 2.

Signfilter

As implemented in this study, the filter is designed to pass coherent reflections with zero apparent dip (Figure 34a). The idea is that the asthenosphere produces laterally continuous reflections due to drag-induced flow, therefore the uppermost asthenosphere is highly reflective in comparison to the lithosphere. This study focused on windows of 7, 9, and 11 traces corresponding to structure continuous over distances of roughly 420, 560, and 700 km. A window length of 9, for example, would show a laterally continuous signal only if it continued for 9 traces in the final gather. This means that less and less signal will be carried over as the window length increases.

The envelope of each sign-filtered trace then was computed to more clearly show the variation in overall reflectivity with TWT. The envelope is defined as the modulus of the signal and its Hilbert transform (Bracewell, 1978; Shearer, 2019) and provides a measure of the instantaneous amplitude of the signal. The envelope functions then were smoothed by computing running averages over 11-sample windows.

As an example, I have included smoothed figures from Line V with a positive polarity and a Gaussian parameter of α=2.0 showing window lengths 7 and 9 (Figures 34b and 35).

Although signfilter plots are useful for analyzing laterally continuous signals, this only works if the signals are not dipping or varying too much. Especially due to the large station spacing of the TA, it is important to note that the signals that this methodology detects are very large-scale, highly continuous features that extend for hundreds of kilometers. Therefore, this methodology works for the purpose of identifying structure generated by horizontal strain, but not the Moho, which is characterized by variations in depth over much smaller distances. It is also important to note that Line L-Z covers almost half the area of the eastern U.S., and therefore subcrustal features may change throughout the area. This means it is possible that some lines may have greater reflectivity in the lithosphere rather than the asthenosphere. It is also possible that layering within the asthenosphere may dip slightly, in which case those reflections will not be passed by the signfilter.

Tallyrun

The tallyrun job takes place after completing the signfilter job. Basically, the tallyrun job sums or stacks the output traces of the signfilter into a signal trace so that at a quick glance one can characterize the differences in reflectivity at all depth ranges for a certain window length and alpha for a line of choice.

As an example, I have included figures of tallyrun plots coinciding with the signfilter jobs (Line V with a negative polarity and a Gaussian parameter of α=2.0 showing all window lengths (5, 7, 9, and 11). Results are shown for both the total number of nonzero samples and the average absolute value of stacked traces (Figures 36-39; Appendix Figures F1-F4).

RESULTS

Results in this section include stacks and color plots but focus mostly on analyzing signfilter and tallyrun plots that help to determine vertical variations in horizontal reflectivity. Figures for part two include color plots, signfilter plots, and tallyrun plots for Lines L-Z.

Stacks and Color Plots

Using the same figures as part one, analysis was done on figures to show deeper subsurface features, related to the LAB and deeper.

Stacks for Line T show a signal around 32 s in the east, while the color plot shows a signal dipping slightly west from 30 s to 32 s (Figures 16 and 17). These signals may mark the LAB, which can be multicyclic and vary in TWT especially depending on the polarity of the plot. Both plots also show a fairly continuous signal around 45 s that may be related to asthenospheric layering. In general, the color plot also showcases an increase in reflectivity beneath the interpreted LAB.

Line U shows a signal at 32 s in the original stack to 36 s in the color plot (Figures 18 and 19). This signal again may be a reflection from within the LAB. The original stacked plot shows a signal around 50 s that is likely due to asthenospheric layering. Like Line T, Line U shows an increase in reflectivity beneath the interpreted LAB.

For Line V, both the stacked and color plot showcase strong signals at 50 s and 54 s that are likely due to asthenospheric layering. (Figures 20 and 21).

For the Line W color plot, a noticeable change in reflectivity is noted below 35 s (Figure 22).

For Line X, the original stacked plot shows signals from 38 s in the east increasing to 40 s in the west, while the color plot shows a signal around 36 s (Figures 23 and 24). All of these signals are likely reflections from within the LAB.

Lastly, for Line Y, the color plot also shows a signal starting at 30 s in the east, increasing to 40 s in the west that is likely the LAB dipping westward (Figures 25 and 26).

Signfilter

The signfilter plots show continuous lateral structures beneath the subsurface using a window length of choice. These plots are useful for objectively identifying continuous signals. In particular, these plots were used to identify the transition from lithosphere to asthenosphere based on variations in horizontal reflectivity as a function of TWT.

A clear example is shown for Line N (Figure 40). This plot shows a slightly weak signal around 14 s TWT in the middle of the section for about 9 stations that likely relate to the Moho. There is also a signal around 35 s that separates the plot by a lack of reflectivity above it and more abundant reflectivity below it. Line T shows a similar variation in horizontal reflectivity above and below 40 s (Figure 41).

Figure 42, generated for Line O, highlights the sensitivity of the images to variations in the parameters used for the sign filter. The general increase in horizontal reflectivity below 40 s is stable. Similar composite figures for the other TA lines can be found in the Appendix D (Figures D1-D14).

For the signfilter plots, three distinct patterns were observed (Figure 43): greater reflectivity below 35-40 s (A), greater reflectivity above 35-40 s (B), and more scattered

reflectivity (C). Composite signfilter plots that highlight each line's general reflectivity are shown in Figures 44a and 44b. Line L shows a general increase in reflectivity above ~35/40 s, while Lines M, N, O, P, R, V, X, and Z all show a general increase in reflectivity below ~35/40 s. The rest of the lines show more scattered reflectivity. In particular, Lines Q and W show a reflection where other plots show an onset in general reflectivity and then a gap below with more signals at later times. Lines S, T, U, and Y show greater reflectivity below ~35/40 s but still contain more signals in the subcrustal lithosphere than some other plots.

Tallyrun

Tallyrun plots are created by stacking or adding together the traces for signfiltered gathers. This can be useful for looking at the general reflectivity patterns of an entire line quickly. Within the tallyrun plots were the same categories as signfilter plots: greater reflectivity above 35-40 s, greater reflectivity below 35-40 s, and more scattered reflectivity.

These plots were generated using a range of Gaussian parameters and window lengths. For the tallyrun plots with both Gaussian parameters of α=1.0 and α=2.0 and window length of 7, Lines L showed increased reflectivity above ~35 s, Lines M, N, R, S, T, W, X and Z show increased reflectivity below ~35 s, and the rest of the lines show more scattered reflectivity (Appendix Figures F5 and F6).

For the tallyrun plots with both Gaussian parameters of α=1.0 and α=2.0 and window length of 9, Line M, N, P, S, T, X, and Z shows increased reflectivity below ~35 s, and the rest of the lines show more scattered reflectivity (Figures F7 and F8).

Corresponding nonzero tallyrun plots can be found in Appendix H Figures F9-F12.

One drawback in using these plots to characterize reflectivity as a function of depth is the fact that they will not show laterally continuous signals if they are dipping, wavy, or changing in anyway- only if they are perfectly horizontal. This is useful for certain purposes, but it is also important to check other plots for signals that vary with TWT.

Overlay Comparisons

Here, reflection profiles produced by sign filtering in this study are compared directly with profiles previously generated at very similar latitudes using Sp receiver functions and with models of S-wave velocity as a function of depth derived from surface waves (Chen et al., 2018). Those previous studies were carried out at latitudes overlapping the coverage provided by TA Lines O, Q, S, U, and V. For each comparison, envelopes of traces from the reflection profiles are plotted directly on sections derived from previous work. In the original sections (prior to computing the envelope), with the direct PKPdf arrival plotted with negative polarity, reflections with positive polarities correspond to positive impedance contrasts (low-velocity layer over high-velocity layer).

Comparison with Sp receiver function profiles

In the receiver-function profiles, red/orange corresponds to a discontinuity (e.g., the Moho) marking an upward decrease in velocity (a low-velocity layer over a high-velocity layer), while blue corresponds to a discontinuity marking an upward increase in velocity (a high-velocity layer over a low-velocity layer).

TA Line O (latitude 40.2°) & Receiver Function Profile G (latitude 40°)

In this profile, a strong positive-polarity reflection closely matches an "orange" receiver function signal (an Sp conversion), both indicating a lower-velocity above and higher velocity below a discontinuity at approximately 140 km depth. This depth also marks an increase in P-wave reflectivity (Figure 45).

TA Line Q (latitude 39°) & Receiver Function Profile A (latitude 38.7°)

In this profile, a strong positive-polarity reflection closely follows an "orange" Sp conversion increasing in depth from 125 along the eastern end of the profile to 150 km farther west. Again, both types of signal indicate a downward increase in velocity. A shallower complex of positive and negative polarity reflections at a depth of 90-100 km along the western section of the profile matches a "blue" receiver function signal, indicating a downward decrease in velocity (Figure 46). Examples for additional filter settings can be found in Appendix E (Figure E1).

TA Line S (latitude 37.7°) & Receiver Function Profile F (latitude 37.7°)

Here again a good match is observed between a positive-polarity reflection and an "orange" Sp conversion increasing in depth westward from 140 km to 150 km, again accompanied by an increase in P-wave reflectivity (Figure 47).

Comparison with S-wave velocity models

In these profiles, shear-wave velocity increases from red to blue.

TA Line Q (latitude 39°) & Shear Wave Velocity Profile A (latitude 38.7°)

For this profile, a strong reflection aligns with the steepest velocity gradient (from fast above to slow at greater depth), beginning at 130-140 km in the eastern portion of the section, rising to ~125 km and finally increasing in depth to ~150 km in the western portion of the section, with a marked increase in reflectivity below these depths. The onset of increased P-wave reflectivity is interpreted as the LAB (Figure 48). Examples for additional filter settings can be found in Appendix E (Figures E2 and E3).

TA Line U (latitude 36.4°) & TA Line V (latitude 35.8°) & Shear Wave Velocity Profile C (latitude 36°)

Both reflection profiles show clear signals following the steepest negative velocity gradient beginning at ~125 km in the east, rising to ~75 km in the central parts of the profiles, and increasing again in depth to ~125 km in the western part of the profiles, again with a marked increase in reflectivity below these depths. Again, the increase in P-

wave reflectivity is interpreted as the LAB (Figures 49 and 50). Additional examples for these lines can be found in Appendix E (Figures E4-E7).

The comparison with models of shear-wave velocities derived from surface waves is particularly compelling, because tracking the depth to the maximum negative velocity gradient has been proposed by several authors as one way to map the depth to the center of the lithosphere-asthenosphere transition zone (Chen et al., 2018). This suggests that P-wave reflectivity can be used as an independent method for constraining thickness of the lithosphere. Moreover, the onset of increased horizontal reflectivity not only closely matches the depth corresponding to the maximum negative velocity gradient, but also provides information about fabric within the asthenosphere that the lower frequencies of surface waves cannot resolve.

DISCUSSION

The Lithosphere-Asthenosphere Boundary

Color versions of the original stacked sections, and in particular, sections filtered to emphasize horizontal reflectivity, show that in general, the LAB starts in the east at about 30 s to 32 s (~109-120 km) or as multicyclic reflections sometimes occurring from 32 s to 36 s (~120-135 km) and even as late as 38 s (~145 km). The LAB deepens westward to about 40 s (~150 km) in the westernmost part of the sections. There is also a general trend of increasing reflectivity below 35- 40 s (130-150 km). This agrees with other results showing the lithosphere thickening towards the North American craton, and motion of the lithosphere causing drag-induced flow in the asthenosphere. Some recent

research has found that the cratonic core can be greater than 180 km thick in the central United States and that lithosphere in the Basin and Range is very thin (Porter & Reid, 2021). Other recent research shows that the LAB increases in depth in a stair-step fashion from east to west from approximately 100 km in the Appalachian Province, to around 150- 200 km in the Grenville Province, to up to 200- 250 km in the North American craton (Gao & Li, 2020). These trends agree with the results of the present study that shows the LAB either stepping down or dipping gradually towards the west.

The key objective of this study was to test a new criterion and protocol for identifying the lithosphere-asthenosphere transition. Reflections identified objectively using the sign test statistic were used to establish a new criterion for mapping the base of the lithosphere based on P-wave reflectivity. Comparison with models of shear-wave velocities derived by inversion of surface waves (Chen et al., 2018) shows that the observed onset of increased horizontal reflectivity closely matches the depth corresponding to the maximum negative velocity gradient, suggesting that P-wave reflectivity can be used as an independent method for constraining thickness of the lithosphere. Moreover, the onset of increased horizontal reflectivity not only closely matches the depth corresponding to the maximum negative velocity gradient, but also provides information about fabric within the asthenosphere that lower-frequency surface waves cannot resolve. The observed, generally abrupt, downward increase in horizontal reflectivity is consistent with the pattern expected for drag-induced flow in the asthenosphere (Figures 51 and 52).

Other Reflections

Some stacked earthquake plots and color plots show signals at 56-58 s (~215-225 km). While layering in the asthenosphere due to drag induced flow is possibly the cause of these signals, it is also possible that these signals mark the Lehmann discontinuity, thought to represent a chemical boundary or the base of a zone of strong anisotropy that represents the base of the zone of drag-induced flow or strong coupling with the lithosphere, which has been found previously at these depths (Eaton et al., 2009; Calo et al., 2016; Verellen et al., 2020).

Future Work

Future work includes identifying MLD's and what may cause them in this study area, a more rigorous assessment of isostasy, further quantifying contrasts in reflections over different depth ranges and the statistical significance of differences between various windows, and extending this analysis to greater depths to test models of anisotropy for the Lehmann discontinuity.

Table 1. Level calculation for the sign test.							
w	t	width (km)	α	nw	N = nw×nt	N×α	(N×α)/12.5
7	7	420	0.00781	24	96,000	750	60
9	9	560	0.00195	22	88,000	172	14
11	11	700	0.00049	20	80,000	39	3

w = number of adjacent traces in spatial window
t = minimum number of positive samples within a window for rejecting H_0
width = (w-1) ×70 km, distance spanned by w
α = level of the sign test, as defined by equation (1). This is the probability that a window containing only noise for t or more traces is identified as signal
nw = ntr – (w-1). the number of windows for a given travel time, where ntr = number of traces in the seismic section = 30
nt = number of samples in each trace = 4000
dt = sampling increment in time = 0.02 s, corresponding to a highest resolvable frequency of 25 Hz
N = total number of windows
N×α = expected number of noise-only windows identified as signal
(N×α)/12.5 = expected number of noise-only windows identified as signal after correcting for waveform oversampling. New dt = 0.25 s, corresponding to a highest resolvable frequency of 2.0 Hz, a more realistic value for global P-wave data.

Table 1. The calculations required for the sign filter test.

Table 2. Power calculation for sign test				
w = t	width (km)	z	$\Phi(z)$	$1 - \beta(z)$
7	420	1.0	0.841	0.298
		1.5	0.933	0.616
		2.0	0.977	0.851
		2.5	0.994	0.957
		3.0	0.999	0.991
9	560	1.0	0.841	0.211
		1.5	0.933	0.537
		2.0	0.977	0.813
		2.5	0.994	0.946
		3.0	0.999	0.988
w = number of adjacent traces in spatial window t = minimum number of positive samples within a window for rejecting H_0 H_0 = null hypothesis: a given window contains only noise width = (w-1) × 70 km, distance spanned by window z = (peak signal level) / (rms noise level) $\Phi(z)$ = cumulative probability for the standardized normal distribution $\beta(z)$ = probability of a type 2 error (probability of characterizing signal as noise) $1 - \beta(z)$ = power = probability, as defined in eqn. (2), of correctly identifying signal				

Table 2. The power calculation for the sign filter test.

Figure 34a. Procedure for computing the sign test statistic and applying the sign filter.

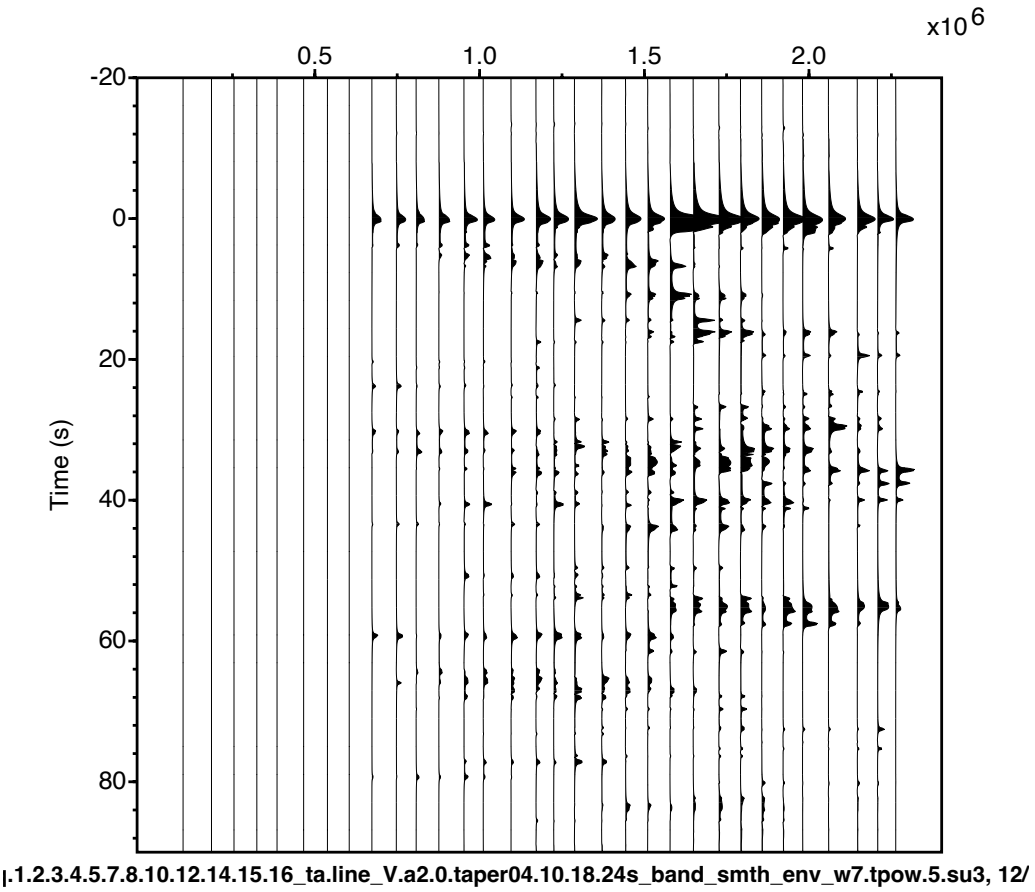


Figure 34b. Stacked section for Line V (α=2.0) after applying a sign filter (window length=7), computing the envelope function, and smoothing over a running average of 11 samples.

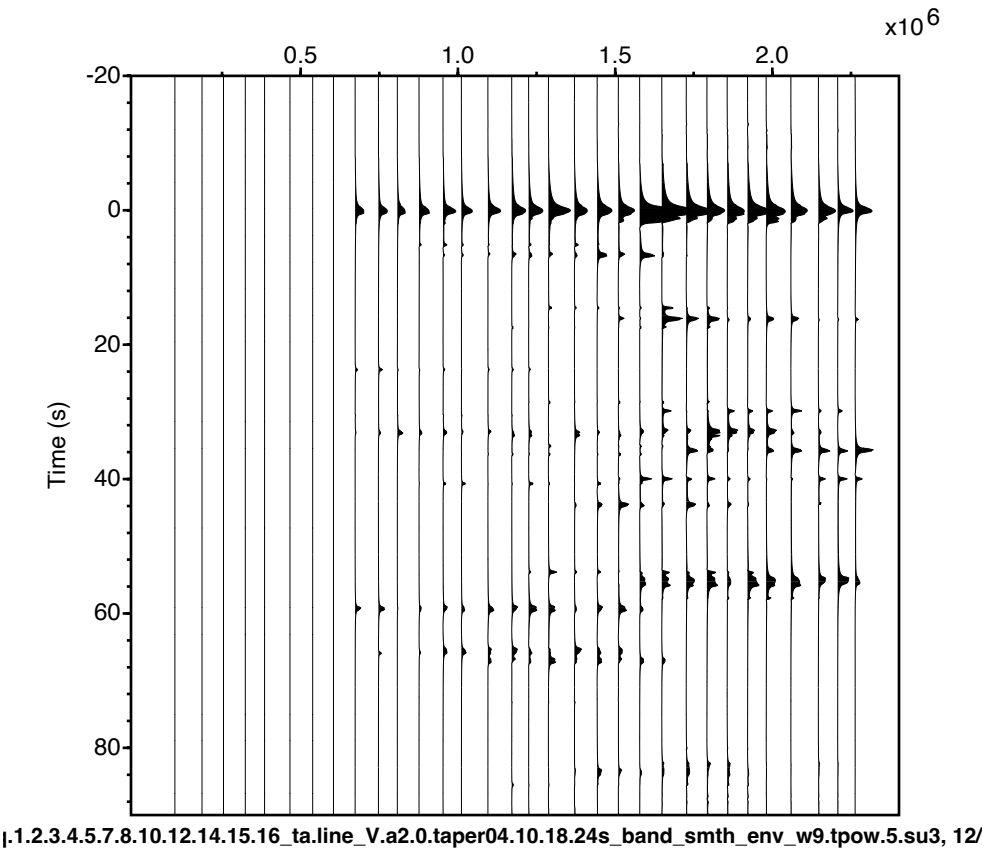


Figure 35. Stacked section for Line V (α=2.0) after applying a sign filter (window length=9), computing the envelope function, and smoothing over a running average of 11 samples.

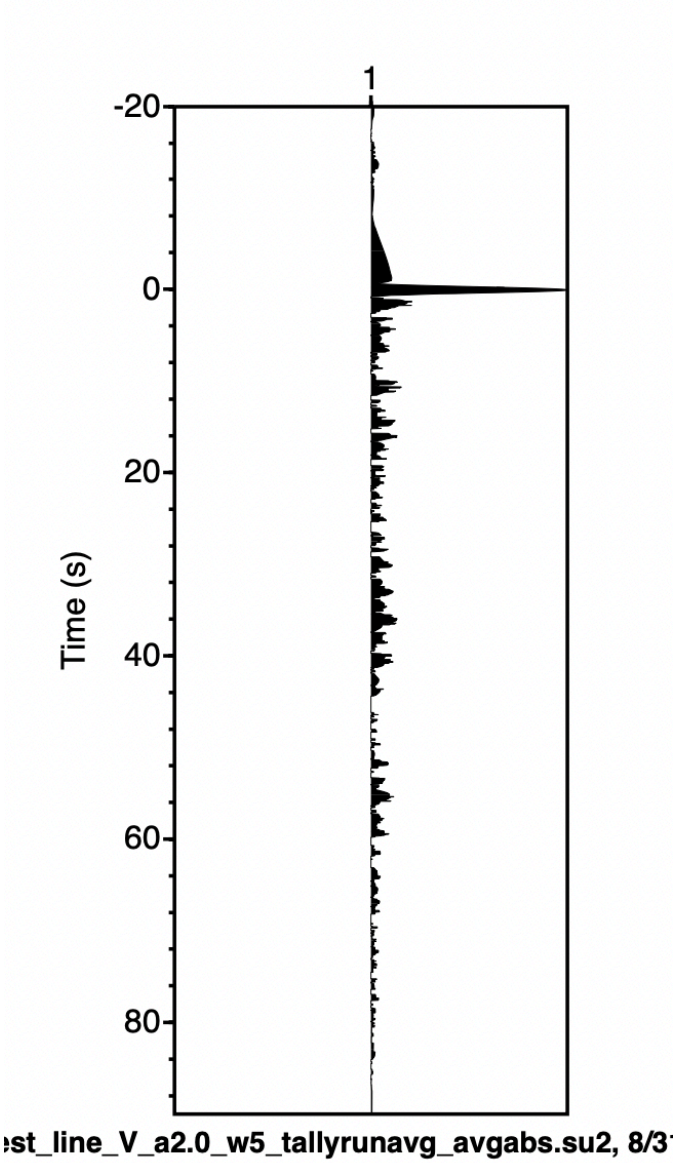


Figure 36. Stack (sum) of the absolute value of all traces in the sign filtered section for Line V (α=2.0) generated for a window length of 5.

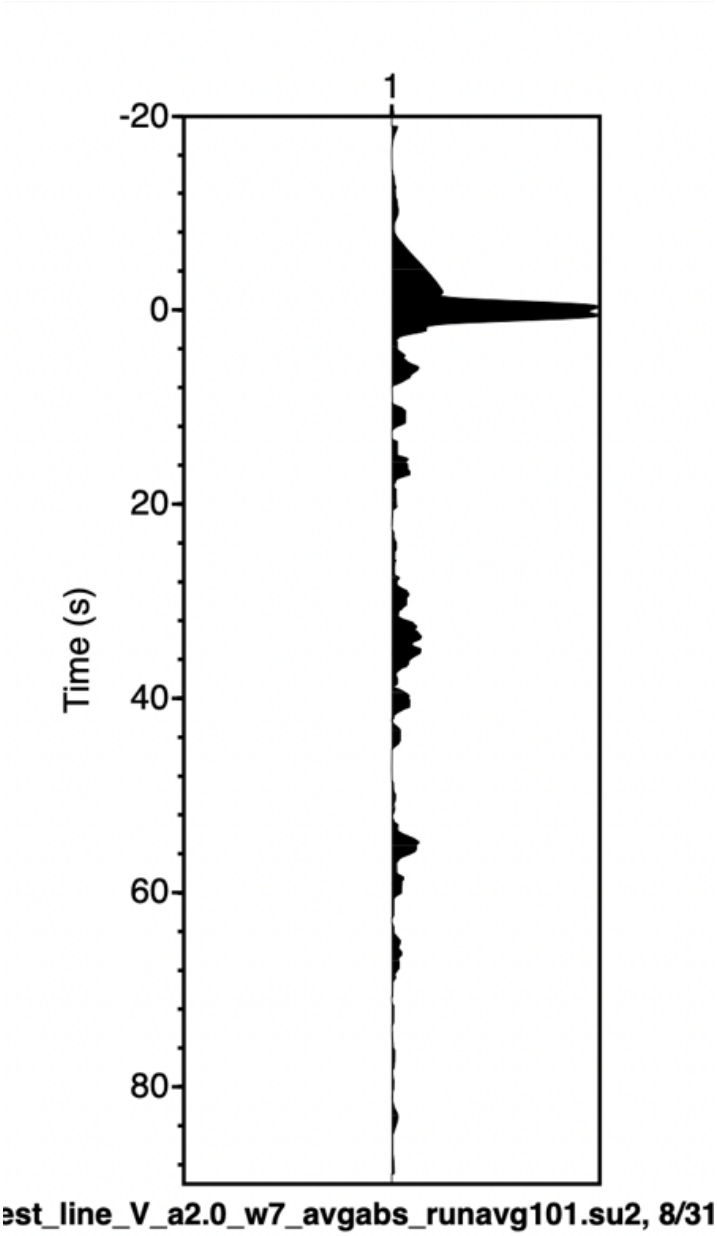


Figure 37. Stack (sum) of the absolute value of all traces in the sign filtered section for Line V (α=2.0) generated for a window length of 7.

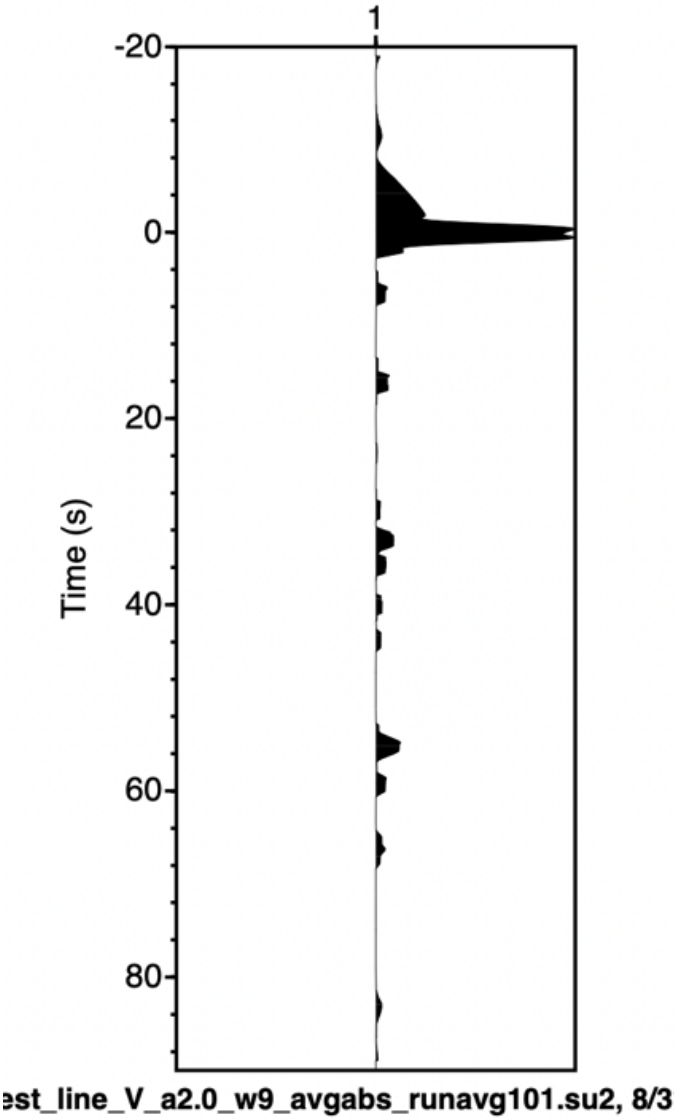


Figure 38. Stack (sum) of the absolute value of all traces in the sign filtered section for Line V (α=2.0) generated for a window length of 9.

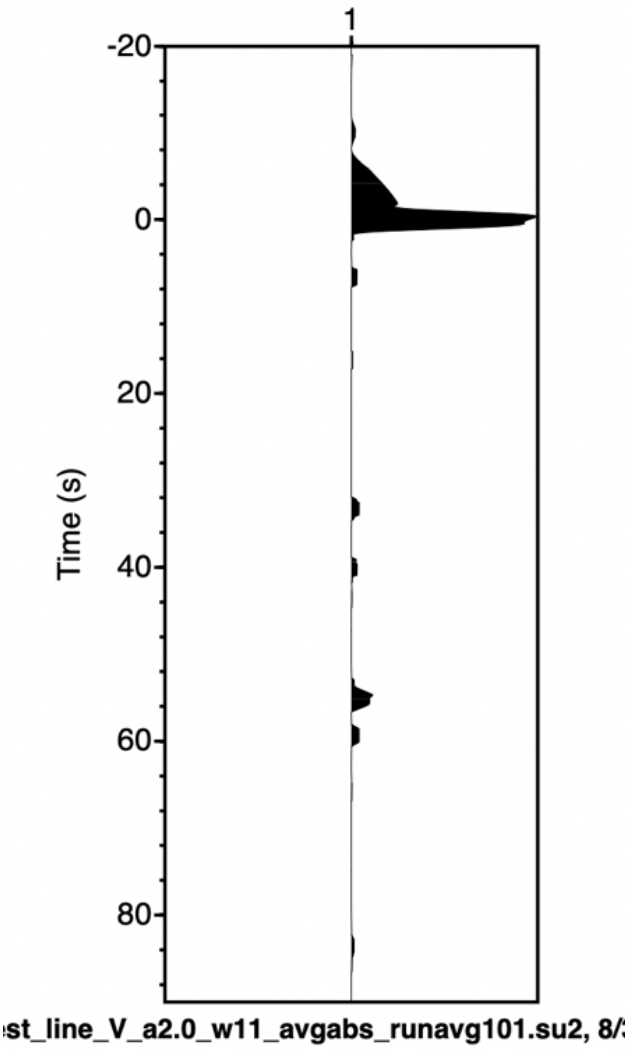


Figure 39. Stack (sum) of the absolute value of all traces in the sign filtered section for Line V (α=2.0) generated for a window length of 11.

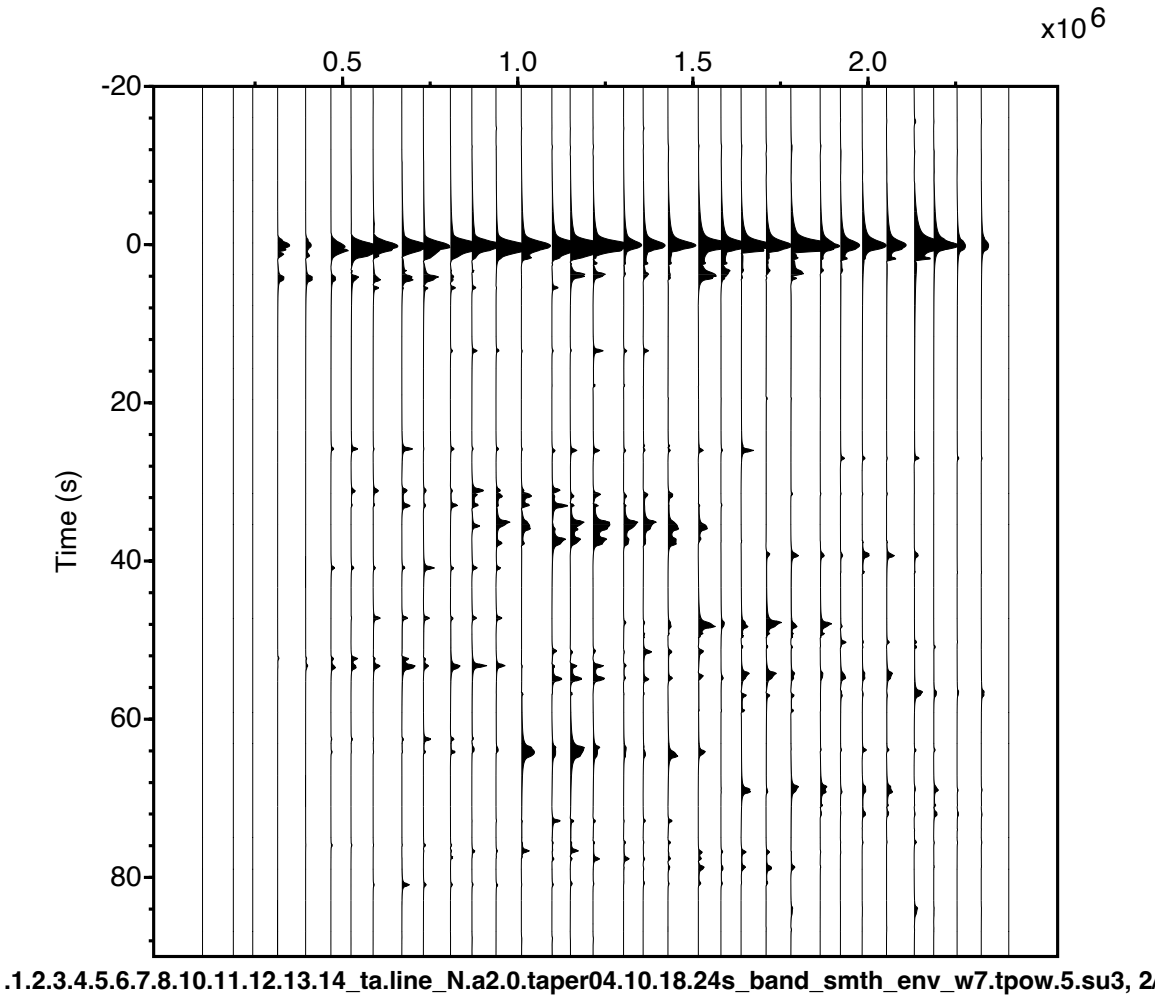


Figure 40. Stacked section for Line N (α=2.0) after applying a sign filter (window length=7), computing the envelope function, and smoothing over a running average of 11 samples. This particular plot highlights greater reflectivity below ~35 s TWT.

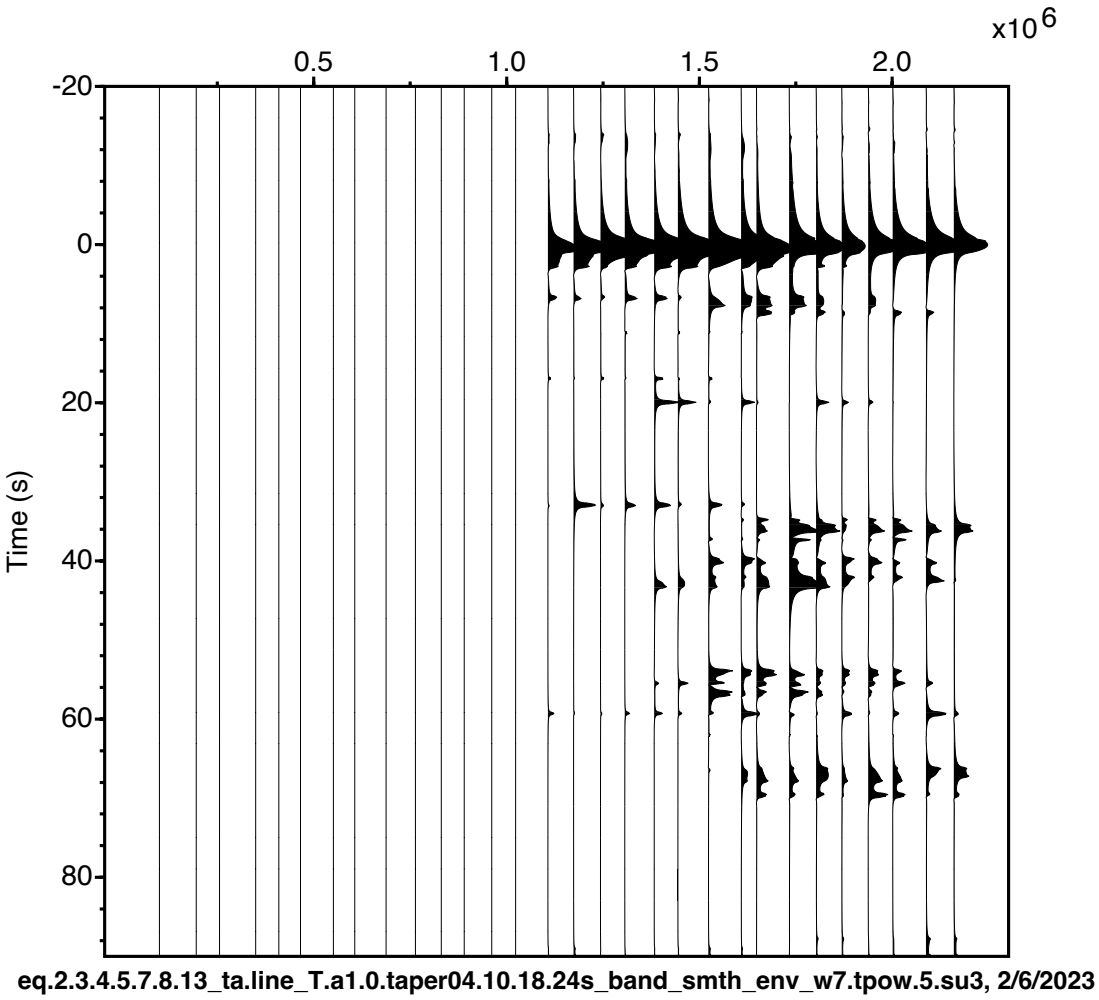


Figure 41. Stacked section for Line T (α=1.0) after applying a sign filter (window length=7), computing the envelope function, and smoothing over a running average of 11 samples. This particular plot highlights greater reflectivity below ~40 s TWT.

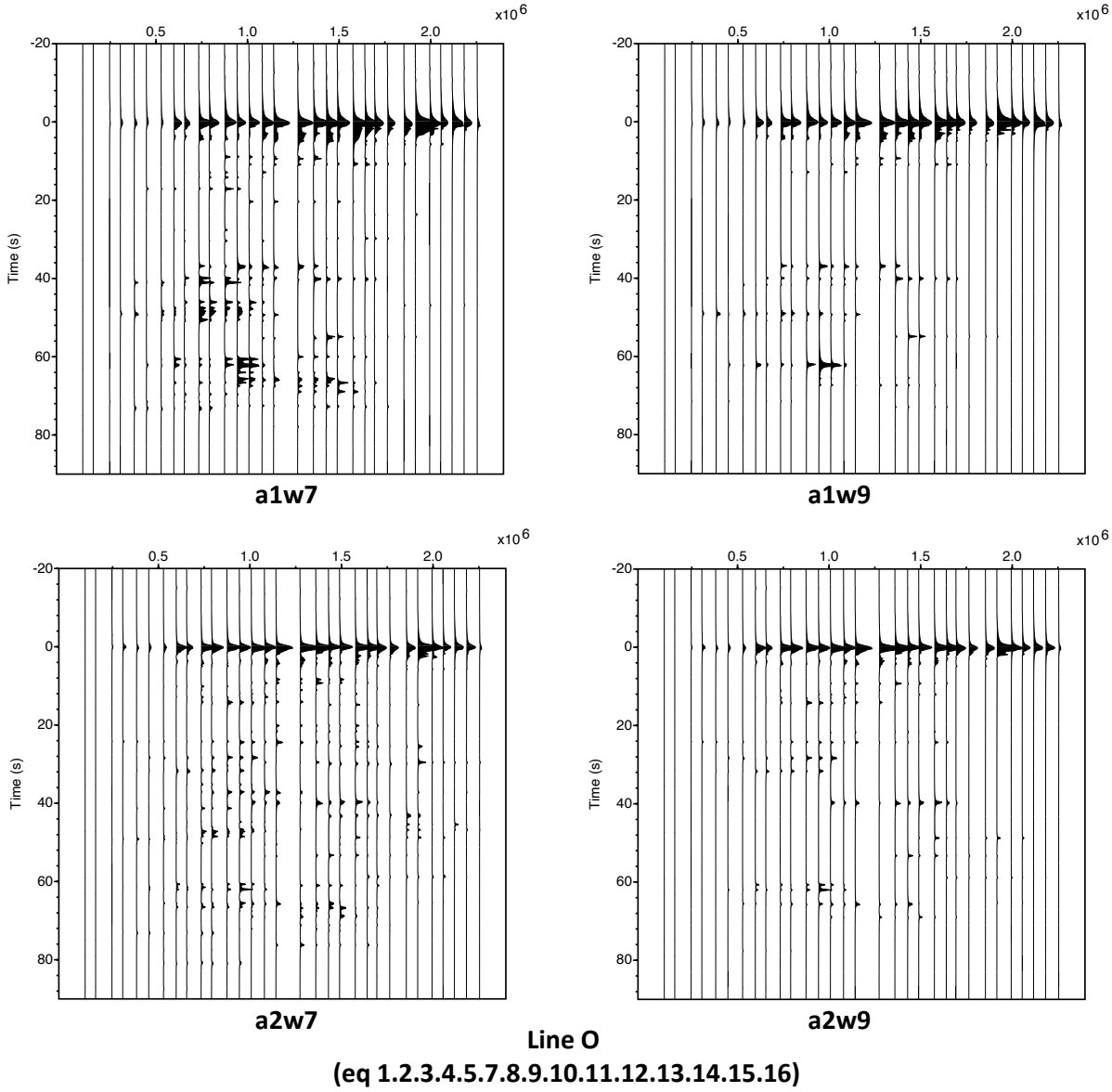


Figure 42. A composite of stacked sections for Line O (α=1.0 and 2.0) after applying a sign filter (window length=7 and 9), computing the envelope function, and smoothing over a running average of 11 samples. Increasing alpha sharpens signals; increasing window length decreases the number of reflection segments passed by the sign filter. Overall, the general increase in reflectivity below 40 s is preserved.

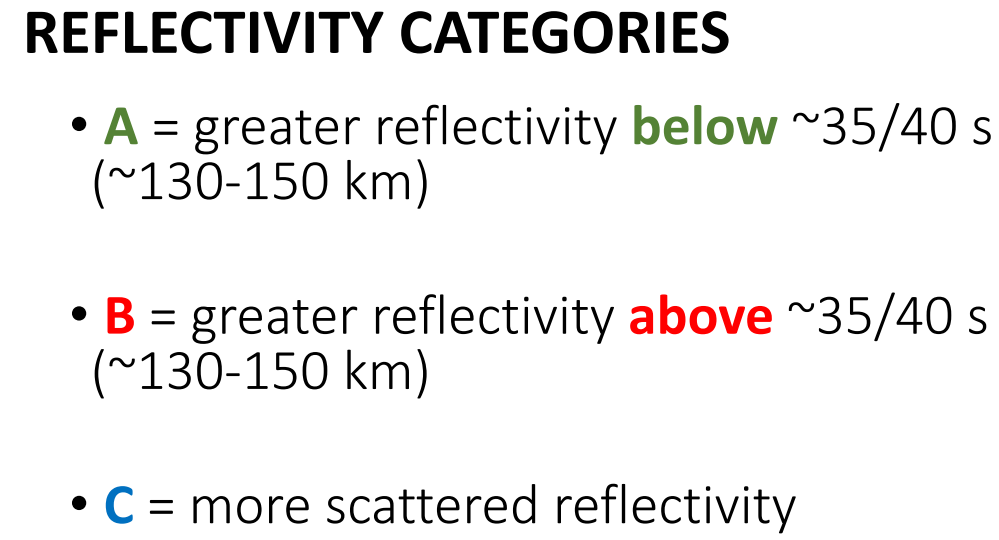


Figure 43. Categories describing the three main reflectivity patterns seen for signfiltered gathers.

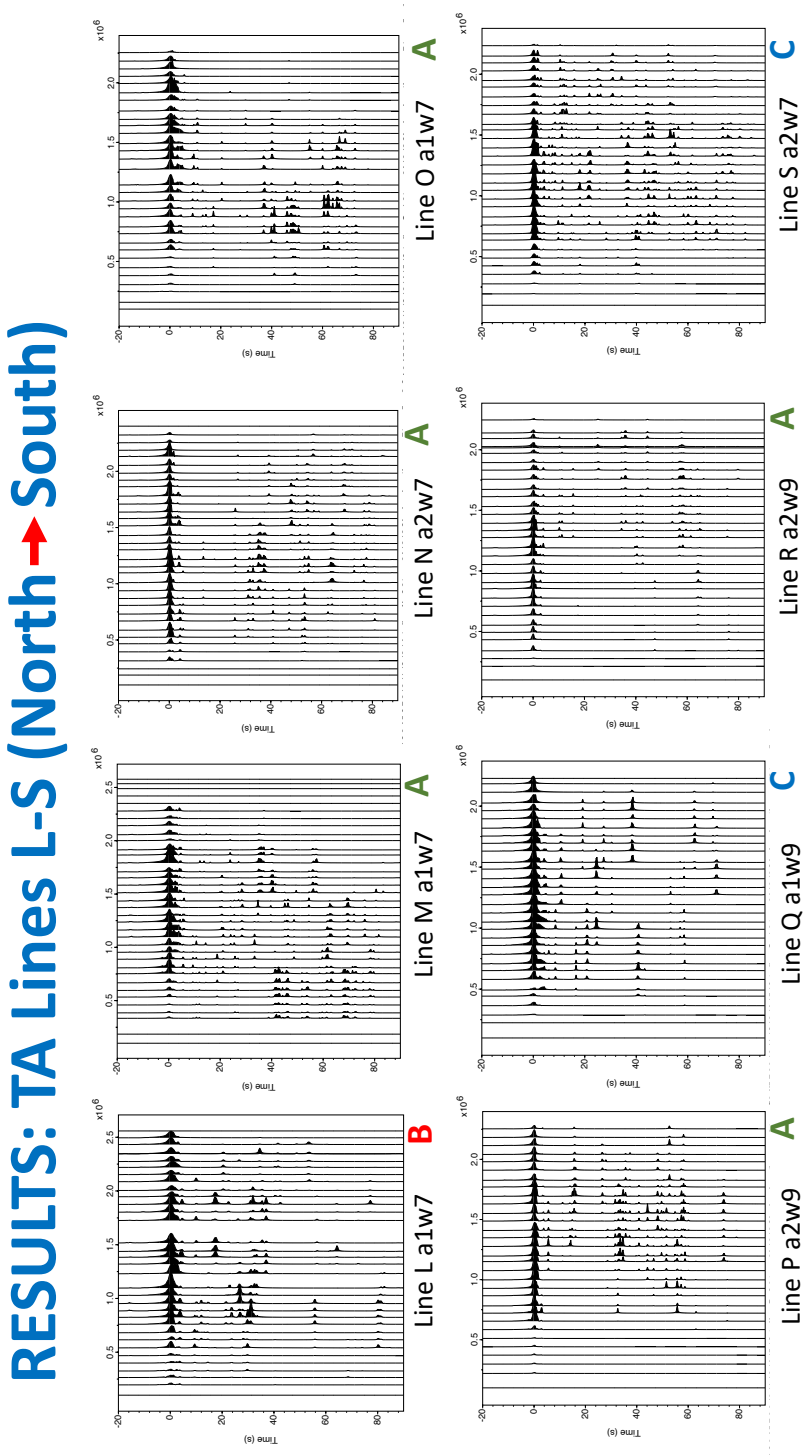


Figure 44a. Composite for Lines L-S showing sections processed as described in Figure 34b.

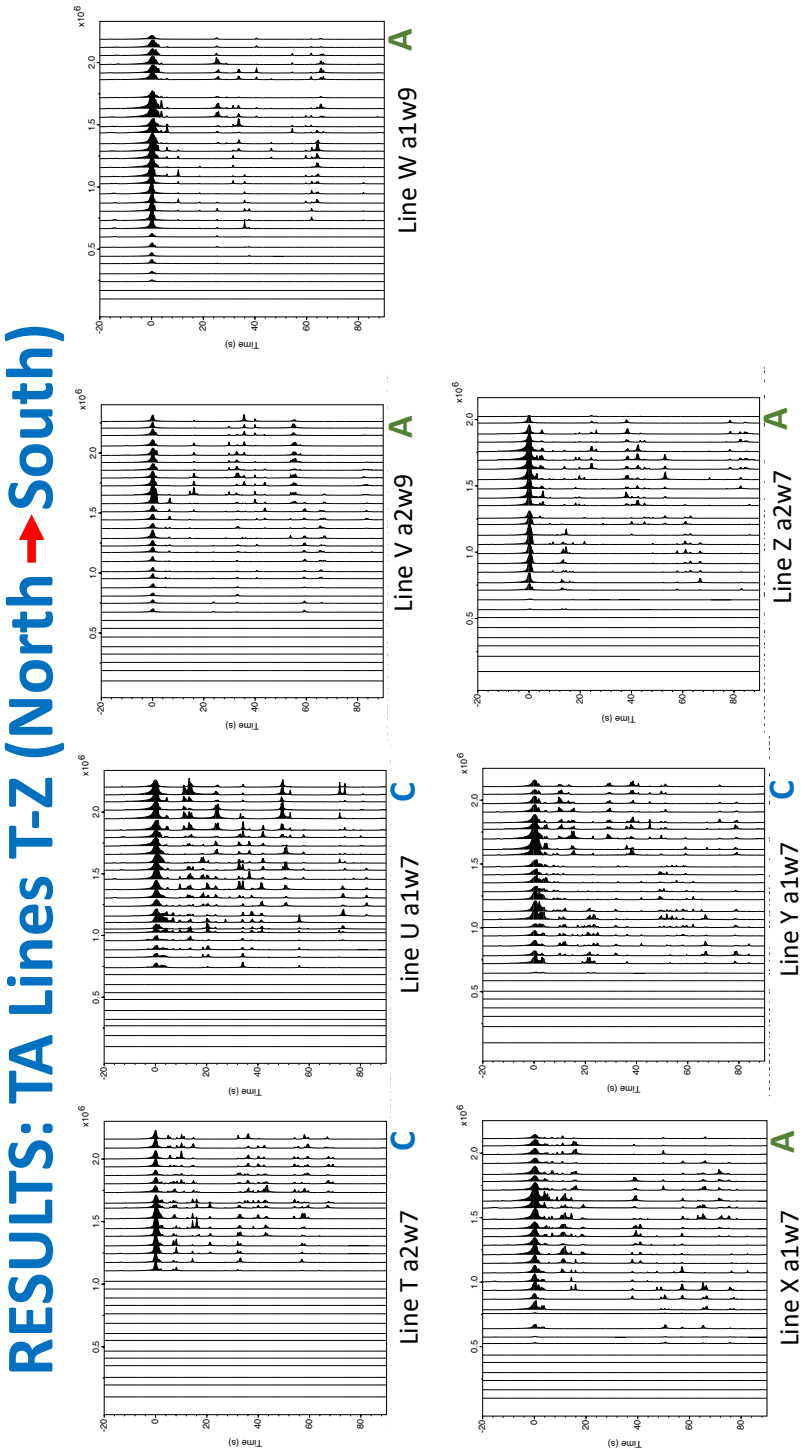


Figure 44b. Composite for Lines T-Z showing sections processed as described in Figure 34b.

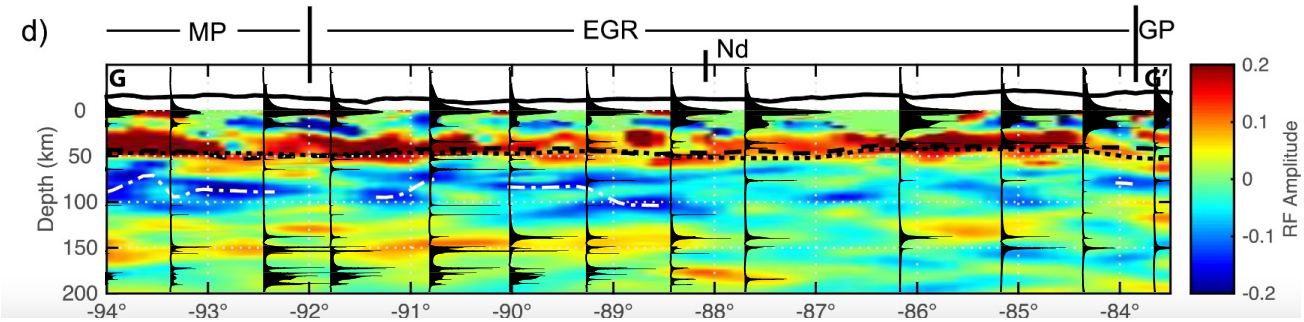


Figure 45. An a1w7 signfilter Line O (40.2°) plot from this study (black waveforms) superimposed on profile G-G' (40°) from Figure 8d (Chen et al., 2018) showing receiver function amplitudes.

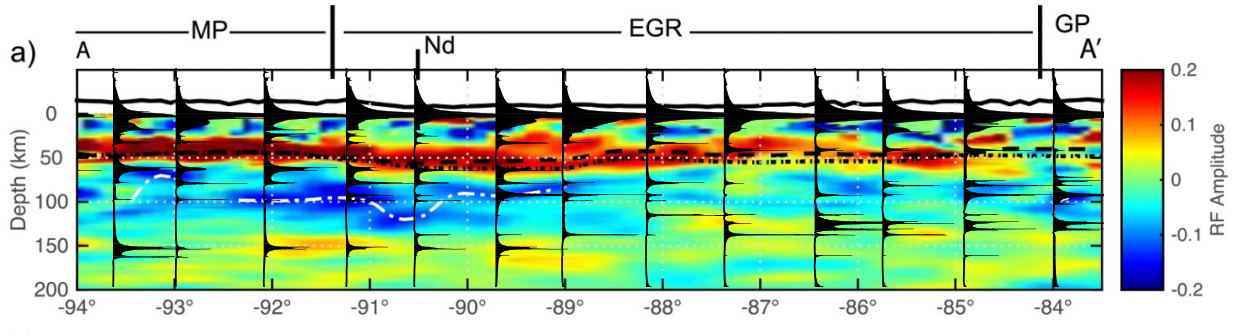


Figure 46. An a1w7 Line Q (39°) signfilter plot from this study (black waveforms) superimposed on the receiver function profile A-A' (38.7°) from Figure 4a (Chen et al., 2018).

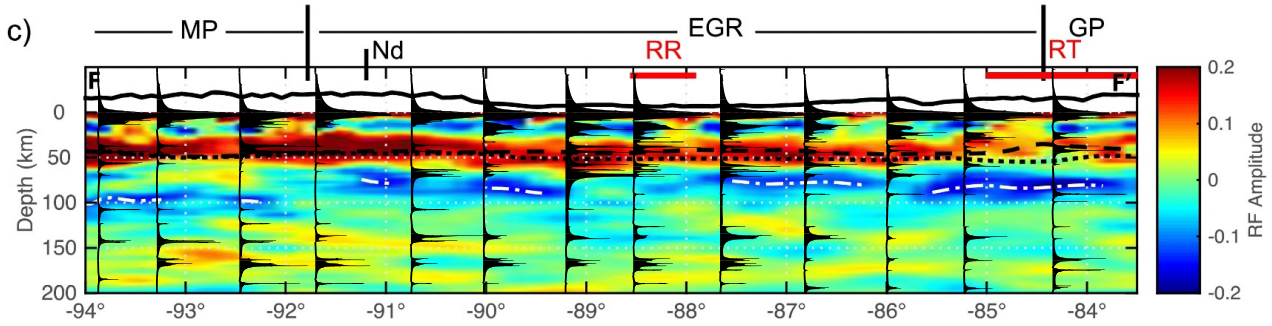


Figure 47. An a1w7 Line S (37.7°) signfilter plot from this study (black waveforms) superimposed on the receiver function profile F-F' (37.7°) from Figure 8c (Chen et al., 2018).

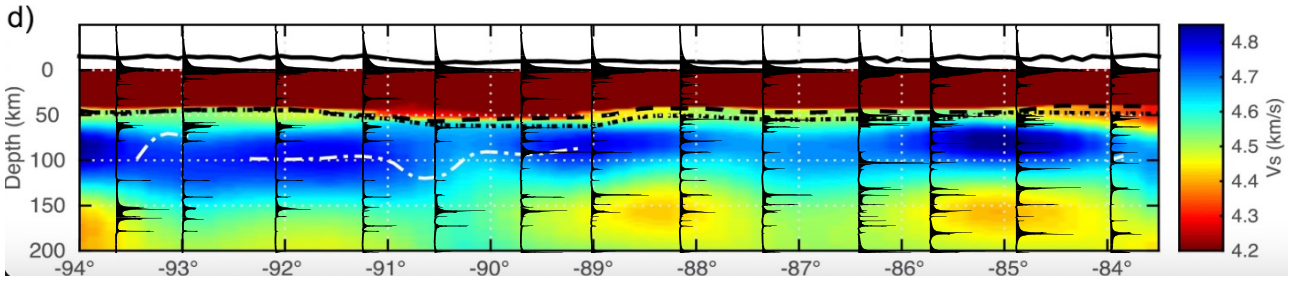


Figure 48. An a2w7 Line Q (39°) signfilter plot from this study (black waveforms) superimposed on the shear wave velocity profile A-A' (38.7°) from Figure 4d (Chen et al., 2018).

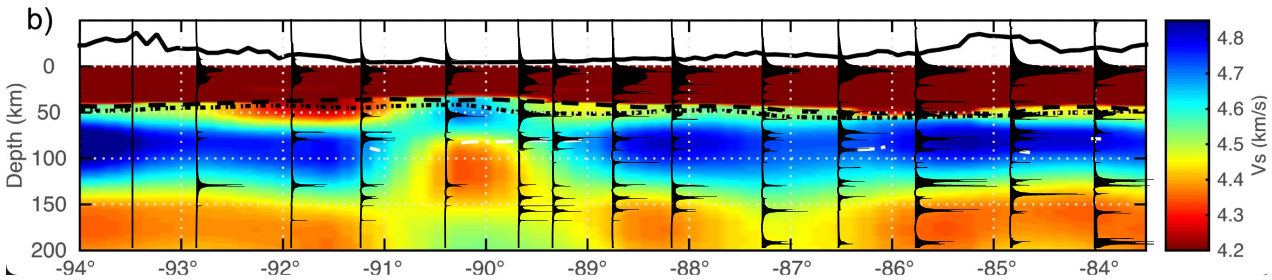


Figure 49. An a1w7 Line U (36.4°) signfilter plot from this study (black waveforms) superimposed on the shear wave velocity profile C-C' (36°) from Figure 7b (Chen et al., 2018).

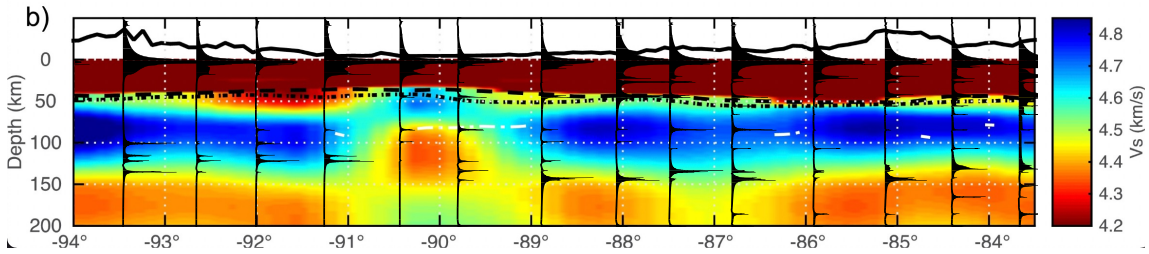


Figure 50. An a1w7 Line V (35.8°) signfilter plot from this study (black waveforms) superimposed on the shear wave velocity profile C-C' (36°) from Figure 7b (Chen et al., 2018).

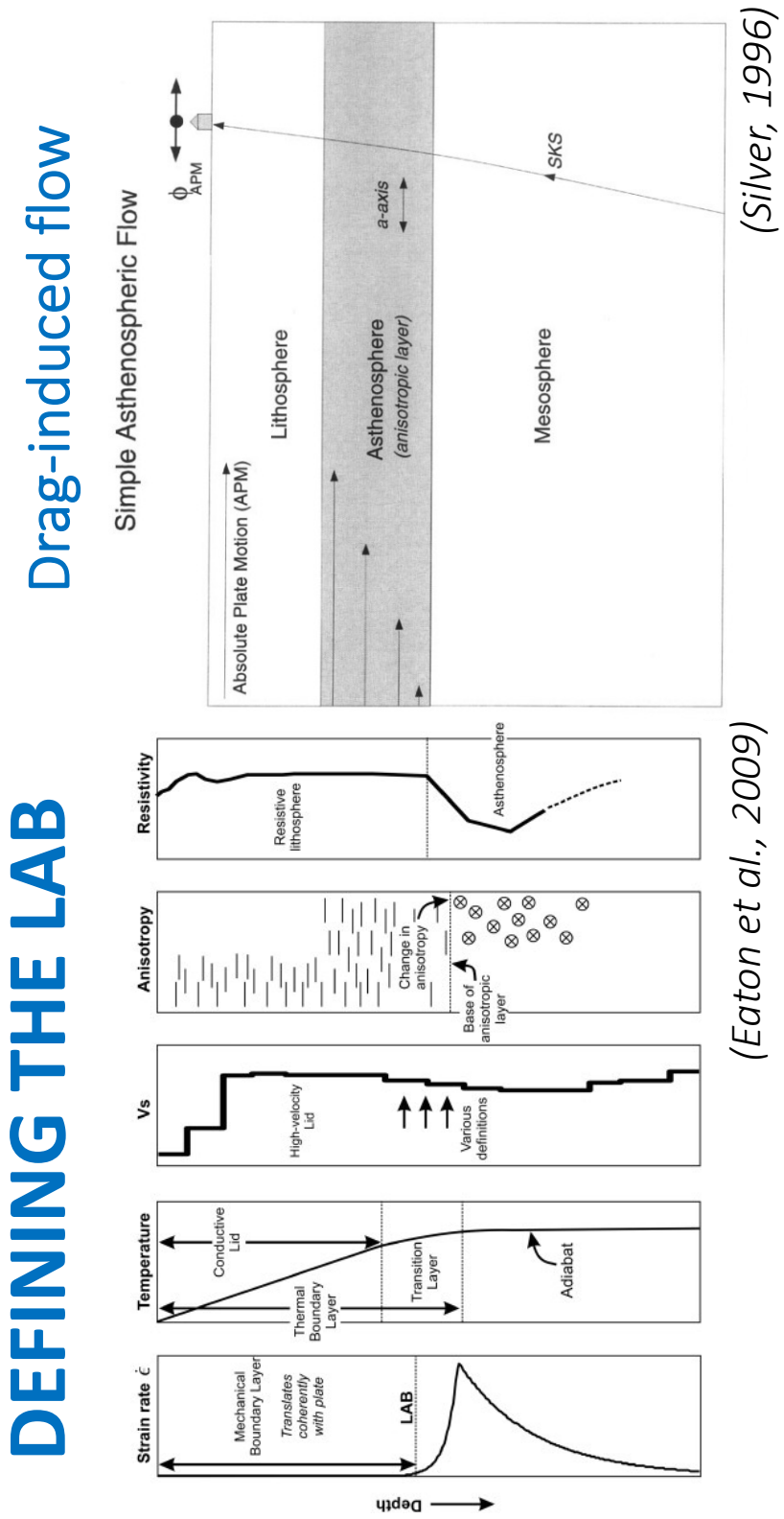


Figure 51. Summary of models for the LAB (Silver, 1996; Eaton et al., 2009).

Figure 52. Models for drag-induced flow in the asthenosphere (Wang & Becker, 2019; Garel & Thoraval, 2021).

CHAPTER FOUR

CONCLUSIONS

The key objective of this study was to test a new criterion and protocol for identifying the lithosphere-asthenosphere transition. Reflections identified objectively using the sign test statistic were used to establish a new criterion for mapping the base of the lithosphere based on P-wave reflectivity. Comparison with models of shear-wave velocities derived by inversion of surface waves (Chen et al., 2018) shows that the observed onset of increased horizontal reflectivity closely matches the depth corresponding to the maximum negative velocity gradient, suggesting that P-wave reflectivity can be used as an independent method for constraining thickness of the lithosphere. Moreover, the onset of increased horizontal reflectivity not only closely matches the depth corresponding to the maximum negative velocity gradient, but also provides information about fabric within the asthenosphere that the lower frequencies of surface waves cannot resolve. The observed, generally abrupt, downward increase in horizontal reflectivity is consistent with the pattern expected for drag-induced flow in the asthenosphere.

Signals identified as reflections from the Moho are also prominent in most of the profiles. These results show a correlation between crustal thickness and elevation. Moho reflections at 10-11 s in the east increase in TWT to 14-18 s under highest elevations and then decrease for a short distance (based on previous work with shorter arrays) before leveling off or deepening further westward. This noticeable thickening of the crust

beneath the highest elevations provides at least part of the support for mountain topography. The correlation of a broad regional Bouguer gravity low with high elevations in the Southern Appalachians supports this interpretation. Additional support of topography may come from lateral variations in density within the upper mantle. In addition to isostatic uplift fed by the substantial crustal root, changes in buoyancy due to convection and other processes in the upper mantle may also play a role in maintaining high relief in the Appalachians. The effect of isostatic uplift may be enhanced by variations in erosion rates with greater rates reported for drainage basins as opposed to mountain summits. Although the correlation of elevation with gravity and Moho depth is consistent with the idea that support for mountain topography is provided by variations in crustal thickness, it does not rule out the possibility that variations in thickness and composition of the lithosphere may also play a role.

Clear reflections from the base of poorly consolidated sediments beneath the Atlantic Coastal Plain and the Mississippi Embayment demonstrate the resolving power that can be achieved using earthquakes as virtual seismic sources.

REFERENCES

Abt, D. L., Fischer, K. M., French, S. W., Ford, H. A., Yuan, H., & Romanowicz, B. (2010). North American lithosphere discontinuity structure imaged by Ps and Sp receiver functions. *Journal of Geophysical Research*. 115, B09301. https://doi.org/10.1029/2009JB006914

Biryol, C.B., Wagner, L.S., Fischer, K.M., & Hawman, R.B. (2016). Relationship between observed upper mantle structures and recent tectonic activity across the Southeastern United States. *Journal of Geophysical Research: Solid Earth*. 121(5), 3393-3414. https://doi.org/10.1002/2015JB012698

Bracewell, R.N. (1978). The Fourier Transform and its Applications. McGraw-Hill, NY, 444 pages.

Braile, L.W. & Chiang, C. S. (1986). The continental Mohorovičić discontinuity results from near-vertical and wide-angle seismic reflection studies. *Reflection Seismology: A Global Perspective, Geodynamic Series*. 13, 257-272. https://doi.org/10.1029/GD013p0257

Buehler, J. S. & Shearer, P. M. (2017). Uppermost mantle seismic velocity structure beneath USArray. *Journal of Geophysical Research: Solid Earth*. 122, 436–448. https://doi.org/10.1002/2016JB013265

Calo, M., Bodin, T. & Romanowicz, B. (2016). Layered structure in the upper mantle across North America from joint inversion of long and short period seismic data. *Earth and Planetary Science Letters.* 449, 164–175. https://doi.org/10.1016/j.epsl.2016.05.054

Chen, C., Gilbert, H., Fischer, K.M., Andronicos, C.L., Pavlis, G.L., Hamburger, M.W., Marshak, S., Larson, T., & Yang, X. (2018). Lithospheric discontinuities beneath the U.S. Midcontinent – signatures of Proterozoic terrane accretion and failed rifting. *Earth and Planetary Science Letters*. 481, 223-235. https://doi.org/10.1016/j.epsl.2017.10.033

Cook, F. A. & Vasudevan, K. (2006). Reprocessing and enhanced interpretation of the initial COCORP southern Appalachian traverse. *Tectonophysics*. 420(1–2), 161–174. https://doi.org/10.1016/j.tecto.2006.01.022

Cooke, W. (1943). Geology of the Coastal Plain of Georgia. *USGS Numbered Series Report.* 941, 1-119. DOI: 10.3133/b941

Cox, R.T. and Van Arsdale, R.B. (2002). The Mississippi Embayment, North America: a first order continental structure generated by the Cretaceous superplume mantle event. *Journal of Geodynamics*. 34 (2), 163-176. https://doi.org/10.1016/S0264-3707(02)00019-4

Cushing, E.M., Boswell, E.H., & Hosman, R.L. (1964). General Geology of the Mississippi Embayment. *Geological Survey Professional Paper*. 448-B, 1-25.

Danielson, J.J. & Gesch, D.B. (2011). World Elevation GMTED. Global multi-resolution terrain elevation data 2010 (GMTED2010): U.S. Geological Survey Open-File Report 2011–1073, 26.

Duff, P. D. & Kellogg, J. N. (2017). Reinterpretation of ADCOH and COCORP seismic reflection data with constraints from detailed forward modeling of potential field data—Implications for Laurentia-Peri-Gondwana suture. *Tectonophysics*. 712–713, 426–437. https://doi.org/10.1016/j.tecto.2017.06.002

Eaton, D.W., Darbyshire, F., Evans, R.L., Grütter, H., Jones, A.G., & Yuan, X. (2009). The elusive lithosphere-asthenosphere boundary (LAB) beneath cratons. *Lithos.* 109(1-2), 1-22. https://doi.org/10.1016/j.lithos.2008.05.009

England, P. & Molnar, P. (1990). Surface uplift, uplift of rocks, and exhumation of rocks. *Geology.* 18(12), 1173-1177. https://doi.org/10.1130/0091-7613(1990)018<1173:SUUORA>2.3.CO;2

Fenneman, N.M., and Johnson, D.W. (1946). Physiographic divisions of the conterminous U.S. USGS.

French, S. W., Fischer, K. M., Syracuse, E. M., & Wysession, M. E. (2009). Crustal structure beneath the Florida-to-Edmonton broadband seismometer array. *Geophysical Research Letters*. 36, L08309. https://doi.org/10.1029/2008GL036331

Fischer, K. (2002). Waning buoyancy in the crustal roots of old mountains. *Nature*. 417, 933-936. https://doi.org/10.1038/nature00855

Fischer, K.M., Ford, H.A., Abt, D.L., & Rychert, C.A. (2010). The Lithosphere-Asthenosphere Boundary. *Annual Review of Earth and Planetary Sciences*. 38, 551-575. doi: 10.1146/annurev-earth-040809-152438

Fischer, K.M., Rychert, C.A., Dalton, C.A., Miller, M.S., Beghein, C., & Schutt, D.L. (2020). A comparison of oceanic and continental mantle. *Physics of the Earth and Planetary Interiors*. 309, 106600. https://doi.org/10.1016/j.pepi.2020.106600

Garel, F. & Thoraval, C. (2021). Lithosphere as a constant-velocity plate: Chasing a dynamical LAB in a homogeneous mantle material. *Physics of the Earth and Planetary Interiors*. 316. https://doi.org/10.1016/j.pepi.2021.106710

Gao, H. & Li, Cong. (2021). Lithospheric Formation and Evolution of Eastern North American Continent. *Geophysical Research Letters*. 48, e2020GL091074. https://doi.org/10.1029/2020GL091074

Hanawalt, L.E., Cuilik, M.P., Hufstetler, B.S., & Hawman, R.B. (2021). Structure of the Lithosphere across the Appalachian Orogen: Reflection Profiling using Earthquakes (abs.) *Southeastern Section of the Geological Society of America, 70th Annual Meeting.* Auburn, AL, April 1-2.

Hanawalt, L.E., Cuilik, M.P., & Hawman, R.B (2022). Mountain Roots, Lithospheric Layering, and Mantle Flow: Imaging P-wave Reflectivity beneath the eastern U.S. (abs.) *Southeastern Section of the Geological Society of America, 71st Annual Meeting.* Cincinnati, OH, April 7-8.

Hancock, G. and Kirwan, M. Summit erosion rates deduced from 10Be: Implications for relief production in the central Appalachians. *Geology*. 35(1), 89-92. https://doi.org/10.1130/G23147A.1

Hansen, K.M., Roy-Chowdhury, K., & Phinney, R.A. (1988). The sign filter for seismic event detection. *Geophysics*. 53, 1024-1033. https://doi.org/10.1190/1.1442539

Hatcher, R. D., Jr. (1989). The Geology of North America, The Appalachian-Ouachita Orogen in the United States. *The Geological Society of America. F-2*. DOI:10.1130/DNAG-GNA-F2.511

Hao, Y., McIntosh, K., & Magnani, M.B. (2015). Long-lived deformation in the southern Mississippi Embayment revealed by high-resolution seismic reflection and sub-bottom profiler data. *Tectonics*. 34(3), 555-570. https://doi.org/10.1002/2014TC003750

Hawman R.B. (2008). Crustal thickness variations across the Blue Ridge Mountains, Southern Appalachians: An alternative procedure for migrating wide-angle reflection data: Bulletin of the Seismological Society of America, v. 98, p. 469–475, doi:10.1785/0120070027.

Hawman, R. B., Khalifa, M. O., & Baker, M. S. (2012). Isostatic compensation for a portion of the southern Appalachians: Evidence from a reconnaissance study using wide-angle, three-component seismic soundings. *Geological Society of America Bulletin.* 124(3–4), 291–317. https://doi.org/10.1130/B30464.1

Jarchow, C. & Thompson, G. (1989). The Nature of the Mohorovičić Discontinuity. *Annual Review of Earth and Planetary Sciences.* 17. 475-506. DOI: 10.1146/annurev.ea.17.050189.002355

Karato, S., Olugboji, T., & Park, J. (2015). Mechanisms and geologic significance of the mid-lithospheric discontinuity in the continents. *Nature Geoscience*. 8, 509-514. https://doi.org/10.1038/ngeo2462

Kennett, B. L. N. (2015). Lithosphere-asthenosphere P-wave reflectivity across Australia. *Earth and Planetary Science*. 431, 225-235. http://dx.doi.org/10.1016/j.epsl.2015.09.039

Kennett, B.L.N., Yoshizawa, K., & Furumura, T. (2017). Interactions of multi-scale heterogeneity in the lithosphere: Australia. *Tectonophysics*. 717, 193-213. http://dx.doi.org/10.1016/j.tecto.2017.07.009

Lamb, S., Moore, J.D.P., Perez-Gussinye, M., & Stern, T. (2020). Global Whole Lithosphere Isostasy: Implications for Surface Elevations, Structure, Strength, and Densities of the

Continental Lithosphere. *Geochemistry, Geophysics, Geosystems*. 21. https://doi.org/10.1029/2020GC009150

Langston, C. A. (1979). Structure under Mount Ranier, Washington, inferred from teleseismic body waves. *Journal of Geophysical Research*. 84(B9), 4749–4762. https://doi.org/10.1029/JB084iB09p04749

Langston, C. A. & Hammer, J. K. (2001). The vertical component *P*-wave receiver function. *Bulletin of the Seismological Society of America*. 91(6), 1805–1819. https://doi.org/10.1785/0120000225

Lehmann, E.L. (1975). Nonparametrics: Statistic Methods Based on Ranks. Holden-Day, Inc. San Francisco

Long, M. D., Jackson, K. G., & McNamara, J. F. (2016). SKS splitting beneath Transportable Array stations in eastern North America and the signature of past lithospheric deformation. *Geochemistry, Geophysics, Geosystems*. 17, 2–15. https://doi.org/10.1002/2015GC006088

Long, M.D., Wagner, L.S., King, S.D., Evans, R.L., Mazza, S.E., Byrnes, J.S., Johnson, E.A., Kirby, E., Bezada, M.J., Gazel, E., Miller, S.R., Aragon, J.C., and Liu, S. (2021). Evaluating models for lithospheric loss and intraplate volcanism beneath the Central Appalachian Mountains. Journal of Geophysical Research: Solid Earth. 126. https://doi.org/10.1029/2021JB022571

Ma, C., Bergeron, P., Foster, D.A., Dutrow, B.L., Mueller, P.A., and Allen, C. (2016) Detrital-zircon geochronology of the Sawtooth metamorphic complex, Idaho: Evidence for metamorphosed lower Paleozoic shelf strata within the Idaho batholith. *Geosphere*. 12 (4), 1136–1153, doi:10.1130/GES01201.1.

MacDougall, J.G., Fischer, K.M., Forsyth, D.W., Hawman, R.B., and Wagner, L.S. (2015). Shallow mantle velocities beneath the southern Appalachians from Pn phases. *Geophysical Research Letters*. 42, 339-345. Doi:10.1002/2014GL062714

Manicini, E.A., Puckett, T.M., and Tew, B.H. (1996). Integrated biostratigraphic and sequence stratigraphic framework for Upper Cretaceous strata of the eastern Gulf Coastal Plain, USA. *Cretaceous Research*. 17(6), 645-669. https://doi.org/10.1006/cres.1996.0035

McBride, J.H. & Nelson, K.D. (1991). Deep Seismic Reflection Constraints on Palaeozoic Crustal Structure and Definition of the Moho in the Buried Southern Appalachian Orogen. *Continental Lithosphere: Deep Seismic Reflections.* DOI:10.1029/GD022P0009

McKeon, R.E., Zeitler, P.K., Pazzaglia, F.J., Idleman, B.D., Enkelmann, E. (2014). Decay of an old orogen: inferences about Appalachian landscape evolution from low-temperature thermochronology. *Geological Society of American Bulletin.* 126, 31-46. https://doi.org/10.1130/B30808.1

Molnar, P. (2004). Late Cenozoic increase in accumulation rates of terrestrial sediment: How might climate change have affected erosion rates? *Annual Review of Earth and Planetary Sciences*. 32, 67-89. doi: 10.1146/annurev.earth.32.091003.143456

Morgan, J.W. (1983). Hotspot tracks and the early rifting of the Atlantic. *Tectonophysics*. 94 (1-4), 123- 139. https://doi.org/10.1016/0040-1951(83)90013-6

Nyamwandha, C.A., Powell, C.A., & Langston, C.A. (2016). A joint local and teleseismic tomography study of the Mississippi Embayment and New Madrid Seismic Zone. J*ournal of Geophysical Research: Solid Earth.* 121(5), 3570-3585. https://doi.org/10.1002/2015JB012761

Parker, E. H. Jr., Hawman, R. B., Fischer, K. M., & Wagner, L. S. (2013). Crustal evolution across the southern Appalachians: Initial results from the SESAME broadband array. *Geophysical Research Letters*. 40, 3853–3857. https://doi.org/10.1002/grl.50761

Parker, E. H. Jr., Hawman, R. B., Fischer, K. M., & Wagner, L. S. (2016). Estimating crustal thickness using SsPmp in regions covered by low-velocity sediments: Imaging the Moho beneath the Southeastern Suture of the Appalachian Margin Experiment (SESAME) array, SE Atlantic coastal plain. *Geophysical Research Letters*. 43, 9627–9635. https://doi.org/10.1002/2016GL070103

Portenga, E.W., Bierman, P.R., Rizzo, D.M., and Rood, D.H. (2013). Low rates of bedrock outcrop erosion in the central Appalachian Mountains inferred from in situ 10Be. *Geological Society of American Bulletin*. 125, 201-215. doi: 10.1130/B30559.1

Porter, R. & Reid, M. (2021). Mapping the Thermal Lithosphere and Melting Across the Continental US. *Geophysical Research Letters*. 48, e2020GL092197. https://doi.org/10.1029/2020GL092197

Rice, T.A. (2019) The resilience of Appalachian topography: A geophysical analysis of the root structure of the southern Appalachians. CURO Symposium, University of Georgia. April 8, 2019.

Ruigrok, E. & Wapenaar, K. (2012). Global-phase seismic interferometry unveils *P*-wave reflectivity below the Himalayas and Tibet. *Geophysical Research Letters*. 39, L11303. https://doi.org/10.1029/2012GL051672

Rychert, C.A., Harmon, N., Constable, S., & Wang, S. (2020). The Nature of the Lithosphere-Asthenosphere Boundary. *Journal of Geophysical Research*. 125(10). https://doi.org/10.1029/2018JB016463

Savage, B., Covellone, B. M., & Shen, Y. (2017). Wave speed structure of the eastern North American margin. *Earth and Planetary Science Letters*. 459, 394–405. https://doi.org/10.1016/j.epsl.2016.11.028

Schmandt, B. & Lin, F. (2014). P and S wave tomography of the mantle beneath the United States. *Geophysical Research Letters*. 41(18), 6342-6349. https://doi.org/10.1002/2014GL061231

Schmandt, B., Lin, F.C., and Karlstrom, K.E. (2015). Distinct crustal isostasy trends east and west of the Rocky Mountain Front. Geophysical Research Letters, 42 (23): 10290-10298. https://doi.org/10.1002/2015GL066593

Shearer, P.M. (2019). Introduction to Seismology. Cambridge University Press: 3rd Edition.

Selway, K., Ford, H., & Keleman, P. (2015). The seismic mid-lithosphere discontinuity. *Earth and Planetary Science Letters.* 414, 45-57. https://doi.org/10.1016/j.epsl.2014.12.029

Spotila, J.A., & Prince, P.S. (2022). Geomorphic complexity and the case for topographic rejuvenation of the Appalachian Mountains. *Geomorphology*. 417. https://doi.org/10.1016/j.geomorph.2022.108449

USGS. North America basement rocks. https://instruct.uwo.ca/earth-sci/300b-001/14strprv.gif

Verellen, D. N., Alberts, E. C., Larramendi, G. A., Parker, E. H., & Hawman, R. B. (2020). *P*-wave reflectivity of the crust and upper mantle beneath the southern Appalachians and Atlantic coastal plain using global phases. *Geophysical Research Letters*. 47, https://doi.org/10.1029/2020GL089648

Wagner, L.S., Fischer, K.M., Hawman, R., Hopper, E., & Howell, D. (2018). The relative roles of inheritance and long-term passive margin lithospheric evolution on the modern

structure and tectonic activity in the southeastern United States. *Geosphere*. 14(4), 1385-1410. https://doi.org/10.1130/GES01593.1

Wirth, E.A. & Long, M.D. (2014). A contrast in anisotropy across mid-lithospheric discontinuities beneath the central United States- A relic of craton formation. *Geology*. 42(10), 851-854. https://doi.org/10.1130/G35804.1

Yang, B.B., Liu, Y., Dahm, H., Liu, K.H., & Gao, S.S. (2017). Seismic azimuthal anisotropy beneath the eastern United States and its geodynamic implications. *Geophysical Research Letters*. 44(6), 2670-2678. https://doi.org/10.1002/2016GL071227

Yang, Q., Liu, K. H., Wang, T., Song, J., & Gao, S. (2021). Crustal and Upper Mantle Structure Beneath the Southeastern United States from Joint Inversion of Receiver Functions and Rayleigh Wave Dispersion. *Journal of Geophysical Research: Solid Earth*. 126, e2021JB021846. https://doi. org/10.1029/2021JB021846

Yuan, H., & Levin, V. (2014). Stratified seismic anisotropy and the lithosphere-asthenosphere boundary beneath eastern North America. *Journal of Geophysical Research: Solid Earth.* 119, 3096–3114. https://doi.org/10.1002/2013JB010785

APPENDICES

APPENDIX A

EARTHQUAKE DATA

TABLE A1

#	Earthquake Date	Latitude (°N)	Longitude (°E)	Depth (km)	Magnitude (Mw)
1	June 13, 2011	2.54	126.46	66.0	6.4
2	July 31, 2011	-3.51	144.97	19.6	6.6
3	Dec 13, 2011	0.05	123.06	167.4	6.1
4	Dec 14, 2011	-7.53	146.81	128.5	7.1
5	Feb 06, 2012	9.92	123.22	17.5	6.7
6	March 21, 2012	-6.22	146.0	117.7	6.6
7	April 17, 2012	-5.53	147.13	208.2	6.9
8	April 21, 2012	-1.69	134.32	24.4	6.7
9	August 26, 2012	2.19	126.84	91.0	6.6
10	August 31, 2012	10.81	126.83	44.4	7.6
11	October 17, 2012	4.18	124.56	338.4	6.0
12	April 06, 2013	-3.51	138.48	69.4	7.0
13	July 07, 2013	-6.04	149.72	65.9	6.6
14	July 07, 2013	-4.01	153.92	387.1	7.3
15	October 15, 2013	9.83	124.12	23.2	7.1
16	April 11, 2014	-6.61	155.03	57.8	7.1

Table A1 shows the 16 earthquakes used for analysis in order by date. This is also the order used for the cross sections. Latitude (°N) is the earthquake latitude of the epicenter in degrees north of the equator and longitude (°E) is the earthquake longitude of the epicenter in degrees east of the prime meridian. Depth (km) is the depth of the earthquake focus. Magnitude (Mw) is the moment magnitude of the earthquake.

TABLE A2

#	Earthquake Date	Latitude (°N)	Longitude (°E)	Depth (km)	Magnitude (Mw)	Back-Azimuth (°)	Distance (°)
1	June 13, 2011	2.54	126.46	66.0	6.4	T: 302.8-309.3 U: 302.3-307.9 V: 303.3-311.3 W: 301.4-310.8 X: 301.7-310.1 Y: 301.3-311.3 Z: 300.7-311.3	T: 122.3-127.0 U: 122.6-126.7 V: 124.0-129.5 W: 123.1-129.8 X: 124.0-130.1 Y: 124.2-131.4 Z: 124.4-132.0
2	July 31, 2011	-3.51	144.97	19.6	6.6	T: 283.5-289.7 U: 283.1-289.8 V: 282.9-289.9 W: 282.5-289.4 X: 282.2-288.9 Y: 282.4-289.7 Z: 282.0-289.6	T: 112.8-119.4 U: 112.9-120.1 V: 113.0-120.9 W: 113.0-120.9 X: 113.1-121.0 Y: 113.7-122.4 Z: 113.8-122.8
3	Dec 13, 2011	0.05	123.06	167.4	6.1	T: 305.3-316.8 U: 303.2-316.2 V: 304.9-315.4 W: 304.4-312.3 X: 303.8-315.1 Y: 303.4-312.9 Z: 303.6-312.8	T: 127.6-134.1 U: 126.8-134.4 V: 128.6-134.8 W: 128.9-133.8 X: 129.2-136.0 Y: 129.5-135.5 Z: 130.2-136.0
4	Dec 14, 2011	-7.53	146.81	128.5	7.1	T: 280.0-287.7 U: 280.0-287.1 V: 279.6-286.5 W: 279.3-284.4 X: 278.9-286.0 Y: 278.6-284.6 Z: 280.5-284.4	T: 115.2-123.57 U: 115.7-123.6 V: 115.7-123.6 W: 115.8-121.9 X: 115.8-124.4 Y: 115.8-123.3 Z: 118.9-123.7
5	Feb 06, 2012	9.92	123.22	17.5	6.7	T: 312.6-323.2 U: 310.7-322.8 V: 312.4-322.2 W: 314.2-321.8	T: 119.9-125.6 U: 119.2-126.0 V: 120.9-126.5 W: 122.8-126.9

						X: 313.1-322.8 Y: 312.0-322.5 Z: 314.4-322.0	X: 122.6-128.1 Y: 122.5-128.5 Z: 124.7-128.9
6	March 21, 2012	-6.22	146.0	117.7	6.6	T: 283.6-289.5 U: 283.9-288.4 V: 283.5-288.3 W: 283.5-287.8 X: 282.5-288.3 Y: 282.7-287.9 Z: 283.2-287.3	T: 117.3-123.3 U: 118.1-122.9 V: 118.1-123.5 W: 118.7-123.6 X: 118.0-124.8 Y: 118.8-124.9 Z: 120.0-124.9
7	April 17, 2012	-5.53	147.13	208.2	6.9	T: 283.4-289.2 U: 283.7-288.8 V: 283.3-288.1 W: 282.9-290.5 X: 282.4-290.0 Y: 282.6-290.0 Z: 282.2-290.0	T: 116.0-122.1 U: 116.8-122.1 V: 116.8-122.2 W: 116.8-125.2 X: 116.7-125.3 Y: 117.5-126.0 Z: 117.6-126.6
8	April 21, 2012	-1.69	134.32	24.4	6.7	T: 296.4-303.5 U: 296.7-303.0 V: 296.3-302.2 W: 295.8-305.3 X: 295.1-304.7 Y: 295.4-304.8 Z: 294.8-304.9	T: 123.1-128.6 U: 124.0-128.8 V: 124.1-129.0 W: 124.3-131.8 X: 124.3-132.1 Y: 125.2-132.9 Z: 125.4-133.6
9	August 26, 2012	2.19	126.84	91.0	6.6	T: 306.2-317.9 U: 306.6-317.9 V: 306.1-317.2 W: 305.6-316.5 X: 304.9-315.9 Y: 305.9-316.2 Z: 304.8-316.4	T: 125.4-132.1 U: 126.3-132.8 V: 126.5-133.2 W: 126.8-133.4 X: 127.0-133.8 Y: 128.4-134.4 Z: 128.2-135.4
10	August 31, 2012	10.81	126.83	44.4	7.6	T: 312.6-323.5 U: 313.0-323.7 V: 312.6-323.1 W: 312.2-322.5 X: 311.6-322.1	T: 118.7-124.7 U: 119.6-125.5 V: 119.9-126.0 W: 120.3-126.2 X: 120.5-126.6

						Y: 312.2-322.4 Z: 311.7-322.7	Y: 121.4-127.5 Z: 121.8-128.2
11	October 17, 2012	4.18	124.56	338.4	6.0	T: 309.9-321.9 U: 310.4-322.0 V: 309.9-321.3 W: 309.4-320.6 X: 308.7-320.1 Y: 309.2-320.4 Z: 308.6-320.7	T: 125.3-131.6 U: 126.2-132.4 V: 126.5-132.8 W: 126.8-133.0 X: 127.0-133.4 Y: 127.9-134.2 Z: 128.3-135.0
12	April 06, 2013	-3.51	138.48	69.4	7.0	T: 294.8-307.5 U: 292.3-305.9 V: 295.8-306.7 W: 290.9-304.9 X: 291.2-304.3 Y: 295.3-303.6 Z: 290.5-301.9	T: 124.2-133.5 U: 122.6-133.3 V: 126.3-134.4 W: 122.3-134.1 X: 123.3-134.1 Y: 127.9-134.3 Z: 123.8-134.0
13	July 07, 2013	-6.04	149.72	65.9	6.6	T: 285.7-294.5 U: 285.1-294.2 V: 284.7-294.0 W: 284.9-292.9 X: 282.3-291.7 Y: 284.5-291.0 Z: 284.5-289.7	T: 119.3-127.6 U: 119.2-128.2 V: 119.4-128.8 W: 119.9-128.2 X: 117.5-127.7 Y: 120.6-127.7 Z: 121.3-127.1
14	July 07, 2013	-4.01	153.92	387.1	7.3	T: 284.5-292.8 U: 284.6-292.6 V: 283.8-292.5 W: 283.9-291.4 X: 282.9-289.8 Y: 283.5-289.8 Z: 283.6-288.5	T: 114.7-123.2 U: 115.4-123.7 V: 114.9-124.4 W: 115.4-123.7 X: 114.8-122.7 Y: 116.1-123.2 Z: 116.8-122.6
15	October 15, 2013	9.83	124.12	23.2	7.1	T: 321.4-333.0 U: 315.4-333.1 V: 321.2-333.4 W: 314.0-332.0 X: 314.6-330.5	T: 125.0-129.3 U: 122.4-130.2 V: 126.1-131.0 W: 122.6-131.0 X: 123.7-131.1

						Y: 320.7-330.0 Z: 314.0-328.4	Y: 127.8-131.5 Z: 124.6-131.7
16	April 11, 2014	-6.61	155.03	57.8	7.1	T: 283.13-289.6 U: 285.4-289.3 V: 284.9-289.2 W: 284.4-288.2 X: 278.4-287.1 Y: 282.4-286.5 Z: 280.9-285.3	T: 117.3-124.1 U: 120.4-124.5 V: 120.5-125.2 W: 120.4-124.5 X: 113.5-123.9 Y: 119.2-123.9 Z: 117.8-123.2

Table A2 shows the 16 earthquakes used for analysis in order by date. This is also the order used for the cross sections. Latitude (°N) is the earthquake latitude of the epicenter in degrees north of the equator and longitude (°E) is the earthquake longitude of the epicenter in degrees east of the prime meridian. Depth (km) is the depth of the earthquake focus. Magnitude (Mw) is the moment magnitude of the earthquake. Back-Azimuth (°) is the range in back-azimuth in degrees clockwise from north from TA stations to the epicenter of the earthquake. T through Z represent the back-azimuths for stations along each TA station line (Figure 1). Distance (°) refers to the range in angular distance between stations and the epicenter of the earthquake.

APPENDIX B

STUDY AREA

FIGURE B1

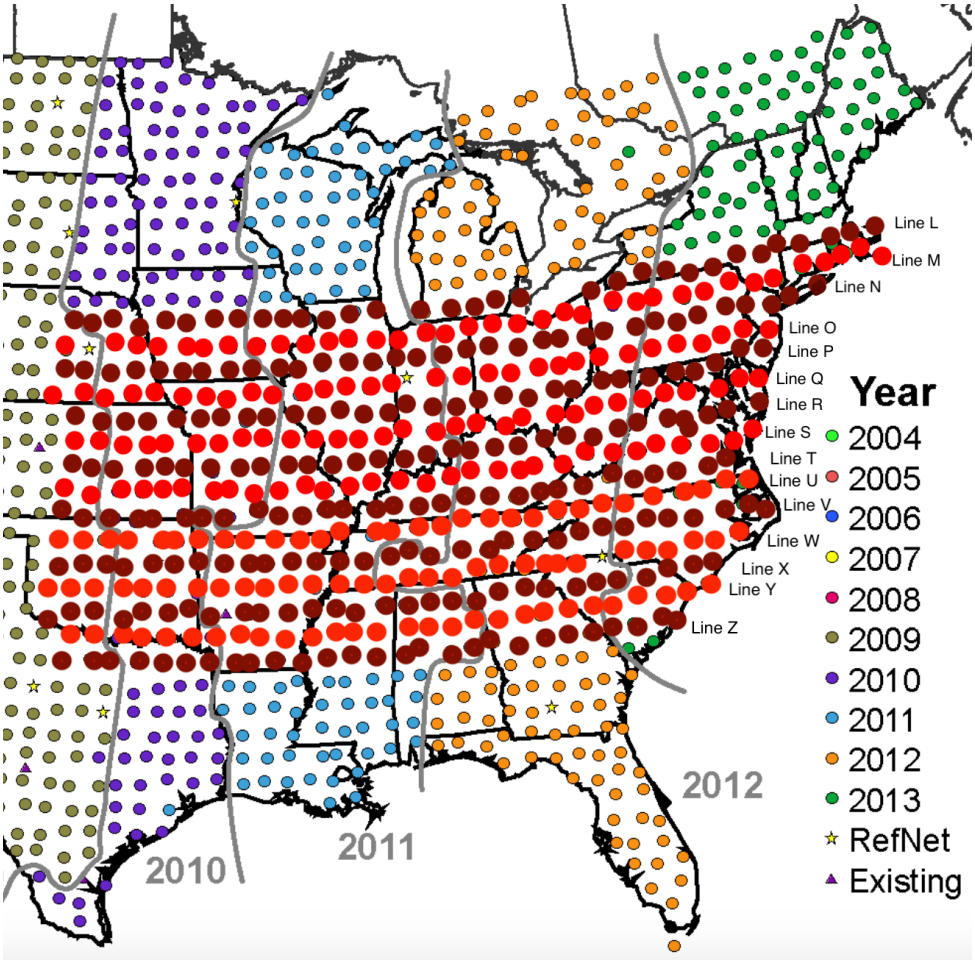


Figure B1 shows all lines used in the complete study, Lines L-Z.

APPENDIX C

METHODOLOGY

The processing for this study involves creating deconvolved stacked gathers for geologic interpretation. Processing begins with data from individual stations (called a trace) for each earthquake and each line (Line T-Z for part one). These traces are formed into a gather by earthquake per line. So, for example, all stations that recorded a single earthquake for Line T would be combined into one gather. Then, for each gather (one gather per earthquake per line- 96 gathers total), a source wavelet is estimated by stacking seismogram traces deployed on crystalline bedrock (Langston & Hammer, 2001). PKPdf (PKIKP) arrivals are aligned by cross-correlation with a source wavelet estimate- either with a previously estimated SESAME wavelet, or a new wavelet that was created by stacking TA traces (Verellen et al., 2020). The source wavelet then is used to deconvolve the traces. This removes the effect of the extended source-time function, compressing the PKPdf arrival and reflections into much shorter duration wavelets, and also placing the PKPdf arrival at time zero. The deconvolved gathers are then stacked, or summed, to suppress noise and enhance signals. Velocity models are used to convert two-way time to depth (Buehler & Shearer, 2017; Parker et al., 2016; Hawman et al., 2012; Kennett, 2015; Verellen et al., 2020). The deconvolved stacks are then used for subsurface interpretation.

STEP 101

The first step in processing is to use the software package "JWEED" to download seismogram data from the IRIS archive for each earthquake that will be used in analysis. This seismogram data for every station that was operating at that time of each earthquake used is taken and sorted into files that are separated by earthquake event for each TA line (Line T-Z for my study). A separate software package, "SAC," removes the mean, trend, and average value of each trace and writes this modified trace into a new output trace.

STEP 102

The next step and all other steps run in the UNIX operating system. The SAC header from each trace is stripped and combined into a single file that extracts a subset of information. The information included is a list of key parameters that specify the stations that were occupied for each earthquake, the stations latitude and longitude, earthquake depth, latitude, longitude, azimuth, back azimuth, and arc-distance. To correct for variations in trace length for different seismograms, this step reads the first 7999 samples and then lengthens all traces to 8001 samples by padding the ends of traces with zeroes. It then takes individual, "plain-vanilla" seismograms (traces with no headers) and combines them into a single file that creates a trace gather from west to east. The TA traces then are resampled from dt=0.025 s to dt=0.02 s to match the sampling increment used for the SESAME experiment. Headers are then added back for plotting and the traces are plotted over a smaller time window. Lastly, a bandpass filter is applied to suppress noise for future steps.

STEP 103

The next job cross-correlates traces to align the PKPdf arrivals for all traces with the source wavelet estimate. The source wavelet estimate can come from a variety of methods. In previous SESAME studies, a source wavelet was estimated for the same earthquakes used in this study. To estimate this wavelet, a reference trace is chosen to use for cross-correlation with the other traces in the gather for aligning the PKPdf arrival. Once aligned, the traces are stacked ("added") together to create the source wavelet estimate. This works because when the traces are added together, reflections cancel out and the PKPdf arrival remains, as it does not vary from station to station like reflections and noise do. The source wavelet is meant to represent the signal created by the earthquake.

Sometimes, especially for the earthquakes that occurred when the western half of the lines were deployed, the SESAME source wavelet estimate was not the best estimation possible for the gathers. This is likely due to the fact that these western stations were much further from the SESAME array and reflections differ. In such cases, a new wavelet was created by stacking all the traces in the gather by using a reference trace to align the PKPdf arrivals. This new wavelet prevents reverberations of signals that occurred from using the SESAME wavelet because the alignment is more exact.

In a similar manner, a few earthquakes were impossible to interpret because seismograms were dominated by low frequency noise. In these scenarios, a new, filtered wavelet was created by stacking all the traces that had a bandpass filtered applied. The filtered traces

and new, filtered wavelet eliminated the low frequencies and enhanced signals for interpretation.

In all cases, the source wavelet estimate was used to cross-correlate all traces by their PKPdf arrival. The source wavelet was used as a reference trace and all other traces in the gather shifted to align with it. The window evaluated for comparison starts slightly before the beginning of the source wavelet and extends to include the most energetic part of the source wavelet. After that, the source wavelet trace and all other traces are combined into one gather, so the source wavelet is now the first trace in the gather followed by the newly cross-correlated traces. This cross-correlation alignment is a form of statics correction. At this point, the source wavelet and all traces are on a common time base. I have included example images of the plots that step 103 created for the SESAME wavelet and a new filtered wavelet with an altered “wh” parameter (Figures C1-C8).

FIGURE C1

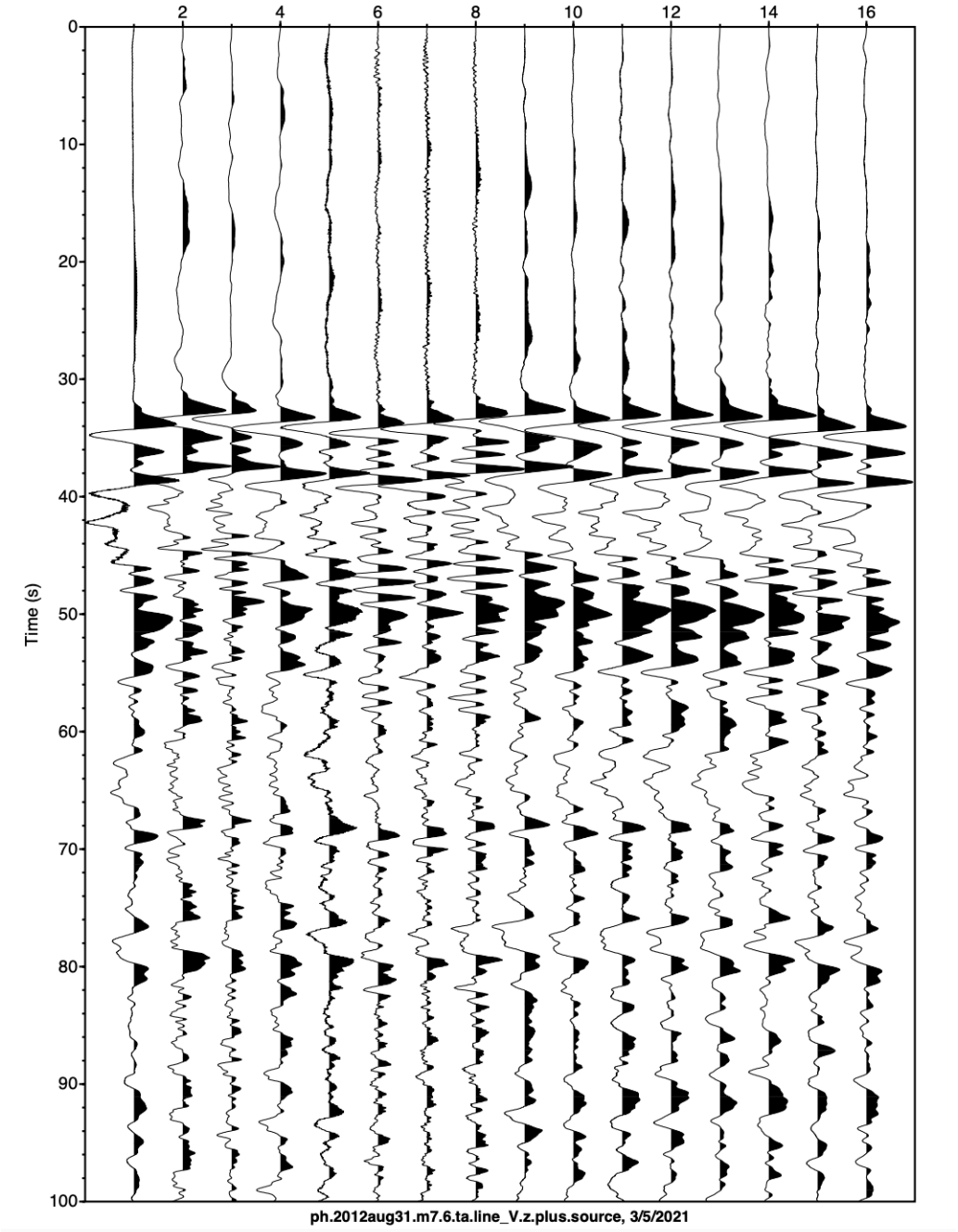


Figure C1 shows step 103 for an earthquake on August 31, 2012, with a magnitude of 7.6 for Line V. This example shows a plot that is unfiltered and without statics correction. This earthquakes source wavelet was estimated by SESAME.

FIGURE C2

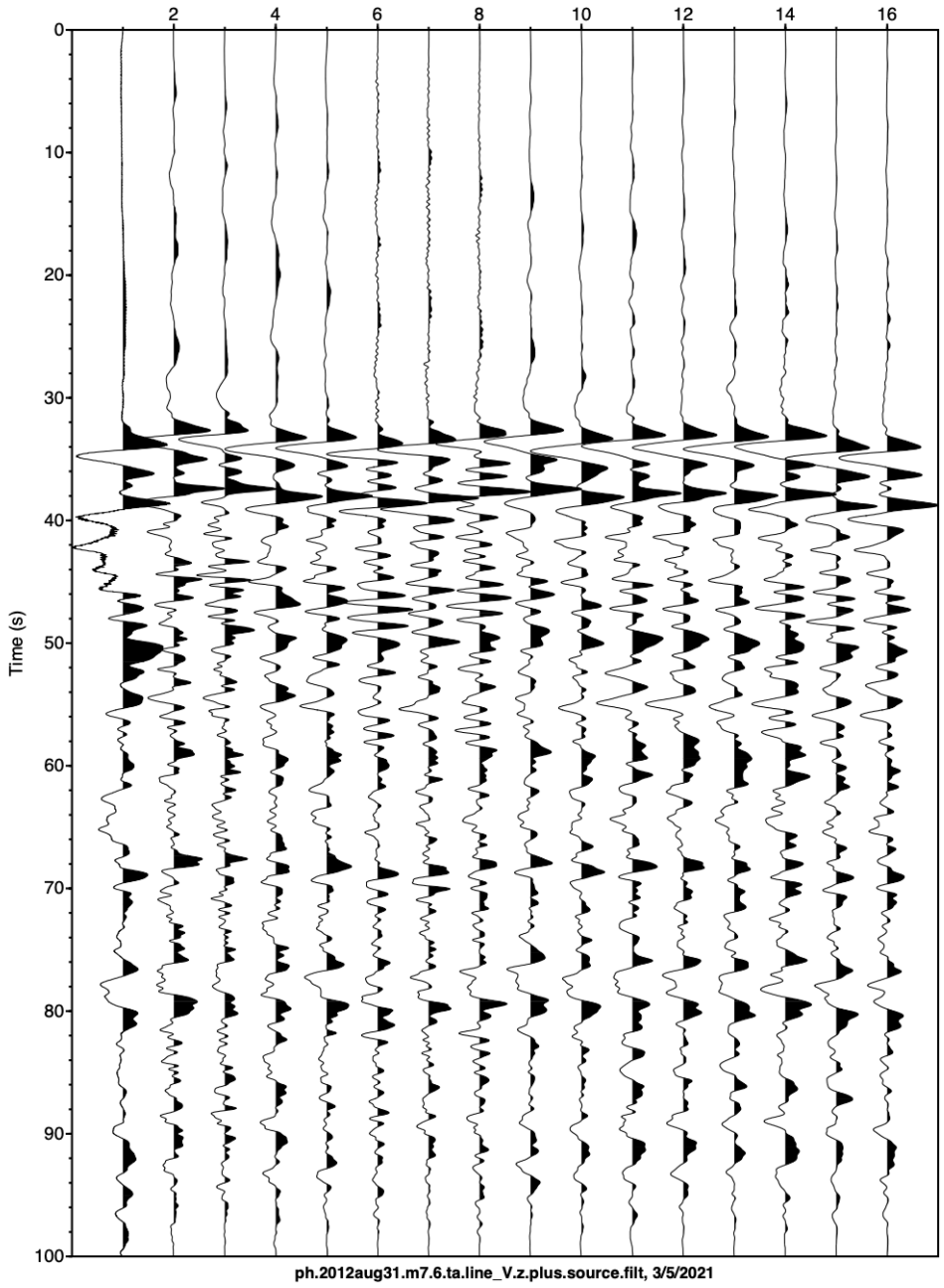


Figure C2 shows step 103 for an earthquake on August 31, 2012, with a magnitude of 7.6 for Line V. This example shows a plot that is filtered but without statics correction. This earthquakes source wavelet was estimated by SESAME.

FIGURE C3

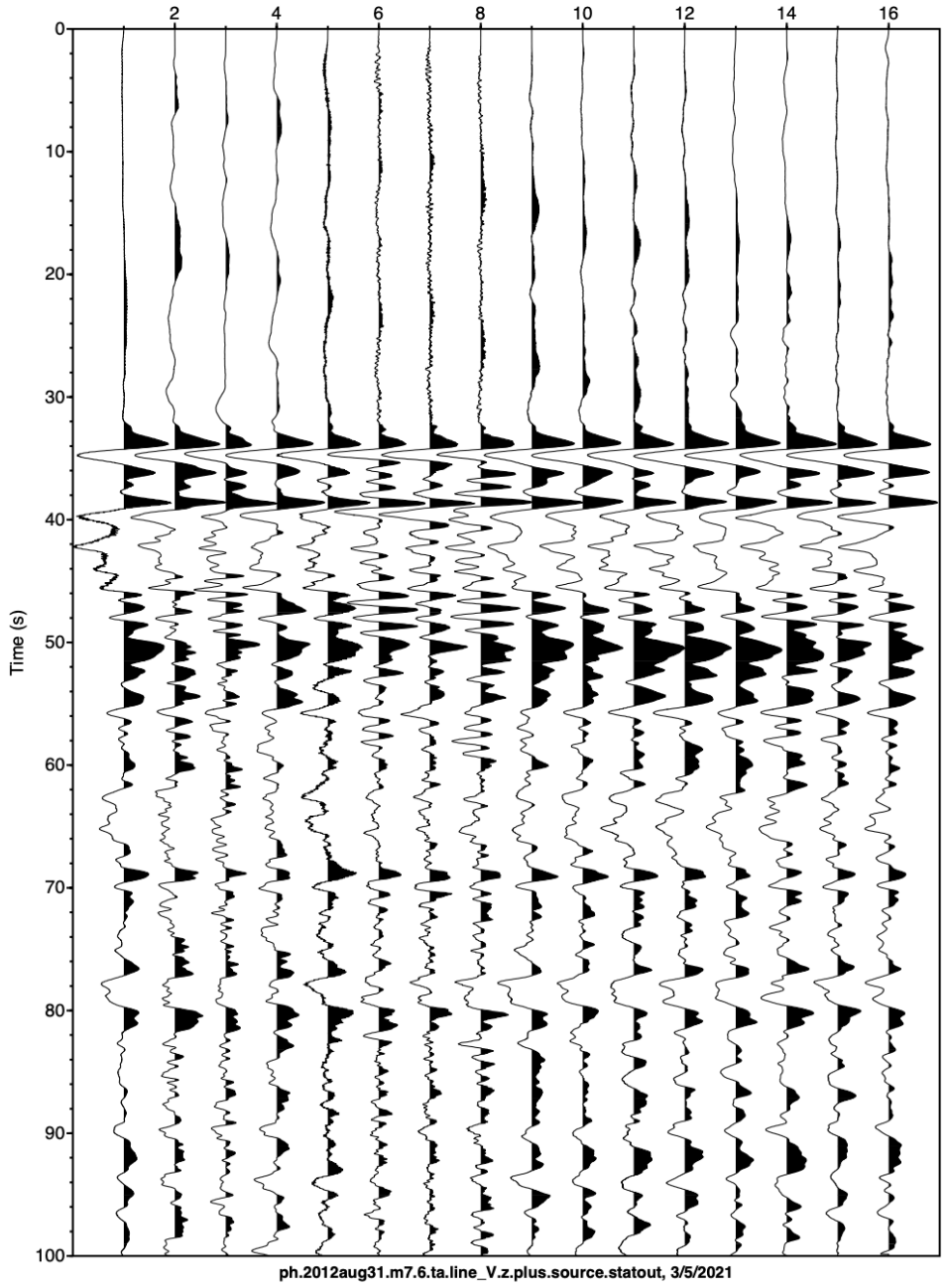


Figure C3 shows step 103 for an earthquake on August 31, 2012, with a magnitude of 7.6 for Line V. This example shows a plot that is unfiltered but with statics correction. This earthquakes source wavelet was estimated by SESAME.

FIGURE C4

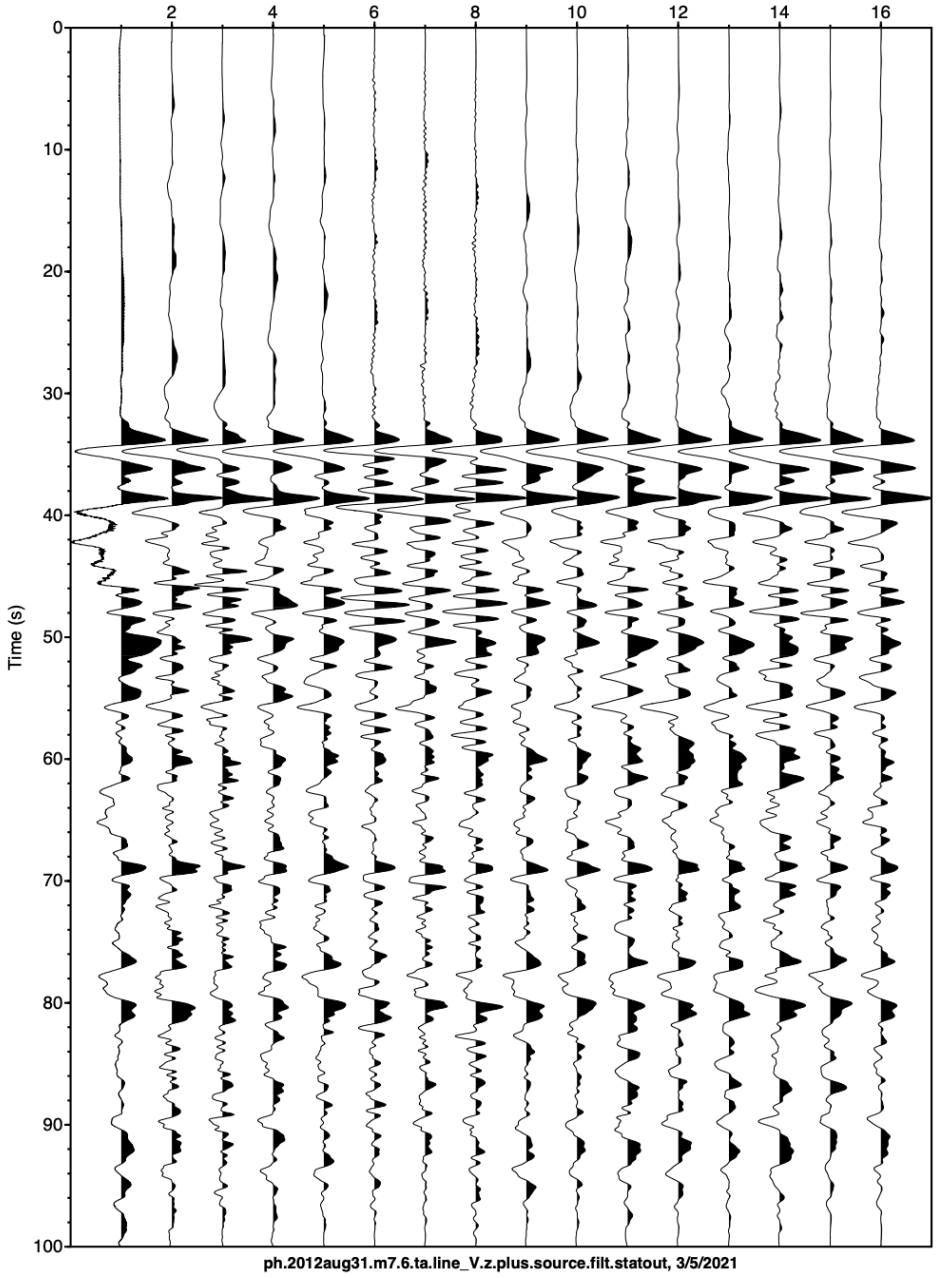


Figure C4 shows step 103 for an earthquake on August 31, 2012, with a magnitude of 7.6 for Line V. This example shows a plot that is filtered and with statics correction. This earthquakes source wavelet was estimated by SESAME.

FIGURE C5

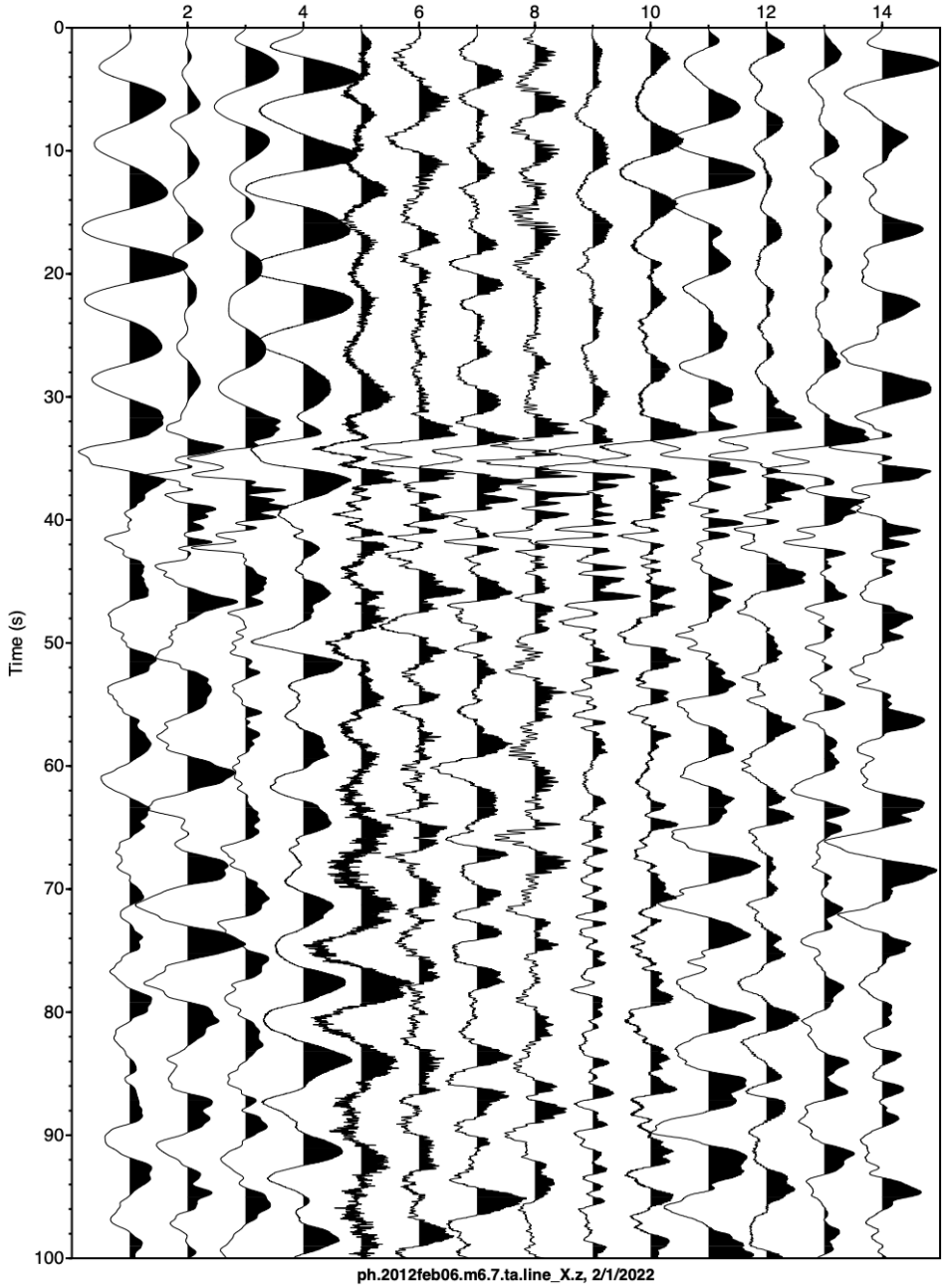


Figure C5 shows step 103 for an earthquake on February 06, 2012, with a magnitude of 6.7 for Line X. This example shows a plot that is unfiltered and without statics correction. This earthquakes source wavelet was estimated by stacking all traces together to form a new wavelet.

FIGURE C6

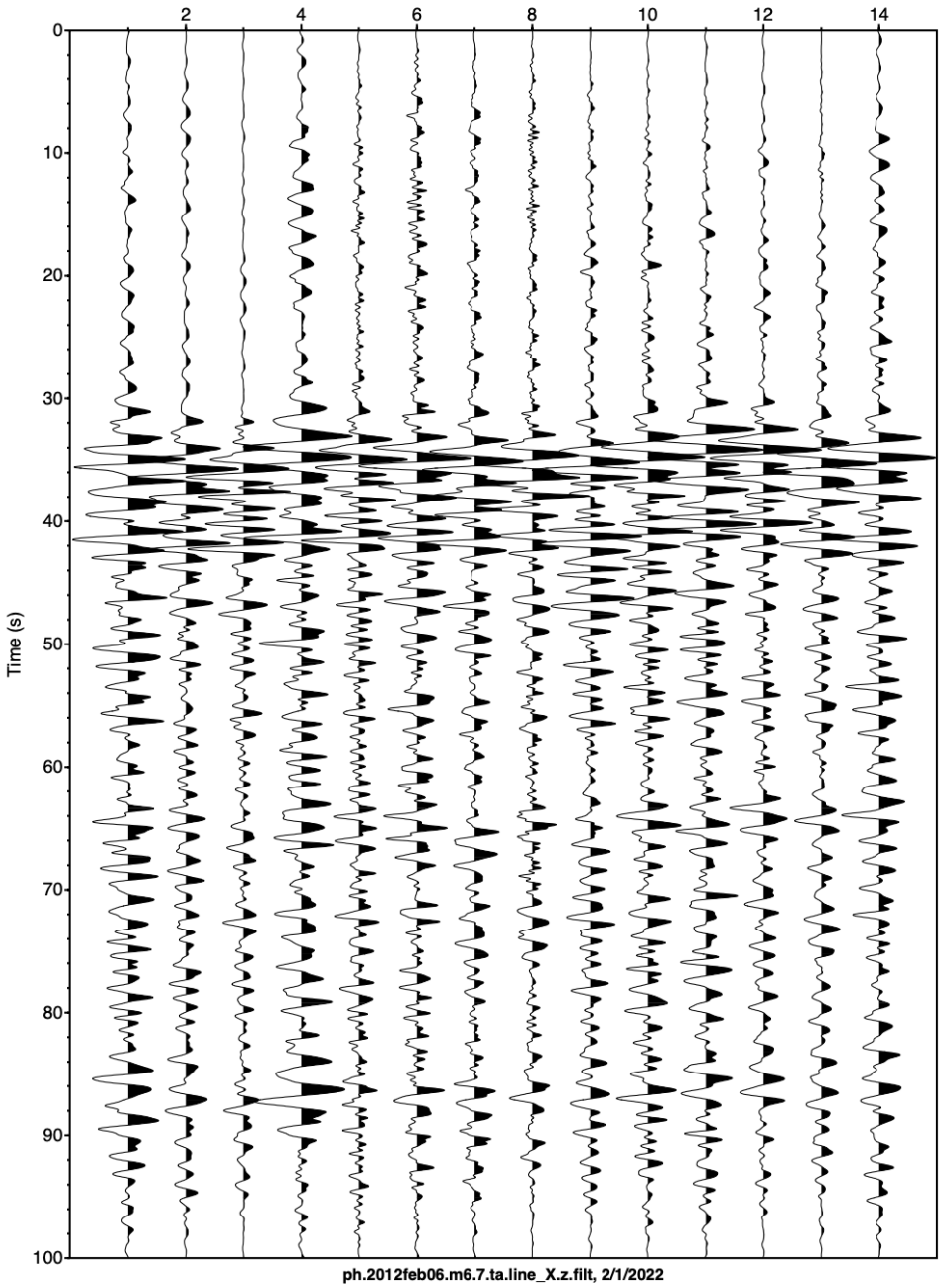


Figure C6 shows step 103 for an earthquake on February 06, 2012, with a magnitude of 6.7 for Line X. This example shows a plot that is filtered but without statics correction. This earthquakes source wavelet was estimated by stacking all traces together to form a new wavelet.

FIGURE C7

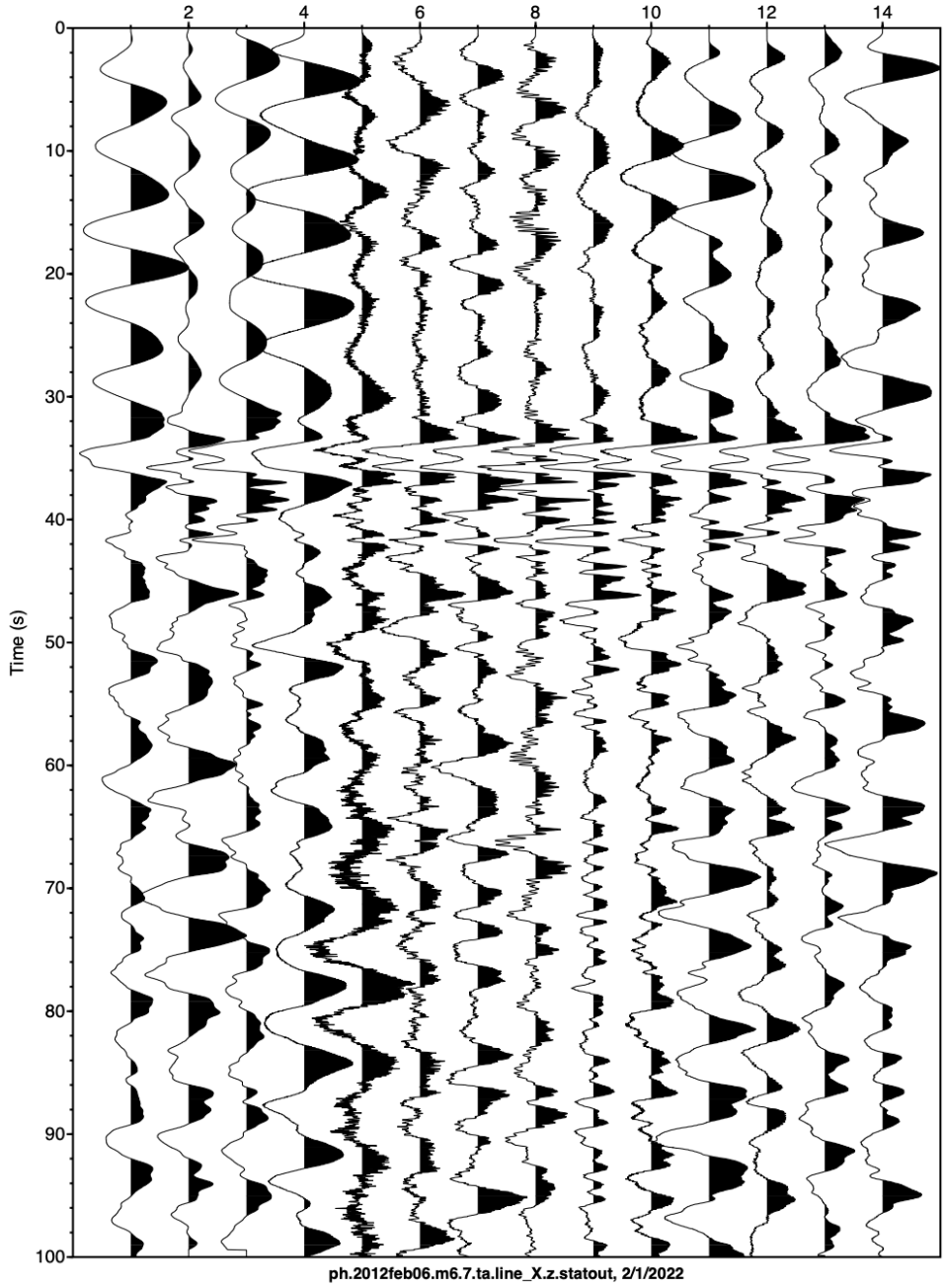


Figure C7 shows step 103 for an earthquake on February 06, 2012, with a magnitude of 6.7 for Line X. This example shows a plot that is unfiltered but with statics correction. This earthquakes source wavelet was estimated by stacking all traces together to form a new wavelet.

FIGURE C8

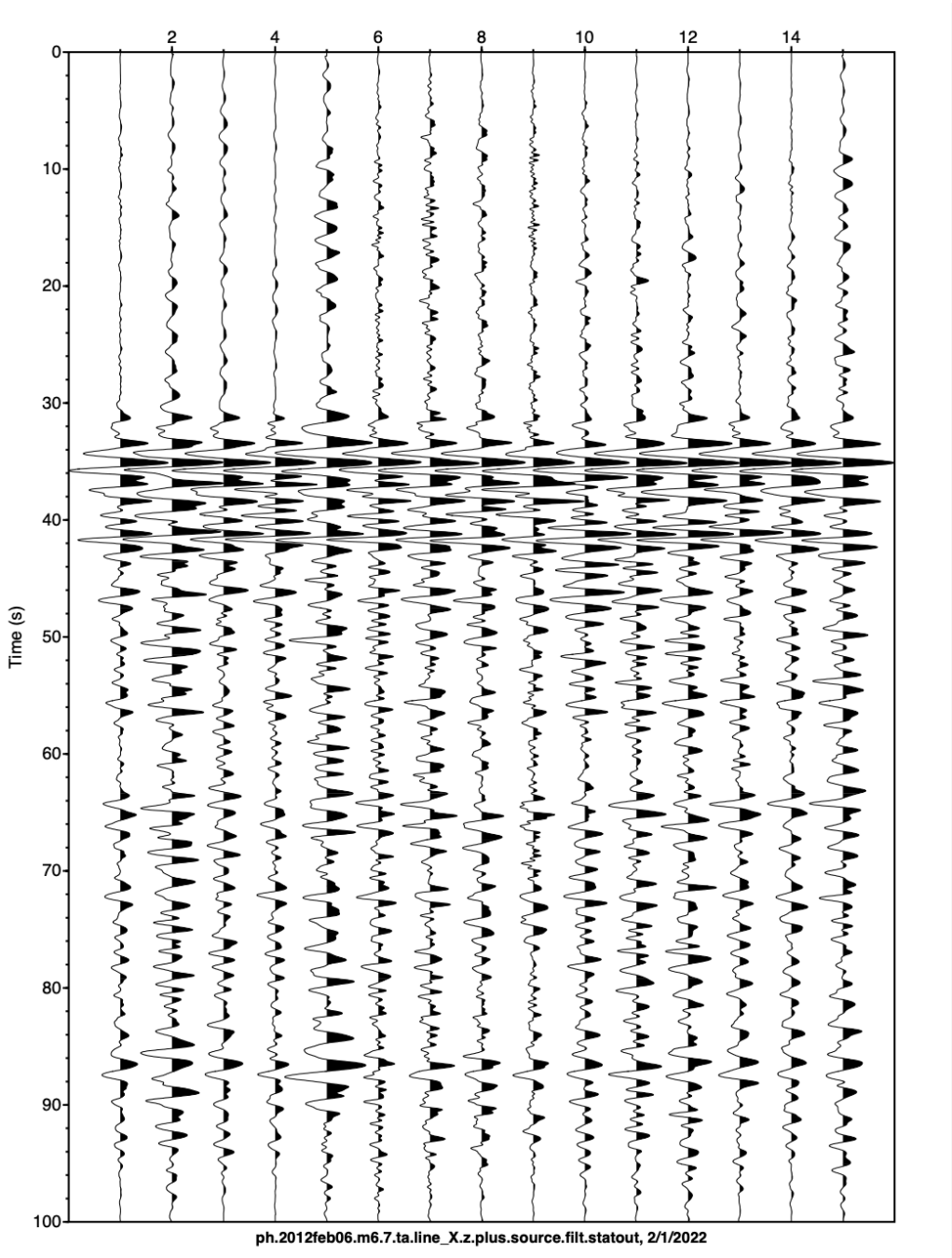


Figure C8 shows step 103 for an earthquake on February 06, 2012, with a magnitude of 6.7 for Line X. This example shows a plot that is filtered and with statics correction. This earthquakes source wavelet (trace 1 of this plot) was estimated by stacking all traces together to form a new wavelet.

STEP 104

This job uses the estimated source wavelet to deconvolve all of the traces in the gather. Deconvolution is the process of removing the effect of the source wavelet by compressing it into a spike. This process is carried out in the frequency domain by dividing the frequency spectrum of each trace by the spectrum of the source wavelet. Deconvolution sharpens reflection signals, so interpretation becomes easier. It removes the effect of the extended source-time function, compressing the PKPdf arrival and reflections into much shorter duration wavelets, and also shifts the time base, placing the PKPdf arrival at time zero. Any of the above source wavelet estimates can be used for this process- the original SESAME wavelet, the new wavelet, and the new, filtered wavelet.

Deconvolution is repeated for a range of Gaussian parameters (α=1.0-5.0) that represent dominant frequencies. Larger values of α tend to preserve more detail and can be more useful for interpretation.

In this job, the “wh” or “water-level parameter” can also be edited. For most earthquakes, this parameter was left as it’s typical value of 0.0001. This parameter stabilizes the spectral division, as the process of dividing spectra for deconvolution sometimes leads to instability, especially if the amplitudes in the source wavelet spectrum are small. One particular earthquake required a larger value of “wh,” which “filled in gaps” in the traces by minimizing both low and high frequency noise to improve signals.

After this process, the job creates plots of the deconvolved gather with the source wavelet as the first trace, followed by the rest of the traces. The plots start at -20 seconds, with the direct arrival at 0 seconds. The pre-event time window (-20-0 s) is plotted as an aid in identifying any instabilities in the deconvolution. The deconvolved gather is plotted with uniform space tracing and plotted with both positive and negative polarities. In the positive, or normal, polarity plots the PKPdf arrival is assigned a positive polarity. However, because of reflection at the free surface, polarities of reflections from the subsurface are reversed, so that reflections from positive impedance contrasts (e.g., the Moho) will show the opposite polarity, i.e., a negative pulse, while interfaces marking negative impedance contrasts (e.g., first-order discontinuity models for the LAB) will show up as a positive pulse. In negative, or reversed, polarity plots the traces are all multiplied by -1, making the PKPdf a negative pulse that in turn reverses the polarities again for all subsurface reflections.

I have included example images of the plots that step 104 created for the SESAME wavelet and a new filtered wavelet with an altered “wh” parameter for Gaussian parameters of α=1.0 and α=4.0 (Figures C9-C16).

FIGURE C9

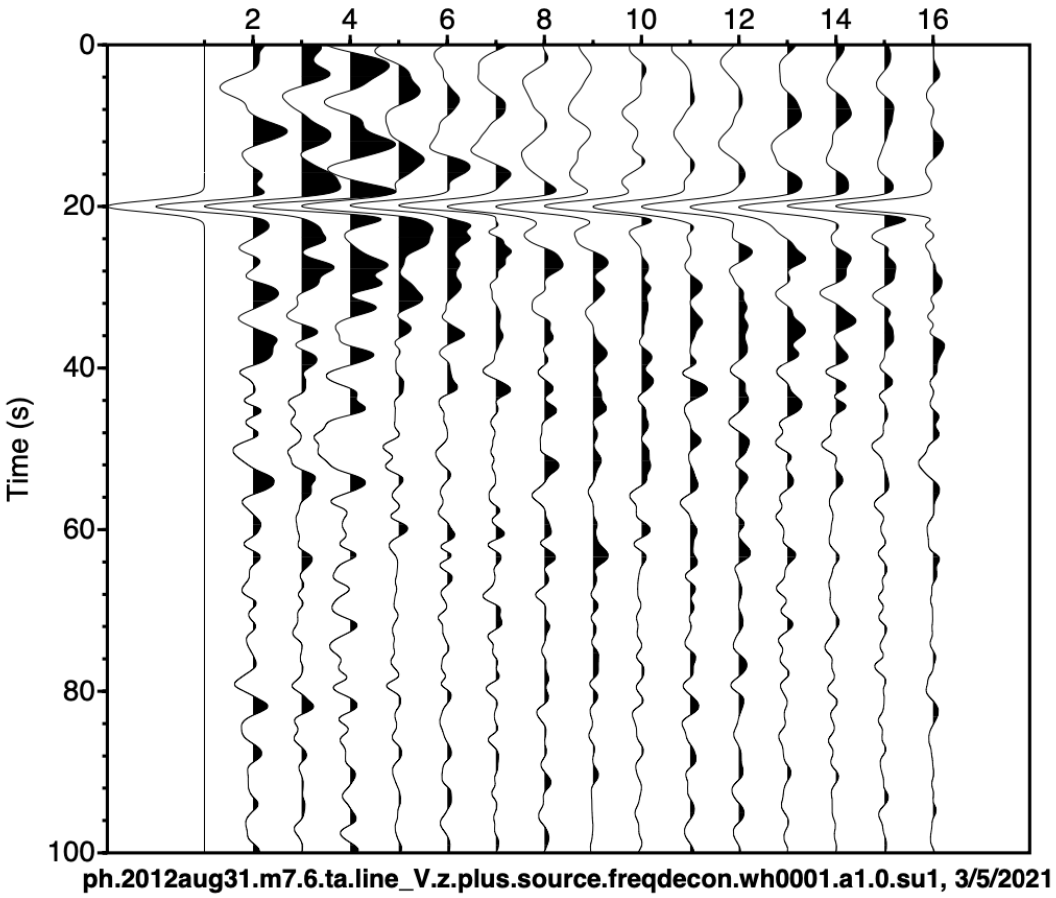


Figure C9 shows step 104 for an earthquake on August 31, 2012, with a magnitude of 7.6 for Line V. This example shows a negative polarity plot with equal station spacing with a Gaussian parameter of α=1.0. This earthquake's source wavelet was estimated by SESAME. Trace 1 is the deconvolved source wavelet.

FIGURE C10

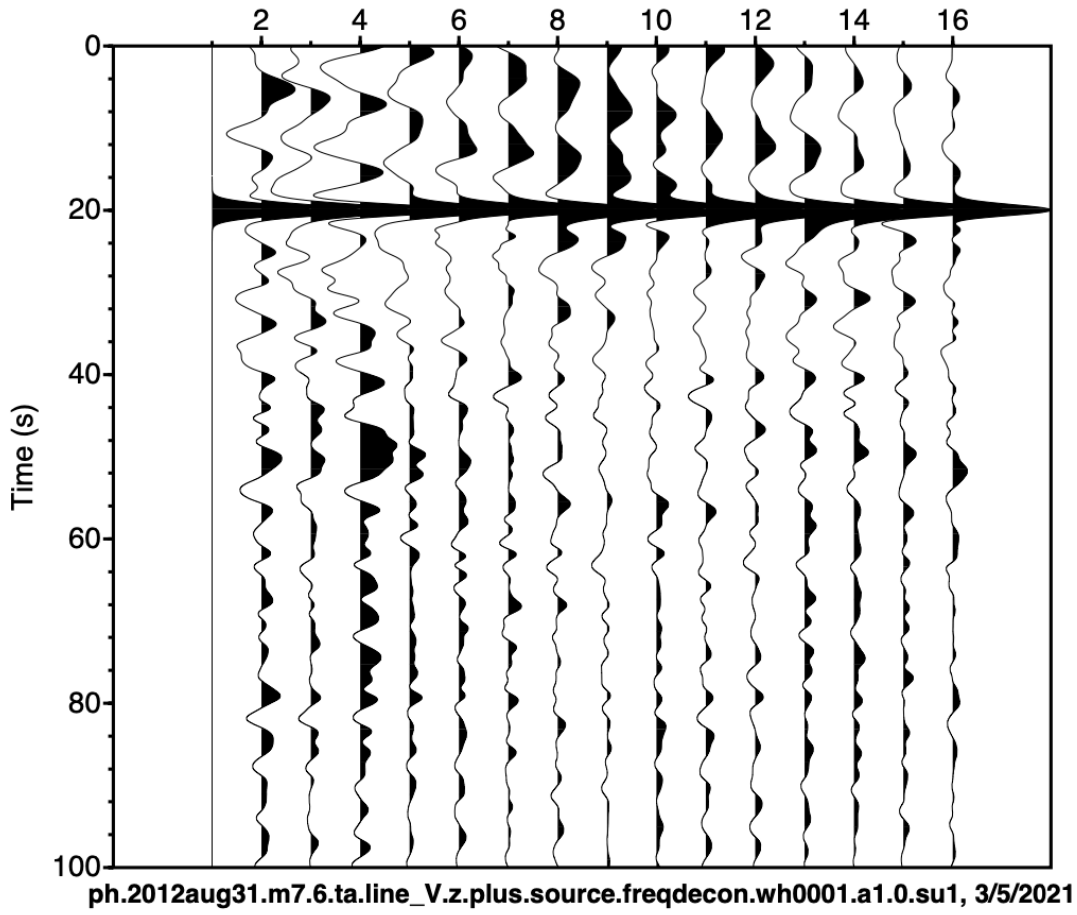


Figure C10 shows step 104 for an earthquake on August 31, 2012, with a magnitude of 7.6 for Line V. This example shows a positive polarity plot with equal station spacing with a Gaussian parameter of α=1.0. This earthquakes source wavelet was estimated by SESAME. Trace 1 is the deconvolved source wavelet.

FIGURE C11

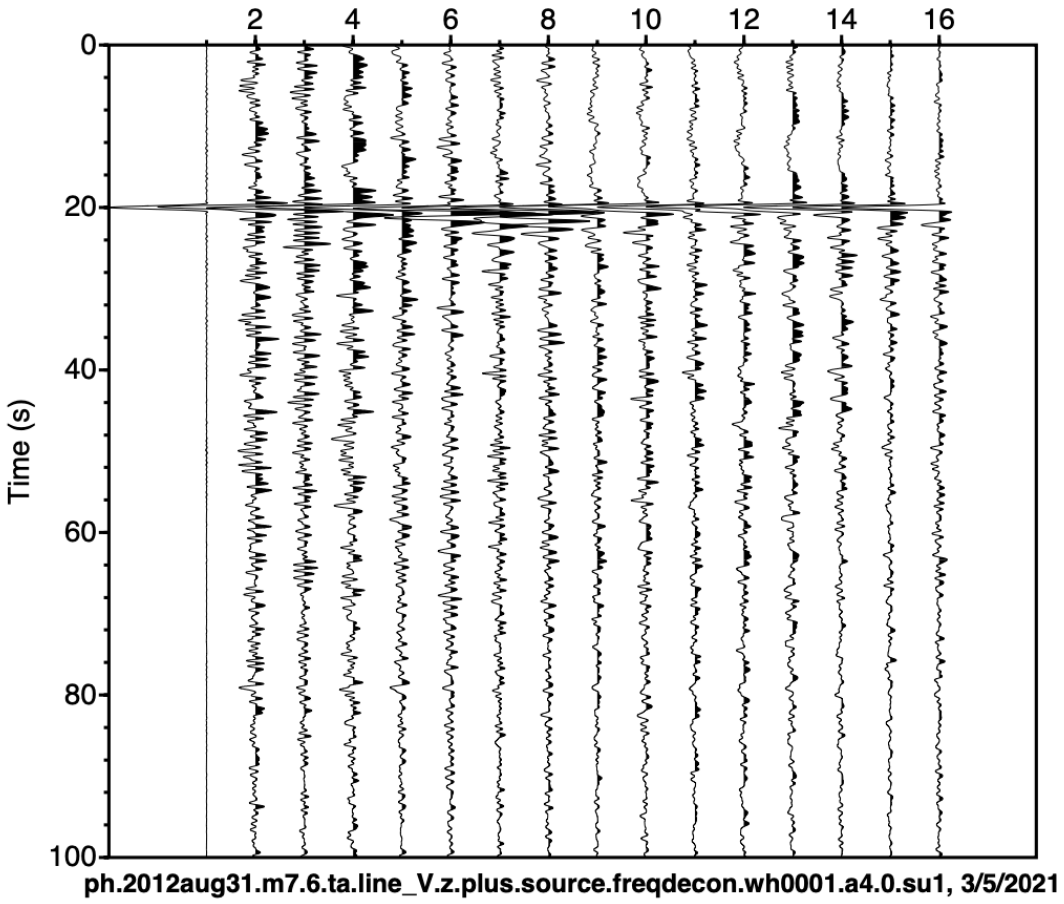


Figure C11 shows step 104 for an earthquake on August 31, 2012, with a magnitude of 7.6 for Line V. This example shows a negative polarity plot with equal station spacing with a Gaussian parameter of α=4.0. This earthquakes source wavelet was estimated by SESAME. Trace 1 is the deconvolved source wavelet.

FIGURE C12

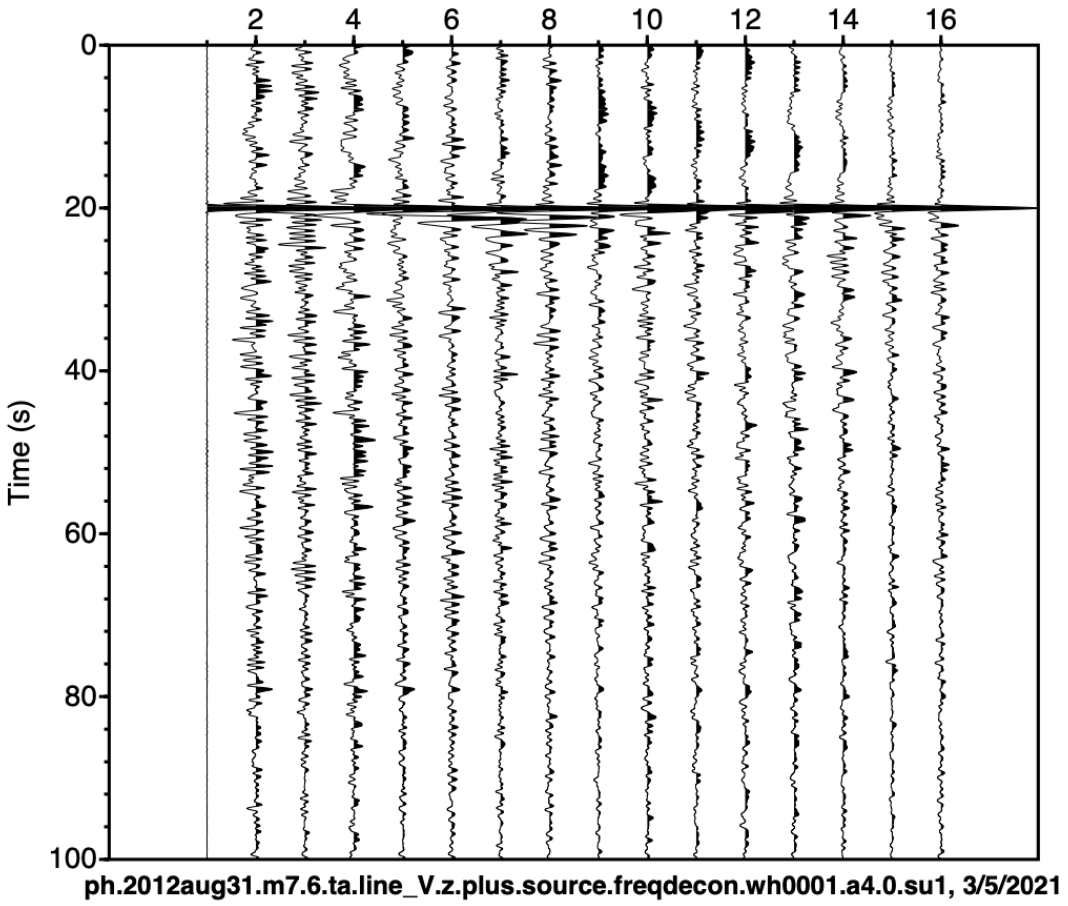


Figure C12 shows step 104 for an earthquake on August 31, 2012, with a magnitude of 7.6 for Line V. This example shows a positive polarity plot with equal station spacing with a Gaussian parameter of α=4.0. This earthquakes source wavelet was estimated by SESAME. Trace 1 is the deconvolved source wavelet.

FIGURE C13

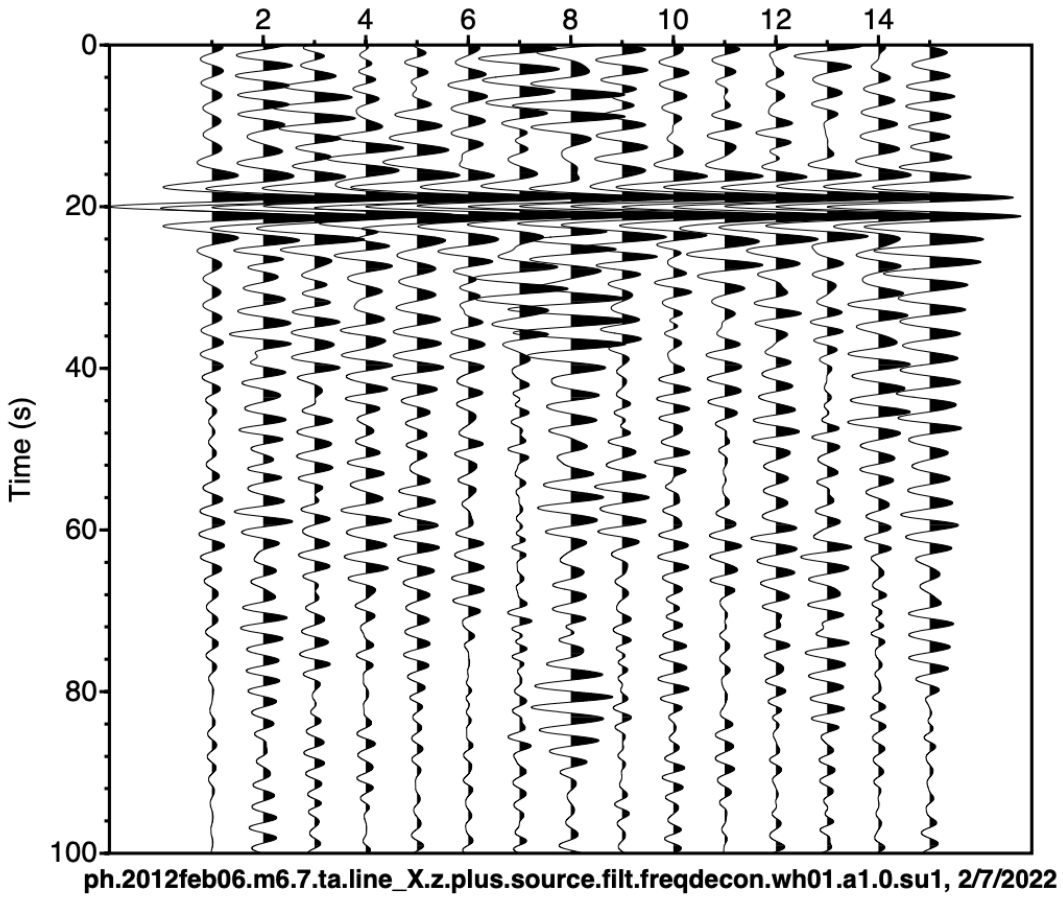


Figure C13 shows step 104 for an earthquake on February 06, 2012, with a magnitude of 6.7 for Line X. This example shows a negative polarity plot with equal station spacing with a Gaussian parameter of α=1.0. This earthquakes source wavelet was estimated by stacking all traces to create a new (filtered) wavelet. The “wh” parameter has also been changed. Trace 1 is the deconvolved source wavelet.

FIGURE C14

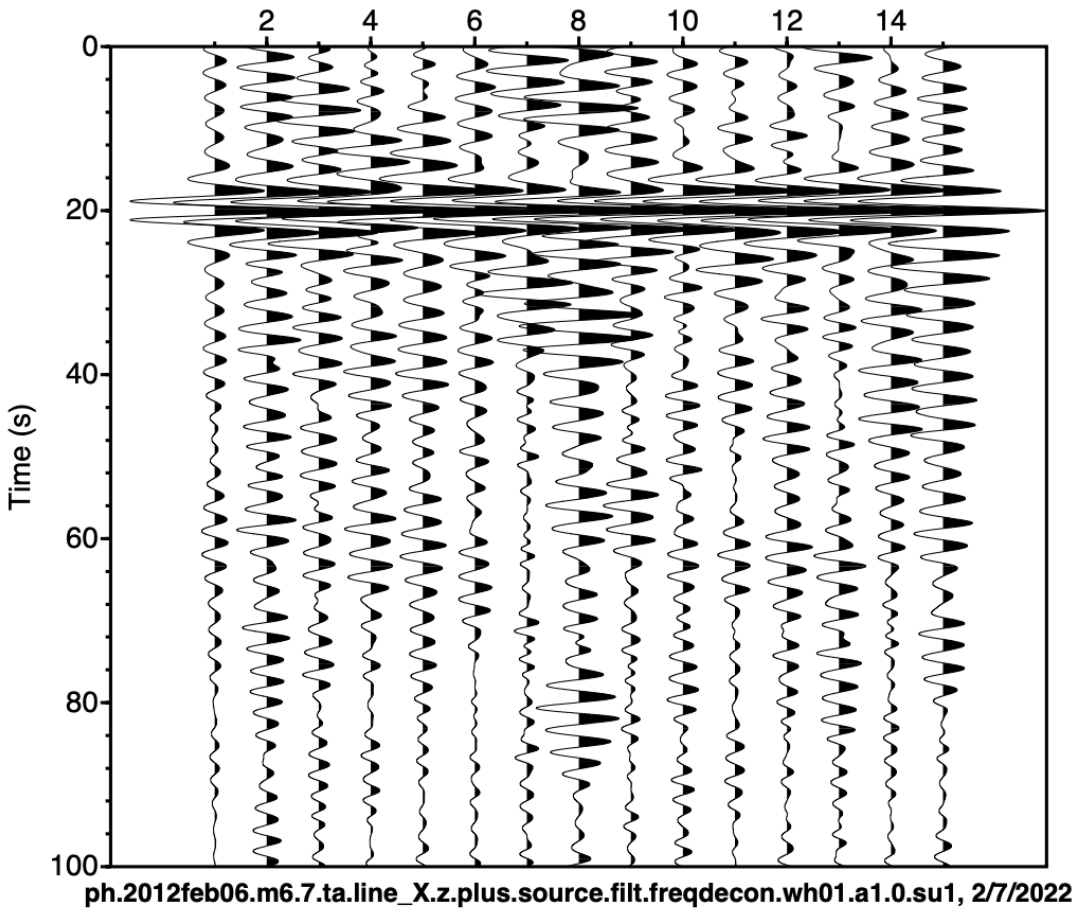


Figure C14 shows step 104 for an earthquake on February 06, 2012, with a magnitude of 6.7 for Line X. This example shows a positive polarity plot with equal station spacing with a Gaussian parameter of α=1.0. This earthquakes source wavelet was estimated by stacking all traces to create a new (filtered) wavelet. The “wh” parameter has also been changed. Trace 1 is the deconvolved source wavelet.

FIGURE C15

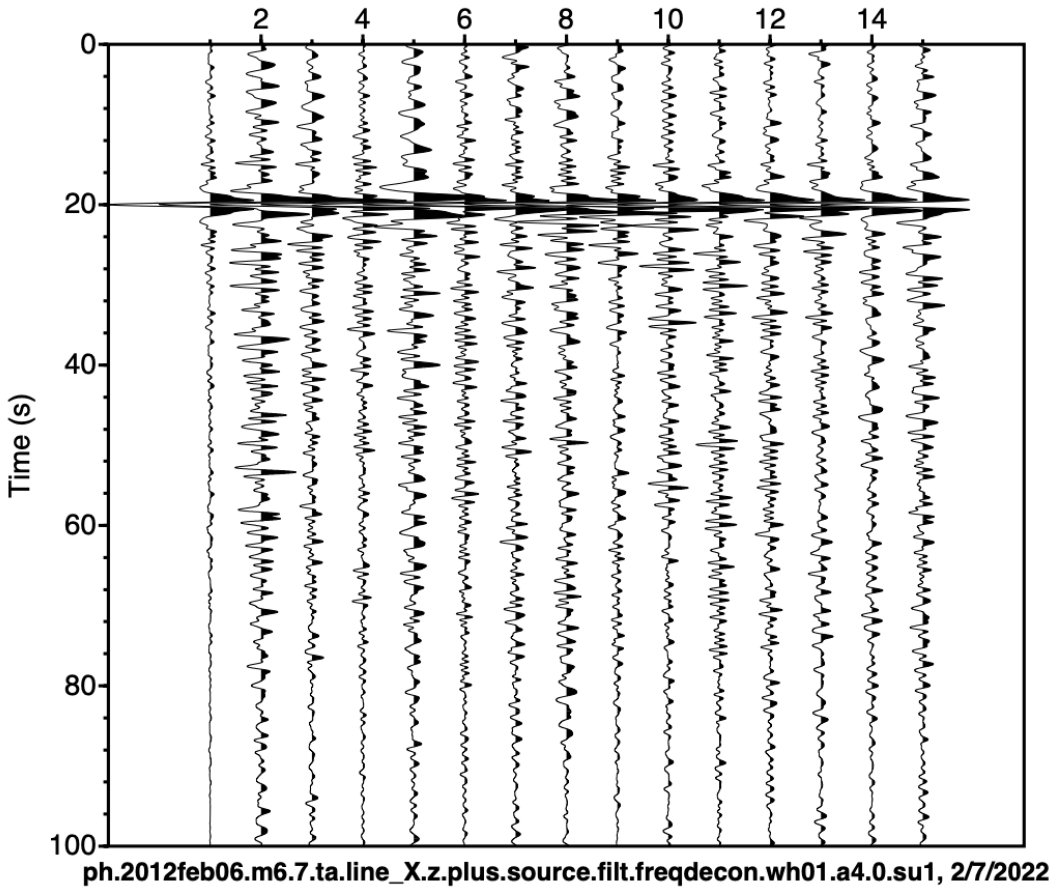


Figure C15 shows step 104 for an earthquake on February 06, 2012, with a magnitude of 6.7 for Line X. This example shows a negative polarity plot with equal station spacing with a Gaussian parameter of α=4.0. This earthquakes source wavelet was estimated by stacking all traces to create a new (filtered) wavelet. The “wh” parameter has also been changed. Trace 1 is the deconvolved source wavelet.

FIGURE C16

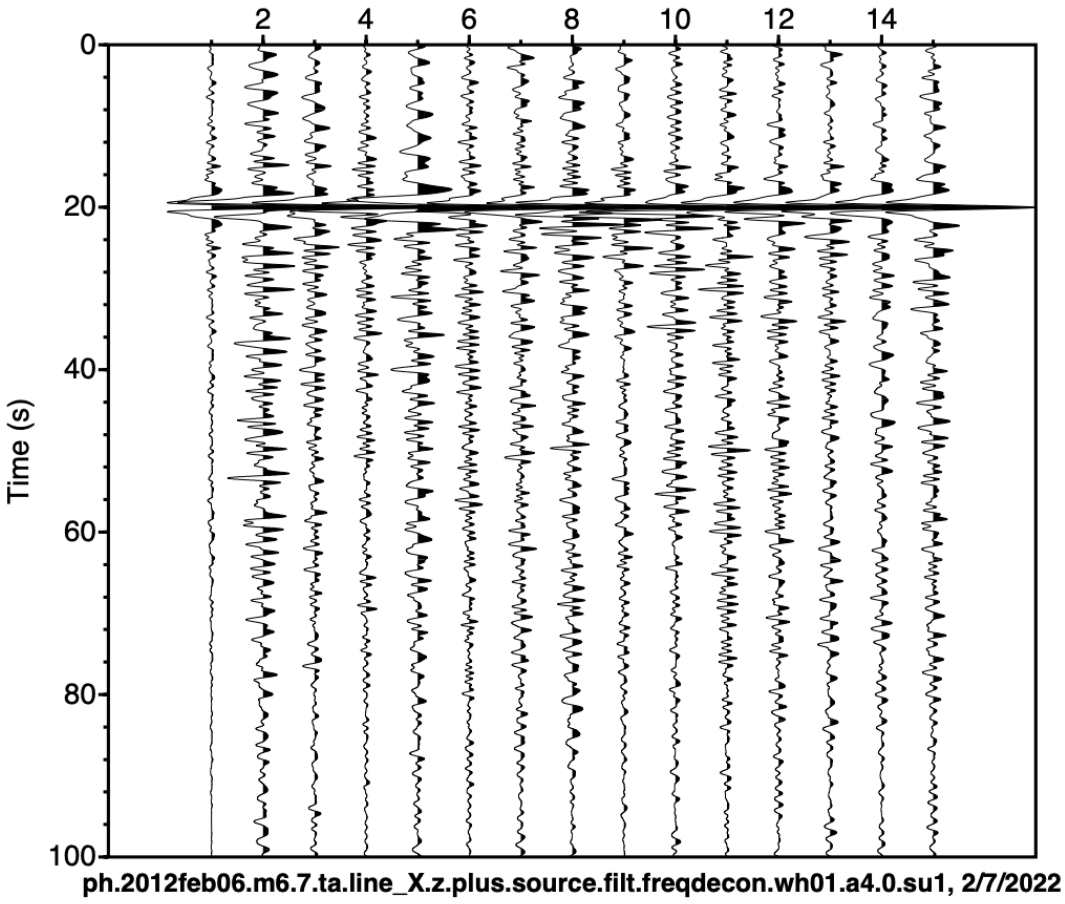


Figure C16 shows step 104 for an earthquake on February 06, 2012, with a magnitude of 6.7 for Line X. This example shows a positive polarity plot with equal station spacing with a Gaussian parameter of α=4.0. This earthquakes source wavelet was estimated by stacking all traces to create a new (filtered) wavelet. The “wh” parameter has also been changed. Trace 1 is the deconvolved source wavelet.

STEP 105

This step takes the deconvolved gather from the previous step and plots each trace in its correct relative space along the gather. Each line in the study has a file that inputs the correct distance to each station from the first station in the western end. So, distances increase from west to east by multiplying the differences in longitude by an appropriate factor to convert longitude to kilometers. Each line will have the same relative spacing for each earthquake. However, for each earthquake only certain stations were occupied, so the stations in the gather that were not occupied will be zeroed out. This is done so all the earthquakes have the same number of traces with the same trace length for the next step of stacking. The traces are then all padded to a length of 5501.

This step can be completed with a SESAME wavelet, a new wavelet, or a new, filtered wavelet. In this step, some last minute low-cut/ bandpass filtering can be applied to further enhance signals. If the "wh" parameter was edited in the previous step, it must also be edited in this step.

I have included example images of the plots that step 105 created for the SESAME wavelet and a new filtered wavelet with an altered "wh" parameter for Gaussian parameters of α=1.0 and α=4.0 (Figures C17-C24).

FIGURE C17

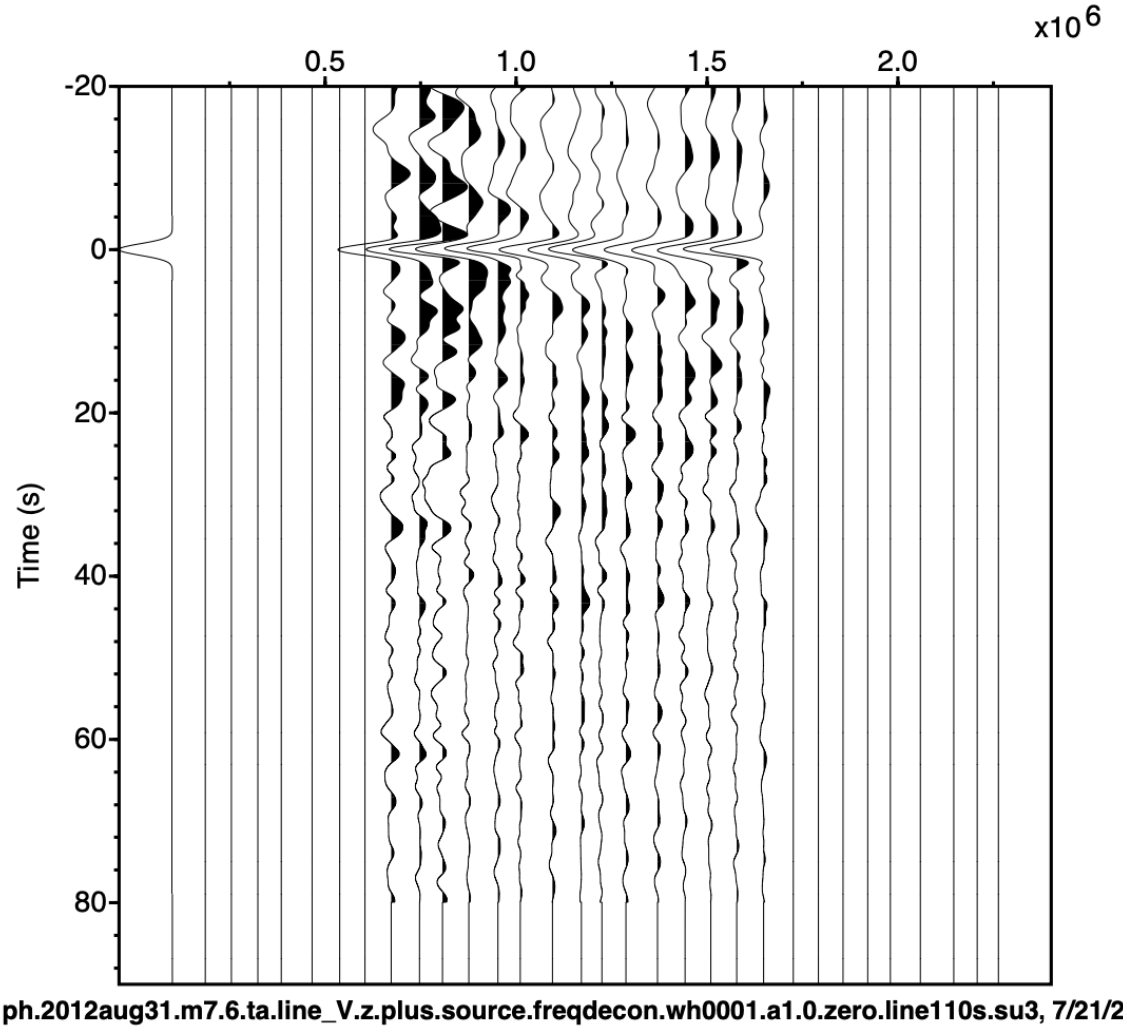


Figure C17 shows step 105 for an earthquake on August 31, 2012, with a magnitude of 7.6 for Line V. This example shows a negative polarity plot with relative station spacing with a Gaussian parameter of α=1.0. This earthquakes source wavelet was estimated by SESAME. Trace 1 is the deconvolved source wavelet.

FIGURE C18

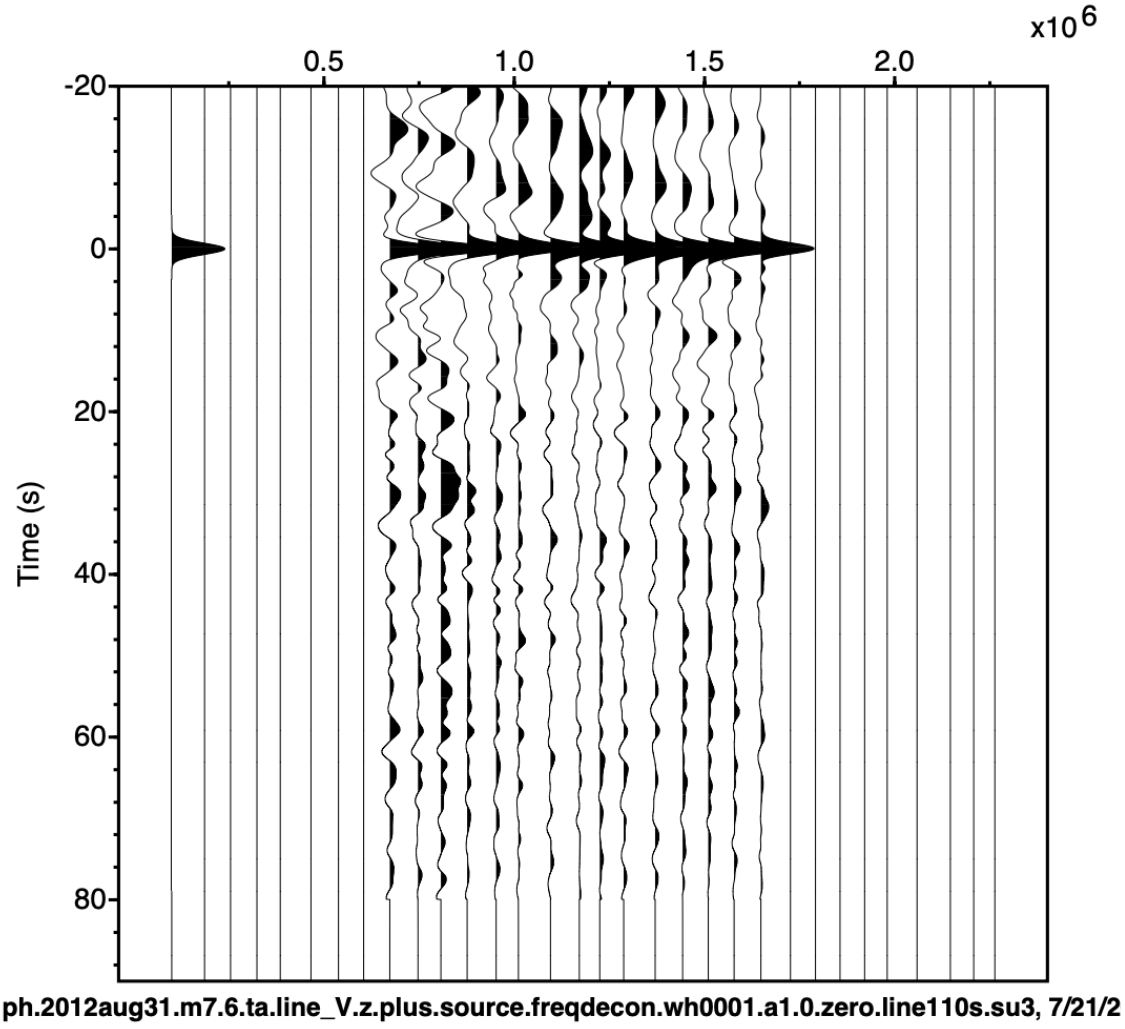


Figure C18 shows step 105 for an earthquake on August 31, 2012, with a magnitude of 7.6 for Line V. This example shows a positive polarity plot with relative station spacing with a Gaussian parameter of α=1.0. This earthquakes source wavelet was estimated by SESAME. Trace 1 is the deconvolved source wavelet.

FIGURE C19

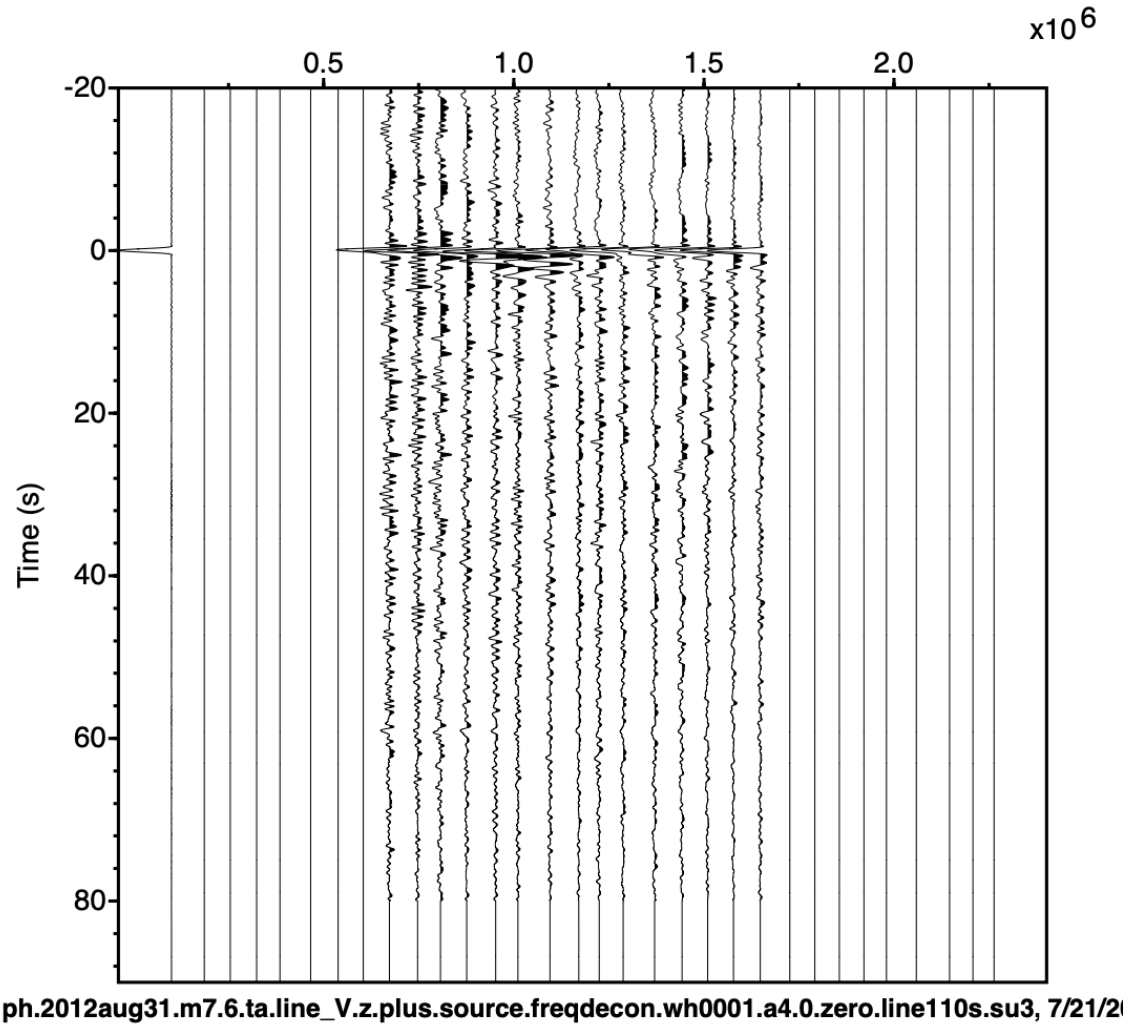


Figure C19 shows step 105 for an earthquake on August 31, 2012, with a magnitude of 7.6 for Line V. This example shows a negative polarity plot with relative station spacing with a Gaussian parameter of α=4.0. This earthquakes source wavelet was estimated by SESAME. Trace 1 is the deconvolved source wavelet.

FIGURE C20

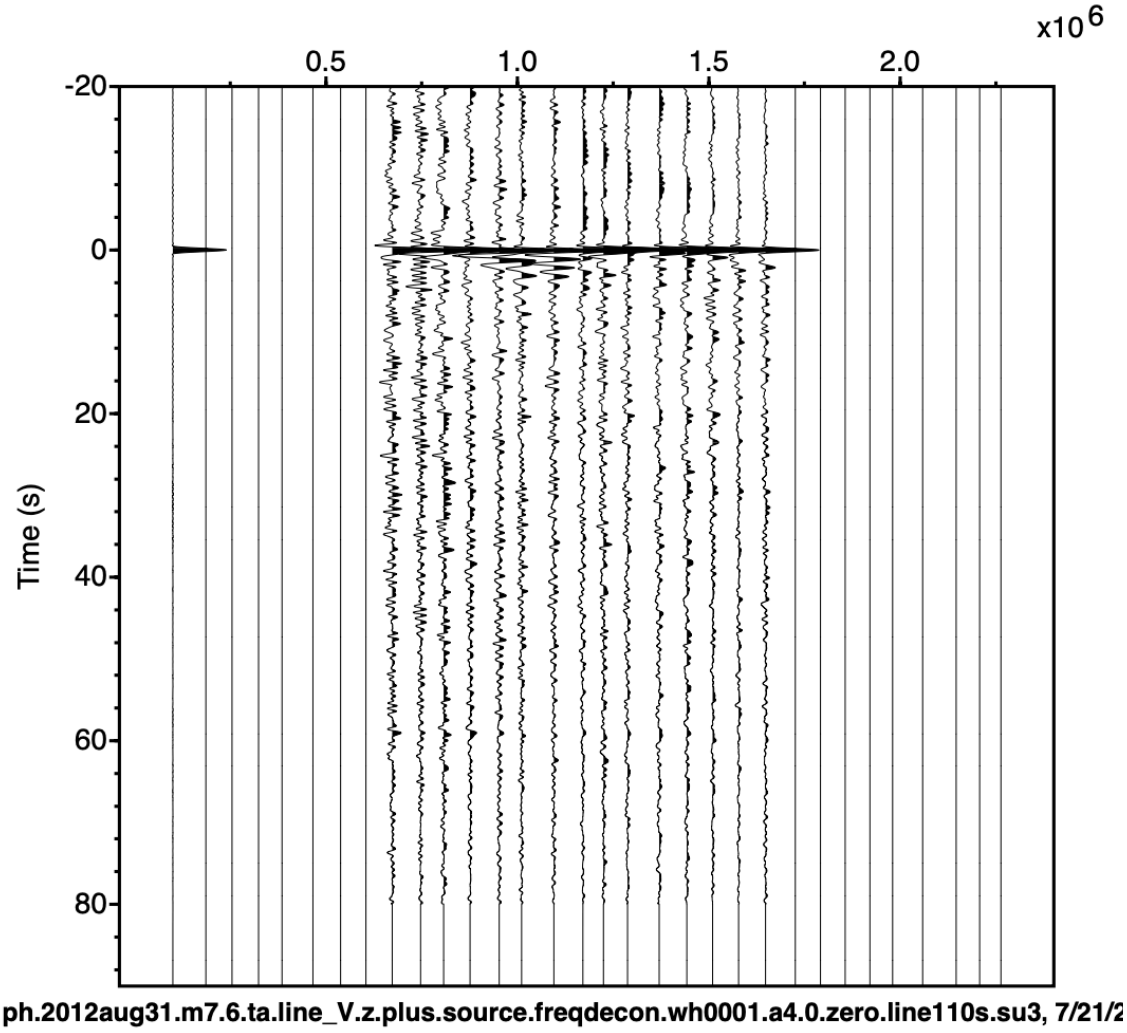


Figure C20 shows step 105 for an earthquake on August 31, 2012, with a magnitude of 7.6 for Line V. This example shows a positive polarity plot with relative station spacing with a Gaussian parameter of α=4.0. This earthquakes source wavelet was estimated by SESAME. Trace 1 is the deconvolved source wavelet.

FIGURE C21

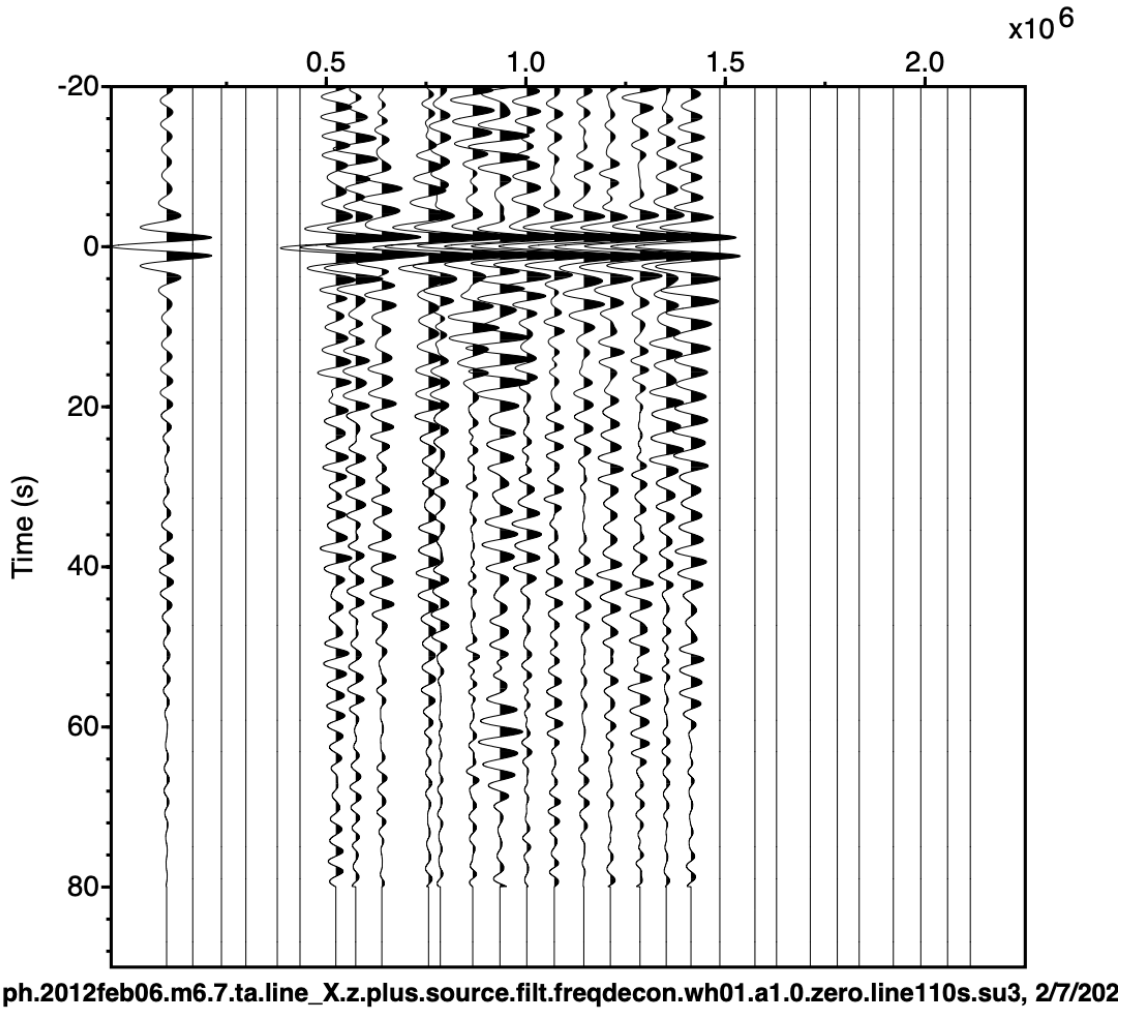


Figure C21 shows step 105 for an earthquake on February 06, 2012, with a magnitude of 6.7 for Line X. This example shows a negative polarity plot with relative station spacing with a Gaussian parameter of α=1.0. This earthquakes source wavelet was estimated by stacking all traces to create a new (filtered) wavelet. The "wh" parameter has also been changed. Trace 1 is the deconvolved source wavelet.

FIGURE C22

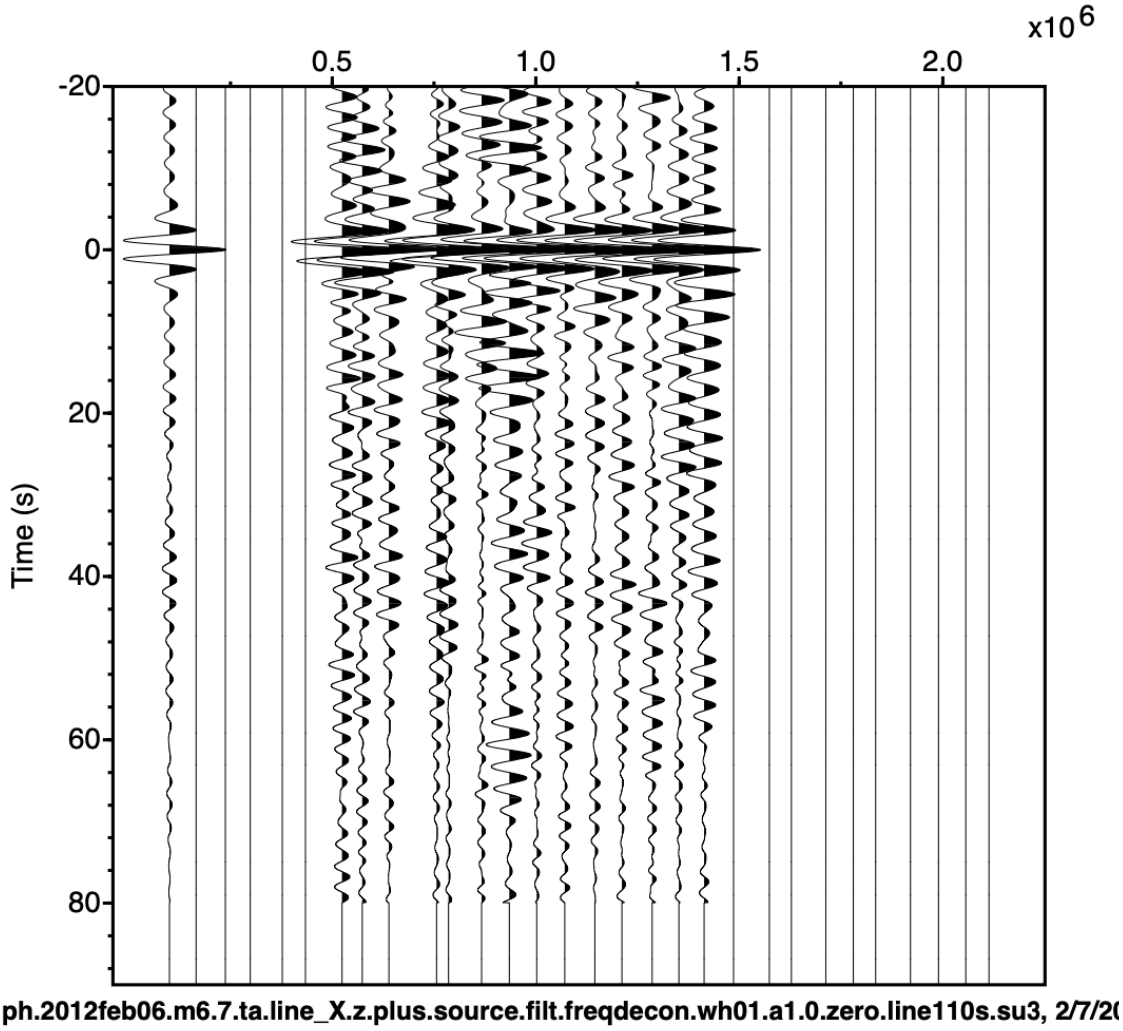


Figure C22 shows step 105 for an earthquake on February 06, 2012, with a magnitude of 6.7 for Line X. This example shows a positive polarity plot with relative station spacing with a Gaussian parameter of α=1.0. This earthquakes source wavelet was estimated by stacking all traces to create a new (filtered) wavelet. The “wh” parameter has also been changed. Trace 1 is the deconvolved source wavelet.

FIGURE C23

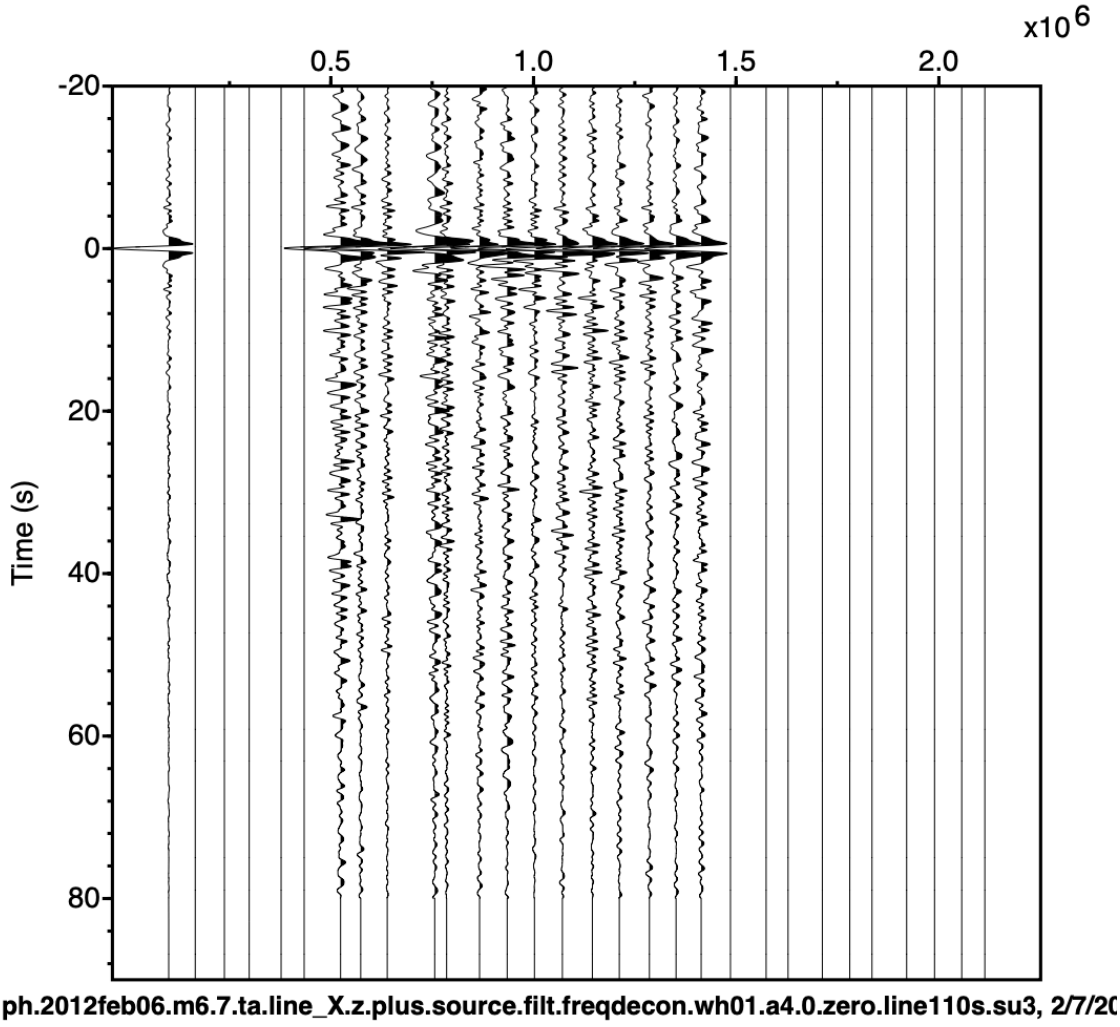


Figure C23 shows step 105 for an earthquake on February 06, 2012, with a magnitude of 6.7 for Line X. This example shows a negative polarity plot with relative station spacing with a Gaussian parameter of α=4.0. This earthquakes source wavelet was estimated by stacking all traces to create a new (filtered) wavelet. The “wh” parameter has also been changed. Trace 1 is the deconvolved source wavelet.

FIGURE C24

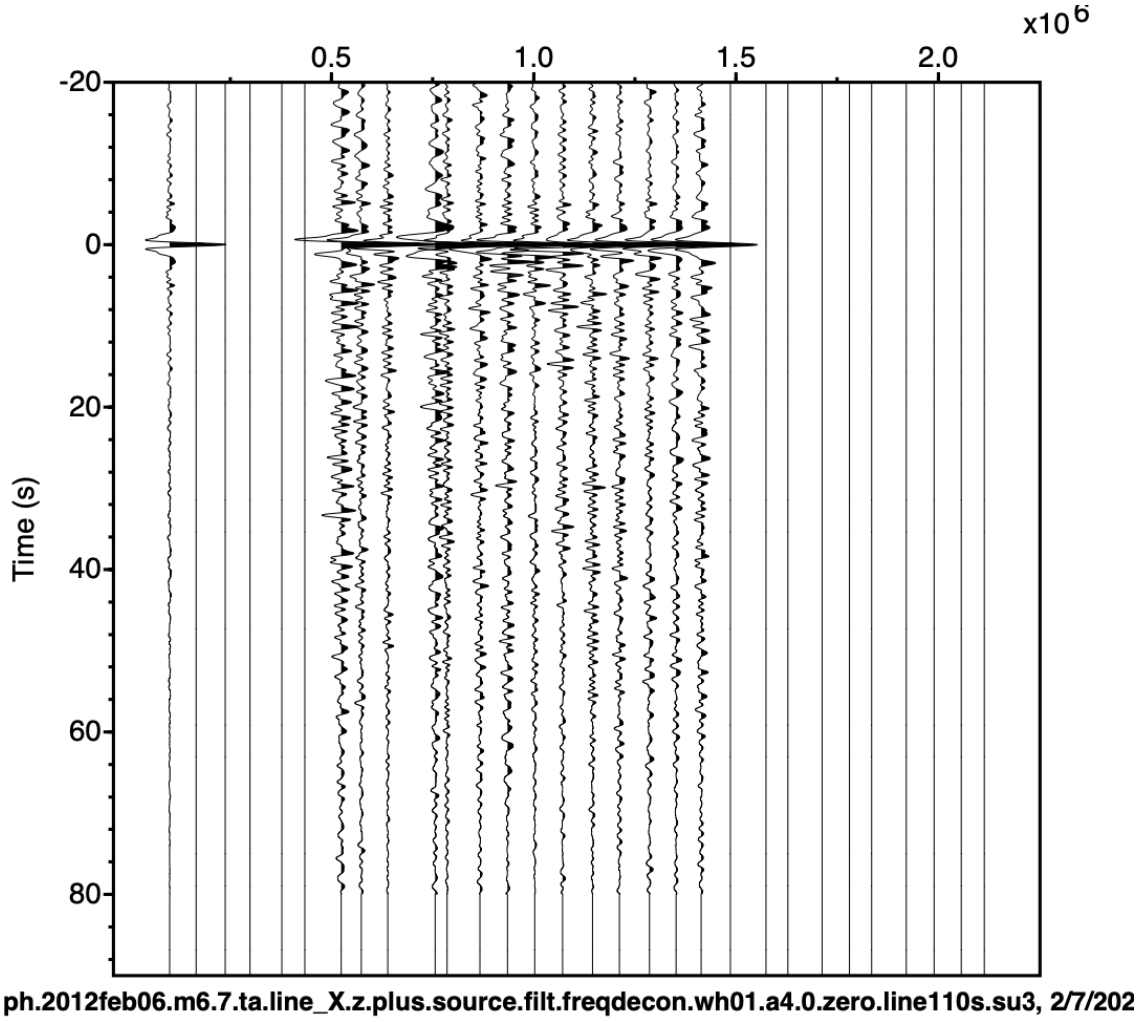


Figure C24 shows step 105 for an earthquake on February 06, 2012, with a magnitude of 6.7 for Line X. This example shows a positive polarity plot with relative station spacing with a Gaussian parameter of α=4.0. This earthquakes source wavelet was estimated by stacking all traces to create a new (filtered) wavelet. The “wh” parameter has also been changed. Trace 1 is the deconvolved source wavelet.

STEP 201

This job takes the previous deconvolved gathers and weighs each trace by its signal level. This is done so noisy traces will not be weighted as much as non-noisy traces for stacking, to enhance the signal to noise ratio. Weighting each trace is done by first normalizing each trace by its maximum value (typically this is the direct arrival) and then going back and normalizing each trace again by the root mean square (RMS) value of noise in the pre-event window before the direct arrival. This decreases the overall amplitude of noisy traces, minimizing their contribution to the stack.

Then, plots of the scaled traces with normal and reversed polarity are created. The normal polarity plots have normalized each trace by its maximum value. The reverse polarity plots have not been normalized to see the effect of the RMS noise division, which appears better in reversed polarity plots.

A mute job for step 201 was created to mute areas affected by bandpass filtering in the window close to the direct arrival to reduce noise from artifacts in shallow reflections.

I have included example images of the plots that step 201 created for the mute job for Gaussian parameters of α=1.0 (Figure C25). The other plots are identical to step 105 plots.

FIGURE C25

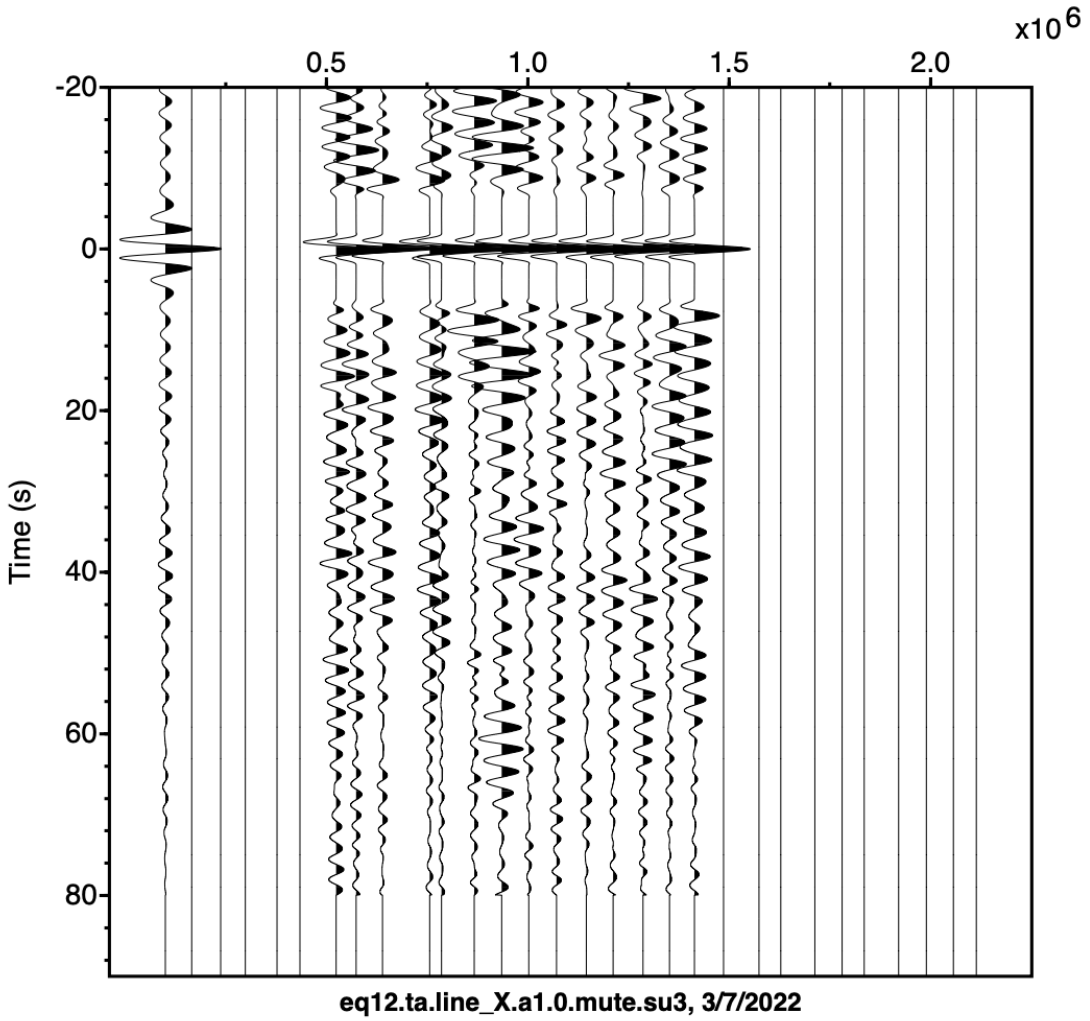


Figure C25 shows step 201 for an earthquake on February 06, 2012, with a magnitude of 6.7 for Line X. This example shows a positive polarity plot with relative station spacing with a Gaussian parameter of α=1.0. This earthquakes source wavelet was estimated by stacking all traces to create a new (filtered) wavelet. The “wh” parameter has also been changed. This plot showcases the muting near the direct arrival to get rid of artifacts of bandpass filtering. Trace 1 is the deconvolved source wavelet.

STEP 202

The final step is to obtain the final stacked gathers. This job works with the weighted traces and sums all of the traces at the same station together. This creates a final, stacked gather. Then, samples are multiplied by a factor equal to the square root of the two-way time to smoothly increase amplitudes of later reflections. This serves to counteract the effect of geometric spreading and attenuation due to scattering and absorption. Plots of stacked gathers are created with both normal and reversed polarity to showcase different signals of different impedance contrasts. For both cases, traces are plotted with their true relative amplitudes. Because amplitudes will normally be proportional to the number of earthquakes used to construct each stacked trace, this serves to indicate the relative reliability of the image over different parts of the stacked section. These are the final stacks that are used for interpretation. These plots show correct relative station spacing for each line and show laterally continuous structures in the lithosphere with enhanced signal to noise levels. These plots are created with a range of Gaussian parameters (α=1.0-4.0) (Langston, 1979). With these gathers, two-way time can be converted to depth with velocity models to show the actual depths to the structures that are seen (Buehler & Shearer, 2017; Parker et al., 2016; Hawman et al., 2012; Kennett, 2015; Verellen et al., 2020).

I have included an example of Step 202 that showcases what a final stacked gather looks like. The example is of Line V with a negative polarity and a Gaussian parameter of α=2.0. All earthquakes that produced more signal than noise was used for the final stack (Figure C26).

FIGURE C26

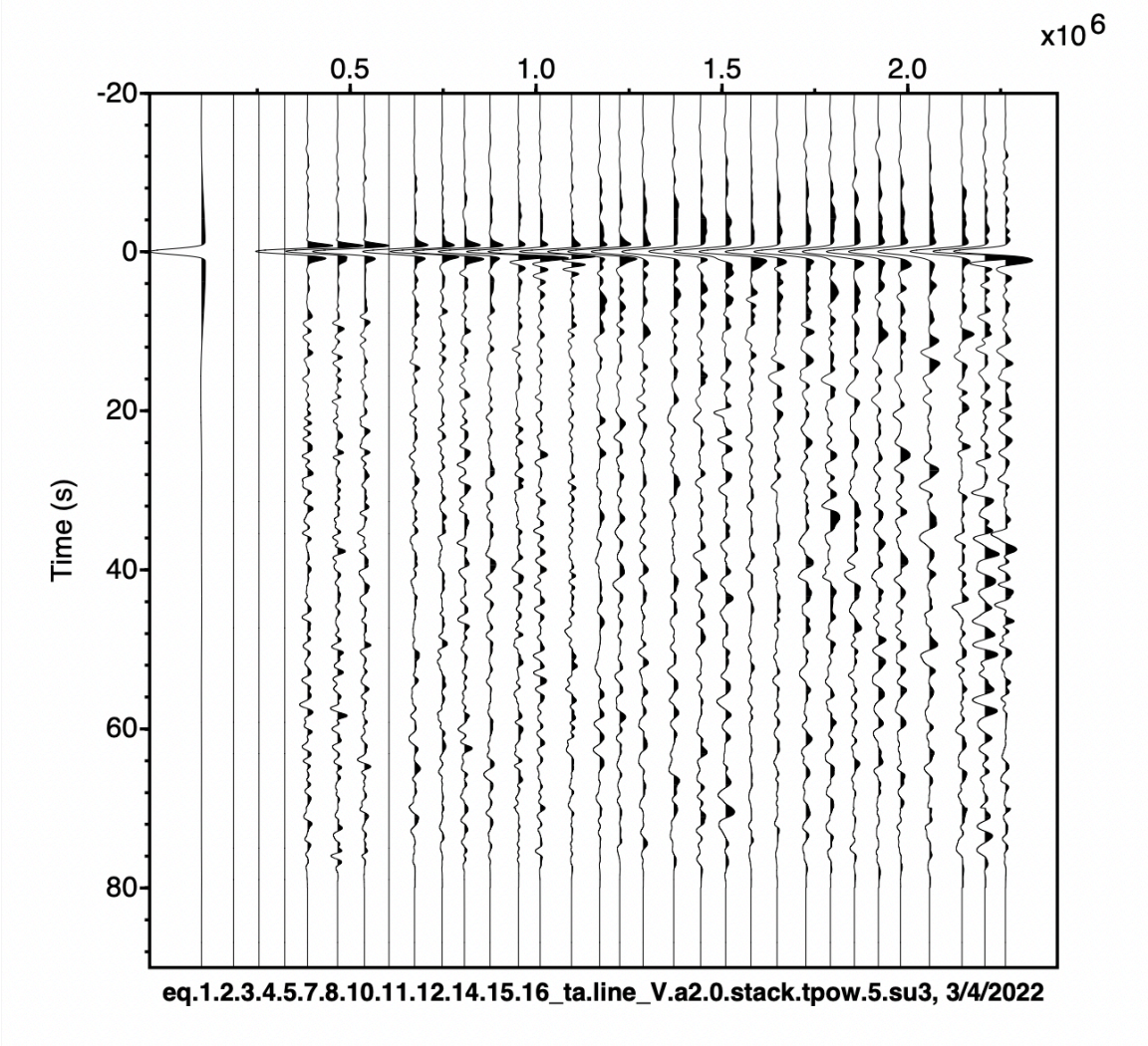


Figure C26 shows an example plot for Line V with all stacked earthquakes that did not create too much noise. This example shows a negative polarity plot with relative station spacing with a Gaussian parameter of α=2.0. Trace 1 is the stack of all the deconvolved source wavelets.

OVERLAY- SIGNFILTER FIGURES AND COLOR PLOTS

While overlay and comparison figures were created to compare recent research to this study, this type of figure was also produced with profiles from this study alone. Figures of signfiltered traces superimposed on their matching color plot were created to compare signals found in both types of plots. Overall, the idea was to look for matching signals to make sure that signals matched where expected as well as to look for places where the signals did not match. For example, signals from the signfilter plot will not match up with dipping structures in the color plots, no matter how continuous or strong these signals are, as signfilter plots preserve only those signals with near-horizontal dip.

Color plot a1 and the signfilter overlay for Line M a1w7 shows a close match of signals (Figure C27). In particular, the signfilter signal matches up with a negative polarity (red/orange signal) color signal at around 35 s TWT in the east and highly reflective signals in the west around 42-46 s TWT. Based on the previous discussion, these signals likely relate to the LAB. It is possible that the LAB signal in the west is more reflective and complex than the signal in the east due to the transition deepening and thickening. Overall, this figure also shows a general increase in reflectivity below around 40 s TWT. This is expected as these signals are presumed to be related to drag-induced flow in the uppermost asthenosphere.

One other notable color plot and signfilter overlay was with signfilter plot Line P a1w7 with color plot a1 (Figure C28). There is a good matching signal around 26 s TWT in the

east to an orange color signal. This may be a reflection from an MLD. Overall, a general increase in reflectivity below around 35 s TWT can be seen in this figure, further highlighting that this methodology is recovering signals that may be related to drag-induced flow in the asthenosphere. Note the very prominent blue signal around 60 s TWT on the color plot that the signfilter does not mimic. This is because the signal is dipping towards the west.

Other color plot with signfilter overlays can be found below (Figures C29-C37).

FIGURE C27

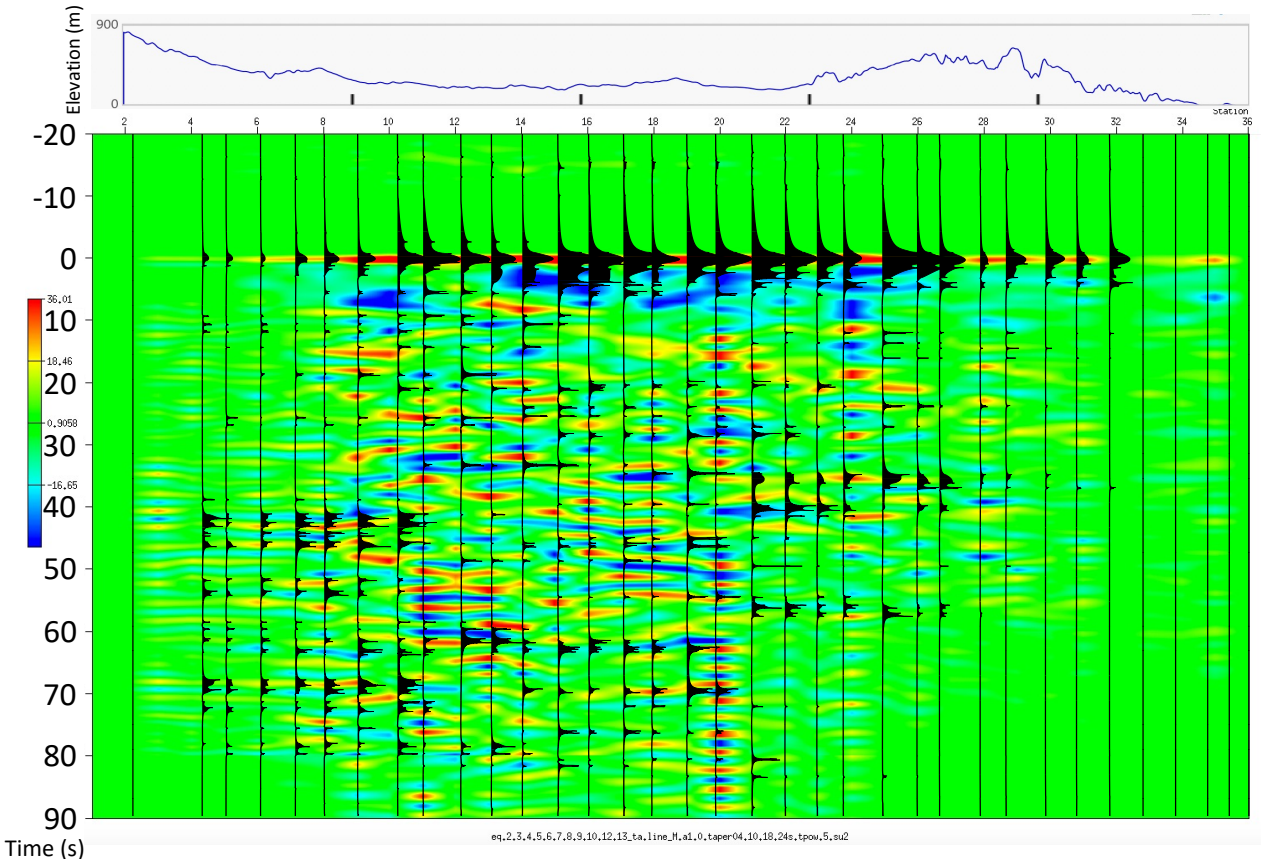


Figure C27 shows a Line M a1w7 signfilter plot superimposed on an a1 Line M color plot.

FIGURE C28

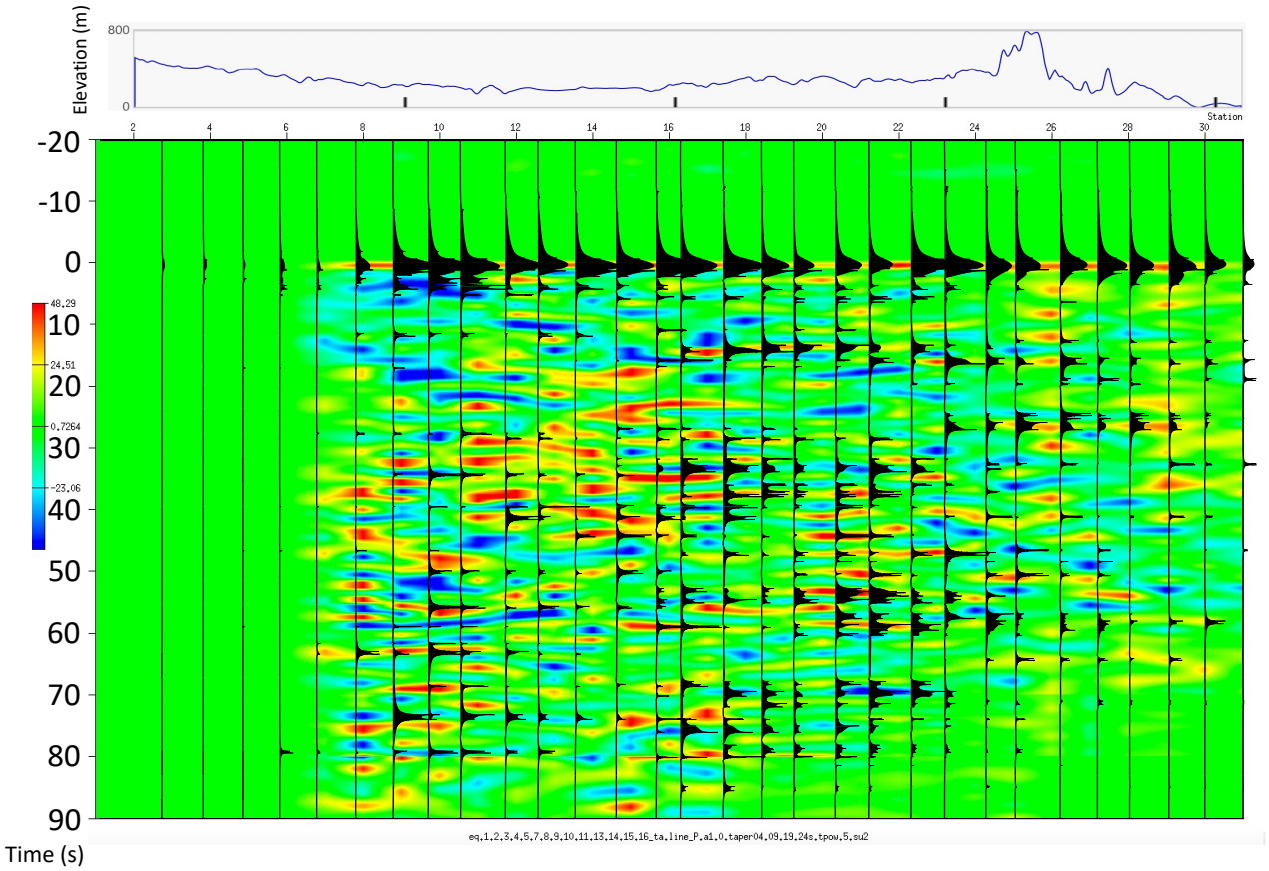


Figure C28 shows a Line P a1w7 signfilter plot superimposed on an a1 Line P color plot.

FIGURE C29

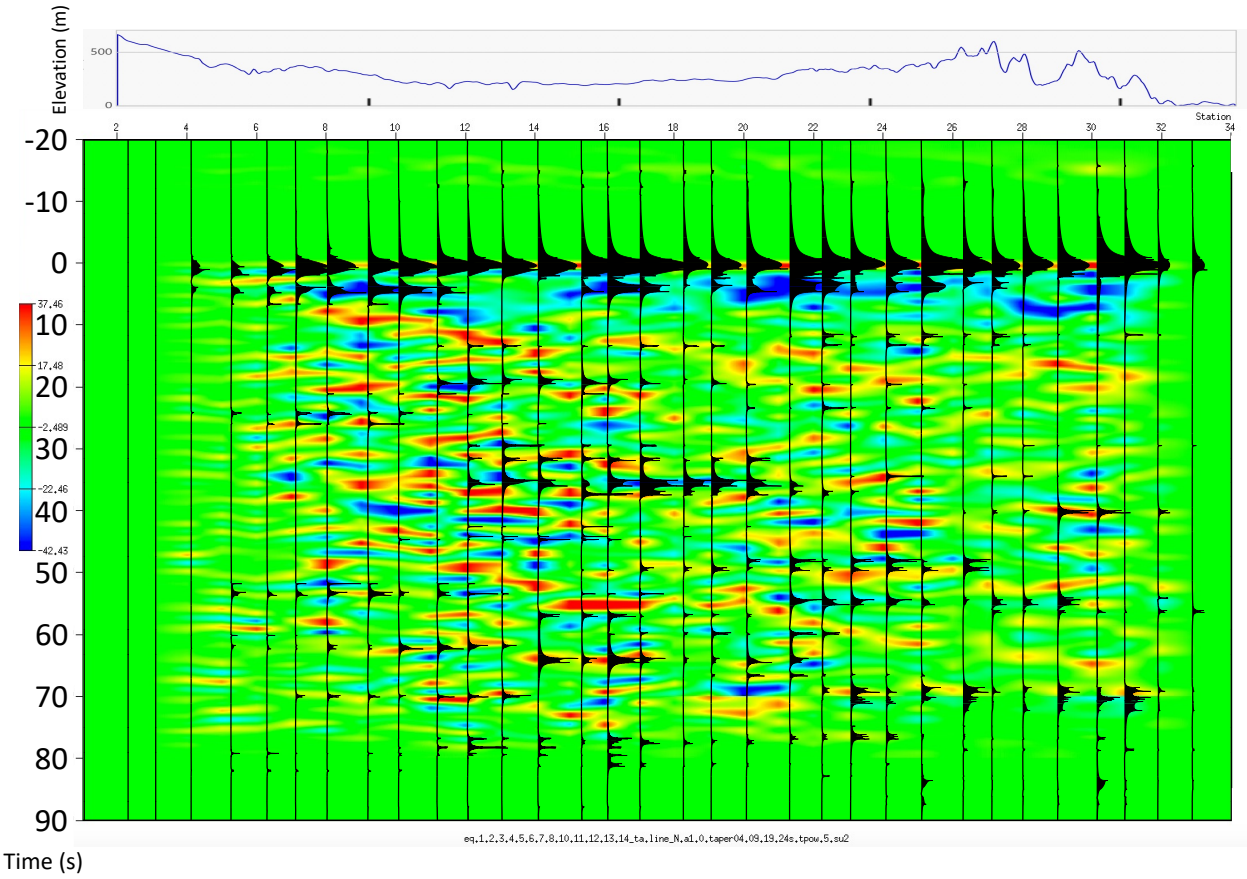


Figure C29 shows a Line N a1w7 signfilter plot superimposed on an a1 Line N color plot. This plot shows matching signals around 35 s in the middle of the section (LAB related), around 49/50 s and 55 s in the east, and around 55 s in the west (asthenosphere related). Overall, a general reflectivity increase below around 40 s is seen.

FIGURE C30

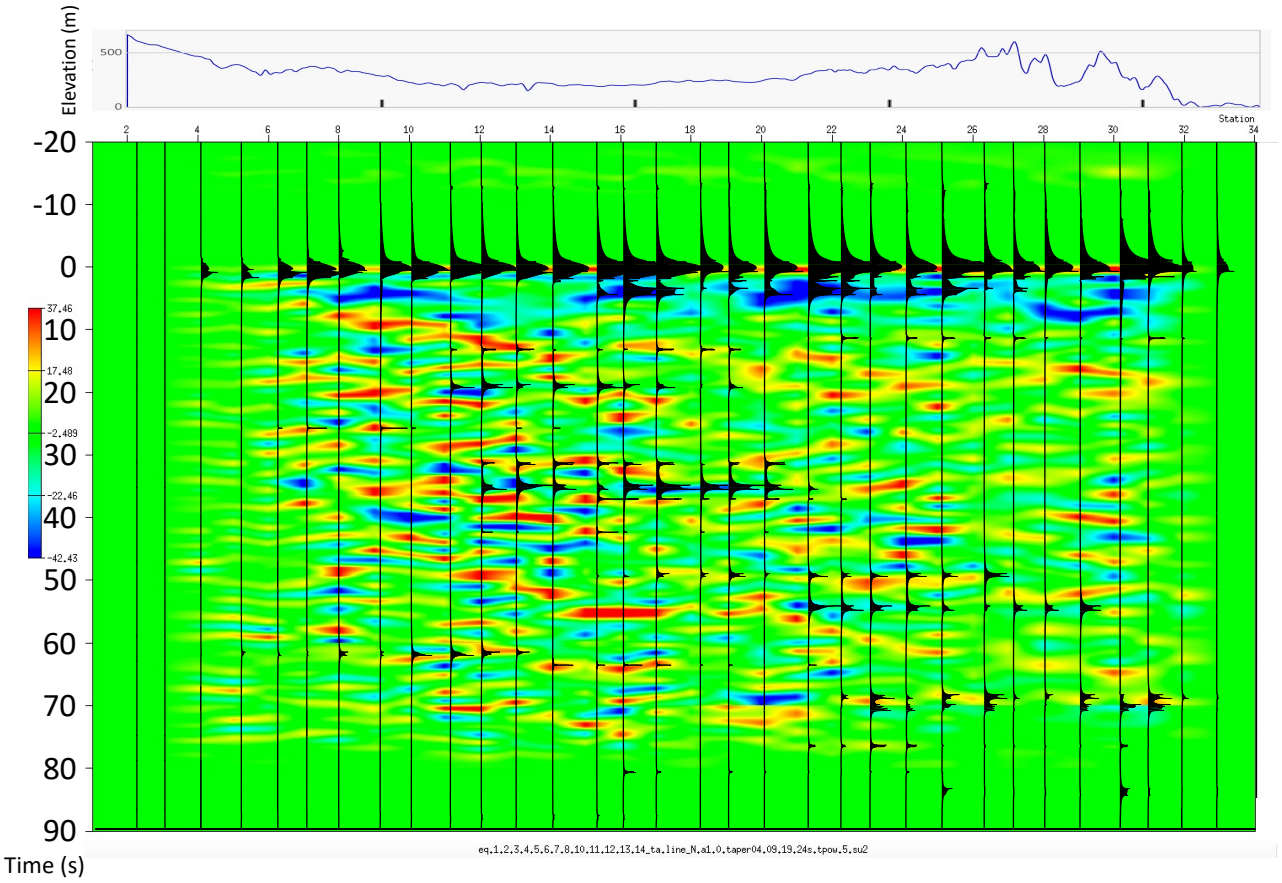


Figure C30 shows a Line N a1w9 signfilter plot superimposed on an a1 Line N color plot. This plot shows matching signals around 35 s in the middle of the section (LAB related), and around 50 s, 55 s, and 70 s in the east (asthenosphere related).

FIGURE C31

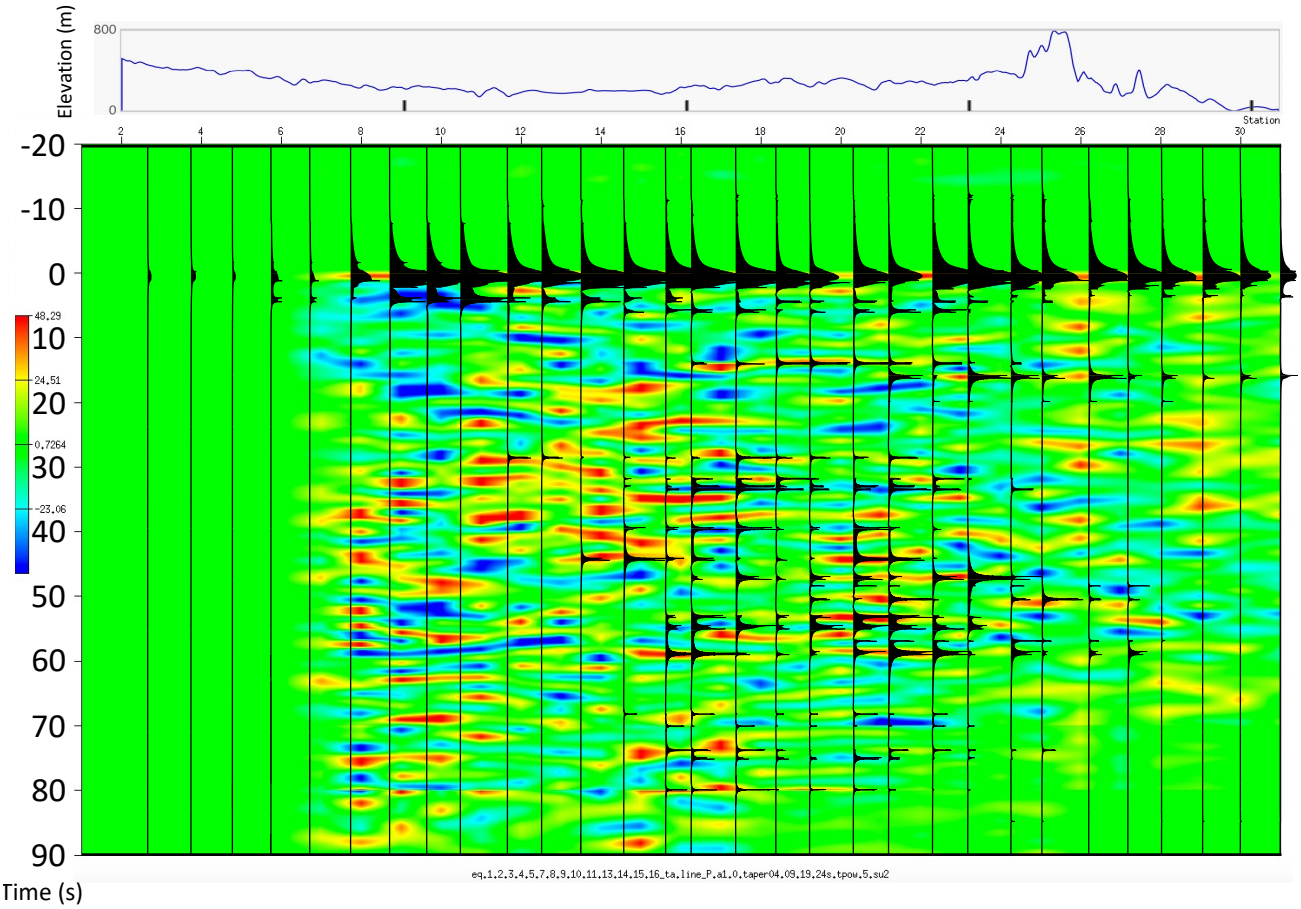


Figure C31 shows a Line P a1w9 signfilter plot superimposed on an a1 Line P color plot. This plot shows matching signals around 29 s, 33 s, and 40 s in the middle of the section (LAB related), and around 17 s in the east towards 14 s in the middle of the section (Moho related). Overall, a general reflectivity increase below around 40 s is seen.

FIGURE C32

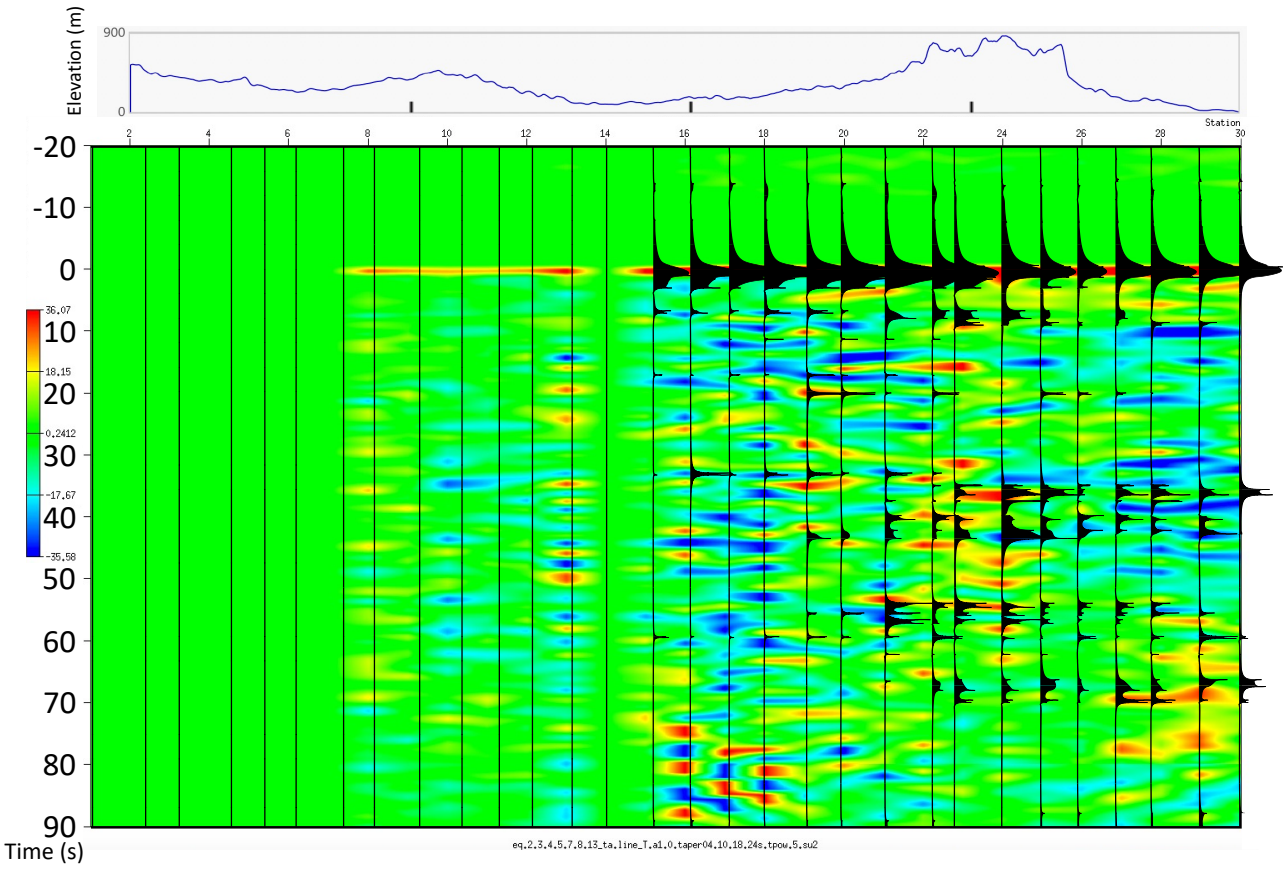


Figure C32 shows a Line T a1w7 signfilter plot superimposed on an a1 Line T color plot. This plot shows matching signals around 33 s in the middle of the section, and around 36 s and 43 s in the east. These signals are likely LAB related. There are also matching signals from 55- 70 s in the east that are likely drag induced flow related. Overall, a general reflectivity increase below around 40 s is seen.

FIGURE C33

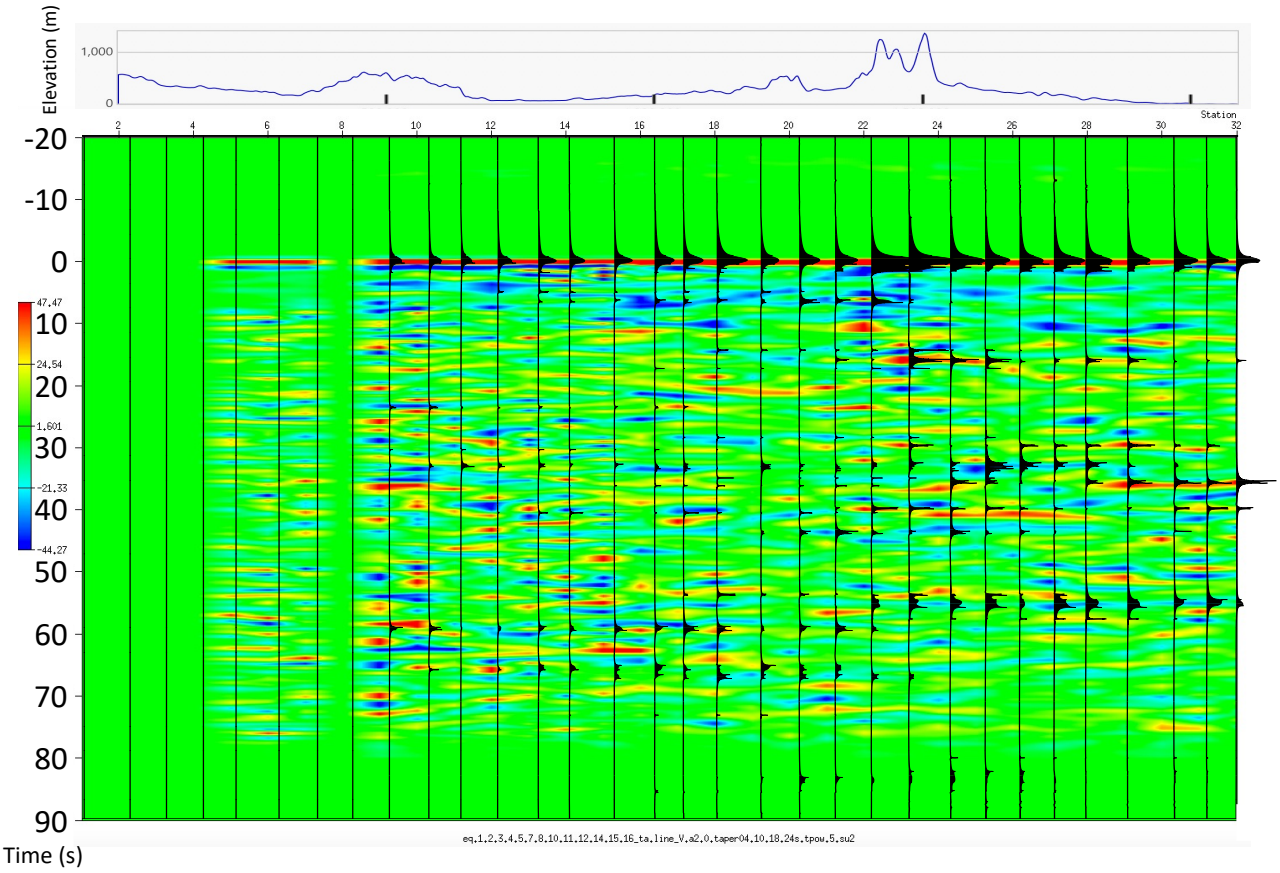


Figure C33 shows a Line V a2w9 signfilter plot superimposed on an a2 Line V color plot. This plot shows matching signals around 33 s in the middle of the section and around 30 s in the east, likely LAB related. There are also matching signals around 55 s in the east that are likely drag induced flow related. Also, matching signals around 17 s in the east are likely Moho related.

FIGURE C34

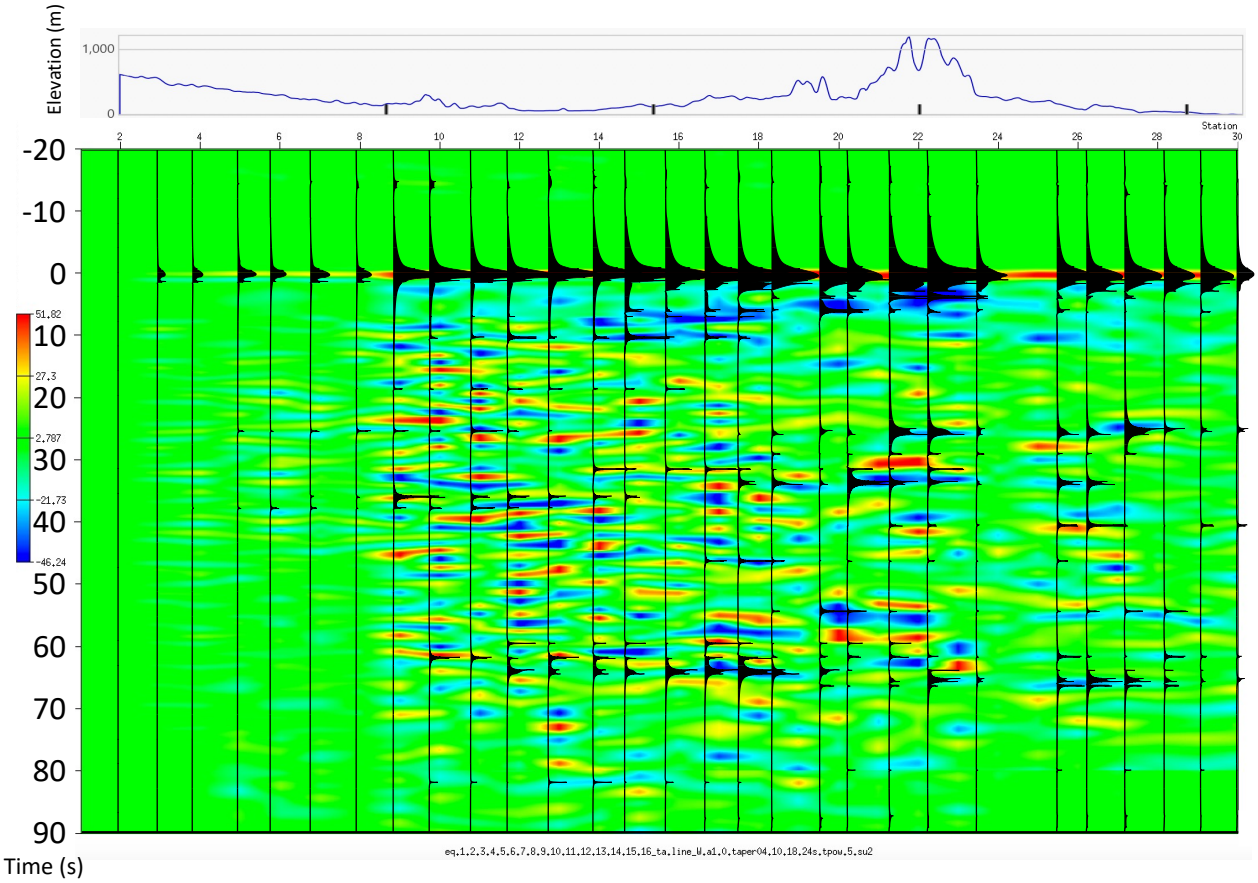


Figure C34 shows a Line W a1w9 signfilter plot superimposed on an a1 Line W color plot. This plot shows matching signals around 33-36 s in the middle of the section that are likely LAB related. There are also matching signals around 65 s in the east that are likely drag induced flow related. Also, matching signals around 25 s in the east are likely MLD related.

FIGURE C35

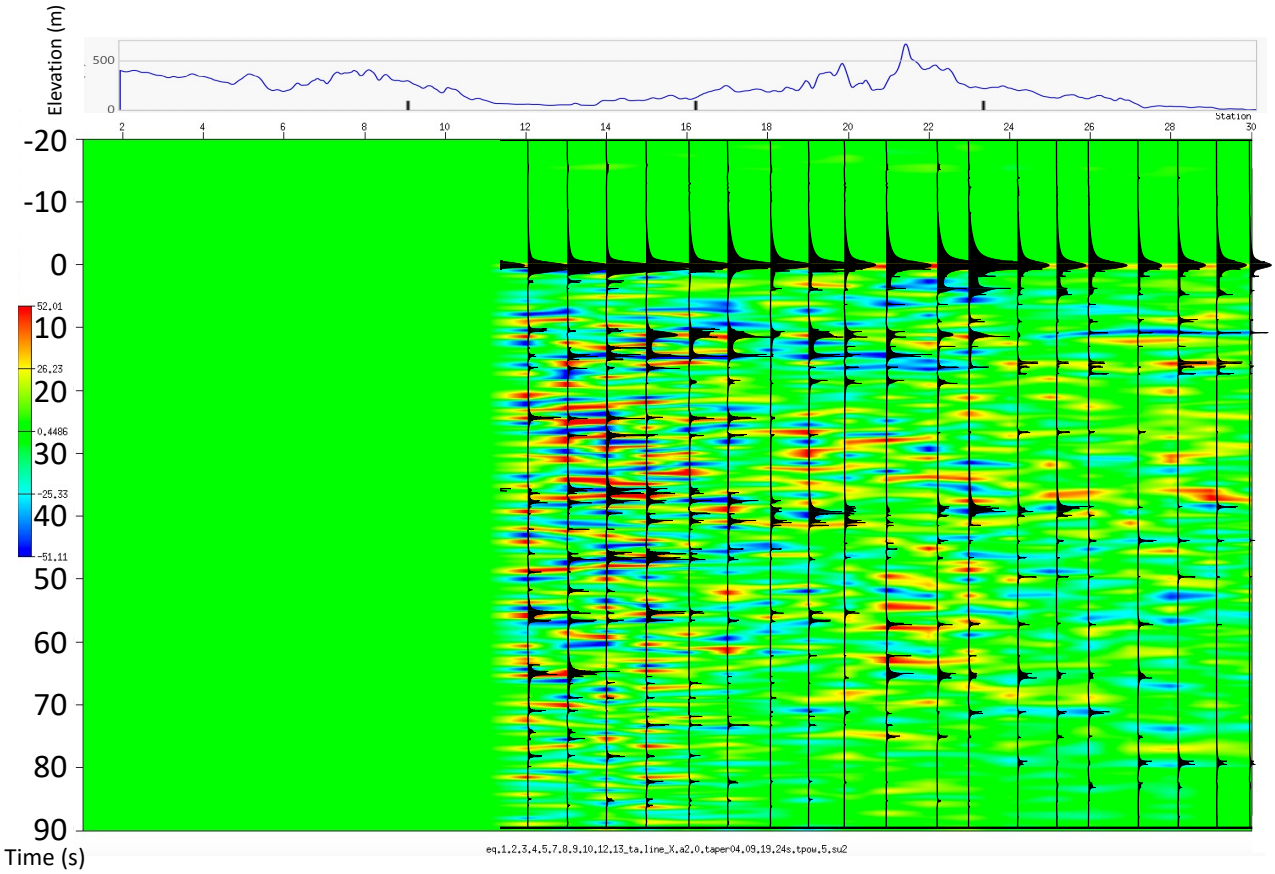


Figure C35 shows a Line X a2w7 signfilter plot superimposed on an a2 Line X color plot. This plot shows matching signals around 37-40 s in the middle of the section that are likely LAB related. There are also matching signals around 55 s throughout that are likely drag induced flow related. Also, matching signals around 12 s in the middle of the section are likely Moho related.

FIGURE C36

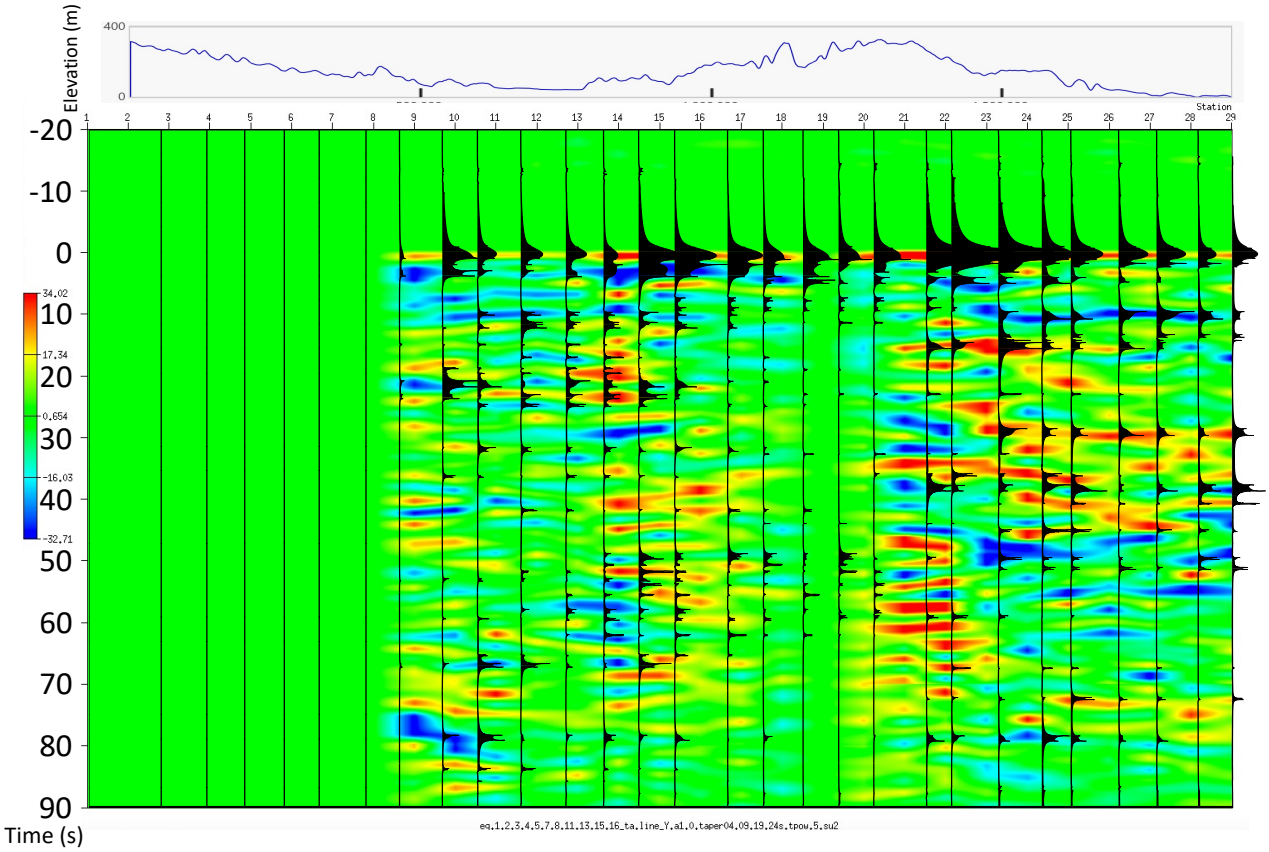


Figure C36 shows a Line Y a1w7 signfilter plot superimposed on an a1 Line Y color plot. This plot shows matching signals around 28 s in the eastof the section that are likely LAB related. Also, matching signals around 10 s in the east and west of the section are likely Moho related. There are also matching signals around 38 s in the east and 20-24 s in the west that may be due to MLD's.

FIGURE C37

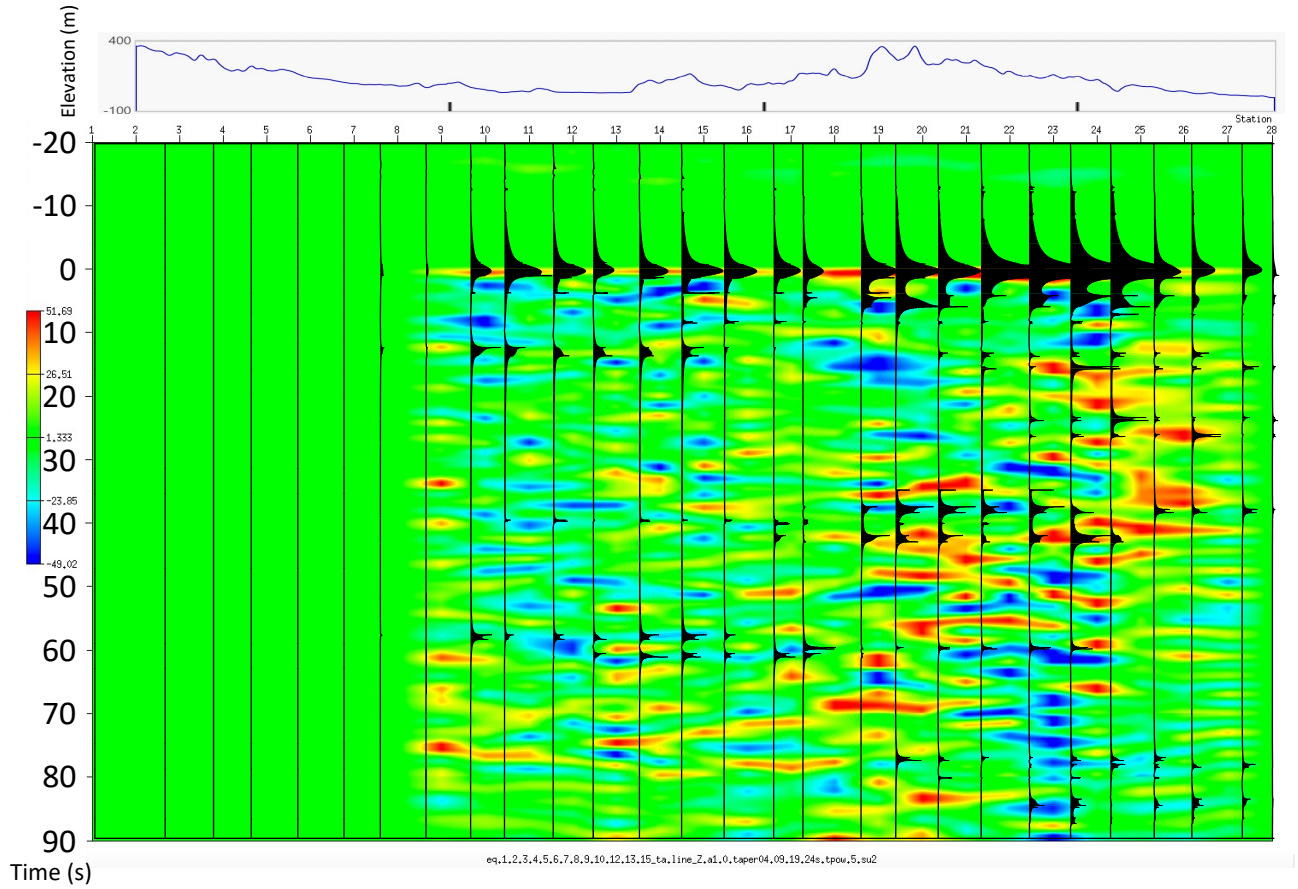
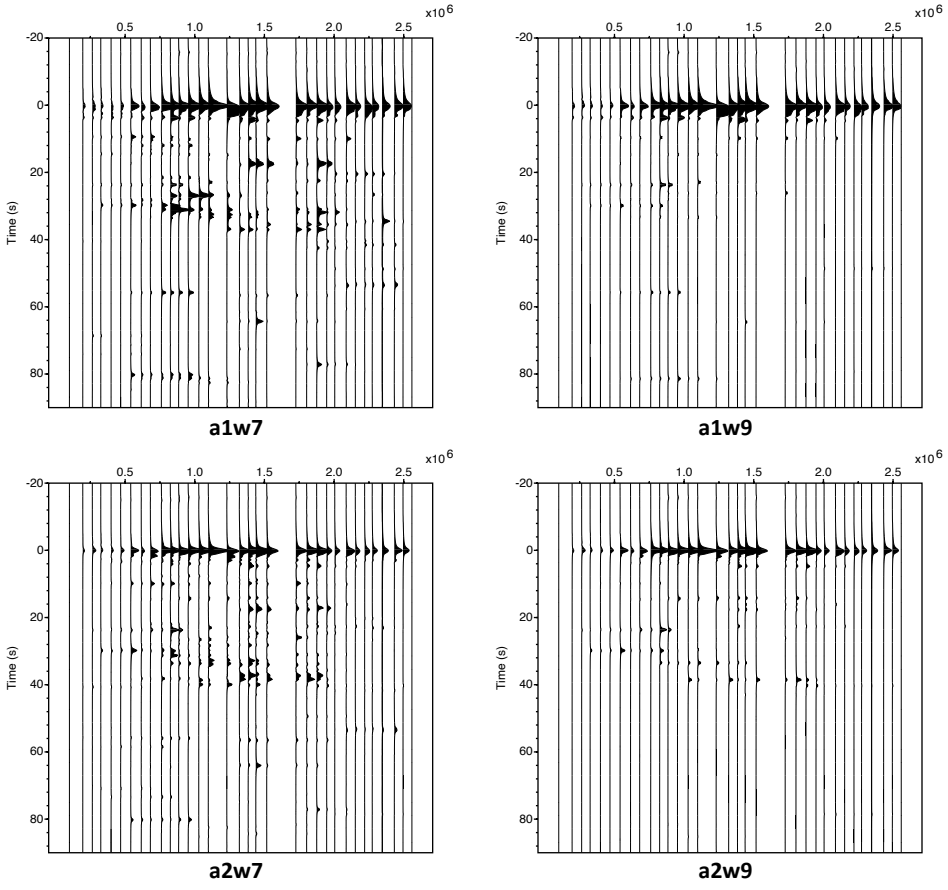


Figure C37 shows a Line Z a1w7 signfilter plot superimposed on an a1 Line Z color plot. This plot shows matching signals around 38 s and 42 s in the east that may be from an MLD.

APPENDIX D

SIGNFILTER FIGURES

FIGURE D1



Line L
(eq 1.2.3.4.5.6.7.8.10.11.12.13.16)

Figure D1 shows the composite plot of all smoothed signfilter plots with differing Gaussian parameters α=1.0 and α=2.0 with a mix of window lengths of 7 and 9 for Line L.

FIGURE D2

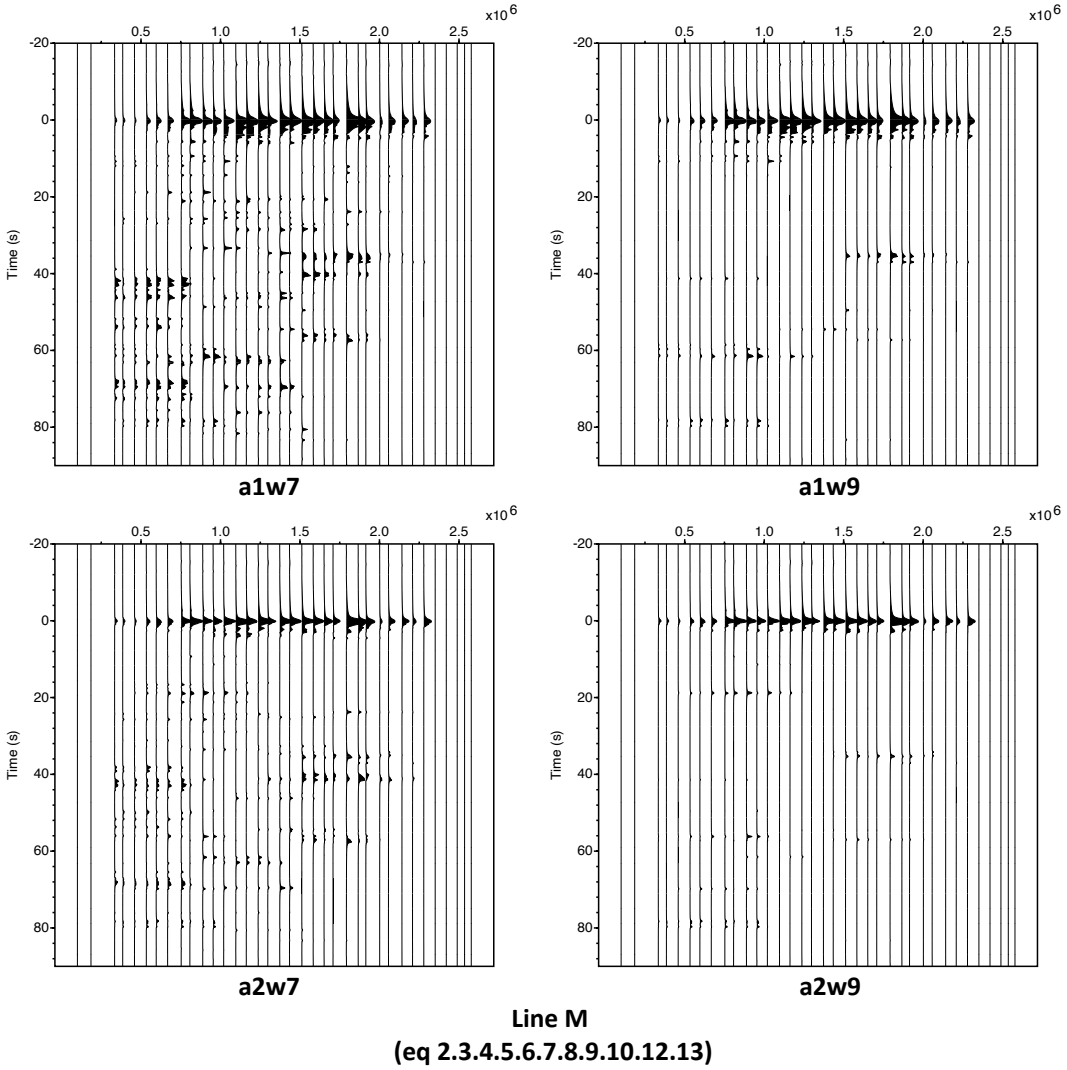


Figure D2 shows the composite plot of all smoothed signfilter plots with differing Gaussian parameters α=1.0 and α=2.0 with a mix of window lengths of 7 and 9 for Line M.

FIGURE D3

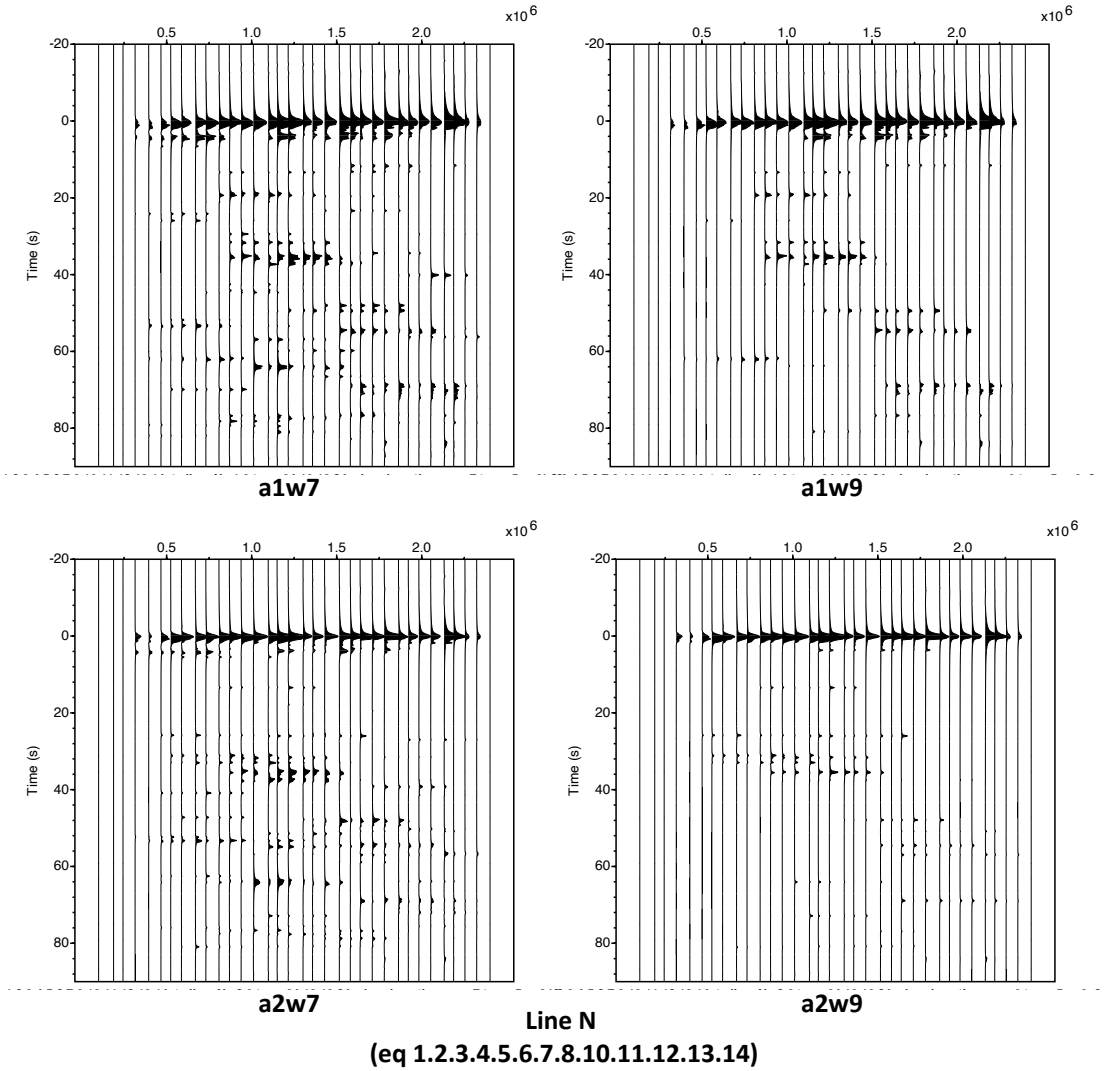


Figure D3 shows the composite plot of all smoothed signfilter plots with differing Gaussian parameters α=1.0 and α=2.0 with a mix of window lengths of 7 and 9 for Line N.

FIGURE D4

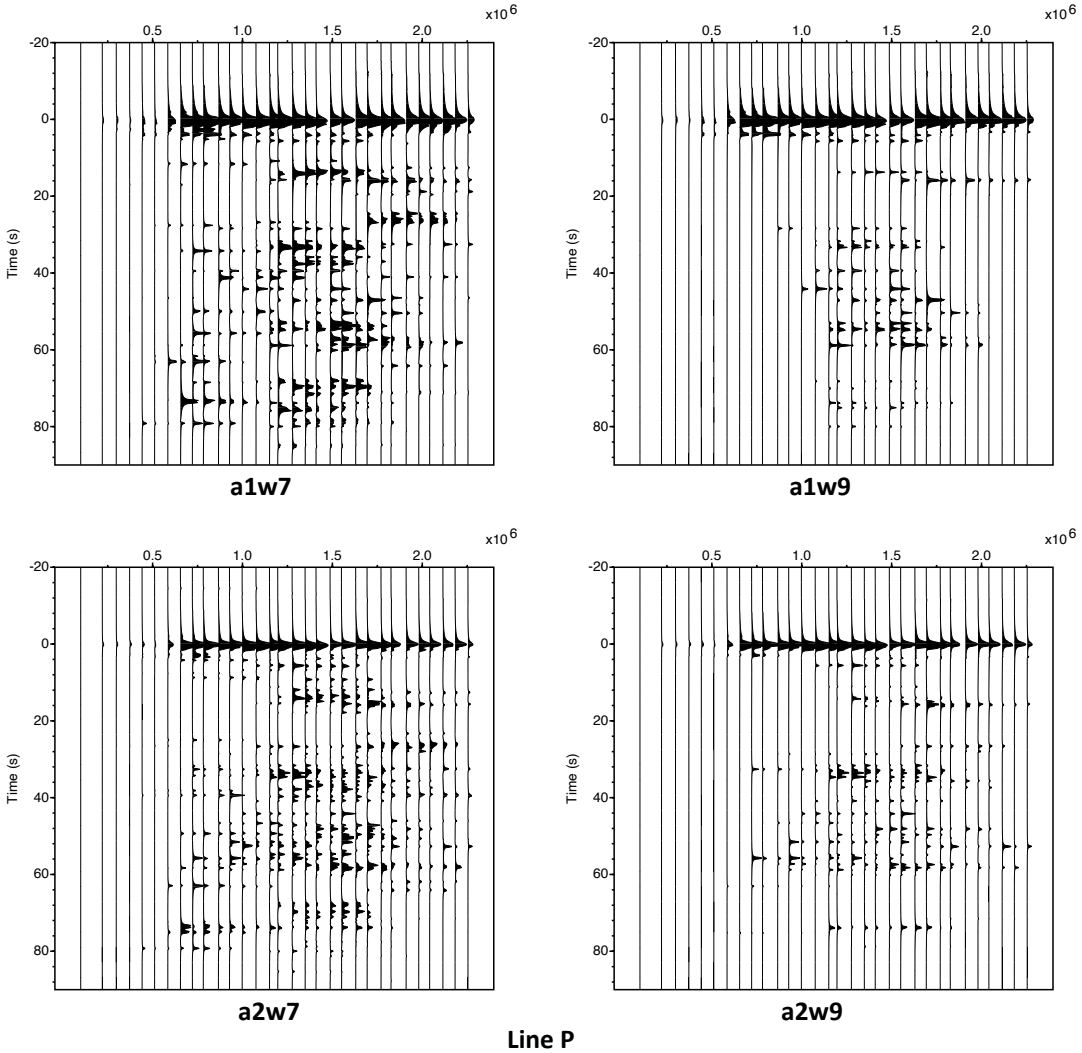


Figure D4 shows the composite plot of all smoothed signfilter plots with differing Gaussian parameters α=1.0 and α=2.0 with a mix of window lengths of 7 and 9 for Line P.

FIGURE D5

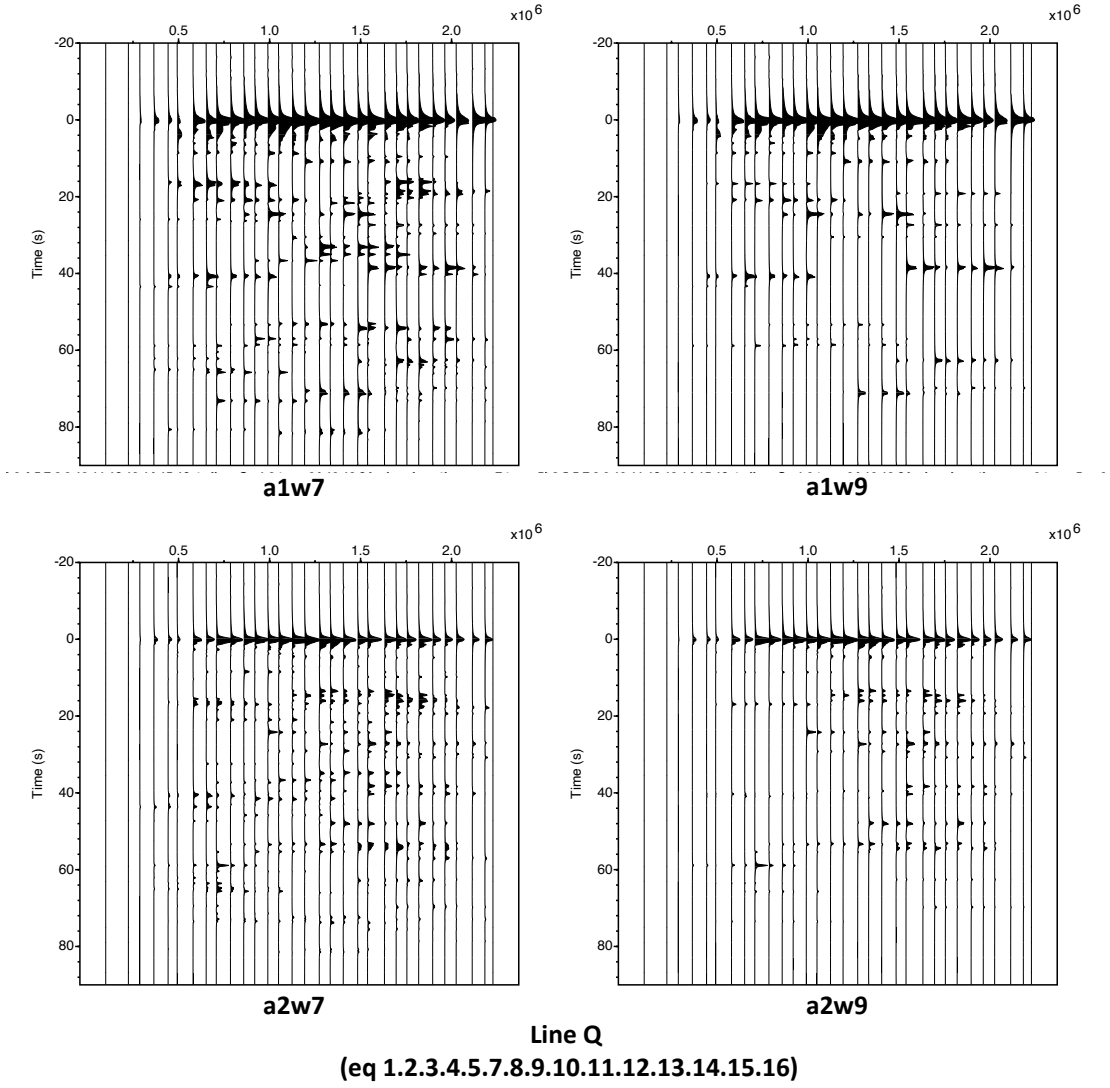


Figure D5 shows the composite plot of all smoothed signfilter plots with differing Gaussian parameters α=1.0 and α=2.0 with a mix of window lengths of 7 and 9 for Line Q.

FIGURE D6

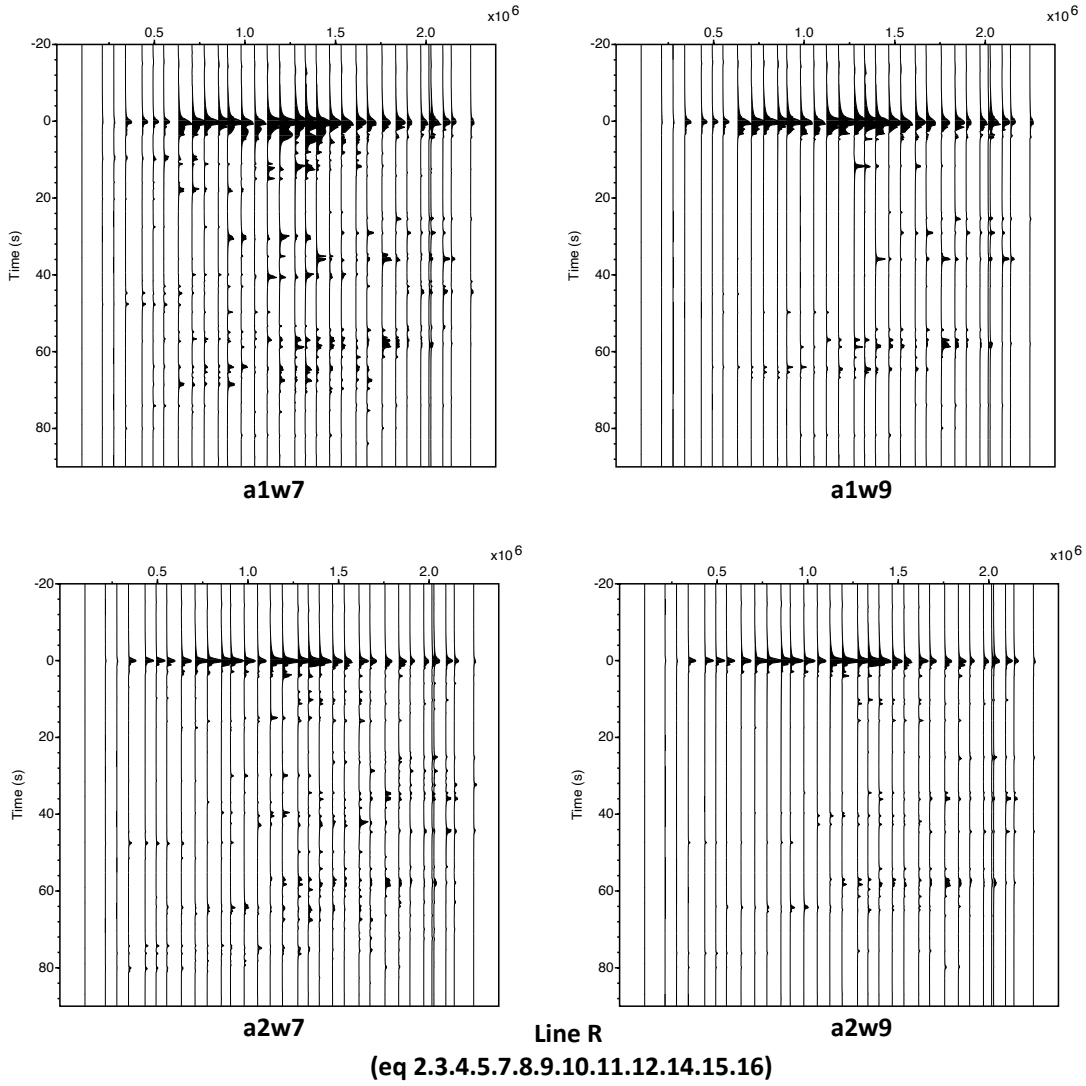


Figure D6 shows the composite plot of all smoothed signfilter plots with differing Gaussian parameters α=1.0 and α=2.0 with a mix of window lengths of 7 and 9 for Line R.

FIGURE D7

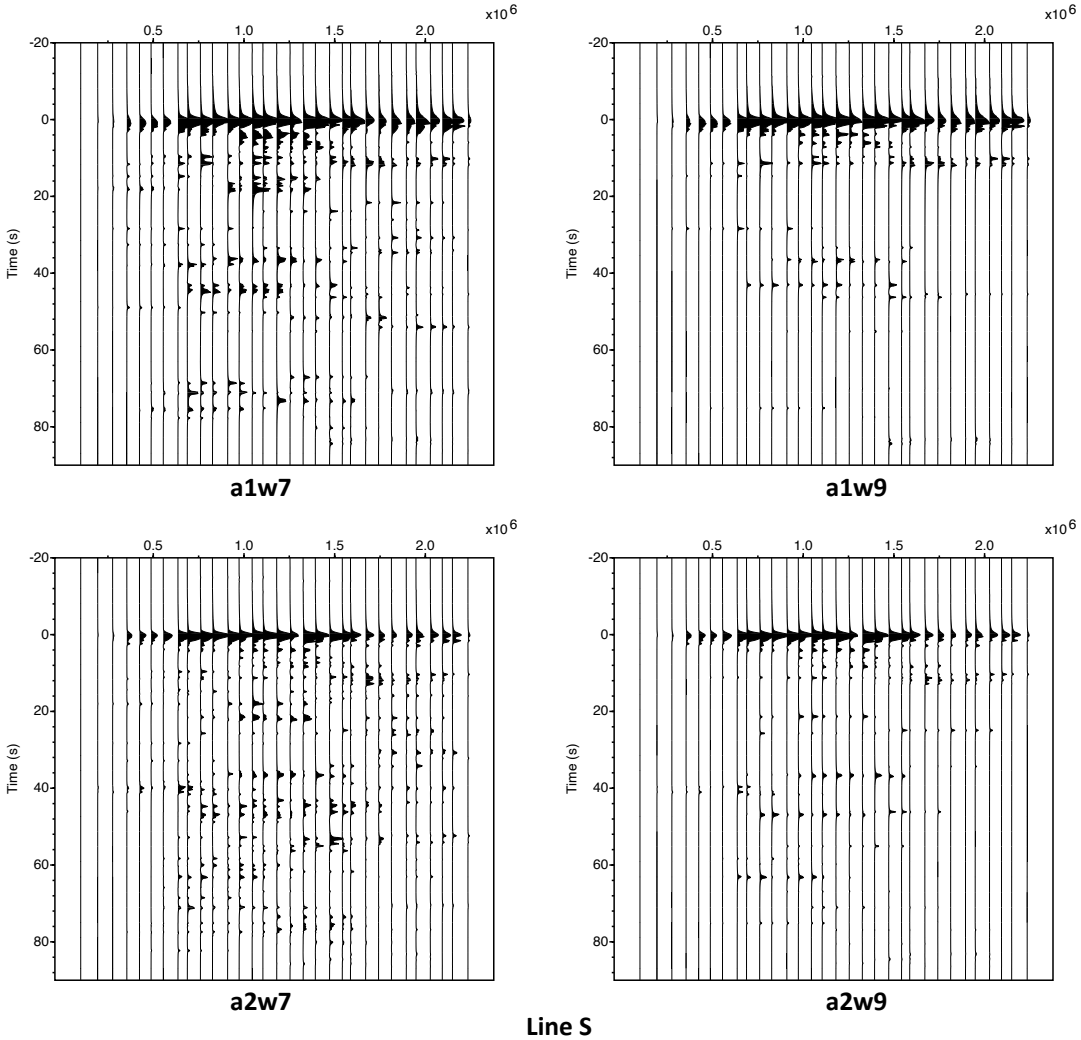


Figure D7 shows the composite plot of all smoothed signfilter plots with differing Gaussian parameters α=1.0 and α=2.0 with a mix of window lengths of 7 and 9 for Line S.

FIGURE D8

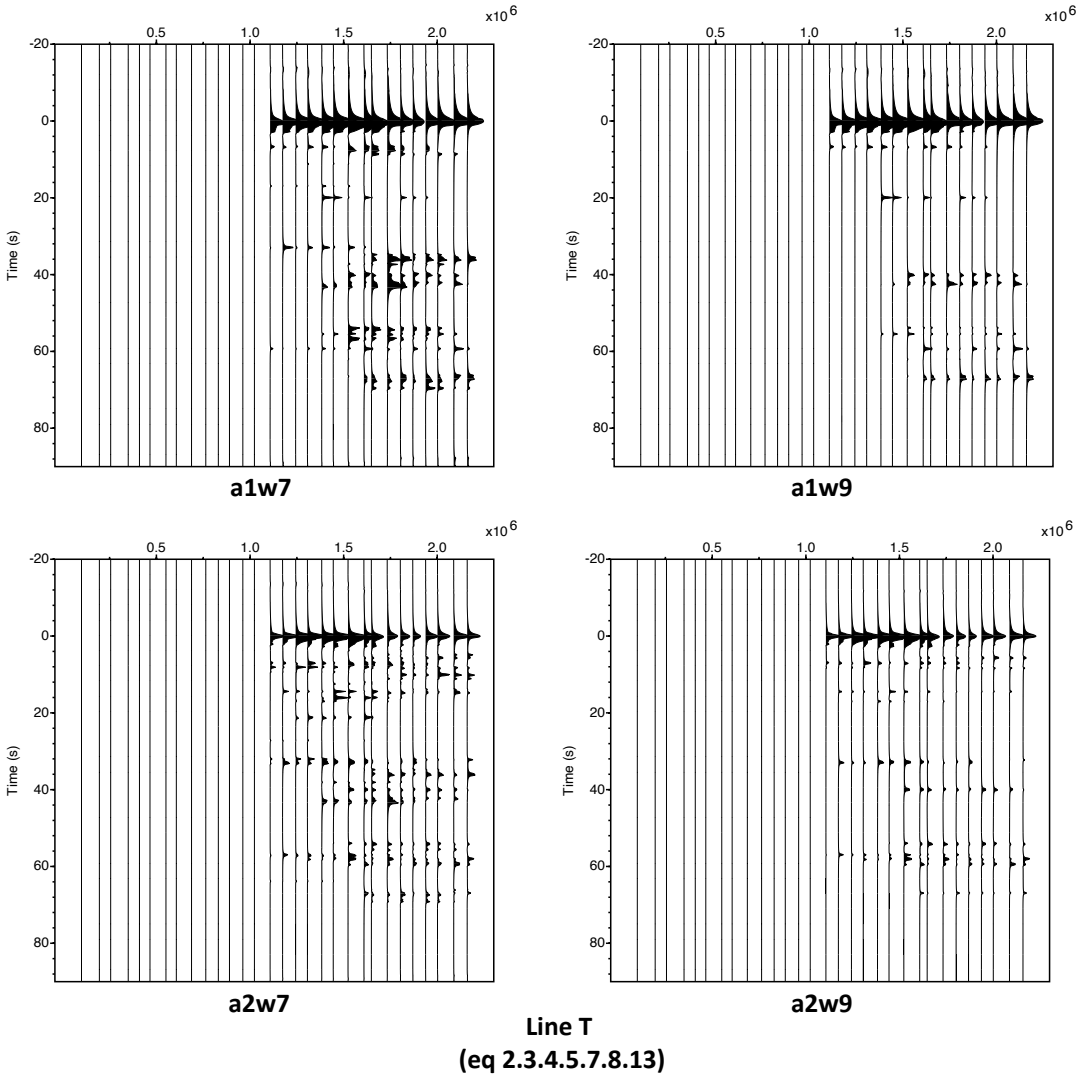


Figure D8 shows the composite plot of all smoothed signfilter plots with differing Gaussian parameters α=1.0 and α=2.0 with a mix of window lengths of 7 and 9 for Line T.

FIGURE D9

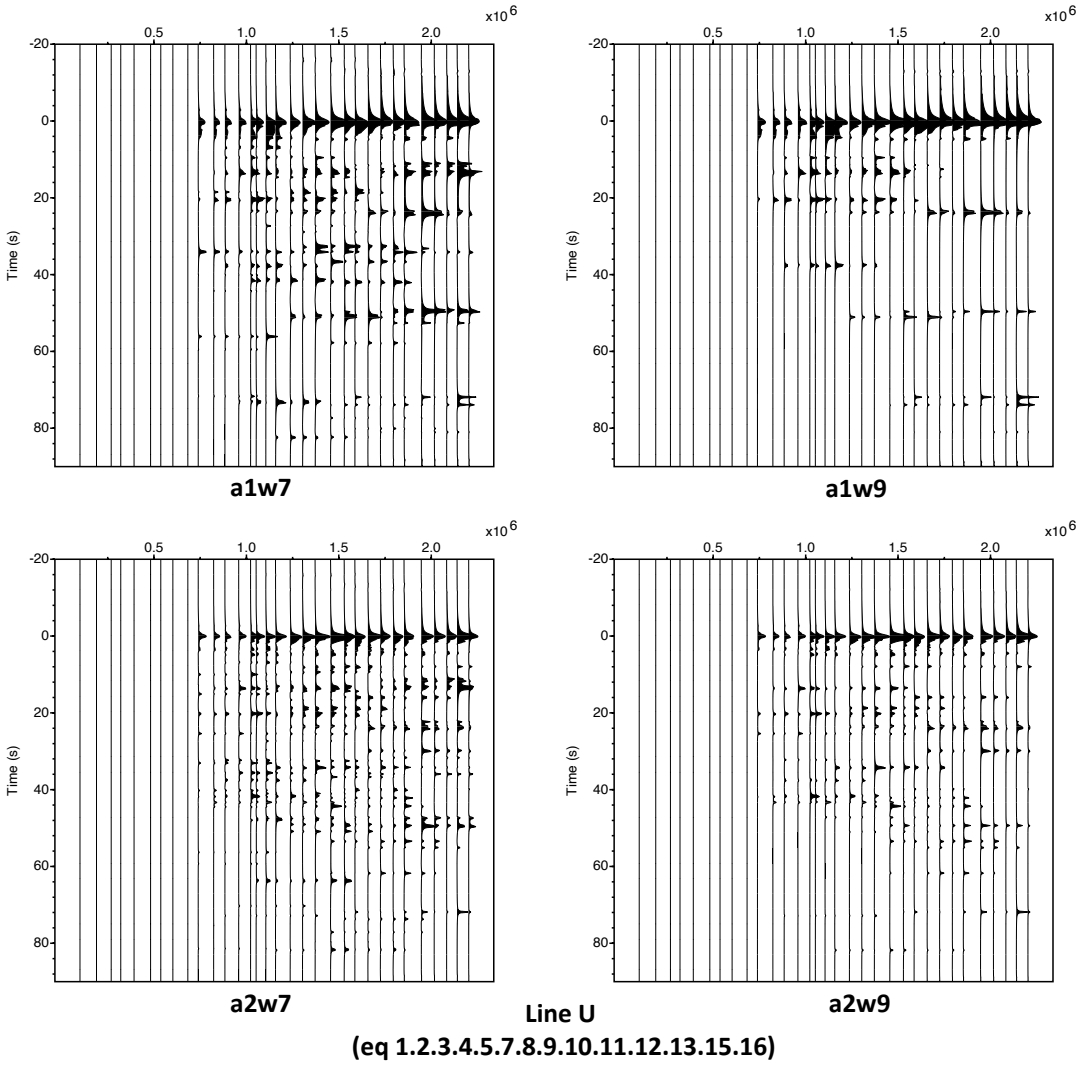


Figure D9 shows the composite plot of all smoothed signfilter plots with differing Gaussian parameters α=1.0 and α=2.0 with a mix of window lengths of 7 and 9 for Line U.

FIGURE D10

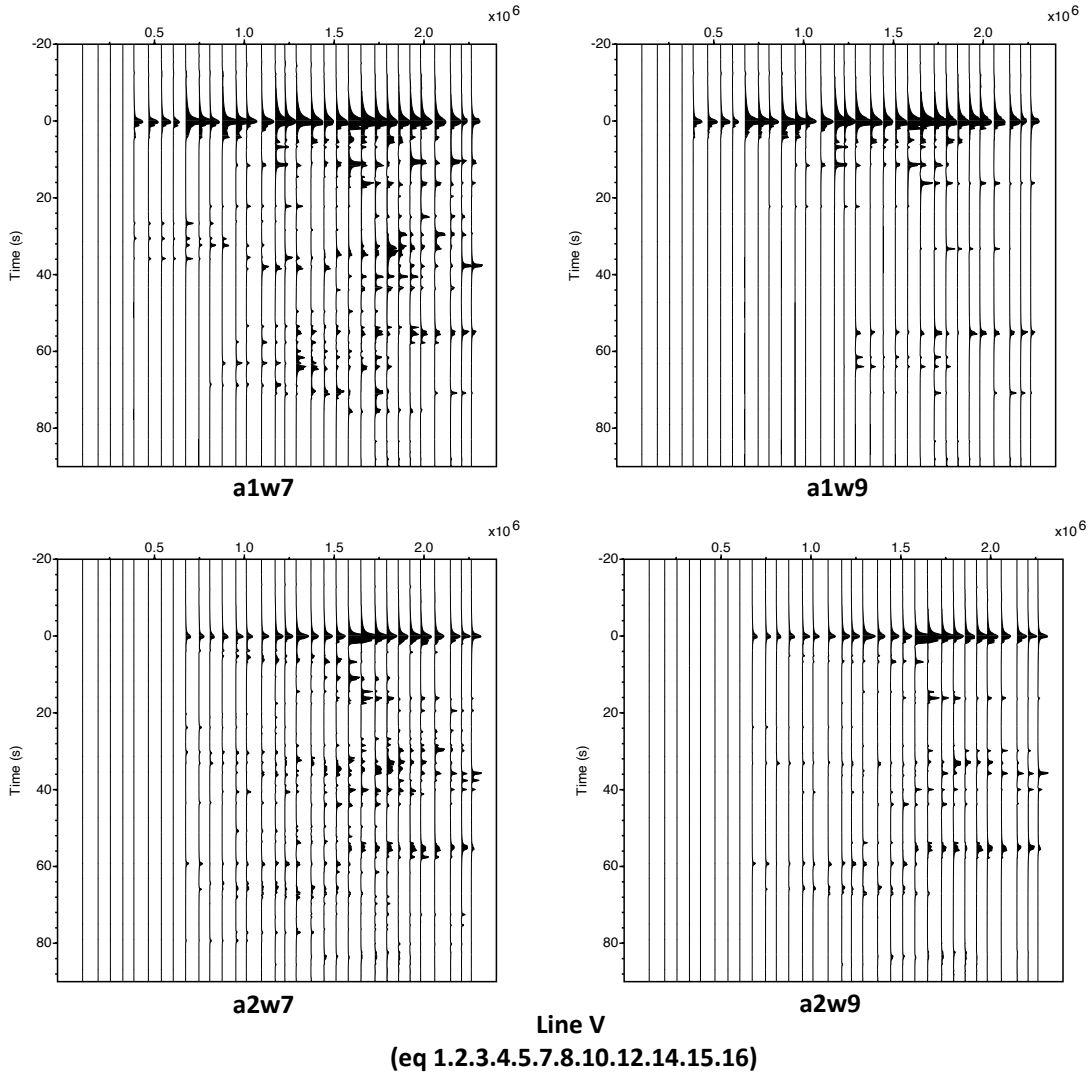


Figure D10 shows the composite plot of all smoothed signfilter plots with differing Gaussian parameters α=1.0 and α=2.0 with a mix of window lengths of 7 and 9 for Line V.

FIGURE D11

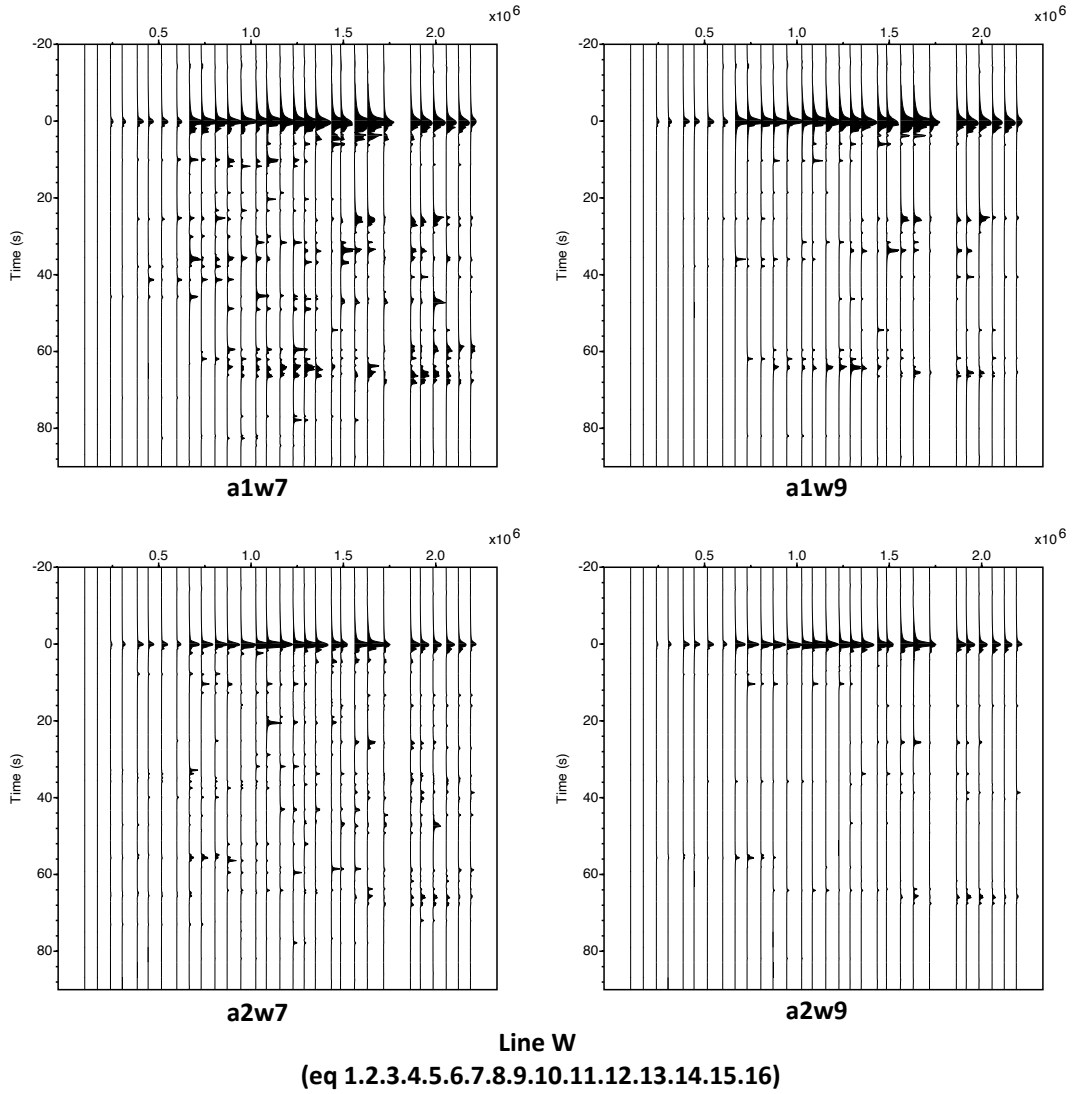


Figure D11 shows the composite plot of all smoothed signfilter plots with differing Gaussian parameters α=1.0 and α=2.0 with a mix of window lengths of 7 and 9 for Line W.

FIGURE D12

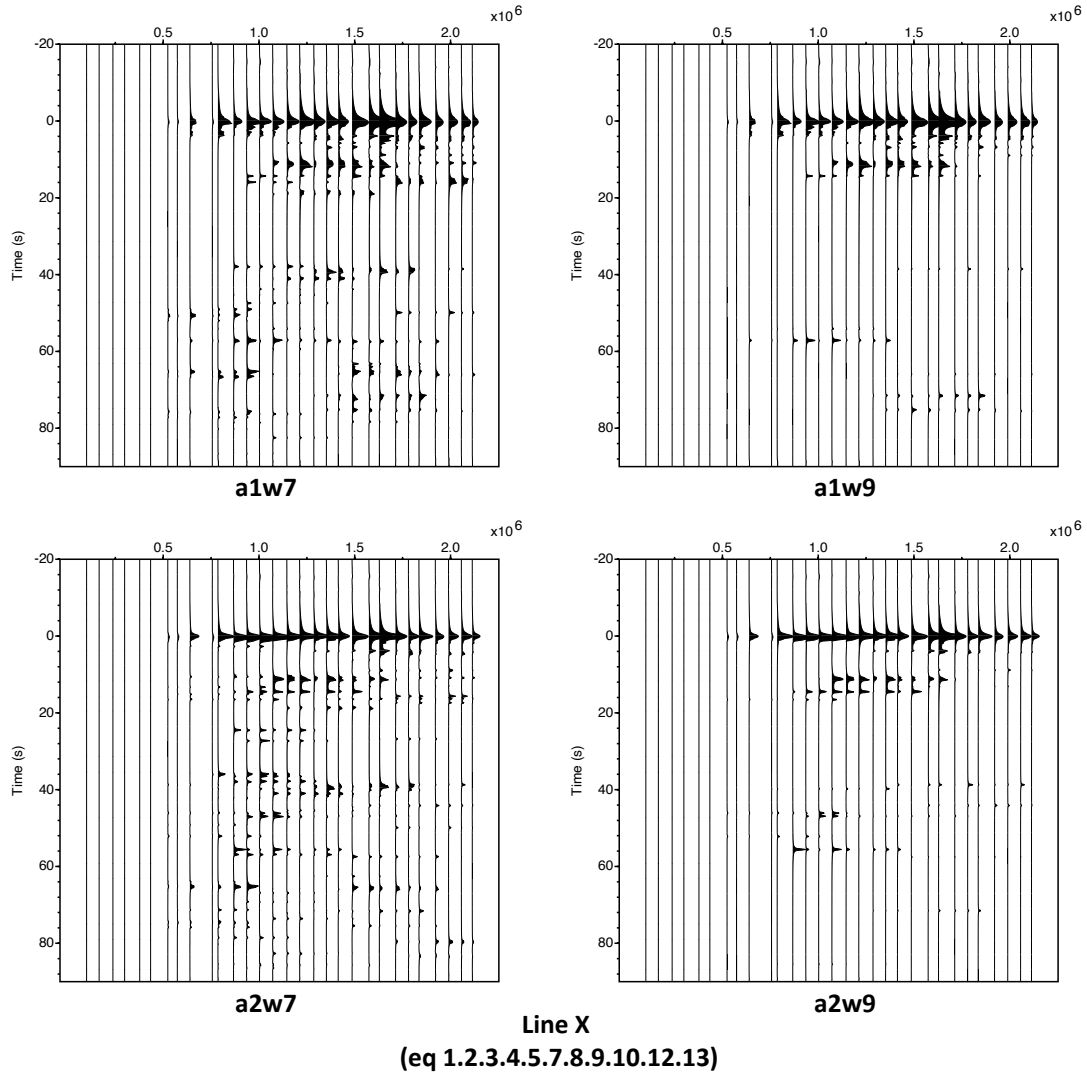


Figure D12 shows the composite plot of all smoothed signfilter plots with differing Gaussian parameters α=1.0 and α=2.0 with a mix of window lengths of 7 and 9 for Line X.

FIGURE D13

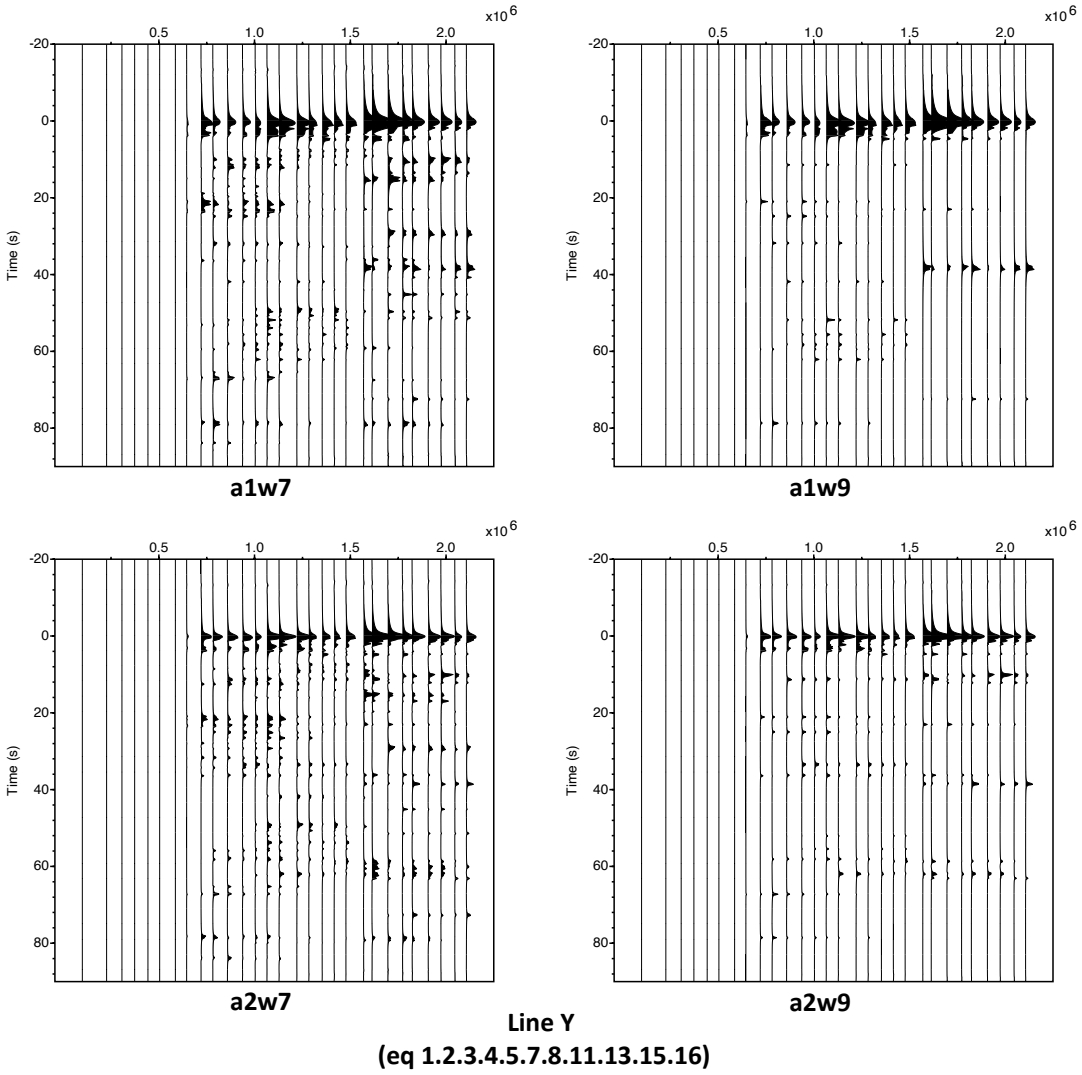


Figure D13 shows the composite plot of all smoothed signfilter plots with differing Gaussian parameters α=1.0 and α=2.0 with a mix of window lengths of 7 and 9 for Line Y.

FIGURE D14

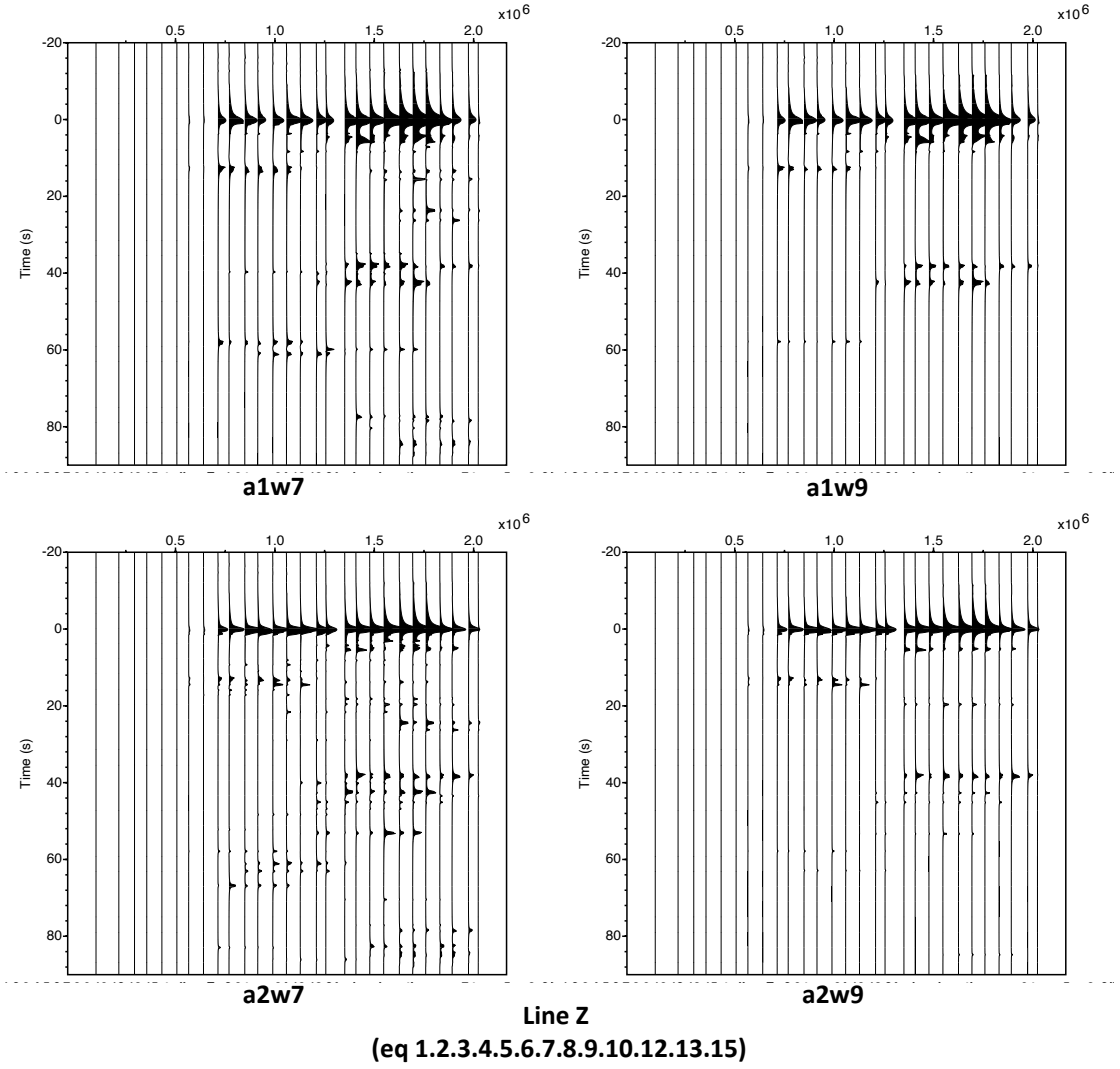


Figure D14 shows the composite plot of all smoothed signfilter plots with differing Gaussian parameters α=1.0 and α=2.0 with a mix of window lengths of 7 and 9 for Line Z.

APPENDIX E

COMPARISON FIGURES

FIGURE E1

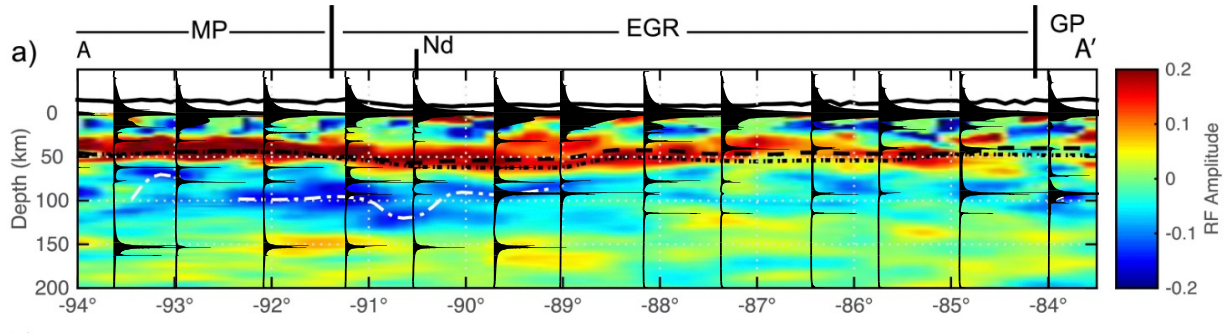


Figure E1 shows an a1w9 Line Q (39°) signfilter plot superimposed on the receiver function profile A-A' (38.7°) from Figure 4a (Chen et al., 2018).

FIGURE E2

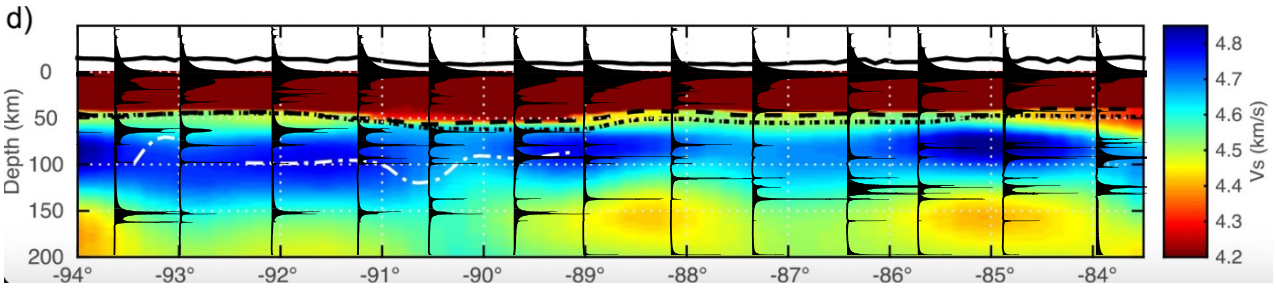


Figure E2 shows an a1w7 Line Q (39°) signfilter plot superimposed on the shear wave velocity profile A-A' (38.7°) from Figure 4d (Chen et al., 2018).

FIGURE E3

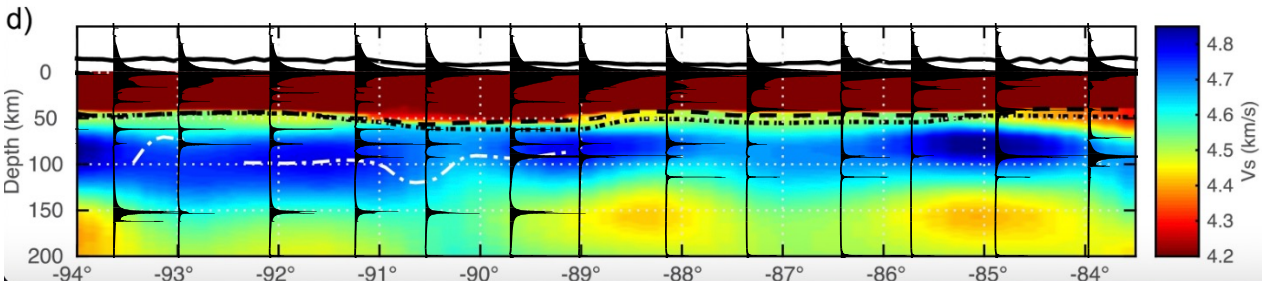


Figure E3 shows an a1w9 Line Q (39°) signfilter plot superimposed on the shear wave velocity profile A-A' (38.7°) from Figure 4d (Chen et al., 2018).

FIGURE E4

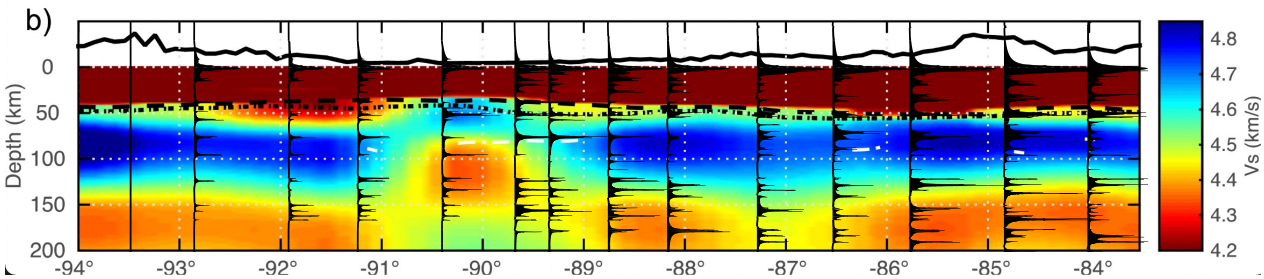


Figure E4 shows an a2w7 Line U (36.4°) signfilter plot superimposed on the shear wave velocity profile C-C' (36°) from Figure 7b (Chen et al., 2018).

FIGURE E5

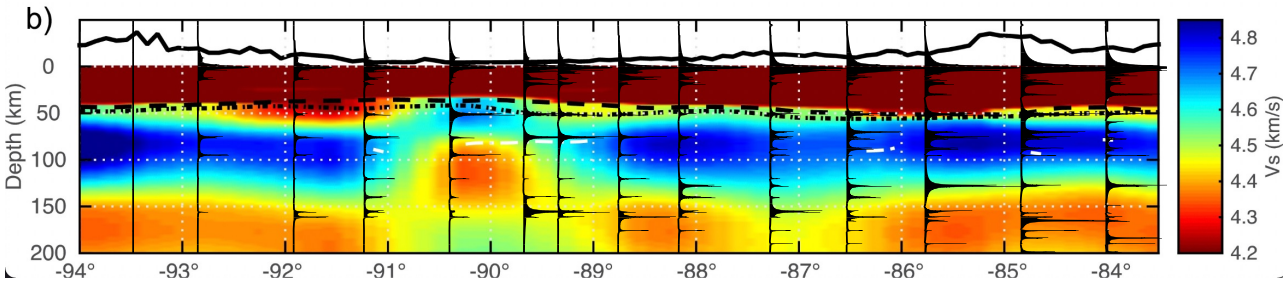


Figure E5 shows an a2w9 Line U (36.4°) signfilter plot superimposed on the shear wave velocity profile C-C' (36°) from Figure 7b (Chen et al., 2018).

FIGURE E6

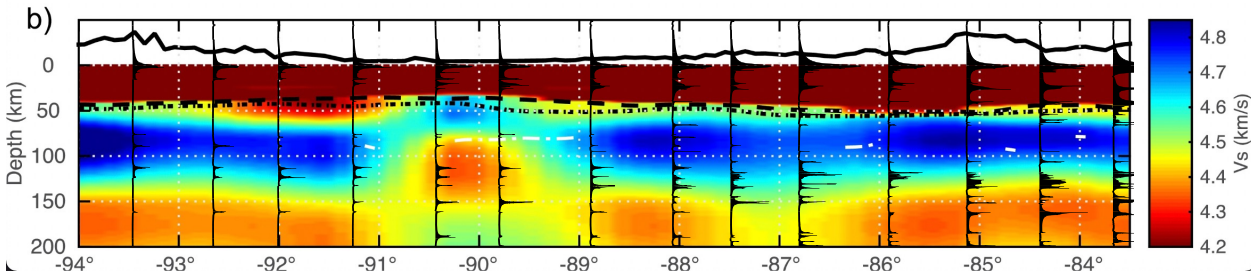


Figure E6 shows an a2w7 Line V (35.8°) signfilter plot superimposed on the shear wave velocity profile C-C' (36°) from Figure 7b (Chen et al., 2018).

FIGURE E7

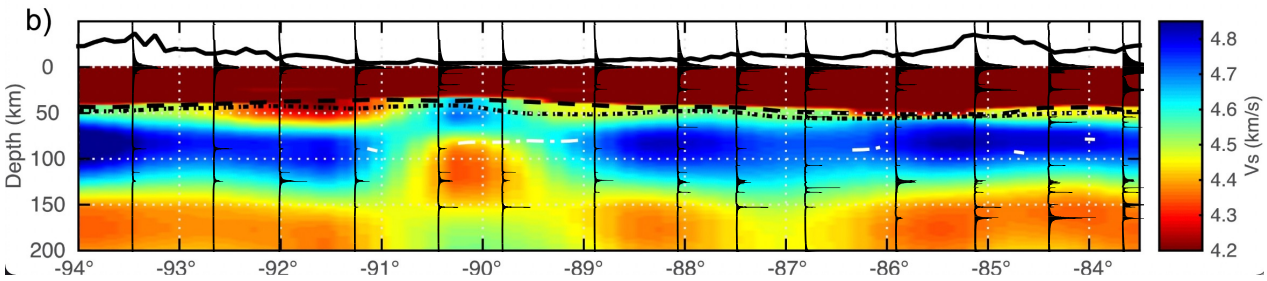


Figure E7 shows an a2w9 Line V (35.8°) signfilter plot superimposed on the shear wave velocity profile C-C' (36°) from Figure 7b (Chen et al., 2018).

APPENDIX F

TALLYRUN

FIGURE F1

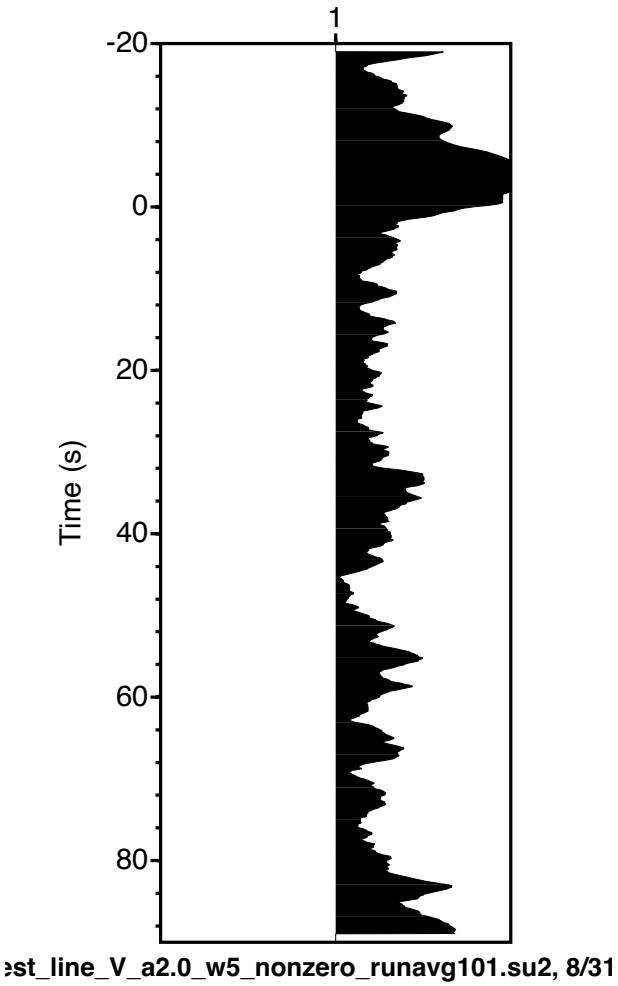


Figure F1 shows example tallyrun nonzero plot for Line V with a positive polarity and a Gaussian parameter of α=2.0. This plot shows a window length of 5, meaning that all signals that are laterally continuous for 5 and more traces are stacked and shown.

FIGURE F2

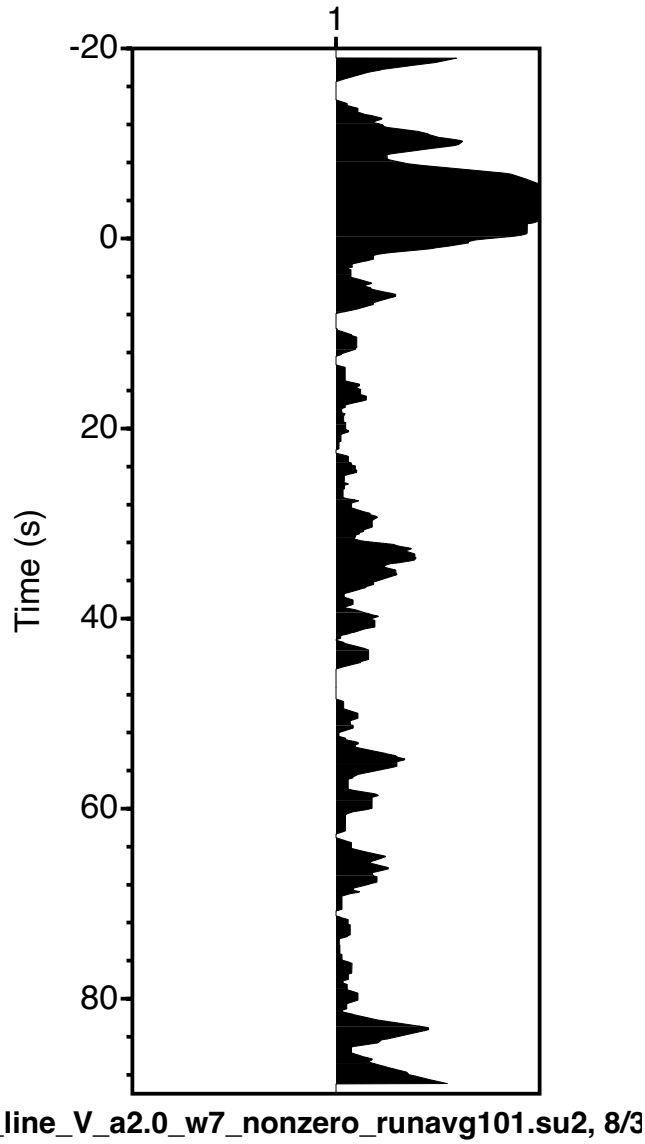


Figure F2 shows example tallyrun nonzero plot for Line V with a positive polarity and a Gaussian parameter of α=2.0. This plot shows a window length of 7, meaning that all signals that are laterally continuous for 7 and more traces are stacked and shown.

FIGURE F3

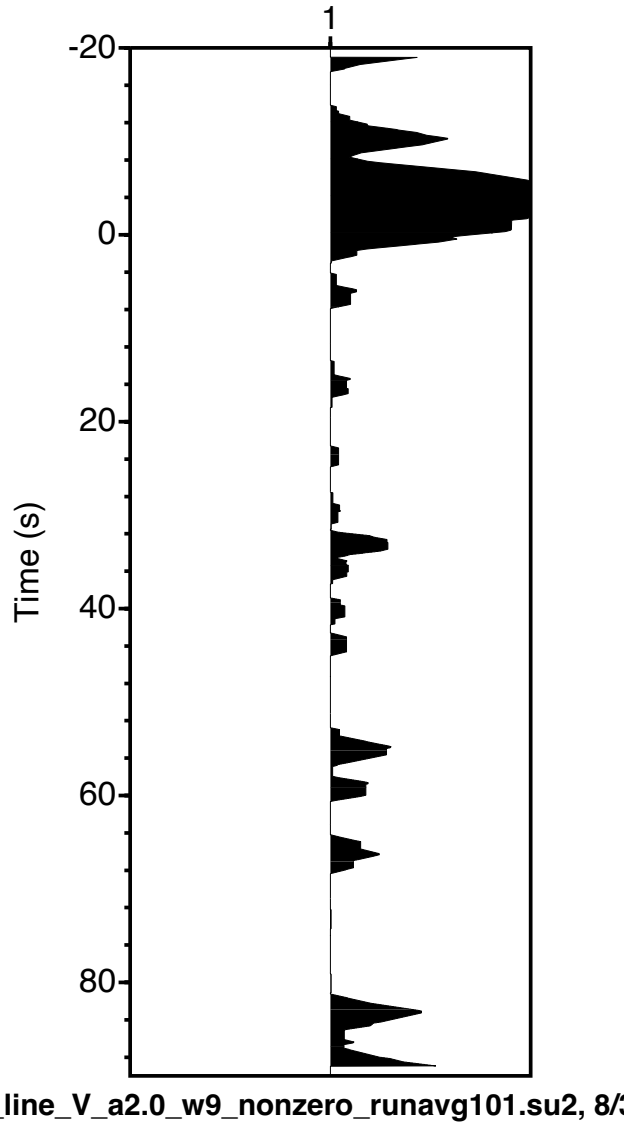
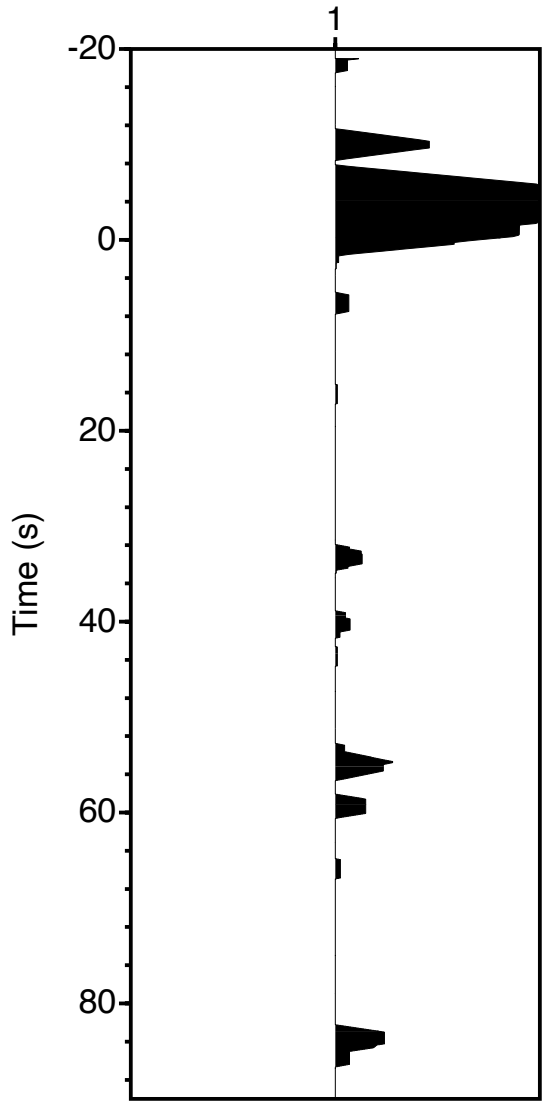


Figure F3 shows example tallyrun nonzero plot for Line V with a positive polarity and a Gaussian parameter of α=2.0. This plot shows a window length of 9, meaning that all signals that are laterally continuous for 9 and more traces are stacked and shown.

FIGURE F4



st_line_V_a2.0_w11_nonzero_runavg101.su2, 8/3

Figure F4 shows example tallyrun nonzero plot for Line V with a positive polarity and a Gaussian parameter of α=2.0. This plot shows a window length of 11, meaning that all signals that are laterally continuous for 11 and more traces are stacked and shown.

FIGURE F5

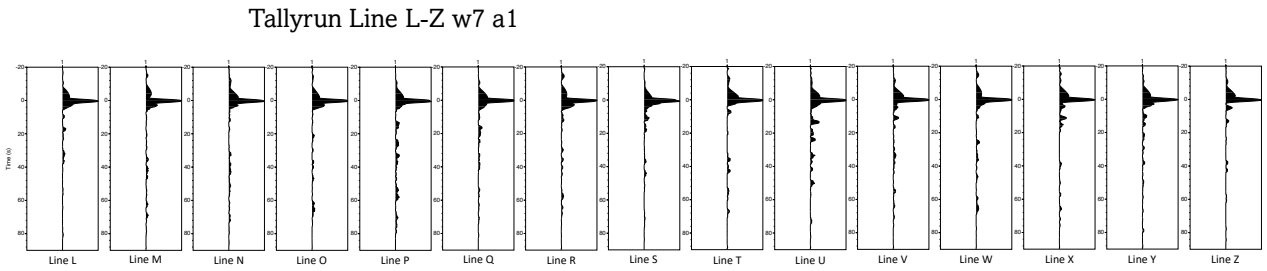


Figure F5 is an average absolute value tallyrun plot for all lines with a positive polarity and with a Gaussian parameter of α=1.0 and with a window length of 7. This plot can at a glance highlight the reflectivity of a line.

FIGURE F6

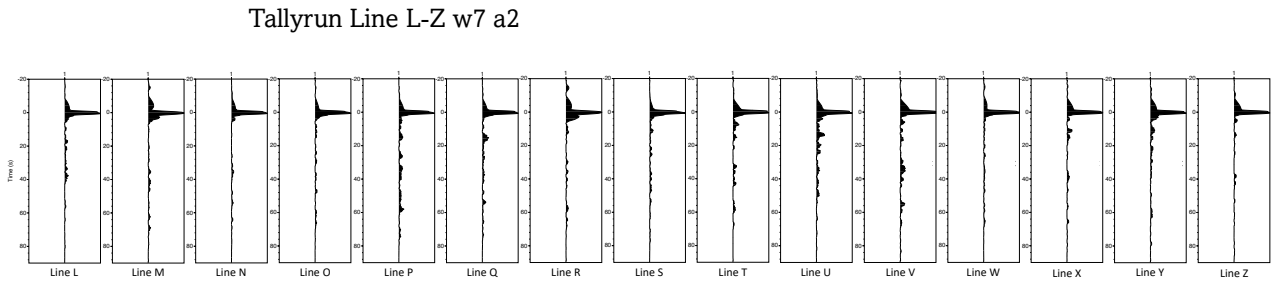


Figure F6 is an average absolute value tallyrun plot for all lines with a positive polarity and with a Gaussian parameter of α=2.0 and with a window length of 7. This plot can at a glance highlight the reflectivity of a line.

FIGURE F7

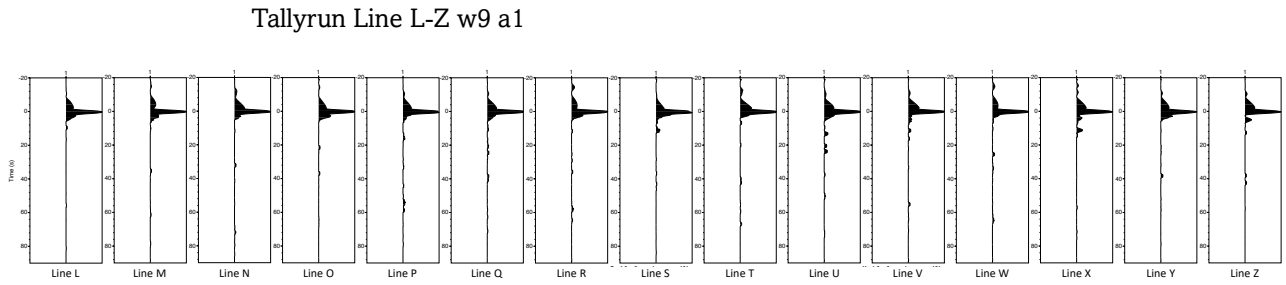


Figure F7 is an average absolute value tallyrun plot for all lines with a positive polarity and with a Gaussian parameter of α=1.0 and with a window length of 9. This plot can at a glance highlight the reflectivity of a line.

FIGURE F8

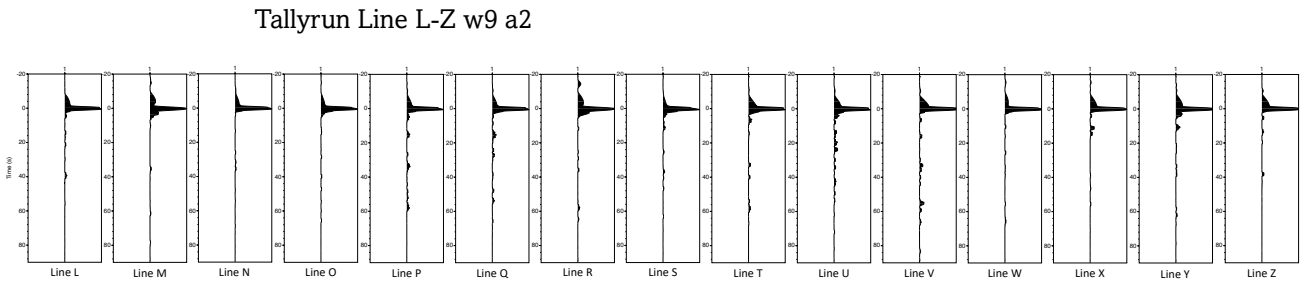


Figure F8 is an average absolute value tallyrun plot for all lines with a positive polarity and with a Gaussian parameter of α=2.0 and with a window length of 9. This plot can at a glance highlight the reflectivity of a line.

FIGURE F9

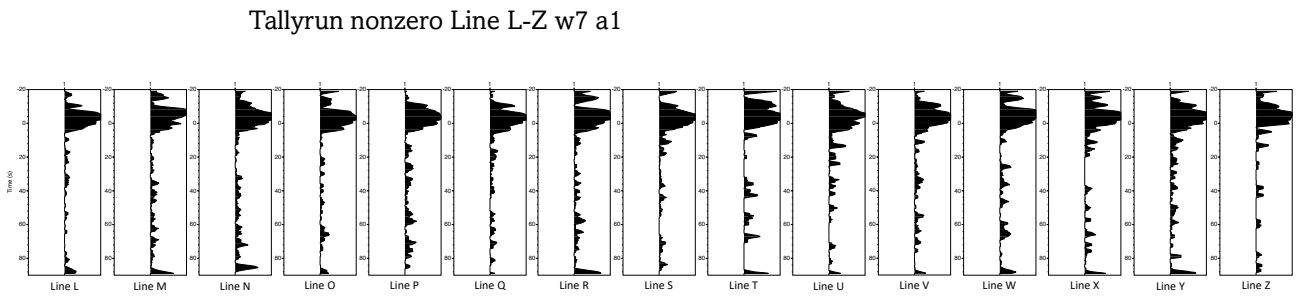


Figure F9 is a tallyrun nonzero plot for all lines with a positive polarity and with a Gaussian parameter of α=1.0 and with a window length of 7. This plot can at a glance highlight the reflectivity of a line.

FIGURE F10

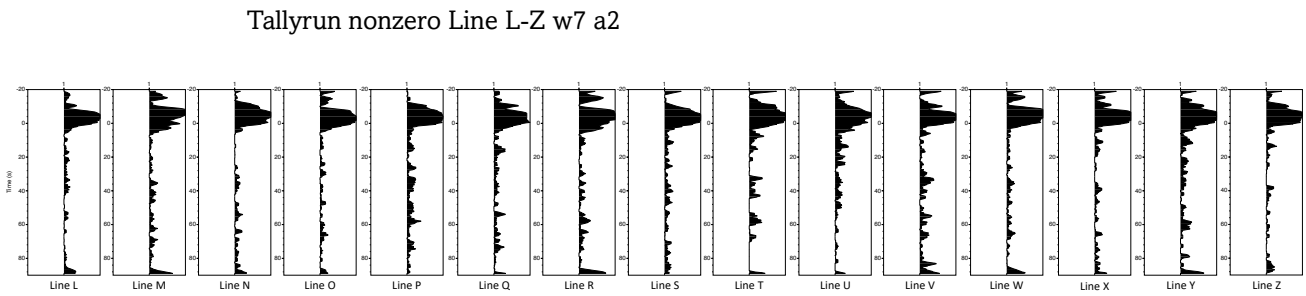


Figure F10 is a tallyrun nonzero plot for all lines with a positive polarity and with a Gaussian parameter of α=2.0 and with a window length of 7. This plot can at a glance highlight the reflectivity of a line.

FIGURE F11

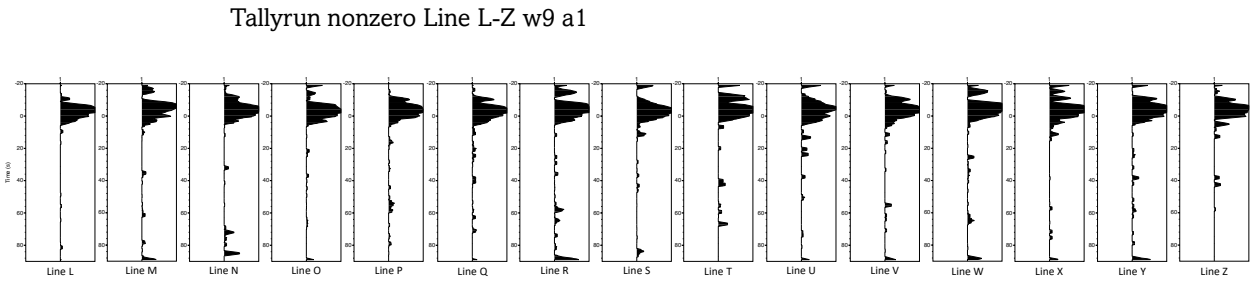


Figure F11 is a tallyrun nonzero plot for all lines with a positive polarity and with a Gaussian parameter of α=1.0 and with a window length of 9. This plot can at a glance highlight the reflectivity of a line.

FIGURE F12

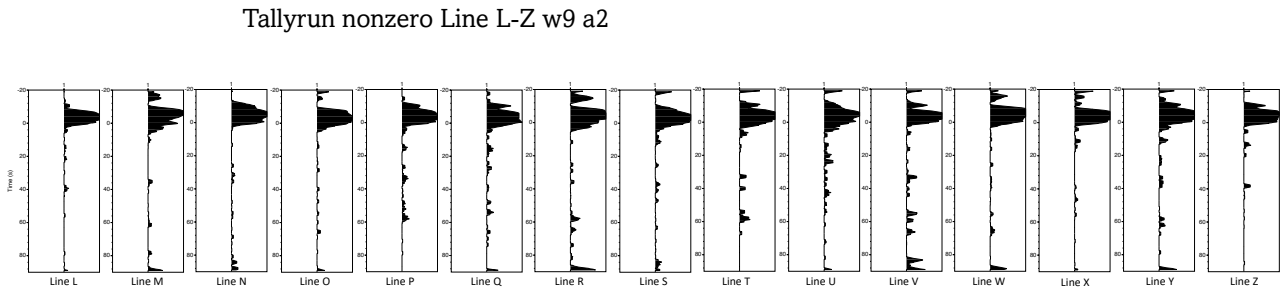


Figure F12 is a tallyrun nonzero plot for all lines with a positive polarity and with a Gaussian parameter of α=2.0 and with a window length of 9. This plot can at a glance highlight the reflectivity of a line.

APPENDIX G

TA STATIONS

TABLE G1

Station	Location	Latitude (°N)	Longitude (°E)	Elevation (m)
T32A	KS	37.18	-98.92	596
T33A	KS	37.08	-98.24	394
T34A	KS	37.02	-97.19	361
T35A	OK	36.92	-96.51	401
T36A	KS	37.06	-95.88	243
T37A	KS	37.12	-94.92	256
T38A	MO	37.04	-94.29	349
T39A	MO	37.02	-93.38	366
T40A	MO	37.15	-92.52	399
T41A	MO	37.04	-91.76	366
T42A	MO	37.03	-91.09	162

T43A	MO	37.08	-90.29	167
T44A	MO	37.09	-89.59	133
T45A	KY	37.02	-88.64	119
T46A	KY	37.04	-87.89	169
T47A	KY	36.99	-87.11	217
T48A	KY	37.11	-86.39	218
T49A	KY	37.1	-85.53	313
T50A	KY	37.02	-84.84	302
T51A	KY	36.97	-83.95	329
T52A	KY	37.11	-82.99	436
T53A	VA	36.98	-82.53	818
T54A	VA	37.06	-81.58	852
T55A	VA	37.12	-80.78	644
T56A	VA	37.03	-80.03	387
T57A	VA	37	-79.25	230
T58A	VA	36.95	-78.53	167

T59A	VA	36.97	-77.55	63
T60A	VA	37.14	-76.73	11
U32A	OK	36.38	-99	525
U33A	OK	36.43	-98.11	393
U34A	OK	36.44	-97.54	345
U35A	OK	36.37	-96.73	303
U36A	OK	36.39	-95.73	187
U37A	OK	36.41	-95.12	248
U38A	AR	36.44	-94.39	389
U39A	AR	36.38	-93.48	433
U40A	AR	36.36	-92.85	374
U41A	AR	36.34	-91.92	300
U42A	AR	36.35	-91.24	119
U43A	AR	36.37	-90.41	96
U44A	MO	36.5	-89.69	89

U44B	TN	36.34	-89.35	136
U45A	TN	36.35	-88.76	144
U46A	TN	36.36	-88.18	146
U47A	TN	36.44	-87.29	145
U48A	TN	36.51	-86.54	268
U49A	TN	36.51	-85.78	234
U50A	TN	36.42	-84.84	474
U51A	TN	36.38	-84.02	472
U52A	TN	36.39	-83.37	510
U53A	TN	36.36	-82.58	559
U54A	TN	36.52	-81.82	837
U55A	NC	36.5	-81.05	863
U56A	NC	36.35	-80.38	363
U57A	NC	36.43	-79.34	178
U58A	NC	36.39	-78.55	169
U59A	NC	36.35	-77.79	99

U60A	NC	36.47	-77.16	8
U61A	NC	36.33	-76.45	4
V32A	OK	35.72	-99.04	533
V33A	OK	35.82	-98.29	420
V34A	OK	35.83	-97.52	329
V35A	OK	35.76	-96.84	280
V36A	OK	35.79	-95.94	236
V37A	OK	35.88	-95.14	219
V38A	AR	35.86	-94.41	372
V39A	AR	35.84	-93.64	744
V40A	AR	35.8	-92.82	570
V41A	AR	35.79	-92.16	413
V42A	AR	35.81	-91.39	134
V43A	AR	35.79	-90.54	74
V44A	AR	35.83	-89.9	78

V45A	TN	35.74	-88.96	126
V46A	TN	35.8	-88.12	162
V47A	TN	35.83	-87.52	240
V48A	TN	35.74	-86.82	278
V49A	TN	35.77	-85.9	329
V50A	TN	35.67	-85.1	287
V51A	TN	35.8	-84.35	243
V52A	TN	35.84	-83.6	328
V53A	NC	35.67	-82.81	681
V54A	NC	35.78	-81.95	448
V55A	NC	35.85	-81.21	313
V56A	NC	35.81	-80.5	237
V57A	NC	35.89	-79.78	223
V58A	NC	35.79	-79.11	127
V59A	NC	35.76	-78.24	58
V60A	NC	35.77	-77.26	8

V61A	NC	35.79	-76.58	4
V62A	NC	35.56	-75.96	-3
W32A	OK	35.12	-99.25	494
W33A	OK	35.15	-98.47	414
W34A	OK	35.24	-97.77	428
W35A	OK	35.15	-96.87	322
W36A	OK	35.14	-96.23	251
W37A	OK	35.14	-95.43	281
W37B	OK	35.14	-95.43	279
W38A	OK	35.07	-94.52	169
W39A	AR	35.2	-93.78	162
W40A	AR	35.19	-93.07	108
W41A	AR	35.17	-92.25	95
W42A	AR	35.27	-91.52	71
W43A	AR	35.09	-90.71	70

W44A	TN	35.14	-89.82	101
W45A	TN	35.16	-89.19	187
W46A	TN	35.13	-88.38	145
W47A	TN	35.25	-87.59	293
W48A	TN	35.14	-86.93	260
W49A	TN	35.12	-86.26	251
W50A	TN	35.2	-85.31	587
W51A	TN	35.16	-84.76	260
W52A	NC	35.09	-83.93	519
W53A	NC	35.17	-83.16	1180
W54A	SC	35.09	-82.19	272
W56A	NC	35.13	-80.58	177
W57A	NC	35.15	-79.99	85
W58A	NC	35.02	-79.23	84
W59A	NC	35.17	-78.44	60
W60A	NC	35.05	-77.71	30

W61A	NC	35.18	-76.99	6
X32A	OK	34.42	-99.29	401
X33A	OK	34.54	-98.5	346
X34A	OK	34.6	-97.83	364
X35A	OK	34.4	-96.97	300
X36A	OK	34.57	-96.35	211
X37A	OK	34.59	-95.37	207
X38A	OK	34.67	-94.83	234
X39A	AR	34.51	-94.11	326
X40A	AR	34.49	-92.83	158
X41A	AR	34.49	-92.51	102
X42A	AR	34.55	-91.63	62
X43A	AR	34.52	-90.88	53
X44A	MS	34.5	-90.15	109
X45A	MS	34.42	-89.39	142

X46A	MS	34.56	-88.58	150
X47A	AL	34.52	-87.86	212
X48A	AL	34.45	-87.05	180
X49A	AL	34.51	-86.33	182
X50A	AL	34.46	-85.65	489
X50B	AL	34.46	-85.65	494
X51A	GA	34.57	-84.86	214
X52A	GA	34.6	-83.89	481
X53A	GA	34.5	-83.3	240
X54A	SC	34.55	-82.37	213
X55A	SC	34.47	-81.63	153
X56A	SC	34.49	-81.03	112
X57A	SC	34.46	-80.09	133
X58A	NC	34.55	-79.34	45
X59A	NC	34.57	-78.6	29
X60A	NC	34.58	-77.98	12

Y33A	TX	34.01	-98.63	321
Y34A	OK	33.96	-97.76	262
Y35A	OK	33.91	-97.04	214
Y36A	OK	33.9	-96.28	186
Y37A	OK	33.98	-95.62	165
Y38A	OK	33.93	-94.73	118
Y39A	AR	33.94	-94.09	108
Y40A	AR	34.01	-93.28	117
Y41A	AR	33.88	-92.61	99
Y42A	AR	33.84	-91.79	77
Y43A	MS	33.91	-90.93	46
Y44A	MS	33.96	-90.21	46
Y45A	MS	33.87	-89.54	106
Y46A	MS	33.88	-88.86	109
Y47A	AL	33.9	-87.85	160

Y48A	AL	33.91	-87.17	170
Y49A	AL	33.86	-86.41	362
Y50A	AL	33.89	-85.73	248
Y51A	GA	33.9	-85.06	380
Y52A	GA	33.86	-84.06	286
Y53A	GA	33.86	-83.58	234
Y54A	GA	33.86	-82.69	176
Y55A	SC	33.94	-81.86	164
Y56A	SC	33.79	-81.3	154
Y57A	SC	34.02	-80.39	56
Y58A	SC	33.91	-79.67	19
Y59A	SC	33.99	-78.87	2
Y60A	NC	34	-78.22	7
Z33A	TX	33.29	-98.76	362
Z34A	TX	33.37	-97.92	341

Z35A	TX	33.33	-97.25	235
Z36A	TX	33.27	-96.43	187
Z37A	TX	33.2	-95.62	146
Z38A	TX	33.26	-94.99	116
Z39A	TX	33.24	-94.18	112
Z40A	AR	33.26	-93.4	78
Z41A	AR	33.26	-92.8	62
Z42A	AR	33.27	-91.95	39
Z43A	AR	33.21	-91.24	39
Z44A	MS	33.28	-90.43	39
Z45A	MS	33.37	-89.69	113
Z46A	MS	33.19	-88.94	125
Z47A	AL	33.2	-88.07	65
Z48A	AL	33.38	-87.56	101
Z49A	AL	33.19	-86.53	134
Z50A	AL	33.25	-85.92	370

Z51A	GA	33.32	-85.17	249
Z52A	GA	33.19	-84.42	252
Z53A	GA	33.28	-83.57	144
Z54A	GA	33.24	-82.84	134
Z55A	GA	33.22	-82.14	100
Z56A	SC	33.33	-81.37	81
Z57A	SC	33.3	-80.7	81
Z58A	SC	33.33	-79.81	18
Z59A	SC	33.24	-79.28	8

Table G1 shows all the TA stations utilized for this research. The TA's station state location is identified along with the latitude (°N) in degrees north of the equator and longitude (°E) in degrees east of the prime meridian. Lastly, the elevation (m) of each station is shown.

TABLE G2

Station	Location	Latitude (°N)	Longitude (°E)	Elevation
L31A	NE	42.18	-98.84	670
L32A	NE	42	-98.01	586
L33A	NE	42.17	-97.27	556
L34A	NE	41.97	-96.38	424
L35A	IA	42.11	-95.54	410
L36A	IA	42.1	-94.67	353
L37A	IA	42.12	-93.75	312
L38A	IA	42.14	-92.96	300
L39A	IA	42.12	-92	261
L40A	IA	42.06	-91.22	242
L41A	IA	42.08	-90.5	238
L42A	IL	42	-89.67	257
L43A	IL	42.18	-88.74	266
L44A	IL	42.18	-87.91	202
L46A	MI	42.01	-86.3	223
L47A	MI	41.98	-85.2	282
L48A	MI	41.94	-84.43	369
L49A	MI	42.11	-83.77	230
L50A	ON, CAN	42.04	-82.81	187

L53A	PA	41.95	-80.26	355
L54A	NY	42.23	-79.32	432
L55A	NY	42.18	-78.44	633
L56A	NY	42.14	-77.56	688
L57A	PA	42	-76.85	546
L58A	NY	42.04	-75.85	447
L59A	NY	42.19	-75.04	677
L60A	NY	41.99	-74.22	388
L61A	NY	42.19	-73.55	275
L61B	MA	42.45	-72.68	261
L62A	CT	42.03	-72.66	49
L63A	RI	41.86	-71.61	109
L64A	MA	41.94	-70.84	17
L65A	MA	42.03	-70.05	50
M31A	NE	41.34	-98.98	699
M33A	NE	41.57	-97.19	503
M34A	NE	41.5	-96.58	415
M35A	IA	41.47	-95.69	363
M36A	IA	41.45	-94.8	430
M37A	IA	41.4	-94.06	325
M38A	IA	41.42	-93.2	258

M39A	IA	41.48	-92.17	264
M40A	IA	41.41	-91.51	223
M41A	IL	41.38	-90.54	226
M42A	IL	41.45	-89.76	212
M43A	IL	41.44	-88.96	190
M44A	IL	41.39	-88.04	207
M45A	IN	41.39	-87.25	216
M46A	IN	41.41	-86.35	242
M47A	IN	41.36	-85.62	283
M48A	OH	41.48	-84.72	258
M49A	OH	41.47	-83.98	203
M50A	OH	41.4	-83.04	176
M51A	OH	41.33	-82.18	239
M52A	OH	41.54	-81.36	382
M53A	OH	41.44	-80.67	334
M54A	PA	41.51	-79.66	488
M55A	PA	41.47	-78.76	531
M56A	PA	41.48	-78.18	493
M57A	PA	41.34	-77.13	319
M58A	PA	41.37	-76.46	529
M59A	PA	41.54	-75.43	471
M60A	NY	41.33	-74.62	292

M61A	NY	41.31	-73.77	190
M62A	CT	41.44	-72.89	24
M63A	CT	41.4	-72.05	44
M64A	RI	41.55	-71.21	17
M65A	MA	41.56	-70.65	22
M66A	MA	41.26	-70.14	9
N31A	NE	40.82	-98.95	687
N33A	NE	40.74	-97.45	475
N34A	NE	40.84	-96.5	401
N35A	IA	40.86	-95.64	353
N36A	IA	40.82	-94.96	349
N37A	IA	40.76	-94.21	351
N38A	IA	40.79	-93.23	317
N39A	IA	40.88	-92.5	260
N40A	IA	40.88	-91.58	208
N41A	IL	40.71	-90.86	226
N42A	IL	40.83	-90.03	205
N43A	IL	40.94	-89.17	215
N44A	IL	40.8	-88.13	202
N45A	IN	40.85	-87.51	206
N46A	IN	40.89	-86.74	209

N47A	IN	40.88	-85.69	252
N48A	IN	40.86	-85.03	250
N49A	OH	40.92	-84.18	225
N50A	OH	40.77	-83.15	277
N51A	OH	40.92	-82.37	343
N52A	OH	40.81	-81.69	331
N53A	OH	40.81	-80.84	360
N54A	PA	40.96	-79.99	408
N55A	PA	40.78	-78.99	559
N56A	PA	40.92	-78.3	561
N57A	PA	40.76	-77.55	306
N58A	PA	40.84	-76.72	200
N59A	PA	40.92	-75.77	508
N60A	PA	40.87	-75.1	189
N61A	NJ	40.75	-74.3	108
N62A	NY	40.93	-73.47	34
N63A	NY	40.99	-72.52	8
O31A	NE	40.15	-99.33	631
O32A	NE	40.26	-98.28	579
O33A	NE	40.08	-97.58	480
O34A	NE	40.18	-96.69	409

O35A	NE	40.27	-95.91	342
O36A	MO	40.13	-94.96	306
O37A	MO	40.17	-94.15	284
O38A	MO	40.12	-93.47	266
O39A	MO	40.25	-92.54	282
O40A	MO	40.12	-91.87	206
O41A	IL	40.12	-90.88	203
O42A	IL	40.2	-90.08	155
O43A	IL	40.29	-89.31	224
O44A	IL	40.15	-88.47	213
O45A	IL	40.25	-87.72	208
O47A	IN	40.24	-86.17	278
O48A	IN	40.26	-85.16	300
O49A	OH	40.19	-84.34	292
O50A	OH	40.15	-83.62	399
O51A	OH	40.15	-82.61	380
O52A	OH	40.12	-81.84	331
O53A	OH	40.25	-81.21	320
O54A	PA	40.18	-80.38	357
O55A	PA	40.21	-79.3	469
O56A	PA	40.27	-78.57	684
O57A	PA	40.21	-77.64	377

O58A	PA	40.12	-76.92	321
O59A	PA	40.31	-76.19	334
O60A	PA	40.32	-75.41	70
O61A	NJ	40.09	-74.55	38
P32A	KS	39.62	-98.6	524
P33A	KS	39.44	-97.69	488
P34A	KS	39.55	-96.83	429
P35A	KS	39.53	-96.02	418
P36A	KS	39.62	-95.21	313
P37A	MO	39.59	-94.35	300
P38A	MO	39.62	-93.53	248
P39A	MO	39.49	-92.75	232
P39B	MO	39.49	-92.75	226
P40A	MO	39.53	-92.05	225
P41A	IL	39.67	-91.06	215
P42A	IL	39.59	-90.34	197
P43A	IL	39.64	-89.52	176
P44A	IL	39.47	-88.62	195
P45A	IL	39.53	-87.74	193
P46A	IN	39.62	-87.21	194
P47A	IN	39.49	-86.27	246

P48A	IN	39.46	-85.43	300
P49A	OH	39.53	-84.72	272
P50A	OH	39.61	-83.8	318
P51A	OH	39.48	-83.06	211
P52A	OH	39.63	-82.13	293
P53A	OH	39.49	-81.39	270
P54A	WV	39.6	-80.48	473
P55A	WV	39.51	-79.83	551
P56A	WV	39.5	-78.84	249
P57A	WV	39.48	-78.01	191
P58A	MD	39.49	-77.3	139
P59A	MD	39.61	-76.43	157
P60A	DE	39.81	-75.64	105
P61A	NJ	39.67	-74.79	22
Q32A	KS	38.99	-98.56	526
Q33A	KS	39	-97.83	422
Q34A	KS	38.92	-96.94	378
Q35A	KS	38.86	-96.04	402
Q36A	KS	38.96	-95.46	306
Q37A	MO	38.88	-94.45	297
Q38A	MO	38.96	-93.62	228

Q39A	MO	39.05	-92.98	225
Q40A	MO	38.99	-92.07	275
Q41A	MO	38.95	-91.23	191
Q42A	IL	38.91	-90.53	175
Q43A	IL	38.94	-89.7	202
Q44A	IL	38.9	-89.02	164
Q45A	IL	38.89	-88.16	162
Q46A	IN	39.02	-87.36	164
Q47A	IN	38.94	-86.43	230
Q48A	IN	38.93	-85.73	185
Q49A	IN	39.01	-84.9	264
Q50A	OH	38.84	-83.98	262
Q51A	OH	39.03	-83.35	362
Q52A	OH	38.96	-82.27	228
Q53A	WV	38.86	-81.53	310
Q54A	WV	38.98	-80.83	254
Q55A	WV	39	-80.08	657
Q56A	WV	39.04	-79.19	430
Q57A	VA	39.04	-78.41	324
Q58A	VA	38.94	-77.68	182
Q59A	MD	38.86	-76.65	34
Q60A	MD	39	-75.84	14

Q61A	DE	38.88	-75.33	5
R32A	KS	38.42	-98.71	573
R33A	KS	38.31	-97.98	497
R34A	KS	38.3	-97.25	437
R35A	KS	38.32	-96.2	365
R36A	KS	38.32	-95.5	354
R37A	KS	38.31	-94.83	298
R38A	MO	38.19	-93.91	237
R39A	MO	38.31	-93.04	290
R40A	MO	38.29	-92.27	213
R41A	MO	38.3	-91.38	257
R42A	MO	38.28	-90.79	218
R43A	IL	38.28	-89.93	186
R44A	IL	38.25	-89.08	144
R45A	IL	38.29	-88.28	143
R46A	IN	38.21	-87.51	164
R47A	IN	38.3	-86.53	181
R48A	IN	38.4	-85.87	243
R49A	KY	38.29	-85.17	251
R50A	KY	38.28	-84.33	255
R51A	KY	38.3	-83.58	231

R52A	KY	38.34	-82.64	300
R53A	WV	38.33	-81.95	294
R54A	WV	38.19	-80.99	512
R55A	WV	38.28	-80.12	833
R56A	VA	38.41	-79.4	902
R57A	VA	38.3	-78.52	230
R58A	VA	38.3	-78	184
R58B	VA	37.96	-77.88	116
R59A	VA	38.2	-77.12	35
R60A	MD	38.27	-76.58	33
R61A	MD	38.33	-75.34	76
S32A	KS	37.7	-98.94	558
S33A	KS	37.59	-98	471
S34A	KS	37.7	-97.11	373
S35A	KS	37.68	-96.32	334
S36A	KS	37.72	-95.59	299
S37A	KS	37.76	-94.83	260
S38A	MO	37.63	-93.91	294
S39A	MO	37.69	-93.32	331
S40A	MO	37.6	-92.5	336
S41A	MO	37.59	-91.75	376

S42A	MO	37.77	-90.79	315
S43A	MO	37.57	-90.08	263
S44A	IL+B264	37.69	-89.26	155
S45A	IL	37.68	-88.58	122
S46A	KY	37.68	-87.72	125
S47A	KY	37.59	-86.88	181
S48A	KY	37.66	-86.06	238
S49A	KY	37.78	-85.29	230
S50A	KY	37.68	-84.4	300
S51A	KY	37.64	-83.59	286
S52A	KY	37.68	-83.08	367
S53A	WV	37.68	-82.13	564
S54A	WV	37.8	-81.31	636
S55A	WV	37.77	-80.5	647
S56A	VA	37.68	-79.57	449
S57A	VA	37.76	-78.95	264
S58A	VA	37.61	-78.05	96
S59A	VA	37.76	-77.29	40
S60A	VA	37.71	-76.65	36
S61A	VA	37.68	-75.67	58

Table G2 is a table that includes all of the TA stations used from Line L-S, their locations, latitudes, longitudes, and elevations.

APPENDIX H

STATION COVERAGE

FIGURE H1

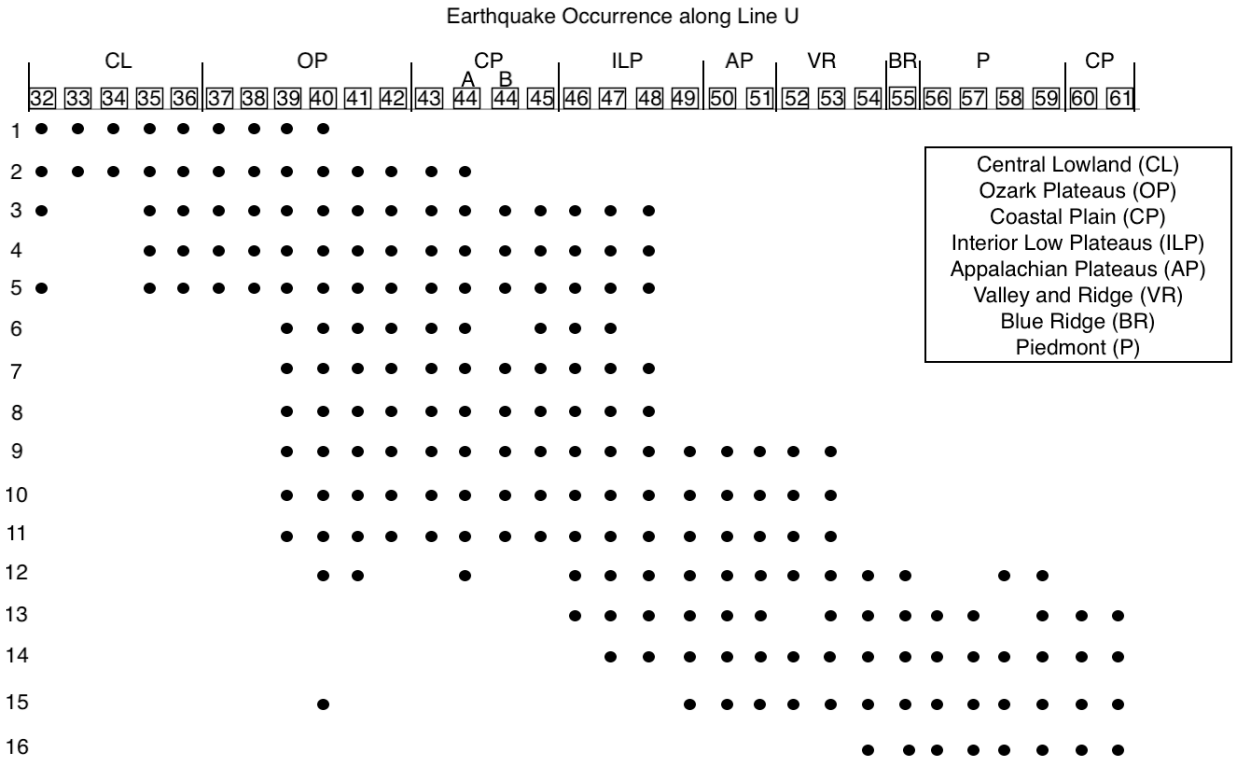


Figure H1 shows station coverage for Line U.

FIGURE H2

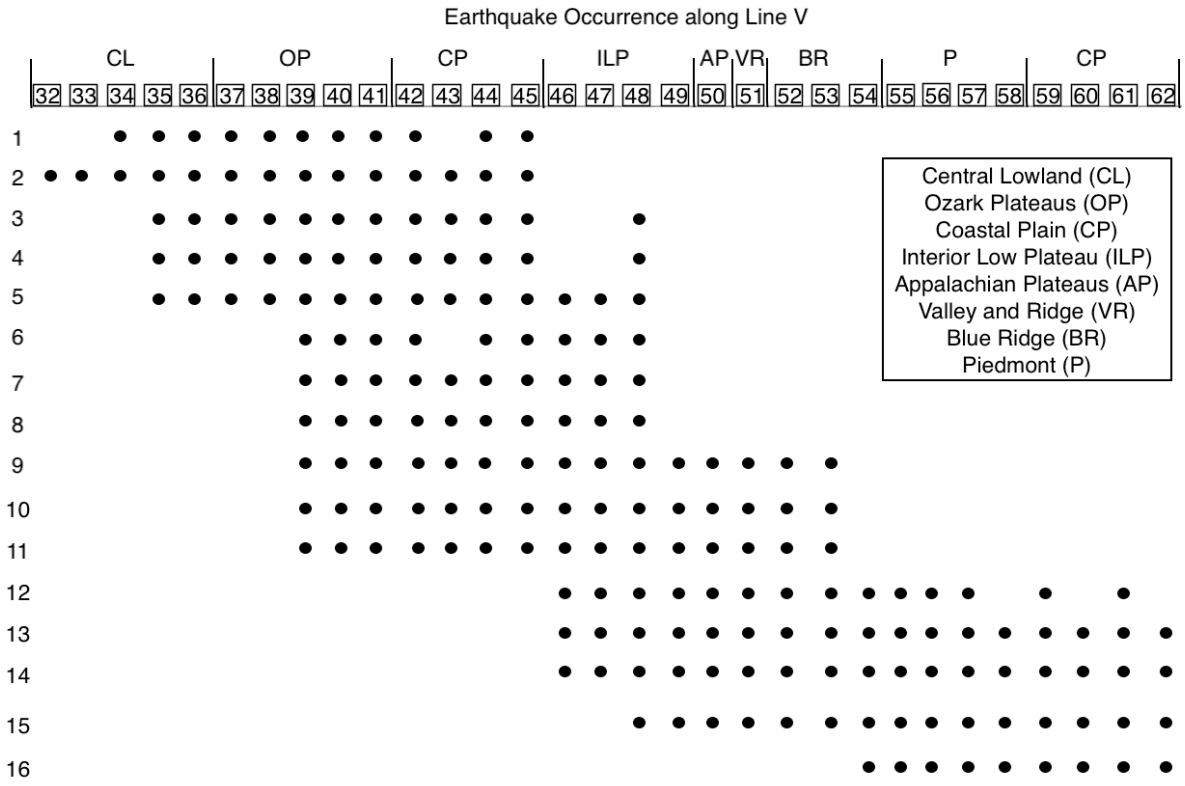


Figure H2 shows station coverage for Line V.

FIGURE H3

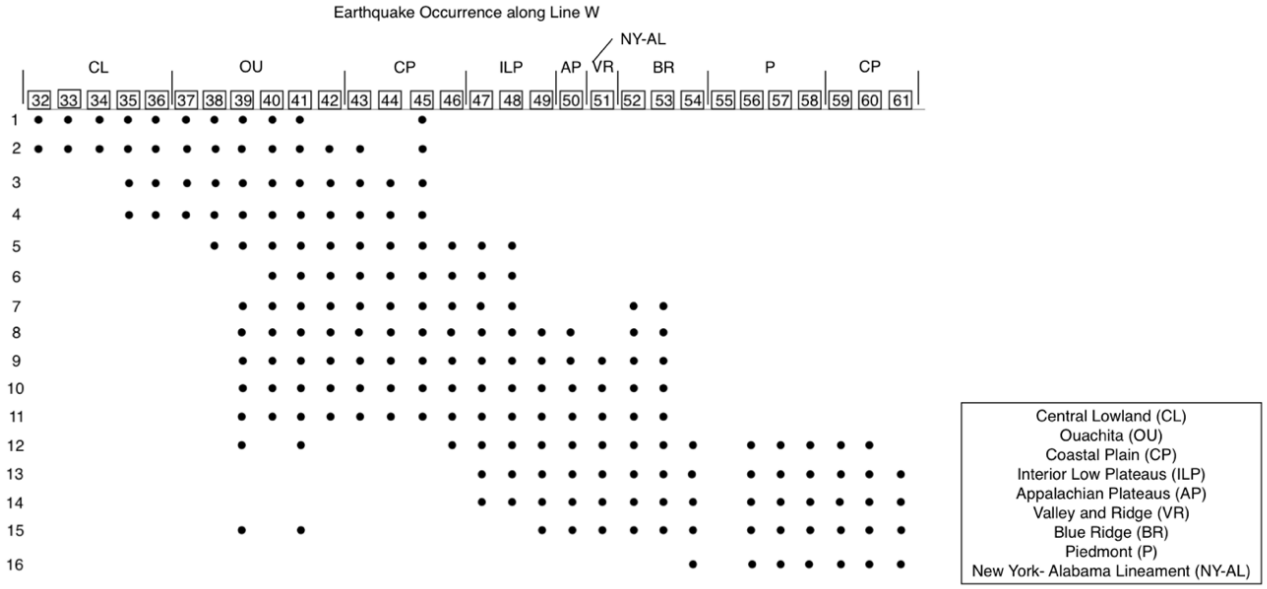


Figure H3 shows station coverage for Line W.

FIGURE H4

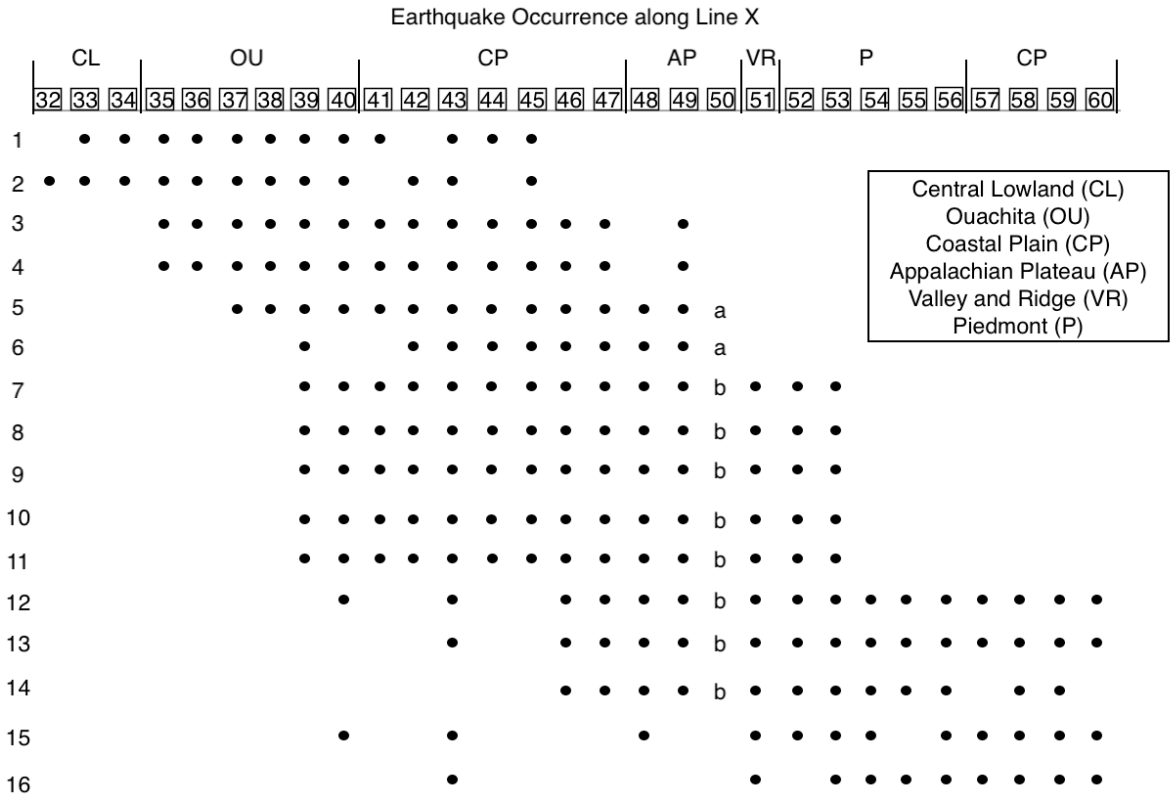


Figure H4 shows station coverage for Line X.

FIGURE H5

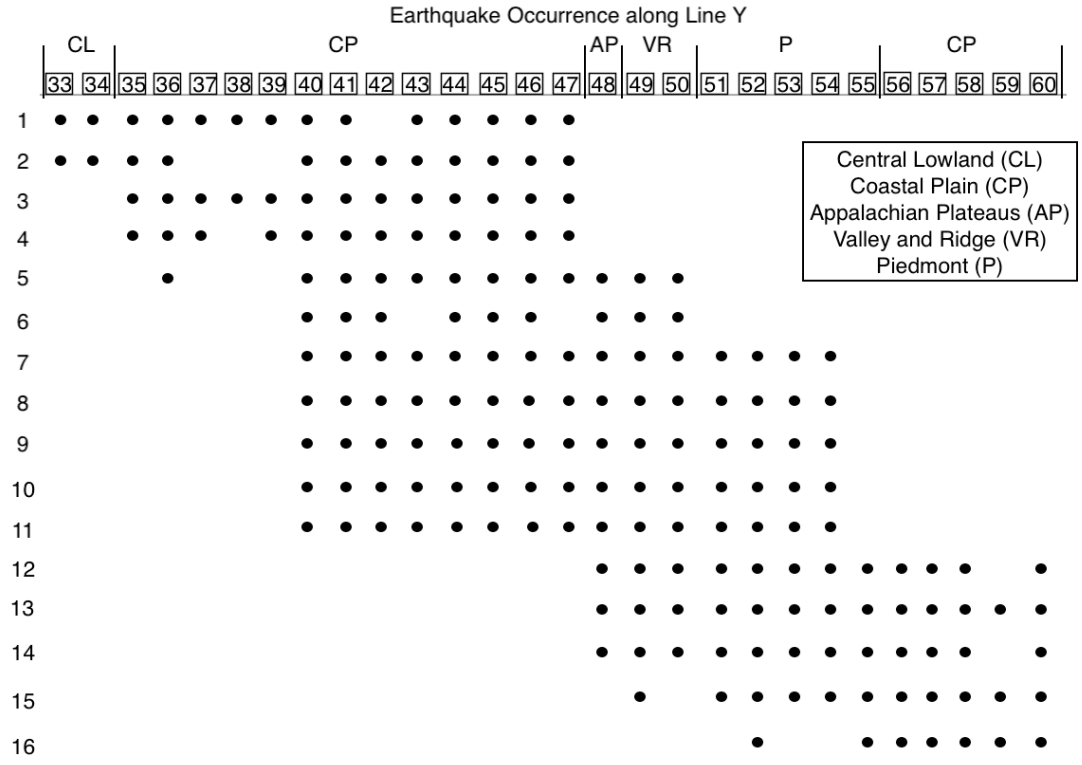


Figure H5 shows station coverage for Line Y.

FIGURE H6

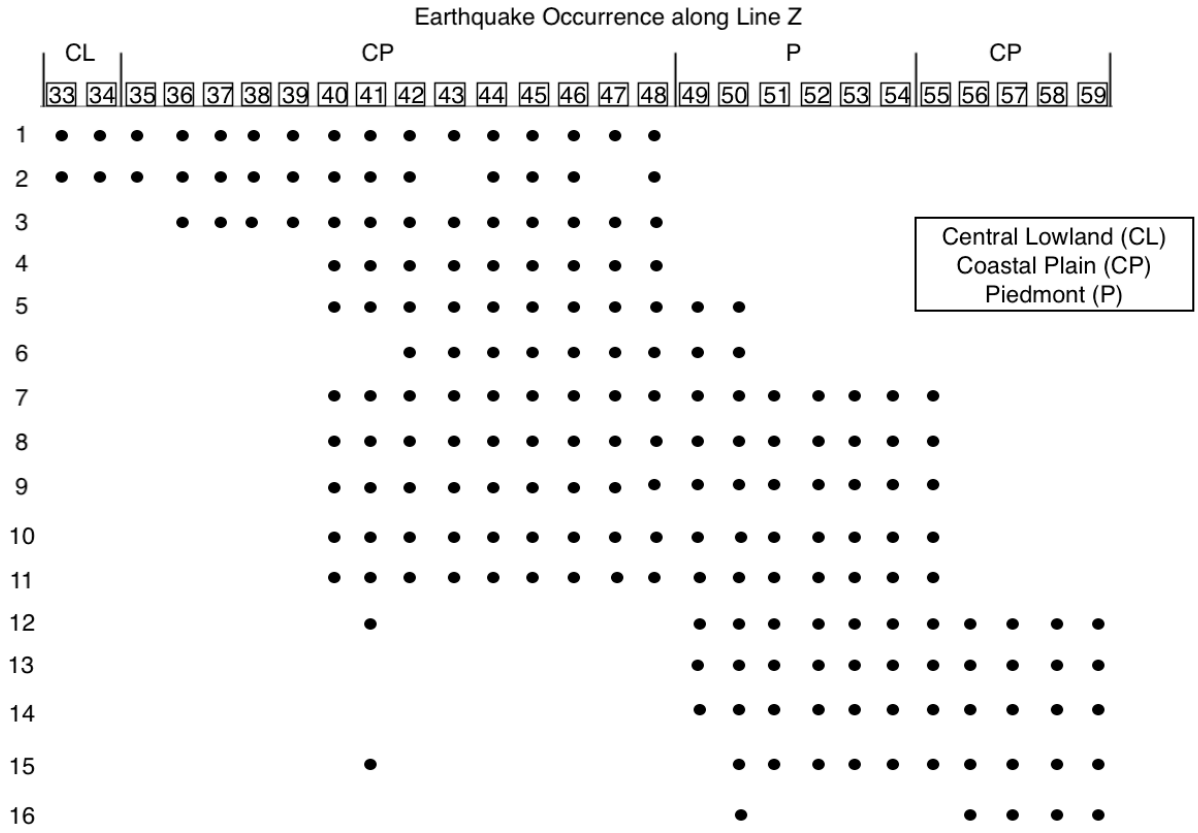


Figure H6 shows station coverage for Line Z.

APPENDIX I

CODING

STEP 101

Example taken from the earthquake of magnitude 7.6 on August 31, 2012, from Line V

```
** pkikp_ta_step101_working_2012aug31.m7.6_TA_line_V.macro

** July 6, 2017; May 17, 2018; Sept. 7, 2018;
** Jan. 9, 2019; Nov. 12, 2020; 11/30/2020; 2/1/2021;
** 2/4/2021; 5/12/2021; 5/26/2021

** SAC job for preliminary processing of TA data
** (dt = 0.025 seconds). (Compared with dt = 0.020 seconds
** used for SESAME data).

** Works on data downloaded from JWEED as follows:

** For Devon's events:
** 20 seconds before "PKIKP" to 180 seconds after "PKIKP"

** For Gustavo's events:
** 30 seconds before "PKIKP" to 170 seconds after "PKIKP"

** Note the following:

**  1. Now (ideally),the input files for all stations will
**     have the same length = (200/0.025) + 1 = 8001 samples
**  2. But traces for a small number of stations will
```

```
**     have 8000 samples (and rarely, 7999 samples),
**     so will need to pad these to 8001 samples. Will do
**     this later in step102.
**  3. As before, the start time for each file will vary,
**     so will need to carefully edit the file names.
**  4. Note: the last part of the name is usually
**     "000Z" but for some stations it may be "025Z".
**  5. The direct PKIKP (PKPdf) arrivals should
**     already be pretty well aligned.
**  6. So this job eliminates the steps for picking
**     the PKIKP arrival and time windowing.
**  7. Just keeps the steps for removing the mean and trend
**     and tapering the output trace.

** TA Station V39A
r TA.V39A..BHZ.M__at__2012-08-31T13.05.50.000Z.SAC
rmean
rtr
taper w 0.01
w ph.2012aug31.m7.6.ta.v39a.BHZ

** TA Station V40A
r TA.V40A..BHZ.M__at__2012-08-31T13.05.51.000Z.SAC
rmean
rtr
taper w 0.01
w ph.2012aug31.m7.6.ta.v40a.BHZ

** TA Station V41A
r TA.V41A..BHZ.M__at__2012-08-31T13.05.51.000Z.SAC
rmean
```

```
rtr
taper w 0.01
w ph.2012aug31.m7.6.ta.v41a.BHZ

** TA Station V42A
r TA.V42A..BHZ.M__at__2012-08-31T13.05.52.000Z.SAC
rmean
rtr
taper w 0.01
w ph.2012aug31.m7.6.ta.v42a.BHZ

** TA Station V43A
r TA.V43A..BHZ.M__at__2012-08-31T13.05.53.000Z.SAC
rmean
rtr
taper w 0.01
w ph.2012aug31.m7.6.ta.v43a.BHZ

** TA Station V44A
r TA.V44A..BHZ.M__at__2012-08-31T13.05.54.000Z.SAC
rmean
rtr
taper w 0.01
w ph.2012aug31.m7.6.ta.v44a.BHZ

** TA Station V45A
r TA.V45A..BHZ.M__at__2012-08-31T13.05.55.000Z.SAC
rmean
rtr
taper w 0.01
w ph.2012aug31.m7.6.ta.v45a.BHZ
```

** TA Station V46A

r TA.V46A..BHZ.M__at__2012-08-31T13.05.56.000Z.SAC

rmean

rtr

taper w 0.01

w ph.2012aug31.m7.6.ta.v46a.BHZ

** TA Station V47A

r TA.V47A..BHZ.M__at__2012-08-31T13.05.56.025Z.SAC

rmean

rtr

taper w 0.01

w ph.2012aug31.m7.6.ta.v47a.BHZ

** TA Station V48A

r TA.V48A..BHZ.M__at__2012-08-31T13.05.57.000Z.SAC

rmean

rtr

taper w 0.01

w ph.2012aug31.m7.6.ta.v48a.BHZ

** TA Station V49A

r TA.V49A..BHZ.M__at__2012-08-31T13.05.58.000Z.SAC

rmean

rtr

taper w 0.01

w ph.2012aug31.m7.6.ta.v49a.BHZ

** TA Station V50A

r TA.V50A..BHZ.M__at__2012-08-31T13.05.59.000Z.SAC

```
rmean
rtr
taper w 0.01
w ph.2012aug31.m7.6.ta.v50a.BHZ

** TA Station V51A
r TA.V51A..BHZ.M__at__2012-08-31T13.06.00.000Z.SAC
rmean
rtr
taper w 0.01
w ph.2012aug31.m7.6.ta.v51a.BHZ

** TA Station V52A
r TA.V52A..BHZ.M__at__2012-08-31T05.06.00.000Z.SAC
rmean
rtr
taper w 0.01
w ph.2012aug31.m7.6.ta.v52a.BHZ


** TA Station V53A
r TA.V53A..BHZ.M__at__2012-08-31T05.06.01.000Z.SAC
rmean
rtr
taper w 0.01
w ph.2012aug31.m7.6.ta.v53a.BHZ
```

STEP 102

Example taken from the earthquake of magnitude 7.6 on August 31, 2012, from Line V

```
# pkikp_ta_step102_working_2012aug31.m7.6.ta.line_V_nt7999.txt
#
# November 12, 2020; 12/1/2020; Feb. 1, 2021;
# 2/8/2021; 5/12/2021; 6/2/2021
#
# Processing of TA data (dt=0.025 seconds, compared
# with dt=0.020 seconds for SESAME data)
#
# Data were downloaded using JWEED as follows:
#
# For Devon's events:
# 20 seconds before "PKIKP" to 180 seconds after "PKIKP".
#
# For Gustavo's events:
# 30 seconds before "PKIKP" to 170 seconds after "PKIKP".

# So (ideally) the input files for all stations will have
# the same length (200/0.025) + 1 = 8001 samples.
#
# But traces for some stations may have only 8000 or 7999 samples.
#
# So far, the data have been processed with a SAC macro
```

```
# (removal of mean and trend, by tapering).
#
# This job performs the following operations:

# 1) Read only the first 7999 samples, strip SAC headers,
#    combine headers into a single
#    file, and then print header listing.
#
# 2) Combine the traces into a gather.
#
# 3) Then lengthen the traces from 7999 to 8001 samples
#    (pad end of each trace with one zero).
#
# 4) Add SU headers, then resample from dt=0.025 seconds
#    to dt=0.020 seconds, to match SESAME data.
#
# 5) Perform bandpass filtering.
#
# 6) Plot.
#
# 7) Strip SU headers in preparation for
#    cross-correlation statics in step103.
#

# Strip the SAC headers; read in the first 7999 samples
# (most traces have 8001 samples)
```

```
sacheaderstrip in=ph.2012aug31.m7.6.ta.v39a.BHZ \
out=trace.v39a.strip \
hdr=trace.v39a.header ntr=1 \
nt=7999

sacheaderstrip in=ph.2012aug31.m7.6.ta.v40a.BHZ \
out=trace.v40a.strip \
hdr=trace.v40a.header ntr=1 \
nt=7999

sacheaderstrip in=ph.2012aug31.m7.6.ta.v41a.BHZ \
out=trace.v41a.strip \
hdr=trace.v41a.header ntr=1 \
nt=7999

sacheaderstrip in=ph.2012aug31.m7.6.ta.v42a.BHZ \
out=trace.v42a.strip \
hdr=trace.v42a.header ntr=1 \
nt=7999

sacheaderstrip in=ph.2012aug31.m7.6.ta.v43a.BHZ \
out=trace.v43a.strip \
hdr=trace.v43a.header ntr=1 \
nt=7999

sacheaderstrip in=ph.2012aug31.m7.6.ta.v44a.BHZ \
out=trace.v44a.strip \
hdr=trace.v44a.header ntr=1 \
```

```
nt=7999

sacheaderstrip in=ph.2012aug31.m7.6.ta.v45a.BHZ \
out=trace.v45a.strip \
hdr=trace.v45a.header ntr=1 \
nt=7999

sacheaderstrip in=ph.2012aug31.m7.6.ta.v46a.BHZ \
out=trace.v46a.strip \
hdr=trace.v46a.header ntr=1 \
nt=7999

sacheaderstrip in=ph.2012aug31.m7.6.ta.v47a.BHZ \
out=trace.v47a.strip \
hdr=trace.v47a.header ntr=1 \
nt=7999

sacheaderstrip in=ph.2012aug31.m7.6.ta.v48a.BHZ \
out=trace.v48a.strip \
hdr=trace.v48a.header ntr=1 \
nt=7999

sacheaderstrip in=ph.2012aug31.m7.6.ta.v49a.BHZ \
out=trace.v49a.strip \
hdr=trace.v49a.header ntr=1 \
nt=7999

sacheaderstrip in=ph.2012aug31.m7.6.ta.v50a.BHZ \
```

```
out=trace.v50a.strip \
hdr=trace.v50a.header ntr=1 \
nt=7999

sacheaderstrip in=ph.2012aug31.m7.6.ta.v51a.BHZ \
out=trace.v51a.strip \
hdr=trace.v51a.header ntr=1 \
nt=7999

sacheaderstrip in=ph.2012aug31.m7.6.ta.v52a.BHZ \
out=trace.v52a.strip \
hdr=trace.v52a.header ntr=1 \
nt=7999

sacheaderstrip in=ph.2012aug31.m7.6.ta.v53a.BHZ \
out=trace.v53a.strip \
hdr=trace.v53a.header ntr=1 \
nt=7999


cp trace.v39a.header header
dd if=trace.v40a.header bs=4096 >> header
dd if=trace.v41a.header bs=4096 >> header
dd if=trace.v42a.header bs=4096 >> header
dd if=trace.v43a.header bs=4096 >> header
dd if=trace.v44a.header bs=4096 >> header
dd if=trace.v45a.header bs=4096 >> header
dd if=trace.v46a.header bs=4096 >> header
```

```
dd if=trace.v47a.header bs=4096 >> header

dd if=trace.v48a.header bs=4096 >> header

dd if=trace.v49a.header bs=4096 >> header

dd if=trace.v50a.header bs=4096 >> header

dd if=trace.v51a.header bs=4096 >> header

dd if=trace.v52a.header bs=4096 >> header

dd if=trace.v53a.header bs=4096 >> header



swapbytes < header in=float > header.swap

sacheaderlist12 in=header inswap=header \

hdr1=headerlist1.ph.2012aug31.m7.6.ta.line_V.txt \

hdr2=headerlist2.ph.2012aug31.m7.6.ta.line_V.txt ntr=15



# form gather

cp trace.v39a.strip ph.2012aug31.m7.6.ta.nt7999.line_V

dd if=trace.v40a.strip bs=4096 >> ph.2012aug31.m7.6.ta.nt7999.line_V

dd if=trace.v41a.strip bs=4096 >> ph.2012aug31.m7.6.ta.nt7999.line_V

dd if=trace.v42a.strip bs=4096 >> ph.2012aug31.m7.6.ta.nt7999.line_V

dd if=trace.v43a.strip bs=4096 >> ph.2012aug31.m7.6.ta.nt7999.line_V

dd if=trace.v44a.strip bs=4096 >> ph.2012aug31.m7.6.ta.nt7999.line_V

dd if=trace.v45a.strip bs=4096 >> ph.2012aug31.m7.6.ta.nt7999.line_V

dd if=trace.v46a.strip bs=4096 >> ph.2012aug31.m7.6.ta.nt7999.line_V

dd if=trace.v47a.strip bs=4096 >> ph.2012aug31.m7.6.ta.nt7999.line_V

dd if=trace.v48a.strip bs=4096 >> ph.2012aug31.m7.6.ta.nt7999.line_V

dd if=trace.v49a.strip bs=4096 >> ph.2012aug31.m7.6.ta.nt7999.line_V

dd if=trace.v50a.strip bs=4096 >> ph.2012aug31.m7.6.ta.nt7999.line_V
```

```
dd if=trace.v51a.strip bs=4096 >> ph.2012aug31.m7.6.ta.nt7999.line_V

dd if=trace.v52a.strip bs=4096 >> ph.2012aug31.m7.6.ta.nt7999.line_V

dd if=trace.v53a.strip bs=4096 >> ph.2012aug31.m7.6.ta.nt7999.line_V

# pad end of traces

padtrace2015 in=ph.2012aug31.m7.6.ta.nt7999.line_V \

out=ph.2012aug31.m7.6.ta.line_V \

ntr=15 ntin=7999 ntout=8001



# Add SU headers: "ns" is the number of samples per trace;

# "a=25000" = 25,000 microseconds = 25 milliseconds = 0.025 seconds = dt


suaddhead < ph.2012aug31.m7.6.ta.line_V ns=8001 | \

sushw key=dt a=25000 > \

ph.2012aug31.m7.6.ta.line_V.su1


# Resample from dt=0.025 s to dt=0.020 s

# Increase the number of samples to keep the

# time window the same: (200/0.020) + 1 = 10,001 samples.


suresamp < ph.2012aug31.m7.6.ta.line_V.su1 \

dt=0.020 nt=10001 > \

ph.2012aug31.m7.6.ta.line_V.z.resamp.dt0.020.nt10001.su1



# Plot traces: all 200 seconds

# Plot trace with dt=0.025s, nt=8001 samples
```

```
suop < ph.2012aug31.m7.6.ta.line_V.su1 op=norm | \
supswigp xcur=1.0 wbox=6 hbox=8.5 style=seismic \
nbpi=300 linewidth=0 \
title="ph.2012aug31.m7.6.ta.line_V.su1, 2/8/2021" \
label1="Time (s)" labelsize=9 n2tic=2 xbeg=-0.2 \
xend=1 interp=1 n1tic=5 titlesize=8 key=offset > \
ph.2012aug31.m7.6.ta.line_V.su1.ps

# Plot trace with dt=0.020s, nt=10,001 samples

suop < ph.2012aug31.m7.6.ta.line_V.z.resamp.dt0.020.nt10001.su1 op=norm | \
supswigp xcur=1.0 wbox=6 hbox=8.5 style=seismic \
nbpi=300 linewidth=0 \
title="ph.2012aug31.m7.6.ta.line_V.z.resamp.dt0.020.nt10001.su1, 2/8/2021" \
label1="Time (s)" labelsize=9 n2tic=2 xbeg=-0.2 \
xend=1 interp=1 n1tic=5 titlesize=8 key=offset > \
ph.2012aug31.m7.6.ta.line_V.z.resamp.dt0.020.nt10001.su1.ps


# Strip header from the resampled trace

sustrip < ph.2012aug31.m7.6.ta.line_V.z.resamp.dt0.020.nt10001.su1 \
> ph.2012aug31.m7.6.ta.line_V.z.resamp.dt0.020.nt10001.strip


# Window the traces to 100 seconds and plot
#
# Note that for Devon's earthquakes:
```

```
# the downloaded traces start 20 seconds before PKIKP
# So output window is 20 s before PKIKP to 80 s after PKIKP
#
# For Gustavo's earthquakes:
# the downloaded traces start 30 seconds before PKIKP
# So output window is 30 s before PKIKP to 70 s after PKIKP

# For resampled trace with dt=0.020 s:

seispickalt_2015 in=ph.2012aug31.m7.6.ta.line_V.z.resamp.dt0.020.nt10001.strip \
out=ph.2012aug31.m7.6.ta.line_V.z.resamp.dt0.020.windowed \
nx=15 nt=10001 nt1=1 nt2=5001

# For original trace with dt=0.025 s:

seispickalt_2015 in=ph.2012aug31.m7.6.ta.line_V \
out=ph.2012aug31.m7.6.ta.line_V.z.windowed \
nx=15 nt=8001 nt1=1 nt2=4001

# Add headers and plot

suaddhead < ph.2012aug31.m7.6.ta.line_V.z.resamp.dt0.020.windowed ns=5001 | \
sushw key=dt a=20000 > \
ph.2012aug31.m7.6.ta.line_V.z.resamp.dt0.020.windowed.su1

suop <ph.2012aug31.m7.6.ta.line_V.z.resamp.dt0.020.windowed.su1 op=norm | \
supswigp xcur=1.0 wbox=6 hbox=8.5 style=seismic \
nbpi=300 linewidth=0 \
```

```
title="ph.2012aug31.m7.6.ta.line_V.z.resamp.dt0.020.windowed, 2/8/2021" \
label1="Time (s)" labelsize=9 n2tic=2 xbeg=-0.2 \
xend=1 interp=1 n1tic=5 titlesize=8 key=offset > \
ph.2012aug31.m7.6.ta.line_V.z.resamp.dt0.020.windowed.su1.ps

suaddhead < ph.2012aug31.m7.6.ta.line_V.z.windowed ns=4001 | \
sushw key=dt a=25000 > \
ph.2012aug31.m7.6.ta.line_V.z.windowed.su1

suop <ph.2012aug31.m7.6.ta.line_V.z.windowed.su1 op=norm | \
supswigp xcur=1.0 wbox=6 hbox=8.5 style=seismic \
nbpi=300 linewidth=0 \
title="ph.2012aug31.m7.6.ta.line_V.z.windowed, 2/8/2021" \
label1="Time (s)" labelsize=9 n2tic=2 xbeg=-0.2 \
xend=1 interp=1 n1tic=5 titlesize=8 key=offset > \
ph.2012aug31.m7.6.ta.line_V.z.windowed.su1.ps

# Taper the ends of the resampled traces (note: SAC has already
# tapered the first and last 3 seconds), then apply
# a series of bandpass filters

suramp < ph.2012aug31.m7.6.ta.line_V.z.resamp.dt0.020.windowed.su1 \
tmin=10 tmax=90 > ph.2012aug31.m7.6.ta.line_V.z.resamp.dt0.020.tap.su1

sufilter < ph.2012aug31.m7.6.ta.line_V.z.resamp.dt0.020.tap.su1 \
f=0,0.01,0.02,3.0,5.0 amps=0,0,1,1,0 > \
ph.2012aug31.m7.6.ta.line_V.z.resamp.filt_0.02_3Hz.su1
```

```
sufilter < ph.2012aug31.m7.6.ta.line_V.z.resamp.dt0.020.tap.su1 \
f=0,0.01,0.02,2.0,3.0 amps=0,0,1,1,0 > \
ph.2012aug31.m7.6.ta.line_V.z.resamp.filt_0.02_2Hz.su1

sufilter < ph.2012aug31.m7.6.ta.line_V.z.resamp.dt0.020.tap.su1 \
f=0,0.05,0.10,2.0,3.0 amps=0,0,1,1,0 > \
ph.2012aug31.m7.6.ta.line_V.z.resamp.filt_0.1_2Hz.su1

sufilter < ph.2012aug31.m7.6.ta.line_V.z.resamp.dt0.020.tap.su1 \
f=0,0.05,0.10,3.0,5.0 amps=0,0,1,1,0 > \
ph.2012aug31.m7.6.ta.line_V.z.resamp.filt_0.1_3Hz.su1

sufilter < ph.2012aug31.m7.6.ta.line_V.z.resamp.dt0.020.tap.su1 \
f=0,0.3,0.5,2.0,3.0 amps=0,0,1,1,0 > \
ph.2012aug31.m7.6.ta.line_V.z.resamp.filt_0.5_2Hz.su1

# strip SU headers to allow use of bandpass filtered traces
# for doing the cross-correlation statics

sustrip < ph.2012aug31.m7.6.ta.line_V.z.resamp.filt_0.02_3Hz.su1 \
 > ph.2012aug31.m7.6.ta.line_V.z.resamp.filt_0.02_3Hz.strip

sustrip < ph.2012aug31.m7.6.ta.line_V.z.resamp.filt_0.02_2Hz.su1 \
 > ph.2012aug31.m7.6.ta.line_V.z.resamp.filt_0.02_2Hz.strip

sustrip < ph.2012aug31.m7.6.ta.line_V.z.resamp.filt_0.1_2Hz.su1 \
 > ph.2012aug31.m7.6.ta.line_V.z.resamp.filt_0.1_2Hz.strip
```

```
sustrip < ph.2012aug31.m7.6.ta.line_V.z.resamp.filt_0.1_3Hz.su1 \
 > ph.2012aug31.m7.6.ta.line_V.z.resamp.filt_0.1_3Hz.strip

sustrip < ph.2012aug31.m7.6.ta.line_V.z.resamp.filt_0.5_2Hz.su1 \
 > ph.2012aug31.m7.6.ta.line_V.z.resamp.filt_0.5_2Hz.strip

# plot the filtered resampled traces

suop <ph.2012aug31.m7.6.ta.line_V.z.resamp.filt_0.02_3Hz.su1 op=norm | \
supswigp xcur=1.0 wbox=6 hbox=8.5 style=seismic \
nbpi=300 linewidth=0 \
title="ph.2012aug31.m7.6.ta.line_V.z.resamp.filt_0.02_3Hz, 2/8/2021" \
label1="Time (s)" labelsize=9 n2tic=2 xbeg=-0.2 \
xend=1 interp=1 n1tic=5 titlesize=8 key=offset > \
ph.2012aug31.m7.6.ta.line_V.z.resamp.filt_0.02_3Hz.su1.ps

suop <ph.2012aug31.m7.6.ta.line_V.z.resamp.filt_0.02_2Hz.su1 op=norm | \
supswigp xcur=1.0 wbox=6 hbox=8.5 style=seismic \
nbpi=300 linewidth=0 \
title="ph.2012aug31.m7.6.ta.line_V.z.resamp.filt_0.02_2Hz, 2/8/2021" \
label1="Time (s)" labelsize=9 n2tic=2 xbeg=-0.2 \
xend=1 interp=1 n1tic=5 titlesize=8 key=offset > \
ph.2012aug31.m7.6.ta.line_V.z.resamp.filt_0.02_2Hz.su1.ps

suop <ph.2012aug31.m7.6.ta.line_V.z.resamp.filt_0.1_2Hz.su1 op=norm | \
supswigp xcur=1.0 wbox=6 hbox=8.5 style=seismic \
nbpi=300 linewidth=0 \
title="ph.2012aug31.m7.6.ta.line_V.z.resamp.filt_0.1_2Hz, 2/8/2021" \
```

```
label1="Time (s)" labelsize=9 n2tic=2 xbeg=-0.2 \
xend=1 interp=1 n1tic=5 titlesize=8 key=offset > \
ph.2012aug31.m7.6.ta.line_V.z.resamp.filt_0.1_2Hz.su1.ps


suop <ph.2012aug31.m7.6.ta.line_V.z.resamp.filt_0.1_3Hz.su1 op=norm | \
supswigp xcur=1.0 wbox=6 hbox=8.5 style=seismic \
nbpi=300 linewidth=0 \
title="ph.2012aug31.m7.6.ta.line_V.z.resamp.filt_0.1_3Hz, 2/8/2021" \
label1="Time (s)" labelsize=9 n2tic=2 xbeg=-0.2 \
xend=1 interp=1 n1tic=5 titlesize=8 key=offset > \
ph.2012aug31.m7.6.ta.line_V.z.resamp.filt_0.1_3Hz.su1.ps

suop <ph.2012aug31.m7.6.ta.line_V.z.resamp.filt_0.5_2Hz.su1 op=norm | \
supswigp xcur=1.0 wbox=6 hbox=8.5 style=seismic \
nbpi=300 linewidth=0 \
title="ph.2012aug31.m7.6.ta.line_V.z.resamp.filt_0.5_2Hz, 2/8/2021" \
label1="Time (s)" labelsize=9 n2tic=2 xbeg=-0.2 \
xend=1 interp=1 n1tic=5 titlesize=8 key=offset > \
ph.2012aug31.m7.6.ta.line_V.z.resamp.filt_0.5_2Hz.su1.ps
```

STEP 103 REGULAR

Example taken from the earthquake of magnitude 7.6 on August 31, 2012, from Line V

```
# pkikp_ta_step103_working_2012aug31.m7.6.ta.line_V.txt
#
# July 6, 2017; May 17, 2018; May 23, 2018; 9/19/18; 10/30/18
# Jan. 11, 2019; Nov. 17, 2020; 11/21/2020; 12/2/2020;
# 2/1/2021 ; 2/27/2021 ; 3/5/2021; 6/30/2021
#
# Processing of TA data (dt=0.025 seconds, compared with
# dt=0.020 seconds for SESAME data).  Traces were
# resampled to 0.020 seconds in the previous job (step102).
#
# "Step103" cross correlates traces with the
# source wavelet (the latter was estimated using SESAME data).
# The final product is the combined gather (source wavelet
# estimate followed by traces) with statics corrections.
#
# Preview of steps after this:
#
# In step104, the source-time function is used to deconvolve
#    the traces. Then plots the gather with uniform trace
#    spacing.
#
```

```
# In step105, will insert blank (all zero) traces for unoccupied
#    stations so eventually can vertically stack traces
#    for multiple earthquakes.  Gathers are plotted with
#    the correct relative trace spacing.
#
# Step106 is similar to step105, except does not insert blank traces.
#    Gathers are still plotted with the correct relative
#    trace spacing.  This will give a cleaner plot, more
#    suitable for presentation of results of individual
#    earthquakes.

# unfiltered traces; windowed -20 -> 80 seconds
# (for some of Devon's events, this will be -20 -> 90 seconds)
# (for Gustavo's events, this will be -30 -> 70 seconds)
#
# NOTE: for the "dd" command, cannot have a space between "if=" and ".."

# insert the source wavelet trace at the beginning of the gather

cp wavelet8.gus.5.2012aug31.m7.6 source_and_traces
dd if=ph.2012aug31.m7.6.ta.line_V.z.resamp.dt0.020.windowed bs=4096 >> source_and_traces
cp source_and_traces ph.2012aug31.m7.6.ta.line_V.z.plus.source
cp wavelet8.gus.5.2012aug31.m7.6  source_and_traces_filt
dd if=ph.2012aug31.m7.6.ta.line_V.z.resamp.filt_0.1_2Hz.strip bs=4096 >> source_and_traces_filt
cp source_and_traces_filt ph.2012aug31.m7.6.ta.line_V.z.plus.source.filt

# Plot gathers
# number of samples in windows:
```

```
#
# for -20 -> 80 & -30 -> 70 seconds: ns=nt=5001
# for -20 -> 90 seconds: ns=nt=5501

suaddhead < ph.2012aug31.m7.6.ta.line_V.z.plus.source ns=5001 | \
sushw key=dt a=20000 > \
ph.2012aug31.m7.6.ta.line_V.z.plus.source.su1

suop < ph.2012aug31.m7.6.ta.line_V.z.plus.source.su1 op=norm | \
supswigp xcur=1.0 wbox=6 hbox=8.5 style=seismic \
nbpi=300 linewidth=0 \
title="ph.2012aug31.m7.6.ta.line_V.z.plus.source, 3/5/2021" \
label1="Time (s)" labelsize=9 n2tic=2 xbeg=-0.2 \
xend=1 interp=1 n1tic=5 titlesize=8 key=offset > \
ph.2012aug31.m7.6.ta.line_V.z.plus.source.su1.ps

suaddhead < ph.2012aug31.m7.6.ta.line_V.z.plus.source.filt ns=5001 | \
sushw key=dt a=20000 > \
ph.2012aug31.m7.6.ta.line_V.z.plus.source.filt.su1

suop < ph.2012aug31.m7.6.ta.line_V.z.plus.source.filt.su1 op=norm | \
supswigp xcur=1.0 wbox=6 hbox=8.5 style=seismic \
nbpi=300 linewidth=0 \
title="ph.2012aug31.m7.6.ta.line_V.z.plus.source.filt, 3/5/2021" \
label1="Time (s)" labelsize=9 n2tic=2 xbeg=-0.2 \
xend=1 interp=1 n1tic=5 titlesize=8 key=offset > \
ph.2012aug31.m7.6.ta.line_V.z.plus.source.filt.su1.ps
```

```
# Cross correlate and plot
#
# Use the first trace (source wavelet estimate) as the pilot trace

crosscorrstatquake in=ph.2012aug31.m7.6.ta.line_V.z.plus.source.filt \
out=ph.2012aug31.m7.6.ta.line_V.z.plus.source.filt.statout \
outc=ph.2012aug31.m7.6.ta.line_V.z.plus.source.filt.shifts \
corr=ph.2012aug31.m7.6.ta.line_V.z.plus.source.filt.crosscor \
ntr=16 nt=5001 t1=28 t2=85 dt=0.02 \
secmax=4 npilot=1

suaddhead < ph.2012aug31.m7.6.ta.line_V.z.plus.source.filt.statout ns=5001 | \
sushw key=dt a=20000 > \
ph.2012aug31.m7.6.ta.line_V.z.plus.source.filt.statout.su1

suop < ph.2012aug31.m7.6.ta.line_V.z.plus.source.filt.statout.su1 op=norm | \
supswigp xcur=1.0 wbox=6 hbox=8.5 style=seismic \
nbpi=300 linewidth=0 \
title="ph.2012aug31.m7.6.ta.line_V.z.plus.source.filt.statout, 3/5/2021" \
label1="Time (s)" labelsize=9 n2tic=2 xbeg=-0.2 \
xend=1 interp=1 n1tic=5 titlesize=8 key=offset > \
ph.2012aug31.m7.6.ta.line_V.z.plus.source.filt.statout.su1.ps

# Apply these static shifts to the unfiltered gather

sampshiftarb in=ph.2012aug31.m7.6.ta.line_V.z.plus.source \
out=ph.2012aug31.m7.6.ta.line_V.z.plus.source.statout \
para=ph.2012aug31.m7.6.ta.line_V.z.plus.source.filt.shifts \
```

```
mode=2 ntr=16 nt=5001


suaddhead < ph.2012aug31.m7.6.ta.line_V.z.plus.source.statout ns=5001 | \
sushw key=dt a=20000 > \
ph.2012aug31.m7.6.ta.line_V.z.plus.source.statout.su1


suop < ph.2012aug31.m7.6.ta.line_V.z.plus.source.statout.su1 op=norm | \
supswigp xcur=1.0 wbox=6 hbox=8.5 style=seismic \
nbpi=300 linewidth=0 \
title="ph.2012aug31.m7.6.ta.line_V.z.plus.source.statout, 3/5/2021" \
label1="Time (s)" labelsize=9 n2tic=2 xbeg=-0.2 \
xend=1 interp=1 n1tic=5 titlesize=8 key=offset > \
ph.2012aug31.m7.6.ta.line_V.z.plus.source.statout.su1.ps
```

STEP 103 NEW WAVELET

Example taken from the earthquake of magnitude 6.6 on August 26, 2012, from Line X

```
# pkikp_ta_step103_new_wavelet_working_2012aug26.m6.6.ta.line_X.txt
#
# July 6, 2017; May 17, 2018; May 23, 2018; 9/19/18; 10/30/18
# Jan. 11, 2019; Nov. 17, 2020; 11/21/2020; 12/2/2020;
# 2/1/2021; 3/8/2021; 3/10/2021; 6/30/2021; 8/25/2021; 1/26/2022
#
# Processing of TA data (dt=0.025 seconds, compared with
# dt=0.020 seconds for SESAME data).  Traces were
# resampled to 0.020 seconds in the previous job (step102).
#
# "Step103" cross correlates the field traces to determine
# statics corrections.  The static-corrected traces then
# are stacked to derive a new estimate of the source
# wavelet.

# The final product is the combined gather (source wavelet
# estimate followed by traces) with statics corrections.
#
# Preview of steps after this:
#
# In step104, the source-time function is used to deconvolve
```

```
#    the traces. Then plots the gather with uniform trace
#    spacing.
#
# In step105, will insert blank (all zero) traces for unoccupied
#    stations so eventually can vertically stack traces
#    for multiple earthquakes.  Gathers are plotted with
#    the correct relative trace spacing.
#
# Step106 is similar to step105, except does not insert blank traces.
#    Gathers are still plotted with the correct relative
#    trace spacing.  This will give a cleaner plot, more
#    suitable for presentation of results of individual
#    earthquakes.

# unfiltered traces; windowed -20 -> 80 seconds
# (for some of Devon's events, this will be -20 -> 90 seconds)
# (for Gustavo's events, this will be -30 -> 70 seconds)
#
# NOTE: for the "dd" command, cannot have a space between "if=" and ".."

cp ph.2012aug26.m6.6.ta.line_X.z.resamp.dt0.020.windowed field_traces
cp ph.2012aug26.m6.6.ta.line_X.z.resamp.filt_0.1_2Hz.strip field_traces_filt

# Plot gathers
# number of samples in windows:
#
# for -20 -> 80 & -30 -> 70 seconds: ns=nt=5501
# for -20 -> 90 seconds: ns=nt=5501
```

```
suaddhead < field_traces nt=5501 | \
sushw key=dt a=20000 > \
ph.2012aug26.m6.6.ta.line_X.z.su1

suop < ph.2012aug26.m6.6.ta.line_X.z.su1 op=norm | \
supswigp xcur=1.0 wbox=6 hbox=8.5 style=seismic \
nbpi=300 linewidth=0 \
title="ph.2012aug26.m6.6.ta.line_X.z, 1/26/2022" \
label1="Time (s)" labelsize=9 n2tic=2 xbeg=-0.2 \
xend=1 interp=1 n1tic=5 titlesize=8 key=offset > \
ph.2012aug26.m6.6.ta.line_X.z.su1.ps

suaddhead < field_traces_filt nt=5501 | \
sushw key=dt a=20000 > \
ph.2012aug26.m6.6.ta.line_X.z.filt.su1

suop < ph.2012aug26.m6.6.ta.line_X.z.filt.su1 op=norm | \
supswigp xcur=1.0 wbox=6 hbox=8.5 style=seismic \
nbpi=300 linewidth=0 \
title="ph.2012aug26.m6.6.ta.line_X.z.filt, 1/26/2022" \
label1="Time (s)" labelsize=9 n2tic=2 xbeg=-0.2 \
xend=1 interp=1 n1tic=5 titlesize=8 key=offset > \
ph.2012aug26.m6.6.ta.line_X.z.filt.su1.ps

# Cross correlate and plot
crosscorrstatquake in=field_traces_filt \
out=ph.2012aug26.m6.6.ta.line_X.z.filt.statout \
```

```
outc=ph.2012aug26.m6.6.ta.line_X.z.filt.shifts \
corr=ph.2012aug26.m6.6.ta.line_X.z.filt.crosscor \
ntr=15 nt=5501 t1=18 t2=45 dt=0.02 \
secmax=4.0 npilot=8

suaddhead < ph.2012aug26.m6.6.ta.line_X.z.filt.statout nt=5501 | \
sushw key=dt a=20000 > \
ph.2012aug26.m6.6.ta.line_X.z.filt.statout.su1

suop < ph.2012aug26.m6.6.ta.line_X.z.filt.statout.su1 op=norm | \
supswigp xcur=1.0 wbox=6 hbox=8.5 style=seismic \
nbpi=300 linewidth=0 \
title="ph.2012aug26.m6.6.ta.line_X.z.filt.statout, 1/26/2022" \
label1="Time (s)" labelsize=9 n2tic=2 xbeg=-0.2 \
xend=1 interp=1 n1tic=5 titlesize=8 key=offset > \
ph.2012aug26.m6.6.ta.line_X.z.filt.statout.su1.ps

# Apply these static shifts to the unfiltered gather

sampshiftarb in=field_traces \
out=ph.2012aug26.m6.6.ta.line_X.z.statout \
para=ph.2012aug26.m6.6.ta.line_X.z.filt.shifts \
mode=2 ntr=15 nt=5501

suaddhead < ph.2012aug26.m6.6.ta.line_X.z.statout nt=5501 | \
sushw key=dt a=20000 > \
ph.2012aug26.m6.6.ta.line_X.z.statout.su1
```

```
suop < ph.2012aug26.m6.6.ta.line_X.z.statout.su1 op=norm | \
supswigp xcur=1.0 wbox=6 hbox=8.5 style=seismic \
nbpi=300 linewidth=0 \
title="ph.2012aug26.m6.6.ta.line_X.z.statout, 1/26/2022" \
label1="Time (s)" labelsize=9 n2tic=2 xbeg=-0.2 \
xend=1 interp=1 n1tic=5 titlesize=8 key=offset > \
ph.2012aug26.m6.6.ta.line_X.z.statout.su1.ps

# Stack the static-shifted traces to get a new estimate
# for the source wavelet

vertstackpick in=ph.2012aug26.m6.6.ta.line_X.z.statout \
out=wavelet.ph.2012aug26.m6.6.ta.line_X \
para=para_stack_2012aug26.m6.6.ta.line_X.txt \
ntr=15 nt=5501

# insert the new source wavelet trace at the beginning of the
# unfiltered gather

cp wavelet.ph.2012aug26.m6.6.ta.line_X source_and_traces
dd if=ph.2012aug26.m6.6.ta.line_X.z.statout bs=4096 >> source_and_traces
cp source_and_traces ph.2012aug26.m6.6.ta.line_X.z.plus.source.statout

# Plot combined source wavelet and static-corrected field traces

# number of samples in windows:
# for -20 -> 80 & -30 -> 70 seconds: ns=nt=5501
# for -20 -> 90 seconds: ns=nt=5501
```

```
suaddhead < ph.2012aug26.m6.6.ta.line_X.z.plus.source.statout nt=5501 | \
sushw key=dt a=20000 > \
ph.2012aug26.m6.6.ta.line_X.z.plus.source.statout.su1

suop < ph.2012aug26.m6.6.ta.line_X.z.plus.source.statout.su1 op=norm | \
supswigp xcur=1.0 wbox=6 hbox=8.5 style=seismic \
nbpi=300 linewidth=0 \
title="ph.2012aug26.m6.6.ta.line_X.z.plus.source.statout, 1/26/2022" \
label1="Time (s)" labelsize=9 n2tic=2 xbeg=-0.2 \
xend=1 interp=1 n1tic=5 titlesize=8 key=offset > \
ph.2012aug26.m6.6.ta.line_X.z.plus.source.statout.su1.ps
```

STEP 103 NEW FILTERED WAVELET

Example taken from the earthquake of magnitude 6.7 on February 06, 2012, from Line X

```
# pkikp_ta_step103_new_wavelet_working_2012feb06.m6.7.ta.line_X.txt
#
# July 6, 2017; May 17, 2018; May 23, 2018; 9/19/18; 10/30/18
# Jan. 11, 2019; Nov. 17, 2020; 11/21/2020; 12/2/2020;
# 2/1/2021; 3/8/2021; 3/10/2021; 6/30/2021; 8/25/2021; 1/15/2022; 1/28/2022; 2/1/2022
#
# Processing of TA data (dt=0.025 seconds, compared with
# dt=0.020 seconds for SESAME data).  Traces were
# resampled to 0.020 seconds in the previous job (step102).
#
# "Step103" cross correlates the field traces to determine
# statics corrections.  The static-corrected traces then
# are stacked to derive a new estimate of the source
# wavelet.

# The final product is the combined gather (source wavelet
# estimate followed by traces) with statics corrections.
#
# Preview of steps after this:
#
# In step104, the source-time function is used to deconvolve
```

```
#    the traces. Then plots the gather with uniform trace
#    spacing.
#
# In step105, will insert blank (all zero) traces for unoccupied
#    stations so eventually can vertically stack traces
#    for multiple earthquakes.  Gathers are plotted with
#    the correct relative trace spacing.
#
# Step106 is similar to step105, except does not insert blank traces.
#    Gathers are still plotted with the correct relative
#    trace spacing.  This will give a cleaner plot, more
#    suitable for presentation of results of individual
#    earthquakes.

# unfiltered traces; windowed -20 -> 80 seconds
# (for some of Devon's events, this will be -20 -> 90 seconds)
# (for Gustavo's events, this will be -30 -> 70 seconds)
#
# NOTE: for the "dd" command, cannot have a space between "if=" and ".."

cp ph.2012feb06.m6.7.ta.line_X.z.resamp.dt0.020.windowed field_traces
cp ph.2012feb06.m6.7.ta.line_X.z.resamp.filt_0.5_2Hz.strip field_traces_filt

# Plot gathers

# number of samples in windows:
#
# for -20 -> 80 & -30 -> 70 seconds: ns=nt=5001
```

```
# for -20 -> 90 seconds: ns=nt=5001

suaddhead < field_traces nt=5001 | \
sushw key=dt a=20000 > \
ph.2012feb06.m6.7.ta.line_X.z.su1

suop < ph.2012feb06.m6.7.ta.line_X.z.su1 op=norm | \
supswigp xcur=1.0 wbox=6 hbox=8.5 style=seismic \
nbpi=300 linewidth=0 \
title="ph.2012feb06.m6.7.ta.line_X.z, 2/1/2022" \
label1="Time (s)" labelsize=9 n2tic=2 xbeg=-0.2 \
xend=1 interp=1 n1tic=5 titlesize=8 key=offset > \
ph.2012feb06.m6.7.ta.line_X.z.su1.ps

suaddhead < field_traces_filt nt=5001 | \
sushw key=dt a=20000 > \
ph.2012feb06.m6.7.ta.line_X.z.filt.su1

suop < ph.2012feb06.m6.7.ta.line_X.z.filt.su1 op=norm | \
supswigp xcur=1.0 wbox=6 hbox=8.5 style=seismic \
nbpi=300 linewidth=0 \
title="ph.2012feb06.m6.7.ta.line_X.z.filt, 2/1/2022" \
label1="Time (s)" labelsize=9 n2tic=2 xbeg=-0.2 \
xend=1 interp=1 n1tic=5 titlesize=8 key=offset > \
ph.2012feb06.m6.7.ta.line_X.z.filt.su1.ps

# Cross correlate and plot
#
```

```
crosscorrstatquake in=field_traces_filt \
out=ph.2012feb06.m6.7.ta.line_X.z.filt.statout \
outc=ph.2012feb06.m6.7.ta.line_X.z.filt.shifts \
corr=ph.2012feb06.m6.7.ta.line_X.z.filt.crosscor \
ntr=14 nt=5001 t1=28 t2=55 dt=0.02 \
secmax=4.0 npilot=7

suaddhead < ph.2012feb06.m6.7.ta.line_X.z.filt.statout nt=5001 | \
sushw key=dt a=20000 > \
ph.2012feb06.m6.7.ta.line_X.z.filt.statout.su1

suop < ph.2012feb06.m6.7.ta.line_X.z.filt.statout.su1 op=norm | \
supswigp xcur=1.0 wbox=6 hbox=8.5 style=seismic \
nbpi=300 linewidth=0 \
title="ph.2012feb06.m6.7.ta.line_X.z.filt.statout, 2/1/2022" \
label1="Time (s)" labelsize=9 n2tic=2 xbeg=-0.2 \
xend=1 interp=1 n1tic=5 titlesize=8 key=offset > \
ph.2012feb06.m6.7.ta.line_X.z.filt.statout.su1.ps

# Apply these static shifts to the unfiltered gather

sampshiftarb in=field_traces \
out=ph.2012feb06.m6.7.ta.line_X.z.statout \
para=ph.2012feb06.m6.7.ta.line_X.z.filt.shifts \
mode=2 ntr=14 nt=5001

suaddhead < ph.2012feb06.m6.7.ta.line_X.z.statout nt=5001 | \
```

```
sushw key=dt a=20000 > \
ph.2012feb06.m6.7.ta.line_X.z.statout.su1

suop < ph.2012feb06.m6.7.ta.line_X.z.statout.su1 op=norm | \
supswigp xcur=1.0 wbox=6 hbox=8.5 style=seismic \
nbpi=300 linewidth=0 \
title="ph.2012feb06.m6.7.ta.line_X.z.statout, 2/1/2022" \
label1="Time (s)" labelsize=9 n2tic=2 xbeg=-0.2 \
xend=1 interp=1 n1tic=5 titlesize=8 key=offset > \
ph.2012feb06.m6.7.ta.line_X.z.statout.su1.ps

# Stack the static-shifted traces to get a new estimate
# for the source wavelet

vertstackpick in=ph.2012feb06.m6.7.ta.line_X.z.filt.statout \
out=wavelet.filt.ph.2012feb06.m6.7.ta.line_X \
para=para_stack_2012feb06.m6.7.ta.line_X.txt \
ntr=14 nt=5001

# insert the new source wavelet trace at the beginning of the
# unfiltered gather

cp wavelet.filt.ph.2012feb06.m6.7.ta.line_X source_and_traces_filt
dd if=ph.2012feb06.m6.7.ta.line_X.z.filt.statout bs=4096 >> source_and_traces_filt
cp source_and_traces_filt ph.2012feb06.m6.7.ta.line_X.z.plus.source.filt.statout

# Plot combined source wavelet and static-corrected field traces
```

```
# number of samples in windows:
#
# for -20 -> 80 & -30 -> 70 seconds: ns=nt=5001
# for -20 -> 90 seconds: ns=nt=5001

suaddhead < ph.2012feb06.m6.7.ta.line_X.z.plus.source.filt.statout nt=5001 | \
sushw key=dt a=20000 > \
ph.2012feb06.m6.7.ta.line_X.z.plus.source.filt.statout.su1

suop < ph.2012feb06.m6.7.ta.line_X.z.plus.source.filt.statout.su1 op=norm | \
supswigp xcur=1.0 wbox=6 hbox=8.5 style=seismic \
nbpi=300 linewidth=0 \
title="ph.2012feb06.m6.7.ta.line_X.z.plus.source.filt.statout, 2/1/2022" \
label1="Time (s)" labelsize=9 n2tic=2 xbeg=-0.2 \
xend=1 interp=1 n1tic=5 titlesize=8 key=offset > \
ph.2012feb06.m6.7.ta.line_X.z.plus.source.filt.statout.su1.ps
```

STEP 104 REGULAR

Example taken from the earthquake of magnitude 7.6 on August 31, 2012, from Line V

```
# pkikp_ta_step104_working_2012aug31.m7.6.ta.line_V.txt
#
# July 6, 2017; May 17, 2018; May 23, 2018; 9/19/18; 10/30/18
# Jan. 11, 2019; Nov. 17, 2020; 11/21/2020; 11/23/2020;
# 12/2/2020; 2/1/2021 ; 2/27/2021 ; 3/5/2021 ; 7/7/2021
#
# Processing of TA data (dt=0.025 seconds, compared with
# dt=0.020 seconds for SESAME data).  Traces were
# resampled to 0.020 seconds in step102.
#
# The previous job ("step103") cross correlated traces with the
# source wavelet (the latter was estimated using SESAME data).
# The final product was the combined gather (source wavelet
# estimate followed by traces) with statics corrections.
#
# In this job ("step104"), the source-time function is used
#    to deconvolve the traces. The gather then is plotted
#    with uniform trace spacing.
#
# Preview of steps after this:
#
```

```
# In step105, will insert blank (all zero) traces for unoccupied
#    stations so eventually can vertically stack traces
#    for multiple earthquakes.  Gathers are plotted with
#    the correct relative trace spacing.
#
# Step106 is similar to step105, except does not insert blank traces.
#    Gathers are still plotted with the correct relative
#    trace spacing.  This will give a cleaner plot, more
#    suitable for presentation of results of individual
#    earthquakes.

# unfiltered traces; windowed -20 -> 80 seconds, so nt=ns=5001
# (for some of Devon's events, this will be -20 -> 90 seconds, so nt=5501)
# (for Gustavo's events, this will be -30 -> 70 seconds, so nt=5001)

# NOTE: for the "dd" command, cannot have a space between "if=" and ".."

# Perform deconvolution
# Input (numer): traces with cross-correlation statics applied

freqdeconsourcemac4extra numer=ph.2012aug31.m7.6.ta.line_V.z.plus.source.statout \
denom=wavelet8.gus.5.2012aug31.m7.6 \
out=ph.2012aug31.m7.6.ta.line_V.z.plus.source.freqdecon.wh0001.a1.0 \
ntr=16 nt=5001 dt=0.02 wh=0.0001 alpha=1.0 pre=20 taper=3

freqdeconsourcemac4extra numer=ph.2012aug31.m7.6.ta.line_V.z.plus.source.statout \
denom=wavelet8.gus.5.2012aug31.m7.6 \
out=ph.2012aug31.m7.6.ta.line_V.z.plus.source.freqdecon.wh0001.a2.0 \
```

```
ntr=16 nt=5001 dt=0.02 wh=0.0001 alpha=2.0 pre=20 taper=3

freqdeconsourcemac4extra numer=ph.2012aug31.m7.6.ta.line_V.z.plus.source.statout \
denom=wavelet8.gus.5.2012aug31.m7.6 \
out=ph.2012aug31.m7.6.ta.line_V.z.plus.source.freqdecon.wh0001.a3.0 \
ntr=16 nt=5001 dt=0.02 wh=0.0001 alpha=3.0 pre=20 taper=3

freqdeconsourcemac4extra numer=ph.2012aug31.m7.6.ta.line_V.z.plus.source.statout \
denom=wavelet8.gus.5.2012aug31.m7.6 \
out=ph.2012aug31.m7.6.ta.line_V.z.plus.source.freqdecon.wh0001.a4.0 \
ntr=16 nt=5001 dt=0.02 wh=0.0001 alpha=4.0 pre=20 taper=3

freqdeconsourcemac4extra numer=ph.2012aug31.m7.6.ta.line_V.z.plus.source.statout \
denom=wavelet8.gus.5.2012aug31.m7.6 \
out=ph.2012aug31.m7.6.ta.line_V.z.plus.source.freqdecon.wh0001.a5.0 \
ntr=16 nt=5001 dt=0.02 wh=0.0001 alpha=5.0 pre=20 taper=3

# Add header but for now, plot with evenly spaced traces
#
# edit "ns" as needed; ns = nt

suaddhead < ph.2012aug31.m7.6.ta.line_V.z.plus.source.freqdecon.wh0001.a1.0 ns=5001 | \
sushw key=dt a=20000 > \
ph.2012aug31.m7.6.ta.line_V.z.plus.source.freqdecon.wh0001.a1.0.su1

suaddhead < ph.2012aug31.m7.6.ta.line_V.z.plus.source.freqdecon.wh0001.a2.0 ns=5001 | \
sushw key=dt a=20000 > \
ph.2012aug31.m7.6.ta.line_V.z.plus.source.freqdecon.wh0001.a2.0.su1
```

```
suaddhead < ph.2012aug31.m7.6.ta.line_V.z.plus.source.freqdecon.wh0001.a3.0 ns=5001 | \
sushw key=dt a=20000 > \
ph.2012aug31.m7.6.ta.line_V.z.plus.source.freqdecon.wh0001.a3.0.su1

suaddhead < ph.2012aug31.m7.6.ta.line_V.z.plus.source.freqdecon.wh0001.a4.0 ns=5001 | \
sushw key=dt a=20000 > \
ph.2012aug31.m7.6.ta.line_V.z.plus.source.freqdecon.wh0001.a4.0.su1

suaddhead < ph.2012aug31.m7.6.ta.line_V.z.plus.source.freqdecon.wh0001.a5.0 ns=5001 | \
sushw key=dt a=20000 > \
ph.2012aug31.m7.6.ta.line_V.z.plus.source.freqdecon.wh0001.a5.0.su1

# Plot

suop < ph.2012aug31.m7.6.ta.line_V.z.plus.source.freqdecon.wh0001.a1.0.su1 op=norm | \
supswigp xcur=2.0 wbox=4 hbox=3.5 style=seismic \
nbpi=300 linewidth=0 \
title="ph.2012aug31.m7.6.ta.line_V.z.plus.source.freqdecon.wh0001.a1.0.su1, 3/5/2021" \
label1="Time (s)" labelsize=9 n2tic=2 xbeg=-0.2 \
xend=1 interp=1 n1tic=5 titlesize=8 key=offset > \
ph.2012aug31.m7.6.ta.line_V.z.plus.source.freqdecon.wh0001.a1.0.su1.ps

suop < ph.2012aug31.m7.6.ta.line_V.z.plus.source.freqdecon.wh0001.a2.0.su1 op=norm | \
supswigp xcur=2.0 wbox=4 hbox=3.5 style=seismic \
nbpi=300 linewidth=0 \
title="ph.2012aug31.m7.6.ta.line_V.z.plus.source.freqdecon.wh0001.a2.0.su1, 3/5/2021" \
label1="Time (s)" labelsize=9 n2tic=2 xbeg=-0.2 \
```

```
xend=1 interp=1 n1tic=5 titlesize=8 key=offset > \
ph.2012aug31.m7.6.ta.line_V.z.plus.source.freqdecon.wh0001.a2.0.su1.ps

suop < ph.2012aug31.m7.6.ta.line_V.z.plus.source.freqdecon.wh0001.a3.0.su1 op=norm | \
supswigp xcur=2.0 wbox=4 hbox=3.5 style=seismic \
nbpi=300 linewidth=0 \
title="ph.2012aug31.m7.6.ta.line_V.z.plus.source.freqdecon.wh0001.a3.0.su1, 3/5/2021" \
label1="Time (s)" labelsize=9 n2tic=2 xbeg=-0.2 \
xend=1 interp=1 n1tic=5 titlesize=8 key=offset > \
ph.2012aug31.m7.6.ta.line_V.z.plus.source.freqdecon.wh0001.a3.0.su1.ps

suop < ph.2012aug31.m7.6.ta.line_V.z.plus.source.freqdecon.wh0001.a4.0.su1 op=norm | \
supswigp xcur=2.0 wbox=4 hbox=3.5 style=seismic \
nbpi=300 linewidth=0 \
title="ph.2012aug31.m7.6.ta.line_V.z.plus.source.freqdecon.wh0001.a4.0.su1, 3/5/2021" \
label1="Time (s)" labelsize=9 n2tic=2 xbeg=-0.2 \
xend=1 interp=1 n1tic=5 titlesize=8 key=offset > \
ph.2012aug31.m7.6.ta.line_V.z.plus.source.freqdecon.wh0001.a4.0.su1.ps

suop < ph.2012aug31.m7.6.ta.line_V.z.plus.source.freqdecon.wh0001.a5.0.su1 op=norm | \
supswigp xcur=2.0 wbox=4 hbox=3.5 style=seismic \
nbpi=300 linewidth=0 \
title="ph.2012aug31.m7.6.ta.line_V.z.plus.source.freqdecon.wh0001.a5.0.su1, 3/5/2021" \
label1="Time (s)" labelsize=9 n2tic=2 xbeg=-0.2 \
xend=1 interp=1 n1tic=5 titlesize=8 key=offset > \
ph.2012aug31.m7.6.ta.line_V.z.plus.source.freqdecon.wh0001.a5.0.su1.ps
```

```
# replot with negative polarity

suop < ph.2012aug31.m7.6.ta.line_V.z.plus.source.freqdecon.wh0001.a1.0.su1 op=norm > tempnorm

suop < tempnorm op=neg | \
supswigp xcur=2.0 wbox=4 hbox=3.5 style=seismic \
nbpi=300 linewidth=0 \
title="ph.2012aug31.m7.6.ta.line_V.z.plus.source.freqdecon.wh0001.a1.0.su1, 3/5/2021" \
label1="Time (s)" labelsize=9 n2tic=2 xbeg=-0.2 \
xend=1 interp=1 n1tic=5 titlesize=8 key=offset > \
ph.2012aug31.m7.6.ta.line_V.z.plus.source.freqdecon.wh0001.a1.0.su1.neg.ps

suop < ph.2012aug31.m7.6.ta.line_V.z.plus.source.freqdecon.wh0001.a2.0.su1 op=norm > tempnorm
suop < tempnorm op=neg | \
supswigp xcur=2.0 wbox=4 hbox=3.5 style=seismic \
nbpi=300 linewidth=0 \
title="ph.2012aug31.m7.6.ta.line_V.z.plus.source.freqdecon.wh0001.a2.0.su1, 3/5/2021" \
label1="Time (s)" labelsize=9 n2tic=2 xbeg=-0.2 \
xend=1 interp=1 n1tic=5 titlesize=8 key=offset > \
ph.2012aug31.m7.6.ta.line_V.z.plus.source.freqdecon.wh0001.a2.0.su1.neg.ps

suop < ph.2012aug31.m7.6.ta.line_V.z.plus.source.freqdecon.wh0001.a3.0.su1 op=norm > tempnorm
suop < tempnorm op=neg | \
supswigp xcur=2.0 wbox=4 hbox=3.5 style=seismic \
nbpi=300 linewidth=0 \
title="ph.2012aug31.m7.6.ta.line_V.z.plus.source.freqdecon.wh0001.a3.0.su1, 3/5/2021" \
label1="Time (s)" labelsize=9 n2tic=2 xbeg=-0.2 \
xend=1 interp=1 n1tic=5 titlesize=8 key=offset > \
```

ph.2012aug31.m7.6.ta.line_V.z.plus.source.freqdecon.wh0001.a3.0.su1.neg.ps

```
suop < ph.2012aug31.m7.6.ta.line_V.z.plus.source.freqdecon.wh0001.a4.0.su1 op=norm > tempnorm
suop < tempnorm op=neg | \
supswigp xcur=2.0 wbox=4 hbox=3.5 style=seismic \
nbpi=300 linewidth=0 \
title="ph.2012aug31.m7.6.ta.line_V.z.plus.source.freqdecon.wh0001.a4.0.su1, 3/5/2021" \
label1="Time (s)" labelsize=9 n2tic=2 xbeg=-0.2 \
xend=1 interp=1 n1tic=5 titlesize=8 key=offset > \
ph.2012aug31.m7.6.ta.line_V.z.plus.source.freqdecon.wh0001.a4.0.su1.neg.ps
```

```
suop < ph.2012aug31.m7.6.ta.line_V.z.plus.source.freqdecon.wh0001.a5.0.su1 op=norm > tempnorm
suop < tempnorm op=neg | \
supswigp xcur=2.0 wbox=4 hbox=3.5 style=seismic \
nbpi=300 linewidth=0 \
title="ph.2012aug31.m7.6.ta.line_V.z.plus.source.freqdecon.wh0001.a5.0.su1, 3/5/2021" \
label1="Time (s)" labelsize=9 n2tic=2 xbeg=-0.2 \
xend=1 interp=1 n1tic=5 titlesize=8 key=offset > \
ph.2012aug31.m7.6.ta.line_V.z.plus.source.freqdecon.wh0001.a5.0.su1.neg.ps
```

STEP 104 NEW WAVELET

Example taken from the earthquake of magnitude 6.6 on August 26, 2012, from Line X

```
# pkikp_ta_step104_new_wavelet_working_2012aug26.m6.6.ta.line_X.txt
#
# July 6, 2017; May 17, 2018; May 23, 2018; 9/19/18; 10/30/18
# Jan. 11, 2019; Nov. 17, 2020; 11/21/2020; 11/23/2020;
# 12/2/2020; 2/1/2021 ; 1/26/2022 ; 7/7/2021; 8/25/2021; 1/26/2022
#
# Processing of TA data (dt=0.025 seconds, compared with
# dt=0.020 seconds for SESAME data).  Traces were
# resampled to 0.020 seconds in step102.
#
# The previous job ("step103") cross correlated traces with the
# source wavelet (the latter was estimated using SESAME data).
# The final product was the combined gather (source wavelet
# estimate followed by traces) with statics corrections.
#
# In this job ("step104"), the source-time function is used
#    to deconvolve the traces. The gather then is plotted
#    with uniform trace spacing.
#
# Preview of steps after this:
#
```

```
# In step105, will insert blank (all zero) traces for unoccupied
#    stations so eventually can vertically stack traces
#    for multiple earthquakes.  Gathers are plotted with
#    the correct relative trace spacing.
#
# Step106 is similar to step105, except does not insert blank traces.
#    Gathers are still plotted with the correct relative
#    trace spacing.  This will give a cleaner plot, more
#    suitable for presentation of results of individual
#    earthquakes.

# unfiltered traces; windowed -20 -> 80 seconds, so nt=ns=5501
# (for some of Devon's events, this will be -20 -> 90 seconds, so nt=5501)
# (for Gustavo's events, this will be -30 -> 70 seconds, so nt=5501)

# NOTE: for the "dd" command, cannot have a space between "if=" and ".."

# Perform deconvolution
# Input (numer): traces with cross-correlation statics applied

freqdeconsourcemac4extra numer=ph.2012aug26.m6.6.ta.line_X.z.plus.source.statout \
denom=wavelet.ph.2012aug26.m6.6.ta.line_X \
out=ph.2012aug26.m6.6.ta.line_X.z.plus.source.freqdecon.wh0001.a1.0 \
ntr=16 nt=5501 dt=0.02 wh=0.0001 alpha=1.0 pre=20 taper=3

freqdeconsourcemac4extra numer=ph.2012aug26.m6.6.ta.line_X.z.plus.source.statout \
denom=wavelet.ph.2012aug26.m6.6.ta.line_X \
out=ph.2012aug26.m6.6.ta.line_X.z.plus.source.freqdecon.wh0001.a2.0 \
```

```
ntr=16 nt=5501 dt=0.02 wh=0.0001 alpha=2.0 pre=20 taper=3

freqdeconsourcemac4extra numer=ph.2012aug26.m6.6.ta.line_X.z.plus.source.statout \
denom=wavelet.ph.2012aug26.m6.6.ta.line_X \
out=ph.2012aug26.m6.6.ta.line_X.z.plus.source.freqdecon.wh0001.a3.0 \
ntr=16 nt=5501 dt=0.02 wh=0.0001 alpha=3.0 pre=20 taper=3

freqdeconsourcemac4extra numer=ph.2012aug26.m6.6.ta.line_X.z.plus.source.statout \
denom=wavelet.ph.2012aug26.m6.6.ta.line_X \
out=ph.2012aug26.m6.6.ta.line_X.z.plus.source.freqdecon.wh0001.a4.0 \
ntr=16 nt=5501 dt=0.02 wh=0.0001 alpha=4.0 pre=20 taper=3

freqdeconsourcemac4extra numer=ph.2012aug26.m6.6.ta.line_X.z.plus.source.statout \
denom=wavelet.ph.2012aug26.m6.6.ta.line_X \
out=ph.2012aug26.m6.6.ta.line_X.z.plus.source.freqdecon.wh0001.a5.0 \
ntr=16 nt=5501 dt=0.02 wh=0.0001 alpha=5.0 pre=20 taper=3

# Add header but for now, plot with evenly spaced traces
#
# edit "ns" as needed; ns = nt

suaddhead < ph.2012aug26.m6.6.ta.line_X.z.plus.source.freqdecon.wh0001.a1.0 ns=5501 | \
sushw key=dt a=20000 > \
ph.2012aug26.m6.6.ta.line_X.z.plus.source.freqdecon.wh0001.a1.0.su1

suaddhead < ph.2012aug26.m6.6.ta.line_X.z.plus.source.freqdecon.wh0001.a2.0 ns=5501 | \
sushw key=dt a=20000 > \
ph.2012aug26.m6.6.ta.line_X.z.plus.source.freqdecon.wh0001.a2.0.su1
```

```
suaddhead < ph.2012aug26.m6.6.ta.line_X.z.plus.source.freqdecon.wh0001.a3.0 ns=5501 | \
sushw key=dt a=20000 > \
ph.2012aug26.m6.6.ta.line_X.z.plus.source.freqdecon.wh0001.a3.0.su1

suaddhead < ph.2012aug26.m6.6.ta.line_X.z.plus.source.freqdecon.wh0001.a4.0 ns=5501 | \
sushw key=dt a=20000 > \
ph.2012aug26.m6.6.ta.line_X.z.plus.source.freqdecon.wh0001.a4.0.su1

suaddhead < ph.2012aug26.m6.6.ta.line_X.z.plus.source.freqdecon.wh0001.a5.0 ns=5501 | \
sushw key=dt a=20000 > \
ph.2012aug26.m6.6.ta.line_X.z.plus.source.freqdecon.wh0001.a5.0.su1

# Plot

suop < ph.2012aug26.m6.6.ta.line_X.z.plus.source.freqdecon.wh0001.a1.0.su1 op=norm | \
supswigp xcur=2.0 wbox=4 hbox=3.5 style=seismic \
nbpi=300 linewidth=0 \
title="ph.2012aug26.m6.6.ta.line_X.z.plus.source.freqdecon.wh0001.a1.0.su1, 1/26/2022" \
label1="Time (s)" labelsize=9 n2tic=2 xbeg=-0.2 \
xend=1 interp=1 n1tic=5 titlesize=8 key=offset > \
ph.2012aug26.m6.6.ta.line_X.z.plus.source.freqdecon.wh0001.a1.0.su1.ps

suop < ph.2012aug26.m6.6.ta.line_X.z.plus.source.freqdecon.wh0001.a2.0.su1 op=norm | \
supswigp xcur=2.0 wbox=4 hbox=3.5 style=seismic \
nbpi=300 linewidth=0 \
title="ph.2012aug26.m6.6.ta.line_X.z.plus.source.freqdecon.wh0001.a2.0.su1, 1/26/2022" \
```

```
label1="Time (s)" labelsize=9 n2tic=2 xbeg=-0.2 \
xend=1 interp=1 n1tic=5 titlesize=8 key=offset > \
ph.2012aug26.m6.6.ta.line_X.z.plus.source.freqdecon.wh0001.a2.0.su1.ps

suop < ph.2012aug26.m6.6.ta.line_X.z.plus.source.freqdecon.wh0001.a3.0.su1 op=norm | \
supswigp xcur=2.0 wbox=4 hbox=3.5 style=seismic \
nbpi=300 linewidth=0 \
title="ph.2012aug26.m6.6.ta.line_X.z.plus.source.freqdecon.wh0001.a3.0.su1, 1/26/2022" \
label1="Time (s)" labelsize=9 n2tic=2 xbeg=-0.2 \
xend=1 interp=1 n1tic=5 titlesize=8 key=offset > \
ph.2012aug26.m6.6.ta.line_X.z.plus.source.freqdecon.wh0001.a3.0.su1.ps

suop < ph.2012aug26.m6.6.ta.line_X.z.plus.source.freqdecon.wh0001.a4.0.su1 op=norm | \
supswigp xcur=2.0 wbox=4 hbox=3.5 style=seismic \
nbpi=300 linewidth=0 \
title="ph.2012aug26.m6.6.ta.line_X.z.plus.source.freqdecon.wh0001.a4.0.su1, 1/26/2022" \
label1="Time (s)" labelsize=9 n2tic=2 xbeg=-0.2 \
xend=1 interp=1 n1tic=5 titlesize=8 key=offset > \
ph.2012aug26.m6.6.ta.line_X.z.plus.source.freqdecon.wh0001.a4.0.su1.ps

suop < ph.2012aug26.m6.6.ta.line_X.z.plus.source.freqdecon.wh0001.a5.0.su1 op=norm | \
supswigp xcur=2.0 wbox=4 hbox=3.5 style=seismic \
nbpi=300 linewidth=0 \
title="ph.2012aug26.m6.6.ta.line_X.z.plus.source.freqdecon.wh0001.a5.0.su1, 1/26/2022" \
label1="Time (s)" labelsize=9 n2tic=2 xbeg=-0.2 \
```

```
xend=1 interp=1 n1tic=5 titlesize=8 key=offset > \
ph.2012aug26.m6.6.ta.line_X.z.plus.source.freqdecon.wh0001.a5.0.su1.ps



# replot with negative polarity

suop < ph.2012aug26.m6.6.ta.line_X.z.plus.source.freqdecon.wh0001.a1.0.su1 op=norm > tempnorm
suop < tempnorm op=neg | \
supswigp xcur=2.0 wbox=4 hbox=3.5 style=seismic \
nbpi=300 linewidth=0 \
title="ph.2012aug26.m6.6.ta.line_X.z.plus.source.freqdecon.wh0001.a1.0.su1, 1/26/2022" \
label1="Time (s)" labelsize=9 n2tic=2 xbeg=-0.2 \
xend=1 interp=1 n1tic=5 titlesize=8 key=offset > \
ph.2012aug26.m6.6.ta.line_X.z.plus.source.freqdecon.wh0001.a1.0.su1.neg.ps

suop < ph.2012aug26.m6.6.ta.line_X.z.plus.source.freqdecon.wh0001.a2.0.su1 op=norm > tempnorm
suop < tempnorm op=neg | \
supswigp xcur=2.0 wbox=4 hbox=3.5 style=seismic \
nbpi=300 linewidth=0 \
title="ph.2012aug26.m6.6.ta.line_X.z.plus.source.freqdecon.wh0001.a2.0.su1, 1/26/2022" \
label1="Time (s)" labelsize=9 n2tic=2 xbeg=-0.2 \
xend=1 interp=1 n1tic=5 titlesize=8 key=offset > \
ph.2012aug26.m6.6.ta.line_X.z.plus.source.freqdecon.wh0001.a2.0.su1.neg.ps

suop < ph.2012aug26.m6.6.ta.line_X.z.plus.source.freqdecon.wh0001.a3.0.su1 op=norm > tempnorm
suop < tempnorm op=neg | \
supswigp xcur=2.0 wbox=4 hbox=3.5 style=seismic \
```

```
nbpi=300 linewidth=0 \
title="ph.2012aug26.m6.6.ta.line_X.z.plus.source.freqdecon.wh0001.a3.0.su1, 1/26/2022" \
label1="Time (s)" labelsize=9 n2tic=2 xbeg=-0.2 \
xend=1 interp=1 n1tic=5 titlesize=8 key=offset > \
ph.2012aug26.m6.6.ta.line_X.z.plus.source.freqdecon.wh0001.a3.0.su1.neg.ps

suop < ph.2012aug26.m6.6.ta.line_X.z.plus.source.freqdecon.wh0001.a4.0.su1 op=norm > tempnorm
suop < tempnorm op=neg | \
supswigp xcur=2.0 wbox=4 hbox=3.5 style=seismic \
nbpi=300 linewidth=0 \
title="ph.2012aug26.m6.6.ta.line_X.z.plus.source.freqdecon.wh0001.a4.0.su1, 1/26/2022" \
label1="Time (s)" labelsize=9 n2tic=2 xbeg=-0.2 \
xend=1 interp=1 n1tic=5 titlesize=8 key=offset > \
ph.2012aug26.m6.6.ta.line_X.z.plus.source.freqdecon.wh0001.a4.0.su1.neg.ps

suop < ph.2012aug26.m6.6.ta.line_X.z.plus.source.freqdecon.wh0001.a5.0.su1 op=norm > tempnorm
suop < tempnorm op=neg | \
supswigp xcur=2.0 wbox=4 hbox=3.5 style=seismic \
nbpi=300 linewidth=0 \
title="ph.2012aug26.m6.6.ta.line_X.z.plus.source.freqdecon.wh0001.a5.0.su1, 1/26/2022" \
label1="Time (s)" labelsize=9 n2tic=2 xbeg=-0.2 \
xend=1 interp=1 n1tic=5 titlesize=8 key=offset > \
ph.2012aug26.m6.6.ta.line_X.z.plus.source.freqdecon.wh0001.a5.0.su1.neg.ps
```

STEP 104 NEW FILTERED WAVELET

Example taken from the earthquake of magnitude 6.7 on February 06, 2012, from Line X

```
# pkikp_ta_step104_working_2012feb06.m6.7.ta.line_X.txt
#
# July 6, 2017; May 17, 2018; May 23, 2018; 9/19/18; 10/30/18
# Jan. 11, 2019; Nov. 17, 2020; 11/21/2020; 11/23/2020;
# 12/2/2020; 2/1/2021 ; 3/8/2022 ; 7/7/2021; Jan. 15, 2022; Jan. 28, 2022
# Feb. 7, 2022


#
# Processing of TA data (dt=0.025 seconds, compared with
# dt=0.020 seconds for SESAME data).  Traces were
# resampled to 0.020 seconds in step102.
#
# The previous job ("step103") cross correlated traces with the
# source wavelet (the latter was estimated using SESAME data).
# The final product was the combined gather (source wavelet
# estimate followed by traces) with statics corrections.
#
# In this job ("step104"), the source-time function is used
#    to deconvolve the traces. The gather then is plotted
#    with uniform trace spacing.
#
```

```
# Preview of steps after this:
#
# In step105, will insert blank (all zero) traces for unoccupied
#    stations so eventually can vertically stack traces
#    for multiple earthquakes.  Gathers are plotted with
#    the correct relative trace spacing.
#
# Step106 is similar to step105, except does not insert blank traces.
#    Gathers are still plotted with the correct relative
#    trace spacing.  This will give a cleaner plot, more
#    suitable for presentation of results of individual
#    earthquakes.

# unfiltered traces; windowed -20 -> 80 seconds, so nt=ns=5001
# (for some of Devon's events, this will be -20 -> 90 seconds, so nt=5501)
# (for Gustavo's events, this will be -30 -> 70 seconds, so nt=5001)

# NOTE: for the "dd" command, cannot have a space between "if=" and ".."

# Perform deconvolution
# Input (numer): traces with cross-correlation statics applied

freqdeconsourcemac4extra numer=ph.2012feb06.m6.7.ta.line_X.z.plus.source.filt.statout \
denom=wavelet.filt.ph.2012feb06.m6.7.ta.line_X \
out=ph.2012feb06.m6.7.ta.line_X.z.plus.source.filt.freqdecon.wh01.a1.0 \
ntr=15 nt=5001 dt=0.02 wh=0.01 alpha=1.0 pre=20 taper=3

freqdeconsourcemac4extra numer=ph.2012feb06.m6.7.ta.line_X.z.plus.source.filt.statout \
```

```
denom=wavelet.filt.ph.2012feb06.m6.7.ta.line_X \
out=ph.2012feb06.m6.7.ta.line_X.z.plus.source.filt.freqdecon.wh01.a2.0 \
ntr=15 nt=5001 dt=0.02 wh=0.01 alpha=2.0 pre=20 taper=3

freqdeconsourcemac4extra numer=ph.2012feb06.m6.7.ta.line_X.z.plus.source.filt.statout \
denom=wavelet.filt.ph.2012feb06.m6.7.ta.line_X \
out=ph.2012feb06.m6.7.ta.line_X.z.plus.source.filt.freqdecon.wh01.a3.0 \
ntr=15 nt=5001 dt=0.02 wh=0.01 alpha=3.0 pre=20 taper=3

freqdeconsourcemac4extra numer=ph.2012feb06.m6.7.ta.line_X.z.plus.source.filt.statout \
denom=wavelet.filt.ph.2012feb06.m6.7.ta.line_X \
out=ph.2012feb06.m6.7.ta.line_X.z.plus.source.filt.freqdecon.wh01.a4.0 \
ntr=15 nt=5001 dt=0.02 wh=0.01 alpha=4.0 pre=20 taper=3

freqdeconsourcemac4extra numer=ph.2012feb06.m6.7.ta.line_X.z.plus.source.filt.statout \
denom=wavelet.filt.ph.2012feb06.m6.7.ta.line_X \
out=ph.2012feb06.m6.7.ta.line_X.z.plus.source.filt.freqdecon.wh01.a5.0 \
ntr=15 nt=5001 dt=0.02 wh=0.01 alpha=5.0 pre=20 taper=3

# Add header but for now, plot with evenly spaced traces
#
# edit "ns" as needed; ns = nt

suaddhead < ph.2012feb06.m6.7.ta.line_X.z.plus.source.filt.freqdecon.wh01.a1.0 ns=5001 | \
sushw key=dt a=20000 > \
ph.2012feb06.m6.7.ta.line_X.z.plus.source.filt.freqdecon.wh01.a1.0.su1

suaddhead < ph.2012feb06.m6.7.ta.line_X.z.plus.source.filt.freqdecon.wh01.a2.0 ns=5001 | \
```

```
sushw key=dt a=20000 > \
ph.2012feb06.m6.7.ta.line_X.z.plus.source.filt.freqdecon.wh01.a2.0.su1

suaddhead < ph.2012feb06.m6.7.ta.line_X.z.plus.source.filt.freqdecon.wh01.a3.0 ns=5001 | \
sushw key=dt a=20000 > \
ph.2012feb06.m6.7.ta.line_X.z.plus.source.filt.freqdecon.wh01.a3.0.su1

suaddhead < ph.2012feb06.m6.7.ta.line_X.z.plus.source.filt.freqdecon.wh01.a4.0 ns=5001 | \
sushw key=dt a=20000 > \
ph.2012feb06.m6.7.ta.line_X.z.plus.source.filt.freqdecon.wh01.a4.0.su1

suaddhead < ph.2012feb06.m6.7.ta.line_X.z.plus.source.filt.freqdecon.wh01.a5.0 ns=5001 | \
sushw key=dt a=20000 > \
ph.2012feb06.m6.7.ta.line_X.z.plus.source.filt.freqdecon.wh01.a5.0.su1

# Plot

suop < ph.2012feb06.m6.7.ta.line_X.z.plus.source.filt.freqdecon.wh01.a1.0.su1 op=norm | \
supswigp xcur=2.0 wbox=4 hbox=3.5 style=seismic \
nbpi=300 linewidth=0 \
title="ph.2012feb06.m6.7.ta.line_X.z.plus.source.filt.freqdecon.wh01.a1.0.su1, 2/7/2022" \
label1="Time (s)" labelsize=9 n2tic=2 xbeg=-0.2 \
xend=1 interp=1 n1tic=5 titlesize=8 key=offset > \
ph.2012feb06.m6.7.ta.line_X.z.plus.source.filt.freqdecon.wh01.a1.0.su1.ps

suop < ph.2012feb06.m6.7.ta.line_X.z.plus.source.filt.freqdecon.wh01.a2.0.su1 op=norm | \
supswigp xcur=2.0 wbox=4 hbox=3.5 style=seismic \
nbpi=300 linewidth=0 \
```

```
title="ph.2012feb06.m6.7.ta.line_X.z.plus.source.filt.freqdecon.wh01.a2.0.su1, 2/7/2022" \
label1="Time (s)" labelsize=9 n2tic=2 xbeg=-0.2 \
xend=1 interp=1 n1tic=5 titlesize=8 key=offset > \
ph.2012feb06.m6.7.ta.line_X.z.plus.source.filt.freqdecon.wh01.a2.0.su1.ps

suop < ph.2012feb06.m6.7.ta.line_X.z.plus.source.filt.freqdecon.wh01.a3.0.su1 op=norm | \
supswigp xcur=2.0 wbox=4 hbox=3.5 style=seismic \
nbpi=300 linewidth=0 \
title="ph.2012feb06.m6.7.ta.line_X.z.plus.source.filt.freqdecon.wh01.a3.0.su1, 2/7/2022" \
label1="Time (s)" labelsize=9 n2tic=2 xbeg=-0.2 \
xend=1 interp=1 n1tic=5 titlesize=8 key=offset > \
ph.2012feb06.m6.7.ta.line_X.z.plus.source.filt.freqdecon.wh01.a3.0.su1.ps

suop < ph.2012feb06.m6.7.ta.line_X.z.plus.source.filt.freqdecon.wh01.a4.0.su1 op=norm | \
supswigp xcur=2.0 wbox=4 hbox=3.5 style=seismic \
nbpi=300 linewidth=0 \
title="ph.2012feb06.m6.7.ta.line_X.z.plus.source.filt.freqdecon.wh01.a4.0.su1, 2/7/2022" \
label1="Time (s)" labelsize=9 n2tic=2 xbeg=-0.2 \
xend=1 interp=1 n1tic=5 titlesize=8 key=offset > \
ph.2012feb06.m6.7.ta.line_X.z.plus.source.filt.freqdecon.wh01.a4.0.su1.ps

suop < ph.2012feb06.m6.7.ta.line_X.z.plus.source.filt.freqdecon.wh01.a5.0.su1 op=norm | \
supswigp xcur=2.0 wbox=4 hbox=3.5 style=seismic \
nbpi=300 linewidth=0 \
title="ph.2012feb06.m6.7.ta.line_X.z.plus.source.filt.freqdecon.wh01.a5.0.su1, 2/7/2022" \
label1="Time (s)" labelsize=9 n2tic=2 xbeg=-0.2 \
xend=1 interp=1 n1tic=5 titlesize=8 key=offset > \
```

```
ph.2012feb06.m6.7.ta.line_X.z.plus.source.filt.freqdecon.wh01.a5.0.su1.ps

# replot with negative polarity

suop < ph.2012feb06.m6.7.ta.line_X.z.plus.source.filt.freqdecon.wh01.a1.0.su1 op=norm > tempnorm
suop < tempnorm op=neg | \
supswigp xcur=2.0 wbox=4 hbox=3.5 style=seismic \
nbpi=300 linewidth=0 \
title="ph.2012feb06.m6.7.ta.line_X.z.plus.source.filt.freqdecon.wh01.a1.0.su1, 2/7/2022" \
label1="Time (s)" labelsize=9 n2tic=2 xbeg=-0.2 \
xend=1 interp=1 n1tic=5 titlesize=8 key=offset > \
ph.2012feb06.m6.7.ta.line_X.z.plus.source.filt.freqdecon.wh01.a1.0.su1.neg.ps

suop < ph.2012feb06.m6.7.ta.line_X.z.plus.source.filt.freqdecon.wh01.a2.0.su1 op=norm > tempnorm
suop < tempnorm op=neg | \
supswigp xcur=2.0 wbox=4 hbox=3.5 style=seismic \
nbpi=300 linewidth=0 \
title="ph.2012feb06.m6.7.ta.line_X.z.plus.source.filt.freqdecon.wh01.a2.0.su1, 2/7/2022" \
label1="Time (s)" labelsize=9 n2tic=2 xbeg=-0.2 \
xend=1 interp=1 n1tic=5 titlesize=8 key=offset > \
ph.2012feb06.m6.7.ta.line_X.z.plus.source.filt.freqdecon.wh01.a2.0.su1.neg.ps

suop < ph.2012feb06.m6.7.ta.line_X.z.plus.source.filt.freqdecon.wh01.a3.0.su1 op=norm > tempnorm
suop < tempnorm op=neg | \
supswigp xcur=2.0 wbox=4 hbox=3.5 style=seismic \
nbpi=300 linewidth=0 \
title="ph.2012feb06.m6.7.ta.line_X.z.plus.source.filt.freqdecon.wh01.a3.0.su1, 2/7/2022" \
label1="Time (s)" labelsize=9 n2tic=2 xbeg=-0.2 \
```

```
xend=1 interp=1 n1tic=5 titlesize=8 key=offset > \
ph.2012feb06.m6.7.ta.line_X.z.plus.source.filt.freqdecon.wh01.a3.0.su1.neg.ps

suop < ph.2012feb06.m6.7.ta.line_X.z.plus.source.filt.freqdecon.wh01.a4.0.su1 op=norm > tempnorm
suop < tempnorm op=neg | \
supswigp xcur=2.0 wbox=4 hbox=3.5 style=seismic \
nbpi=300 linewidth=0 \
title="ph.2012feb06.m6.7.ta.line_X.z.plus.source.filt.freqdecon.wh01.a4.0.su1, 2/7/2022" \
label1="Time (s)" labelsize=9 n2tic=2 xbeg=-0.2 \
xend=1 interp=1 n1tic=5 titlesize=8 key=offset > \
ph.2012feb06.m6.7.ta.line_X.z.plus.source.filt.freqdecon.wh01.a4.0.su1.neg.ps

suop < ph.2012feb06.m6.7.ta.line_X.z.plus.source.filt.freqdecon.wh01.a5.0.su1 op=norm > tempnorm
suop < tempnorm op=neg | \
supswigp xcur=2.0 wbox=4 hbox=3.5 style=seismic \
nbpi=300 linewidth=0 \
title="ph.2012feb06.m6.7.ta.line_X.z.plus.source.filt.freqdecon.wh01.a5.0.su1, 2/7/2022" \
label1="Time (s)" labelsize=9 n2tic=2 xbeg=-0.2 \
xend=1 interp=1 n1tic=5 titlesize=8 key=offset > \
ph.2012feb06.m6.7.ta.line_X.z.plus.source.filt.freqdecon.wh01.a5.0.su1.neg.ps
```

STEP 105

Example taken from the earthquake of magnitude 7.6 on August 31, 2012, from Line V

Step 105 will run the same regardless of any wavelet used.

```
# pkikp_ta_step105_working_2012aug31.m7.6.ta.line_V.txt
#
# July 6, 2017; May 17, 2018; May 23, 2018; Sept. 15, 2018;
# Sept. 19, 2018; Jan. 11, 2019; Jan. 26, 2019; July 19, 2019
# Aug. 3, 2019; Dec. 9, 2020; Feb. 1, 2021; Mar. 16, 2021; July 21, 2021

# NOTE:
#
# For program "tracezero2019", "ntr" is the number of
# occupied stations plus 1 more trace for the source wavelet.
# So this number will vary from earthquake to earthquake.
#
# For program "zerotraceinsertmac", "nx" is the total number
# stations (both occupied and unoccupied), plus one trace
# for the source wavelet.  So this number will be the
# same for every earthquake.

# This job does the following:
#
```

```
# 1) works on output files generated by "step104".
# 2) length of input traces:
#    for Gustavo's and some of Devon's events:
#        5001 samples (-20 -> 80 seconds)
#    for the rest of Devon's events:
#        5501 samples (-20 -> 90 seconds)
# 3) zeroes out any bad traces
# 4) inserts blank (all zero) traces for unoccupied
#    stations
# 5) pads all traces to a length of nt=5501 samples
#    (-20 -> 90 seconds)
# 6) plots gathers with correct relative trace spacings.

# First: Set up distance files for TA "W" W-E array for
# all the original stations (W31A-W65A, including W41B)
#
# NOTE: The distance for the first trace (source wavelet)
# will be a dummy distance.

a2b < plot_dist_all_TA_line_V.txt n1=1 > \
plot_dist_all_TA_line_V.bin

# zero out bad traces
#
# Note: for "tracezero2019", ntr is the number of occupied stations, plus one for
# the source wavelet.
```

```
tracezero2019 in=ph.2012aug31.m7.6.ta.line_V.z.plus.source.freqdecon.wh0001.a1.0 \
out=ph.2012aug31.m7.6.ta.line_V.z.plus.source.freqdecon.wh0001.a1.zap \
ntr=16 nt=5001 para=zap_2012aug31.m7.6_ta_line_V.txt

tracezero2019 in=ph.2012aug31.m7.6.ta.line_V.z.plus.source.freqdecon.wh0001.a2.0 \
out=ph.2012aug31.m7.6.ta.line_V.z.plus.source.freqdecon.wh0001.a2.zap \
ntr=16 nt=5001 para=zap_2012aug31.m7.6_ta_line_V.txt

tracezero2019 in=ph.2012aug31.m7.6.ta.line_V.z.plus.source.freqdecon.wh0001.a3.0 \
out=ph.2012aug31.m7.6.ta.line_V.z.plus.source.freqdecon.wh0001.a3.zap \
ntr=16 nt=5001 para=zap_2012aug31.m7.6_ta_line_V.txt

tracezero2019 in=ph.2012aug31.m7.6.ta.line_V.z.plus.source.freqdecon.wh0001.a4.0 \
out=ph.2012aug31.m7.6.ta.line_V.z.plus.source.freqdecon.wh0001.a4.zap \
ntr=16 nt=5001 para=zap_2012aug31.m7.6_ta_line_V.txt

tracezero2019 in=ph.2012aug31.m7.6.ta.line_V.z.plus.source.freqdecon.wh0001.a5.0 \
out=ph.2012aug31.m7.6.ta.line_V.z.plus.source.freqdecon.wh0001.a5.zap \
ntr=16 nt=5001 para=zap_2012aug31.m7.6_ta_line_V.txt

# insert dummy traces (samples: all zeroes) for unoccupied stations
#
# NOTE: For zerotraceinsertmac, "nx" is the total number of stations for each line
# (both occupied and unoccupied), plus one trace for the source wavelet.
#
# Note: Line W has station "W41B" as well as "W41A".
#
# So for TA W-E line "W":
```

```
#  "nx" will always be (65-31+1) + 1 (for W41B) + 1 (for wavelet) = 37
#

# 8/3/19: Also, pad output traces to 5501 samples


zerotraceinsertmac in=ph.2012aug31.m7.6.ta.line_V.z.plus.source.freqdecon.wh0001.a1.zap \
out=ph.2012aug31.m7.6.ta.line_V.z.plus.source.freqdecon.wh0001.a1.0.zero.line110s \
nx=32 ntin=5001 ntout=5501 inc=insert_2012aug31.m7.6_ta_line_V.txt

zerotraceinsertmac in=ph.2012aug31.m7.6.ta.line_V.z.plus.source.freqdecon.wh0001.a2.zap \
out=ph.2012aug31.m7.6.ta.line_V.z.plus.source.freqdecon.wh0001.a2.0.zero.line110s \
nx=32 ntin=5001 ntout=5501 inc=insert_2012aug31.m7.6_ta_line_V.txt

zerotraceinsertmac in=ph.2012aug31.m7.6.ta.line_V.z.plus.source.freqdecon.wh0001.a3.zap \
out=ph.2012aug31.m7.6.ta.line_V.z.plus.source.freqdecon.wh0001.a3.0.zero.line110s \
nx=32 ntin=5001 ntout=5501 inc=insert_2012aug31.m7.6_ta_line_V.txt

zerotraceinsertmac in=ph.2012aug31.m7.6.ta.line_V.z.plus.source.freqdecon.wh0001.a4.zap \
out=ph.2012aug31.m7.6.ta.line_V.z.plus.source.freqdecon.wh0001.a4.0.zero.line110s \
nx=32 ntin=5001 ntout=5501 inc=insert_2012aug31.m7.6_ta_line_V.txt

zerotraceinsertmac in=ph.2012aug31.m7.6.ta.line_V.z.plus.source.freqdecon.wh0001.a5.zap \
out=ph.2012aug31.m7.6.ta.line_V.z.plus.source.freqdecon.wh0001.a5.0.zero.line110s \
nx=32 ntin=5001 ntout=5501 inc=insert_2012aug31.m7.6_ta_line_V.txt

# Add headers
```

```
# NOTE that dt is in microseconds and delrt is in milliseconds

# dt = 0.02 seconds = 20 milliseconds = 20,000 microseconds

# delrt = -20 seconds = -20,000 milliseconds (trace starts
# 20 seconds before first arrival)

suaddhead < ph.2012aug31.m7.6.ta.line_V.z.plus.source.freqdecon.wh0001.a1.0.zero.line110s ns=5501 | \
sushw key=dt a=20000 > \
ph.2012aug31.m7.6.ta.line_V.z.plus.source.freqdecon.wh0001.a1.0.zero.line110s.su1

sushw < ph.2012aug31.m7.6.ta.line_V.z.plus.source.freqdecon.wh0001.a1.0.zero.line110s.su1 \
key=delrt a=-20000 > \
ph.2012aug31.m7.6.ta.line_V.z.plus.source.freqdecon.wh0001.a1.0.zero.line110s.su2

sushw < ph.2012aug31.m7.6.ta.line_V.z.plus.source.freqdecon.wh0001.a1.0.zero.line110s.su2 \
infile=plot_dist_all_ta_line_V.bin key=offset > \
ph.2012aug31.m7.6.ta.line_V.z.plus.source.freqdecon.wh0001.a1.0.zero.line110s.su3

suaddhead < ph.2012aug31.m7.6.ta.line_V.z.plus.source.freqdecon.wh0001.a2.0.zero.line110s ns=5501 | \
sushw key=dt a=20000 > \
ph.2012aug31.m7.6.ta.line_V.z.plus.source.freqdecon.wh0001.a2.0.zero.line110s.su1

sushw < ph.2012aug31.m7.6.ta.line_V.z.plus.source.freqdecon.wh0001.a2.0.zero.line110s.su1 \
key=delrt a=-20000 > \
ph.2012aug31.m7.6.ta.line_V.z.plus.source.freqdecon.wh0001.a2.0.zero.line110s.su2

sushw < ph.2012aug31.m7.6.ta.line_V.z.plus.source.freqdecon.wh0001.a2.0.zero.line110s.su2 \
```

```
infile=plot_dist_all_ta_line_V.bin key=offset > \
ph.2012aug31.m7.6.ta.line_V.z.plus.source.freqdecon.wh0001.a2.0.zero.line110s.su3

suaddhead < ph.2012aug31.m7.6.ta.line_V.z.plus.source.freqdecon.wh0001.a3.0.zero.line110s ns=5501 | \
sushw key=dt a=20000 > \
ph.2012aug31.m7.6.ta.line_V.z.plus.source.freqdecon.wh0001.a3.0.zero.line110s.su1

sushw < ph.2012aug31.m7.6.ta.line_V.z.plus.source.freqdecon.wh0001.a3.0.zero.line110s.su1 \
key=delrt a=-20000 > \
ph.2012aug31.m7.6.ta.line_V.z.plus.source.freqdecon.wh0001.a3.0.zero.line110s.su2

sushw < ph.2012aug31.m7.6.ta.line_V.z.plus.source.freqdecon.wh0001.a3.0.zero.line110s.su2 \
infile=plot_dist_all_ta_line_V.bin key=offset > \
ph.2012aug31.m7.6.ta.line_V.z.plus.source.freqdecon.wh0001.a3.0.zero.line110s.su3

suaddhead < ph.2012aug31.m7.6.ta.line_V.z.plus.source.freqdecon.wh0001.a4.0.zero.line110s ns=5501 | \
sushw key=dt a=20000 > \
ph.2012aug31.m7.6.ta.line_V.z.plus.source.freqdecon.wh0001.a4.0.zero.line110s.su1

sushw < ph.2012aug31.m7.6.ta.line_V.z.plus.source.freqdecon.wh0001.a4.0.zero.line110s.su1 \
key=delrt a=-20000 > \
ph.2012aug31.m7.6.ta.line_V.z.plus.source.freqdecon.wh0001.a4.0.zero.line110s.su2

sushw < ph.2012aug31.m7.6.ta.line_V.z.plus.source.freqdecon.wh0001.a4.0.zero.line110s.su2 \
infile=plot_dist_all_ta_line_V.bin key=offset > \
ph.2012aug31.m7.6.ta.line_V.z.plus.source.freqdecon.wh0001.a4.0.zero.line110s.su3
```

```
suaddhead < ph.2012aug31.m7.6.ta.line_V.z.plus.source.freqdecon.wh0001.a5.0.zero.line110s ns=5501 | \
sushw key=dt a=20000 > \
ph.2012aug31.m7.6.ta.line_V.z.plus.source.freqdecon.wh0001.a5.0.zero.line110s.su1

sushw < ph.2012aug31.m7.6.ta.line_V.z.plus.source.freqdecon.wh0001.a5.0.zero.line110s.su1 \
key=delrt a=-20000 > \
ph.2012aug31.m7.6.ta.line_V.z.plus.source.freqdecon.wh0001.a5.0.zero.line110s.su2

sushw < ph.2012aug31.m7.6.ta.line_V.z.plus.source.freqdecon.wh0001.a5.0.zero.line110s.su2 \
infile=plot_dist_all_ta_line_V.bin key=offset > \
ph.2012aug31.m7.6.ta.line_V.z.plus.source.freqdecon.wh0001.a5.0.zero.line110s.su3

# Plot
# use op=norm for normalizing each trace separately
# use op=neg to reverse polarity (otherwise same normalization as op=norm)

# For vertical scale: hbox=3.5 inches for 100 seconds,
# so use hbox=3.85 inches for 110 seconds

suop < ph.2012aug31.m7.6.ta.line_V.z.plus.source.freqdecon.wh0001.a1.0.zero.line110s.su3 op=norm | \
supswigp xcur=2.0 wbox=4 hbox=3.85 style=seismic \
nbpi=300 linewidth=0 \
title="ph.2012aug31.m7.6.ta.line_V.z.plus.source.freqdecon.wh0001.a1.0.zero.line110s.su3, 7/21/2021" \
label1="Time (s)" labelsize=9 n2tic=2 xbeg=-0.2 \
xend=1 interp=1 n1tic=5 titlesize=8 key=offset > \
ph.2012aug31.m7.6.ta.line_V.z.plus.source.freqdecon.wh0001.a1.0.zero.line110s.su3.ps

suop < ph.2012aug31.m7.6.ta.line_V.z.plus.source.freqdecon.wh0001.a2.0.zero.line110s.su3 op=norm | \
```

```
supswigp xcur=2.0 wbox=4 hbox=3.85 style=seismic \
nbpi=300 linewidth=0 \
title="ph.2012aug31.m7.6.ta.line_V.z.plus.source.freqdecon.wh0001.a2.0.zero.line110s.su3, 7/21/2021" \
label1="Time (s)" labelsize=9 n2tic=2 xbeg=-0.2 \
xend=1 interp=1 n1tic=5 titlesize=8 key=offset > \
ph.2012aug31.m7.6.ta.line_V.z.plus.source.freqdecon.wh0001.a2.0.zero.line110s.su3.ps

suop < ph.2012aug31.m7.6.ta.line_V.z.plus.source.freqdecon.wh0001.a3.0.zero.line110s.su3 op=norm | \
supswigp xcur=2.0 wbox=4 hbox=3.85 style=seismic \
nbpi=300 linewidth=0 \
title="ph.2012aug31.m7.6.ta.line_V.z.plus.source.freqdecon.wh0001.a3.0.zero.line110s.su3, 7/21/2021" \
label1="Time (s)" labelsize=9 n2tic=2 xbeg=-0.2 \
xend=1 interp=1 n1tic=5 titlesize=8 key=offset > \
ph.2012aug31.m7.6.ta.line_V.z.plus.source.freqdecon.wh0001.a3.0.zero.line110s.su3.ps

suop < ph.2012aug31.m7.6.ta.line_V.z.plus.source.freqdecon.wh0001.a4.0.zero.line110s.su3 op=norm | \
supswigp xcur=2.0 wbox=4 hbox=3.85 style=seismic \
nbpi=300 linewidth=0 \
title="ph.2012aug31.m7.6.ta.line_V.z.plus.source.freqdecon.wh0001.a4.0.zero.line110s.su3, 7/21/2021" \
label1="Time (s)" labelsize=9 n2tic=2 xbeg=-0.2 \
xend=1 interp=1 n1tic=5 titlesize=8 key=offset > \
ph.2012aug31.m7.6.ta.line_V.z.plus.source.freqdecon.wh0001.a4.0.zero.line110s.su3.ps

# Now replot with negative polarity (op=neg).  Then direct arrival will
# be negative and a positive impedance contrast (e.g. Moho if it's a
# first-order discontinuity) will be positive.
```

```
suop < ph.2012aug31.m7.6.ta.line_V.z.plus.source.freqdecon.wh0001.a1.0.zero.line110s.su3 op=norm >
tempnorm
suop < tempnorm op=neg | \
supswigp xcur=2.0 wbox=4 hbox=3.85 style=seismic \
nbpi=300 linewidth=0 \
title="ph.2012aug31.m7.6.ta.line_V.z.plus.source.freqdecon.wh0001.a1.0.zero.line110s.su3, 7/21/2021" \
label1="Time (s)" labelsize=9 n2tic=2 xbeg=-0.2 \
xend=1 interp=1 n1tic=5 titlesize=8 key=offset > \
ph.2012aug31.m7.6.ta.line_V.z.plus.source.freqdecon.wh0001.a1.0.zero.line110s.su3.neg.ps

suop < ph.2012aug31.m7.6.ta.line_V.z.plus.source.freqdecon.wh0001.a2.0.zero.line110s.su3 op=norm >
tempnorm
suop < tempnorm op=neg | \
supswigp xcur=2.0 wbox=4 hbox=3.85 style=seismic \
nbpi=300 linewidth=0 \
title="ph.2012aug31.m7.6.ta.line_V.z.plus.source.freqdecon.wh0001.a2.0.zero.line110s.su3, 7/21/2021" \
label1="Time (s)" labelsize=9 n2tic=2 xbeg=-0.2 \
xend=1 interp=1 n1tic=5 titlesize=8 key=offset > \
ph.2012aug31.m7.6.ta.line_V.z.plus.source.freqdecon.wh0001.a2.0.zero.line110s.su3.neg.ps

suop < ph.2012aug31.m7.6.ta.line_V.z.plus.source.freqdecon.wh0001.a3.0.zero.line110s.su3 op=norm >
tempnorm
suop < tempnorm op=neg | \
supswigp xcur=2.0 wbox=4 hbox=3.85 style=seismic \
nbpi=300 linewidth=0 \
title="ph.2012aug31.m7.6.ta.line_V.z.plus.source.freqdecon.wh0001.a3.0.zero.line110s.su3, 7/21/2021" \
label1="Time (s)" labelsize=9 n2tic=2 xbeg=-0.2 \
xend=1 interp=1 n1tic=5 titlesize=8 key=offset > \
```

ph.2012aug31.m7.6.ta.line_V.z.plus.source.freqdecon.wh0001.a3.0.zero.line110s.su3.neg.ps

suop < ph.2012aug31.m7.6.ta.line_V.z.plus.source.freqdecon.wh0001.a4.0.zero.line110s.su3 op=norm >

tempnorm

suop < tempnorm op=neg | \

supswigp xcur=2.0 wbox=4 hbox=3.85 style=seismic \

nbpi=300 linewidth=0 \

title="ph.2012aug31.m7.6.ta.line_V.z.plus.source.freqdecon.wh0001.a4.0.zero.line110s.su3, 7/21/2021" \

label1="Time (s)" labelsize=9 n2tic=2 xbeg=-0.2 \

xend=1 interp=1 n1tic=5 titlesize=8 key=offset > \

ph.2012aug31.m7.6.ta.line_V.z.plus.source.freqdecon.wh0001.a4.0.zero.line110s.su3.neg.ps

STEP 105 BANDPASS FILTER AND REDUCED WINDOW ADDED

Example taken from the earthquake of magnitude 6.6 on July 07, 2013, from Line X

```
# pkikp_ta_step105_filt_master_2013july07.m6.6.ta.line_X.txt
#
# July 6, 2017; May 17, 2018; May 23, 2018; Sept. 15, 2018;
# Sept. 19, 2018; Jan. 11, 2019; Jan. 26, 2019; July 19, 2019
# Aug. 3, 2019; Dec. 9, 2020; Feb. 1, 2021; Jan. 12, 2022; Feb. 11, 2022

# Jan. 12, 2022: added lines to taper and bandpass filter the
# deconvolved output

# NOTE:
#
# For program "tracezero2019", "ntr" is the number of
# occupied stations plus 1 more trace for the source wavelet.
# So this number will vary from earthquake to earthquake.
#
# For program "zerotraceinsertmac", "nx" is the total number
# stations (both occupied and unoccupied), plus one trace
# for the source wavelet.  So this number will be the
# same for every earthquake.
```

```
# This job does the following:
#
# 1) works on output files generated by "step104".
# 2) length of input traces:
#    for Gustavo's and some of Devon's events:
#        5001 samples (-20 -> 80 seconds)
#    for the rest of Devon's events:
#        5501 samples (-20 -> 90 seconds)
# 3) zeroes out any bad traces
# 4) inserts blank (all zero) traces for unoccupied
#    stations
# 5) pads all traces to a length of nt=5001 samples
#    (-20 -> 90 seconds)
# 6) plots gathers with correct relative trace spacings.

# First: Set up distance files for TA "W" W-E array for
# all the original stations (W31A-W65A, including W41B)
#
# NOTE: The distance for the first trace (source wavelet)
# will be a dummy distance.

a2b < plot_dist_all_TA_line_X n1=1 > \
plot_dist_all_TA_line_X.bin

# zero out bad traces
#
# Note: for "tracezero2019", ntr is the number of occupied stations, plus one for
# the source wavelet.
```

```
tracezero2019 in=ph.2013july07.m6.6.ta.line_X.z.plus.source.freqdecon.100s.wh0001.a1.0 \
out=ph.2013july07.m6.6.ta.line_X.z.plus.source.freqdecon.100s.wh0001.a1.zap \
ntr=17 nt=5001 para=zap_2013july07.m6.6_ta_line_X.txt

tracezero2019 in=ph.2013july07.m6.6.ta.line_X.z.plus.source.freqdecon.100s.wh0001.a2.0 \
out=ph.2013july07.m6.6.ta.line_X.z.plus.source.freqdecon.100s.wh0001.a2.zap \
ntr=17 nt=5001 para=zap_2013july07.m6.6_ta_line_X.txt

tracezero2019 in=ph.2013july07.m6.6.ta.line_X.z.plus.source.freqdecon.100s.wh0001.a3.0 \
out=ph.2013july07.m6.6.ta.line_X.z.plus.source.freqdecon.100s.wh0001.a3.zap \
ntr=17 nt=5001 para=zap_2013july07.m6.6_ta_line_X.txt

tracezero2019 in=ph.2013july07.m6.6.ta.line_X.z.plus.source.freqdecon.100s.wh0001.a4.0 \
out=ph.2013july07.m6.6.ta.line_X.z.plus.source.freqdecon.100s.wh0001.a4.zap \
ntr=17 nt=5001 para=zap_2013july07.m6.6_ta_line_X.txt

tracezero2019 in=ph.2013july07.m6.6.ta.line_X.z.plus.source.freqdecon.100s.wh0001.a5.0 \
out=ph.2013july07.m6.6.ta.line_X.z.plus.source.freqdecon.100s.wh0001.a5.zap \
ntr=17 nt=5001 para=zap_2013july07.m6.6_ta_line_X.txt

# taper the first and last 10 seconds (first and last 500 samples) of each trace
#
# note that “nx1” must be 0

tapernew2015 in=ph.2013july07.m6.6.ta.line_X.z.plus.source.freqdecon.100s.wh0001.a1.zap \
out=ph.2013july07.m6.6.ta.line_X.z.plus.source.freqdecon.100s.wh0001.a1.taper \
nx=17 nt=5001 nt1=500 nx1=0
```

```
tapernew2015 in=ph.2013july07.m6.6.ta.line_X.z.plus.source.freqdecon.100s.wh0001.a2.zap \
out=ph.2013july07.m6.6.ta.line_X.z.plus.source.freqdecon.100s.wh0001.a2.taper \
nx=17 nt=5001 nt1=500 nx1=0

tapernew2015 in=ph.2013july07.m6.6.ta.line_X.z.plus.source.freqdecon.100s.wh0001.a3.zap \
out=ph.2013july07.m6.6.ta.line_X.z.plus.source.freqdecon.100s.wh0001.a3.taper \
nx=17 nt=5001 nt1=500 nx1=0

tapernew2015 in=ph.2013july07.m6.6.ta.line_X.z.plus.source.freqdecon.100s.wh0001.a4.zap \
out=ph.2013july07.m6.6.ta.line_X.z.plus.source.freqdecon.100s.wh0001.a4.taper \
nx=17 nt=5001 nt1=500 nx1=0

tapernew2015 in=ph.2013july07.m6.6.ta.line_X.z.plus.source.freqdecon.100s.wh0001.a5.zap \
out=ph.2013july07.m6.6.ta.line_X.z.plus.source.freqdecon.100s.wh0001.a5.taper \
nx=17 nt=5001 nt1=500 nx1=0

# Bandpass Filter

bandnew2015 in=ph.2013july07.m6.6.ta.line_X.z.plus.source.freqdecon.100s.wh0001.a1.taper \
out=ph.2013july07.m6.6.ta.line_X.z.plus.source.freqdecon.100s.wh0001.a1.bnd \
nt=5001 dt=0.02 a=0.1 b=0.2 c=3.0 d=5.0

bandnew2015 in=ph.2013july07.m6.6.ta.line_X.z.plus.source.freqdecon.100s.wh0001.a2.taper \
out=ph.2013july07.m6.6.ta.line_X.z.plus.source.freqdecon.100s.wh0001.a2.bnd \
nt=5001 dt=0.02 a=0.1 b=0.2 c=3.0 d=5.0

bandnew2015 in=ph.2013july07.m6.6.ta.line_X.z.plus.source.freqdecon.100s.wh0001.a3.taper \
```

```
out=ph.2013july07.m6.6.ta.line_X.z.plus.source.freqdecon.100s.wh0001.a3.bnd \
nt=5001 dt=0.02 a=0.1 b=0.2 c=3.0 d=5.0

bandnew2015 in=ph.2013july07.m6.6.ta.line_X.z.plus.source.freqdecon.100s.wh0001.a4.taper \
out=ph.2013july07.m6.6.ta.line_X.z.plus.source.freqdecon.100s.wh0001.a4.bnd \
nt=5001 dt=0.02 a=0.1 b=0.2 c=3.0 d=5.0

bandnew2015 in=ph.2013july07.m6.6.ta.line_X.z.plus.source.freqdecon.100s.wh0001.a5.taper \
out=ph.2013july07.m6.6.ta.line_X.z.plus.source.freqdecon.100s.wh0001.a5.bnd \
nt=5001 dt=0.02 a=0.1 b=0.2 c=3.0 d=5.0

# insert dummy traces (samples: all zeroes) for unoccupied stations
#
# NOTE: For zerotraceinsertmac, "nx" is the total number of stations for each line
# (both occupied and unoccupied), plus one trace for the source wavelet.
#
# Note: Line W has station "W41B" as well as "W41A".
#
# So for TA W-E line "W":
#  "nx" will always be (65-31+1) + 1 (for W41B) + 1 (for wavelet) = 37

# 8/3/19: Also, pad output traces to 5501 samples

zerotraceinsertmac in=ph.2013july07.m6.6.ta.line_X.z.plus.source.freqdecon.100s.wh0001.a1.bnd \
out=ph.2013july07.m6.6.ta.line_X.z.plus.source.freqdecon.100s.wh0001.a1.0.zero.line110s \
nx=30 ntin=5001 ntout=5501 inc=insert_2013july07.m6.6_ta_line_X.txt

zerotraceinsertmac in=ph.2013july07.m6.6.ta.line_X.z.plus.source.freqdecon.100s.wh0001.a2.bnd \
```

```
out=ph.2013july07.m6.6.ta.line_X.z.plus.source.freqdecon.100s.wh0001.a2.0.zero.line110s \
nx=30 ntin=5001 ntout=5501 inc=insert_2013july07.m6.6_ta_line_X.txt

zerotraceinsertmac in=ph.2013july07.m6.6.ta.line_X.z.plus.source.freqdecon.100s.wh0001.a3.bnd \
out=ph.2013july07.m6.6.ta.line_X.z.plus.source.freqdecon.100s.wh0001.a3.0.zero.line110s \
nx=30 ntin=5001 ntout=5501 inc=insert_2013july07.m6.6_ta_line_X.txt

zerotraceinsertmac in=ph.2013july07.m6.6.ta.line_X.z.plus.source.freqdecon.100s.wh0001.a4.bnd \
out=ph.2013july07.m6.6.ta.line_X.z.plus.source.freqdecon.100s.wh0001.a4.0.zero.line110s \
nx=30 ntin=5001 ntout=5501 inc=insert_2013july07.m6.6_ta_line_X.txt

zerotraceinsertmac in=ph.2013july07.m6.6.ta.line_X.z.plus.source.freqdecon.100s.wh0001.a5.bnd \
out=ph.2013july07.m6.6.ta.line_X.z.plus.source.freqdecon.100s.wh0001.a5.0.zero.line110s \
nx=30 ntin=5001 ntout=5501 inc=insert_2013july07.m6.6_ta_line_X.txt

# Add headers & apply bandpass filter
# NOTE that dt is in microseconds and delrt is in milliseconds
# dt = 0.02 seconds = 20 milliseconds = 20,000 microseconds
# delrt = -20 seconds = -20,000 milliseconds (trace starts
# 20 seconds before first arrival)

suaddhead < ph.2013july07.m6.6.ta.line_X.z.plus.source.freqdecon.100s.wh0001.a1.0.zero.line110s
ns=5501 | \
sushw key=dt a=20000 > \
ph.2013july07.m6.6.ta.line_X.z.plus.source.freqdecon.100s.wh0001.a1.0.zero.line110s.su1

sushw < ph.2013july07.m6.6.ta.line_X.z.plus.source.freqdecon.100s.wh0001.a1.0.zero.line110s.su1 \
key=delrt a=-20000 > \
```

```
ph.2013july07.m6.6.ta.line_X.z.plus.source.freqdecon.100s.wh0001.a1.0.zero.line110s.su2

sushw < ph.2013july07.m6.6.ta.line_X.z.plus.source.freqdecon.100s.wh0001.a1.0.zero.line110s.su2 \
infile=plot_dist_all_ta_line_X.bin key=offset > \
ph.2013july07.m6.6.ta.line_X.z.plus.source.freqdecon.100s.wh0001.a1.0.zero.line110s.su3

sustrip < ph.2013july07.m6.6.ta.line_X.z.plus.source.freqdecon.100s.wh0001.a1.0.zero.line110s.su3 > \
ph.2013july07.m6.6.ta.line_X.z.plus.source.freqdecon.100s.wh0001.a1.0.zero.line110s

suaddhead < ph.2013july07.m6.6.ta.line_X.z.plus.source.freqdecon.100s.wh0001.a2.0.zero.line110s
ns=5501 | \
sushw key=dt a=20000 > \
ph.2013july07.m6.6.ta.line_X.z.plus.source.freqdecon.100s.wh0001.a2.0.zero.line110s.su1

sushw < ph.2013july07.m6.6.ta.line_X.z.plus.source.freqdecon.100s.wh0001.a2.0.zero.line110s.su1 \
key=delrt a=-20000 > \
ph.2013july07.m6.6.ta.line_X.z.plus.source.freqdecon.100s.wh0001.a2.0.zero.line110s.su2

sushw < ph.2013july07.m6.6.ta.line_X.z.plus.source.freqdecon.100s.wh0001.a2.0.zero.line110s.su2 \
infile=plot_dist_all_ta_line_X.bin key=offset > \
ph.2013july07.m6.6.ta.line_X.z.plus.source.freqdecon.100s.wh0001.a2.0.zero.line110s.su3

sustrip < ph.2013july07.m6.6.ta.line_X.z.plus.source.freqdecon.100s.wh0001.a2.0.zero.line110s.su3 > \
ph.2013july07.m6.6.ta.line_X.z.plus.source.freqdecon.100s.wh0001.a2.0.zero.line110s

suaddhead < ph.2013july07.m6.6.ta.line_X.z.plus.source.freqdecon.100s.wh0001.a3.0.zero.line110s
ns=5501 | \
sushw key=dt a=20000 > \
```

ph.2013july07.m6.6.ta.line_X.z.plus.source.freqdecon.100s.wh0001.a3.0.zero.line110s.su1

sushw < ph.2013july07.m6.6.ta.line_X.z.plus.source.freqdecon.100s.wh0001.a3.0.zero.line110s.su1 \
key=delrt a=-20000 > \
ph.2013july07.m6.6.ta.line_X.z.plus.source.freqdecon.100s.wh0001.a3.0.zero.line110s.su2

sushw < ph.2013july07.m6.6.ta.line_X.z.plus.source.freqdecon.100s.wh0001.a3.0.zero.line110s.su2 \
infile=plot_dist_all_ta_line_X.bin key=offset > \
ph.2013july07.m6.6.ta.line_X.z.plus.source.freqdecon.100s.wh0001.a3.0.zero.line110s.su3

sustrip < ph.2013july07.m6.6.ta.line_X.z.plus.source.freqdecon.100s.wh0001.a3.0.zero.line110s.su3 > \
ph.2013july07.m6.6.ta.line_X.z.plus.source.freqdecon.100s.wh0001.a3.0.zero.line110s

suaddhead < ph.2013july07.m6.6.ta.line_X.z.plus.source.freqdecon.100s.wh0001.a4.0.zero.line110s \
ns=5501 | \
sushw key=dt a=20000 > \
ph.2013july07.m6.6.ta.line_X.z.plus.source.freqdecon.100s.wh0001.a4.0.zero.line110s.su1

sushw < ph.2013july07.m6.6.ta.line_X.z.plus.source.freqdecon.100s.wh0001.a4.0.zero.line110s.su1 \
key=delrt a=-20000 > \
ph.2013july07.m6.6.ta.line_X.z.plus.source.freqdecon.100s.wh0001.a4.0.zero.line110s.su2

sushw < ph.2013july07.m6.6.ta.line_X.z.plus.source.freqdecon.100s.wh0001.a4.0.zero.line110s.su2 \
infile=plot_dist_all_ta_line_X.bin key=offset > \
ph.2013july07.m6.6.ta.line_X.z.plus.source.freqdecon.100s.wh0001.a4.0.zero.line110s.su3

sustrip < ph.2013july07.m6.6.ta.line_X.z.plus.source.freqdecon.100s.wh0001.a4.0.zero.line110s.su3 > \
ph.2013july07.m6.6.ta.line_X.z.plus.source.freqdecon.100s.wh0001.a4.0.zero.line110s

```
suaddhead < ph.2013july07.m6.6.ta.line_X.z.plus.source.freqdecon.100s.wh0001.a5.0.zero.line110s
ns=5501 | \
sushw key=dt a=20000 > \
ph.2013july07.m6.6.ta.line_X.z.plus.source.freqdecon.100s.wh0001.a5.0.zero.line110s.su1

sushw < ph.2013july07.m6.6.ta.line_X.z.plus.source.freqdecon.100s.wh0001.a5.0.zero.line110s.su1 \
key=delrt a=-20000 > \
ph.2013july07.m6.6.ta.line_X.z.plus.source.freqdecon.100s.wh0001.a5.0.zero.line110s.su2

sushw < ph.2013july07.m6.6.ta.line_X.z.plus.source.freqdecon.100s.wh0001.a5.0.zero.line110s.su2 \
infile=plot_dist_all_ta_line_X.bin key=offset > \
ph.2013july07.m6.6.ta.line_X.z.plus.source.freqdecon.100s.wh0001.a5.0.zero.line110s.su3

sustrip < ph.2013july07.m6.6.ta.line_X.z.plus.source.freqdecon.100s.wh0001.a5.0.zero.line110s.su3 > \
ph.2013july07.m6.6.ta.line_X.z.plus.source.freqdecon.100s.wh0001.a5.0.zero.line110s

# Plot
# use op=norm for normalizing each trace separately
# use op=neg to reverse polarity (otherwise same normalization as op=norm)

# For vertical scale: hbox=3.5 inches for 100 seconds,
# so use hbox=3.85 inches for 110 seconds
```

```
suop < ph.2013july07.m6.6.ta.line_X.z.plus.source.freqdecon.100s.wh0001.a1.0.zero.line110s.su3
op=norm | \
supswigp xcur=2.0 wbox=4 hbox=3.85 style=seismic \
nbpi=300 linewidth=0 \
title="ph.2013july07.m6.6.ta.line_X.z.plus.source.freqdecon.100s.wh0001.a1.0.zero.line110s.su3,
2/11/2022" \
label1="Time (s)" labelsize=9 n2tic=2 xbeg=-0.2 \
xend=1 interp=1 n1tic=5 titlesize=8 key=offset > \
ph.2013july07.m6.6.ta.line_X.z.plus.source.freqdecon.100s.wh0001.a1.0.zero.line110s.su3.ps

suop < ph.2013july07.m6.6.ta.line_X.z.plus.source.freqdecon.100s.wh0001.a2.0.zero.line110s.su3
op=norm | \
supswigp xcur=2.0 wbox=4 hbox=3.85 style=seismic \
nbpi=300 linewidth=0 \
title="ph.2013july07.m6.6.ta.line_X.z.plus.source.freqdecon.100s.wh0001.a2.0.zero.line110s.su3,
2/11/2022" \
label1="Time (s)" labelsize=9 n2tic=2 xbeg=-0.2 \
xend=1 interp=1 n1tic=5 titlesize=8 key=offset > \
ph.2013july07.m6.6.ta.line_X.z.plus.source.freqdecon.100s.wh0001.a2.0.zero.line110s.su3.ps

suop < ph.2013july07.m6.6.ta.line_X.z.plus.source.freqdecon.100s.wh0001.a3.0.zero.line110s.su3
op=norm | \
supswigp xcur=2.0 wbox=4 hbox=3.85 style=seismic \
nbpi=300 linewidth=0 \
title="ph.2013july07.m6.6.ta.line_X.z.plus.source.freqdecon.100s.wh0001.a3.0.zero.line110s.su3,
2/11/2022" \
label1="Time (s)" labelsize=9 n2tic=2 xbeg=-0.2 \
xend=1 interp=1 n1tic=5 titlesize=8 key=offset > \
```

```
ph.2013july07.m6.6.ta.line_X.z.plus.source.freqdecon.100s.wh0001.a3.0.zero.line110s.su3.ps



suop < ph.2013july07.m6.6.ta.line_X.z.plus.source.freqdecon.100s.wh0001.a4.0.zero.line110s.su3
op=norm | \
supswigp xcur=2.0 wbox=4 hbox=3.85 style=seismic \
nbpi=300 linewidth=0 \
title="ph.2013july07.m6.6.ta.line_X.z.plus.source.freqdecon.100s.wh0001.a4.0.zero.line110s.su3,
2/11/2022" \
label1="Time (s)" labelsize=9 n2tic=2 xbeg=-0.2 \
xend=1 interp=1 n1tic=5 titlesize=8 key=offset > \
ph.2013july07.m6.6.ta.line_X.z.plus.source.freqdecon.100s.wh0001.a4.0.zero.line110s.su3.ps

# Now replot with negative polarity (op=neg).  Then direct arrival will
# be negative and a positive impedance contrast (e.g. Moho if it's a
# first-order discontinuity) will be positive.

suop < ph.2013july07.m6.6.ta.line_X.z.plus.source.freqdecon.100s.wh0001.a1.0.zero.line110s.su3
op=norm > tempnorm
suop < tempnorm op=neg | \
supswigp xcur=2.0 wbox=4 hbox=3.85 style=seismic \
nbpi=300 linewidth=0 \
title="ph.2013july07.m6.6.ta.line_X.z.plus.source.freqdecon.100s.wh0001.a1.0.zero.line110s.su3,
2/11/2022" \
label1="Time (s)" labelsize=9 n2tic=2 xbeg=-0.2 \
xend=1 interp=1 n1tic=5 titlesize=8 key=offset > \
ph.2013july07.m6.6.ta.line_X.z.plus.source.freqdecon.100s.wh0001.a1.0.zero.line110s.su3.neg.ps
```

```
suop < ph.2013july07.m6.6.ta.line_X.z.plus.source.freqdecon.100s.wh0001.a2.0.zero.line110s.su3
op=norm > tempnorm
suop < tempnorm op=neg | \
supswigp xcur=2.0 wbox=4 hbox=3.85 style=seismic \
nbpi=300 linewidth=0 \
title="ph.2013july07.m6.6.ta.line_X.z.plus.source.freqdecon.100s.wh0001.a2.0.zero.line110s.su3,
2/11/2022" \
label1="Time (s)" labelsize=9 n2tic=2 xbeg=-0.2 \
xend=1 interp=1 n1tic=5 titlesize=8 key=offset > \
ph.2013july07.m6.6.ta.line_X.z.plus.source.freqdecon.100s.wh0001.a2.0.zero.line110s.su3.neg.ps

suop < ph.2013july07.m6.6.ta.line_X.z.plus.source.freqdecon.100s.wh0001.a3.0.zero.line110s.su3
op=norm > tempnorm
suop < tempnorm op=neg | \
supswigp xcur=2.0 wbox=4 hbox=3.85 style=seismic \
nbpi=300 linewidth=0 \
title="ph.2013july07.m6.6.ta.line_X.z.plus.source.freqdecon.100s.wh0001.a3.0.zero.line110s.su3,
2/11/2022" \
label1="Time (s)" labelsize=9 n2tic=2 xbeg=-0.2 \
xend=1 interp=1 n1tic=5 titlesize=8 key=offset > \
ph.2013july07.m6.6.ta.line_X.z.plus.source.freqdecon.100s.wh0001.a3.0.zero.line110s.su3.neg.ps

suop < ph.2013july07.m6.6.ta.line_X.z.plus.source.freqdecon.100s.wh0001.a4.0.zero.line110s.su3
op=norm > tempnorm
suop < tempnorm op=neg | \
supswigp xcur=2.0 wbox=4 hbox=3.85 style=seismic \
nbpi=300 linewidth=0 \
```

```
title="ph.2013july07.m6.6.ta.line_X.z.plus.source.freqdecon.100s.wh0001.a4.0.zero.line110s.su3,
2/11/2022" \
label1="Time (s)" labelsize=9 n2tic=2 xbeg=-0.2 \
xend=1 interp=1 n1tic=5 titlesize=8 key=offset > \
ph.2013july07.m6.6.ta.line_X.z.plus.source.freqdecon.100s.wh0001.a4.0.zero.line110s.su3.neg.ps
```

STEP 201

This step works on all earthquakes for a particular line and Gaussian parameter. In this example I show Line T and α=1.

```
# pkikp_ta_step201_working_ta_line_T_a1.txt
#
# (Original job name, for SESAME lines:
# "pkikp_scale_devon_line_T_a1.txt")
#
# July 6, 2017; May 17, 2018; May 23, 2018; Sept. 15, 2018;
# Sept. 19, 2018; Jan. 11, 2019; Jan. 26, 2019; July 19, 2019
# Aug. 3, 2019; Aug. 8, 2019; August 10, 2019;
# Dec. 10, 2020; Feb. 1, 2021; March 27, 2021; August 17, 2021
# Feb. 21, 2022

# This job is run prior to vertically stacking deconvolved
# records for several earthquakes.  It operates on earthquakes
# recorded by stations of the Transportable Array (TA).
# These traces were resampled (from dt=0.025 s to dt=0.020 s)
# in Step102 and Step103 and then deconvolved in Step104
# using estimates of the earthquake source wavelets derived
# from analysis of data recorded by the SESAME array
# (as described in Verellen et al., 2020, GRL).  For some
# of the earthquakes, new source wavelets were estimated
```

```
# by stacking traces recorded by TA stations (after aligning
# first arrivals by cross-correlation with the SESAME wavelet
# estimate).
#
# Works on the output file of job
# pkikp_ta_step105_master_2013julyl07.m7.3.ta.line_T.txt,
# etc., for other earthquakes.
#
# It first renames the input files, then runs program
# tracezero2019 to zero out especially noisy traces, e.g.,
# traces contaminated by contributions from the PP arrival.
# One strategy is to perform the step104 deconvolution twice,
# first with the original trace length, then again with a
# shorter trace length (if required) to cut out the PP arrival on
# traces from the westernmost stations.  Then use tracezero2019
# to eliminate the PP-contaminated traces for the longer
# window, and also to eliminate the traces for the shorter
# time window that correspond to the easternmost stations
# of the longer time window that show no contamination.

# It then normalizes each trace by its maximum value.  In
# general, the maxumum value will correspond to the sample
# at "zero time", corresponding to the peak of the deconvolved
# direct PKIKP arrival. Then it goes back and normalizes
# each trace by the RMS value of noise in a window
# preceding the direct PKIKP arrival.
#
# Step105, the preceding jobs, inserted blank traces
```

```
# for unoccupied stations for each W-E TA subarray
# for each earthquake.
#
# The output time window for all the Step105 jobs was
# -20 -> 90 seconds (nt=5501 samples).
#
# Step201 renames the output files of Step105 using the
# following renaming scheme.  Events are numbered by
# date, starting with the most recent earthquake (recorded
# by the westernmost stations of the TA array)
#
# Depths are also listed. "dev" refers to events worked on
# by Devon Verellen; "gus" refers to events worked on
# by Gustavo Larramendi (a few events were worked on
# by both):
#                                                  Depth (km)
#
# eq.1   ph.2014.04.11.m7.1      dev.2   gus.2     61 km
# eq.2   ph.2013.10.15.m7.1      gus.7             23
# eq.3   ph.2013.07.07.m7.3      dev.1   gus.1     386
# eq.4   ph.2013.07.07.m6.6      dev.3             62
# eq.5   ph.2013.04.06.m7.0      dev.6   gus.8     66
# eq.6   ph.2012.10.17.m6.0      dev.7             338
# eq.7   ph.2012.08.31.m7.6      gus.5             44
# eq.8   ph.2012.08.26.m6.6      dev.e4  gus.10    91
# eq.9   ei.2012.04.21.m6.7      gus.9             24
# eq.10  ph.2012.04.17.m6.9      dev.4   gus.3     208
# eq.11  ph.2012.03.21.m6.6      dev.e3            118
```

```
# eq.12   ph.2012.02.06.m6.7      gus.6          18
# eq.13   ph.2011.12.14.m7.1      dev.5          129
# eq.14   ph.2011.12.13.m6.1      dev.8          167
# eq.15   ei.2011.07.31.m6.6      gus.4          20
# eq.16   ph.2011.06.13.m6.4      dev.e5         66
# ----    ph.2013.08.12.m6.0      dev.9          95

# Set up distance files for TA "W" W-E array for
# all the original stations (W32A-W61A). Note that
# Station W55A was never deployed.  Stations W37A and
# W37B were deployed at different times at the same location
# and so have been combined into a single station, "W37AB".
# The same goes for stations W41A and W41B.
#
# So: the total number of traces, including the first trace
# which is the deconvolved source wavelet ("WAVE"), is 30.
#
# NOTE: The distance for the first trace (source wavelet)
# will be a dummy distance.

# Convert distance files from ascii to binary format

a2b < plot_dist_all_TA_line_T.txt n1=1 > \
plot_dist_all_TA_line_T.bin

# Rename the output files from step105

cp ph.2014apr11.m7.1.ta.line_T.z.plus.source.freqdecon.90s.wh0001.a1.0.zero.line110s \
```

```
 eq1.ta.line_T.a1.0
cp ph.2013oct15.m7.1.ta.line_T.z.plus.source.freqdecon.wh0001.a1.0.zero.line110s \
 eq2.ta.line_T.a1.0
cp ph.2013july07.m7.3.ta.line_T.z.plus.source.freqdecon.80s.wh0001.a1.0.zero.line110s.filt_0.2_3Hz \
 eq3West.ta.line_T.a1.0
cp ph.2013july07.m7.3.ta.line_T.z.plus.source.freqdecon.80s.wh0001.a1.0.zero.line110s \
 eq3East.ta.line_T.a1.0
cp ph.2013july07.m6.6.ta.line_T.z.plus.source.freqdecon.wh0001.a1.0.zero.line110s \
 eq4.ta.line_T.a1.0
cp ph.2013apr06.m7.0.ta.line_T.z.plus.source.freqdecon.wh0001.a1.0.zero.line110s \
 eq5.ta.line_T.a1.0
cp ph.2012oct17.m6.0.ta.line_T.z.plus.source.freqdecon.wh0001.a1.0.zero.line110s \
 eq6.ta.line_T.a1.0
cp ph.2012aug31.m7.6.ta.line_T.z.plus.source.freqdecon.wh0001.a1.0.zero.line110s.filt_0.2_3Hz \
 eq7.ta.line_T.a1.0
cp ph.2012aug26.m6.6.ta.line_T.z.plus.source.freqdecon.wh0001.a1.0.zero.line110s \
 eq8.ta.line_T.a1.0
cp ph.2012apr21.m6.7.ta.line_T.z.plus.source.freqdecon.wh0001.a1.0.zero.line110s \
 eq9.ta.line_T.a1.0
cp ph.2012apr17.m6.9.ta.line_T.z.plus.source.freqdecon.90s.wh0001.a1.0.zero.line110s.filt_0.2_3Hz \
 eq10.ta.line_T.a1.0
cp ph.2012mar21.m6.6.ta.line_T.z.plus.source.freqdecon.90s.wh0001.a1.0.zero.line110s \
 eq11.ta.line_T.a1.0
cp ph.2012feb06.m6.7.ta.line_T.z.plus.source.filt.freqdecon.wh0001.a1.0.zero.line110s \
 eq12.ta.line_T.a1.0
cp ph.2011dec14.m7.1.ta.line_T.z.plus.source.freqdecon.wh0001.a1.0.zero.line110s \
 eq13.ta.line_T.a1.0
cp ph.2011dec13.m6.1.ta.line_T.z.plus.source.freqdecon.wh0001.a1.0.zero.line110s.filt_0.2_3Hz \
```

```
 eq14.ta.line_T.a1.0
cp ph.2011july31.m6.6.ta.line_T.z.plus.source.freqdecon.wh0001.a1.0.zero.line110s.filt_0.20_3Hz \
 eq15.ta.line_T.a1.0
cp ph.2011june13.m6.4.ta.line_T.z.plus.source.freqdecon.wh0001.a1.0.zero.line110s \
 eq16.ta.line_T.a1.0

# Zero out bad traces (i.e., assign "zero" to all samples for the selected traces)

tracezero2019 in=eq1.ta.line_T.a1.0 out=eq1.ta.line_T.a1.0.zap ntr=30 nt=5501 \
 para=zap_eq1_ta_line_T.txt
tracezero2019 in=eq2.ta.line_T.a1.0 out=eq2.ta.line_T.a1.0.zap ntr=30 nt=5501 \
 para=zap_eq2_ta_line_T.txt
tracezero2019 in=eq3West.ta.line_T.a1.0 out=eq3West.ta.line_T.a1.0.zap ntr=30 nt=5501 \
 para=zap_eq3West_ta_line_T.txt
tracezero2019 in=eq3East.ta.line_T.a1.0 out=eq3East.ta.line_T.a1.0.zap ntr=30 nt=5501 \
 para=zap_eq3East_ta_line_T.txt
tracezero2019 in=eq4.ta.line_T.a1.0 out=eq4.ta.line_T.a1.0.zap ntr=30 nt=5501 \
 para=zap_eq4_ta_line_T.txt
tracezero2019 in=eq5.ta.line_T.a1.0 out=eq5.ta.line_T.a1.0.zap ntr=30 nt=5501 \
 para=zap_eq5_ta_line_T.txt
tracezero2019 in=eq6.ta.line_T.a1.0 out=eq6.ta.line_T.a1.0.zap ntr=30 nt=5501 \
 para=zap_eq6_ta_line_T.txt
tracezero2019 in=eq7.ta.line_T.a1.0 out=eq7.ta.line_T.a1.0.zap ntr=30 nt=5501 \
 para=zap_eq7_ta_line_T.txt
tracezero2019 in=eq8.ta.line_T.a1.0 out=eq8.ta.line_T.a1.0.zap ntr=30 nt=5501 \
 para=zap_eq8_ta_line_T.txt
tracezero2019 in=eq9.ta.line_T.a1.0 out=eq9.ta.line_T.a1.0.zap ntr=30 nt=5501 \
 para=zap_eq9_ta_line_T.txt
```

```
tracezero2019 in=eq10.ta.line_T.a1.0 out=eq10.ta.line_T.a1.0.zap ntr=30 nt=5501 \
 para=zap_eq10_ta_line_T.txt
tracezero2019 in=eq11.ta.line_T.a1.0 out=eq11.ta.line_T.a1.0.zap ntr=30 nt=5501 \
 para=zap_eq11_ta_line_T.txt
tracezero2019 in=eq12.ta.line_T.a1.0 out=eq12.ta.line_T.a1.0.zap ntr=30 nt=5501 \
 para=zap_eq12_ta_line_T.txt
tracezero2019 in=eq13.ta.line_T.a1.0 out=eq13.ta.line_T.a1.0.zap ntr=30 nt=5501 \
 para=zap_eq13_ta_line_T.txt
tracezero2019 in=eq14.ta.line_T.a1.0 out=eq14.ta.line_T.a1.0.zap ntr=30 nt=5501 \
 para=zap_eq14_ta_line_T.txt
tracezero2019 in=eq15.ta.line_T.a1.0 out=eq15.ta.line_T.a1.0.zap ntr=30 nt=5501 \
 para=zap_eq15_ta_line_T.txt
tracezero2019 in=eq16.ta.line_T.a1.0 out=eq16.ta.line_T.a1.0.zap ntr=30 nt=5501 \
 para=zap_eq16_ta_line_T.txt

# NOTE: "ntr" will be different for each W-E TA subarray.  It represents
# the number of deployed stations for that array, plus one more for the
# source wavelet.

scalebynoisewindow in=eq1.ta.line_T.a1.0.zap out=eq1.ta.line_T.a1.0.scale \
outc=eq1.ta.line_T.a1.0.noisetally.txt \
ntr=30 nt=5501 dt=0.02 t1=2 t2=18

scalebynoisewindow in=eq2.ta.line_T.a1.0.zap out=eq2.ta.line_T.a1.0.scale \
outc=eq2.ta.line_T.a1.0.noisetally.txt \
ntr=30 nt=5501 dt=0.02 t1=2 t2=18

scalebynoisewindow in=eq3West.ta.line_T.a1.0.zap out=eq3West.ta.line_T.a1.0.scale \
```

```
outc=eq3West.ta.line_T.a1.0.noisetally.txt \
ntr=30 nt=5501 dt=0.02 t1=2 t2=18

scalebynoisewindow in=eq3East.ta.line_T.a1.0.zap out=eq3East.ta.line_T.a1.0.scale \
outc=eq3East.ta.line_T.a1.0.noisetally.txt \
ntr=30 nt=5501 dt=0.02 t1=2 t2=18

scalebynoisewindow in=eq4.ta.line_T.a1.0.zap out=eq4.ta.line_T.a1.0.scale \
outc=eq4.ta.line_T.a1.0.noisetally.txt \
ntr=30 nt=5501 dt=0.02 t1=2 t2=18

scalebynoisewindow in=eq5.ta.line_T.a1.0.zap out=eq5.ta.line_T.a1.0.scale \
outc=eq5.ta.line_T.a1.0.noisetally.txt \
ntr=30 nt=5501 dt=0.02 t1=2 t2=18

scalebynoisewindow in=eq6.ta.line_T.a1.0.zap out=eq6.ta.line_T.a1.0.scale \
outc=eq6.ta.line_T.a1.0.noisetally.txt \
ntr=30 nt=5501 dt=0.02 t1=2 t2=18

scalebynoisewindow in=eq7.ta.line_T.a1.0.zap out=eq7.ta.line_T.a1.0.scale \
outc=eq7.ta.line_T.a1.0.noisetally.txt \
ntr=30 nt=5501 dt=0.02 t1=2 t2=18

scalebynoisewindow in=eq8.ta.line_T.a1.0.zap out=eq8.ta.line_T.a1.0.scale \
outc=eq8.ta.line_T.a1.0.noisetally.txt \
ntr=30 nt=5501 dt=0.02 t1=2 t2=18

scalebynoisewindow in=eq9.ta.line_T.a1.0.zap out=eq9.ta.line_T.a1.0.scale \
```

```
outc=eq9.ta.line_T.a1.0.noisetally.txt \
ntr=30 nt=5501 dt=0.02 t1=2 t2=18

scalebynoisewindow in=eq10.ta.line_T.a1.0.zap out=eq10.ta.line_T.a1.0.scale \
outc=eq10.ta.line_T.a1.0.noisetally.txt \
ntr=30 nt=5501 dt=0.02 t1=2 t2=18

scalebynoisewindow in=eq11.ta.line_T.a1.0.zap out=eq11.ta.line_T.a1.0.scale \
outc=eq11.ta.line_T.a1.0.noisetally.txt \
ntr=30 nt=5501 dt=0.02 t1=2 t2=18

scalebynoisewindow in=eq12.ta.line_T.a1.0.zap out=eq12.ta.line_T.a1.0.scale \
outc=eq12.ta.line_T.a1.0.noisetally.txt \
ntr=30 nt=5501 dt=0.02 t1=2 t2=18

scalebynoisewindow in=eq13.ta.line_T.a1.0.zap out=eq13.ta.line_T.a1.0.scale \
outc=eq13.ta.line_T.a1.0.noisetally.txt \
ntr=30 nt=5501 dt=0.02 t1=2 t2=18

scalebynoisewindow in=eq14.ta.line_T.a1.0.zap out=eq14.ta.line_T.a1.0.scale \
outc=eq14.ta.line_T.a1.0.noisetally.txt \
ntr=30 nt=5501 dt=0.02 t1=2 t2=18

scalebynoisewindow in=eq15.ta.line_T.a1.0.zap out=eq15.ta.line_T.a1.0.scale \
outc=eq15.ta.line_T.a1.0.noisetally.txt \
ntr=30 nt=5501 dt=0.02 t1=2 t2=18

scalebynoisewindow in=eq16.ta.line_T.a1.0.zap out=eq16.ta.line_T.a1.0.scale \
```

```
outc=eq16.ta.line_T.a1.0.noisetally.txt \
ntr=30 nt=5501 dt=0.02 t1=2 t2=18


# The above program scales each trace by a different constant, depending
# on the level of noise preceding the direct PKIKP arrival.  The RMS
# values of noise are tallied in the "outc" file.  Can also check this
# by plotting traces WITHOUT first running the program "suop" with
# "op=norm". Try comparing the two ways of plotting.

# Add headers
# NOTE that dt is in microseconds and delrt is in milliseconds
# dt = 0.02 seconds = 20 milliseconds = 20,000 microseconds
# delrt = -20 seconds = -20,000 milliseconds (trace starts
# 20 seconds before first arrival)

suaddhead < eq1.ta.line_T.a1.0.scale ns=5501 | \
sushw key=dt a=20000 > eq1.ta.line_T.a1.0.scale.su1

sushw < eq1.ta.line_T.a1.0.scale.su1 \
key=delrt a=-20000 > eq1.ta.line_T.a1.0.scale.su2

sushw < eq1.ta.line_T.a1.0.scale.su2 \
infile=plot_dist_all_TA_line_T.bin key=offset > eq1.ta.line_T.a1.0.scale.su3

suaddhead < eq2.ta.line_T.a1.0.scale ns=5501 | \
sushw key=dt a=20000 > eq2.ta.line_T.a1.0.scale.su1
```

```
sushw < eq2.ta.line_T.a1.0.scale.su1 \
key=delrt a=-20000 > eq2.ta.line_T.a1.0.scale.su2

sushw < eq2.ta.line_T.a1.0.scale.su2 \
infile=plot_dist_all_TA_line_T.bin key=offset > eq2.ta.line_T.a1.0.scale.su3

suaddhead < eq3West.ta.line_T.a1.0.scale ns=5501 | \
sushw key=dt a=20000 > eq3West.ta.line_T.a1.0.scale.su1

sushw < eq3West.ta.line_T.a1.0.scale.su1 \
key=delrt a=-20000 > eq3West.ta.line_T.a1.0.scale.su2

sushw < eq3West.ta.line_T.a1.0.scale.su2 \
infile=plot_dist_all_TA_line_T.bin key=offset > eq3West.ta.line_T.a1.0.scale.su3

suaddhead < eq3East.ta.line_T.a1.0.scale ns=5501 | \
sushw key=dt a=20000 > eq3East.ta.line_T.a1.0.scale.su1

sushw < eq3East.ta.line_T.a1.0.scale.su1 \
key=delrt a=-20000 > eq3East.ta.line_T.a1.0.scale.su2

sushw < eq3East.ta.line_T.a1.0.scale.su2 \
infile=plot_dist_all_TA_line_T.bin key=offset > eq3East.ta.line_T.a1.0.scale.su3


suaddhead < eq4.ta.line_T.a1.0.scale ns=5501 | \
sushw key=dt a=20000 > eq4.ta.line_T.a1.0.scale.su1
```

```
sushw < eq4.ta.line_T.a1.0.scale.su1 \
key=delrt a=-20000 > eq4.ta.line_T.a1.0.scale.su2

sushw < eq4.ta.line_T.a1.0.scale.su2 \
infile=plot_dist_all_TA_line_T.bin key=offset > eq4.ta.line_T.a1.0.scale.su3

suaddhead < eq5.ta.line_T.a1.0.scale ns=5501 | \
sushw key=dt a=20000 > eq5.ta.line_T.a1.0.scale.su1

sushw < eq5.ta.line_T.a1.0.scale.su1 \
key=delrt a=-20000 > eq5.ta.line_T.a1.0.scale.su2

sushw < eq5.ta.line_T.a1.0.scale.su2 \
infile=plot_dist_all_TA_line_T.bin key=offset > eq5.ta.line_T.a1.0.scale.su3

suaddhead < eq6.ta.line_T.a1.0.scale ns=5501 | \
sushw key=dt a=20000 > eq6.ta.line_T.a1.0.scale.su1

sushw < eq6.ta.line_T.a1.0.scale.su1 \
key=delrt a=-20000 > eq6.ta.line_T.a1.0.scale.su2

sushw < eq6.ta.line_T.a1.0.scale.su2 \
infile=plot_dist_all_TA_line_T.bin key=offset > eq6.ta.line_T.a1.0.scale.su3

suaddhead < eq7.ta.line_T.a1.0.scale ns=5501 | \
sushw key=dt a=20000 > eq7.ta.line_T.a1.0.scale.su1

sushw < eq7.ta.line_T.a1.0.scale.su1 \
```

```
key=delrt a=-20000 > eq7.ta.line_T.a1.0.scale.su2

sushw < eq7.ta.line_T.a1.0.scale.su2 \
infile=plot_dist_all_TA_line_T.bin key=offset > eq7.ta.line_T.a1.0.scale.su3



suaddhead < eq8.ta.line_T.a1.0.scale ns=5501 | \
sushw key=dt a=20000 > eq8.ta.line_T.a1.0.scale.su1

sushw < eq8.ta.line_T.a1.0.scale.su1 \
key=delrt a=-20000 > eq8.ta.line_T.a1.0.scale.su2

sushw < eq8.ta.line_T.a1.0.scale.su2 \
infile=plot_dist_all_TA_line_T.bin key=offset > eq8.ta.line_T.a1.0.scale.su3

suaddhead < eq9.ta.line_T.a1.0.scale ns=5501 | \
sushw key=dt a=20000 > eq9.ta.line_T.a1.0.scale.su1

sushw < eq9.ta.line_T.a1.0.scale.su1 \
key=delrt a=-20000 > eq9.ta.line_T.a1.0.scale.su2

sushw < eq9.ta.line_T.a1.0.scale.su2 \
infile=plot_dist_all_TA_line_T.bin key=offset > eq9.ta.line_T.a1.0.scale.su3

suaddhead < eq10.ta.line_T.a1.0.scale ns=5501 | \
sushw key=dt a=20000 > eq10.ta.line_T.a1.0.scale.su1
```

```
sushw < eq10.ta.line_T.a1.0.scale.su1 \
key=delrt a=-20000 > eq10.ta.line_T.a1.0.scale.su2

sushw < eq10.ta.line_T.a1.0.scale.su2 \
infile=plot_dist_all_TA_line_T.bin key=offset > eq10.ta.line_T.a1.0.scale.su3

suaddhead < eq11.ta.line_T.a1.0.scale ns=5501 | \
sushw key=dt a=20000 > eq11.ta.line_T.a1.0.scale.su1

sushw < eq11.ta.line_T.a1.0.scale.su1 \
key=delrt a=-20000 > eq11.ta.line_T.a1.0.scale.su2

sushw < eq11.ta.line_T.a1.0.scale.su2 \
infile=plot_dist_all_TA_line_T.bin key=offset > eq11.ta.line_T.a1.0.scale.su3

suaddhead < eq12.ta.line_T.a1.0.scale ns=5501 | \
sushw key=dt a=20000 > eq12.ta.line_T.a1.0.scale.su1

sushw < eq12.ta.line_T.a1.0.scale.su1 \
key=delrt a=-20000 > eq12.ta.line_T.a1.0.scale.su2

sushw < eq12.ta.line_T.a1.0.scale.su2 \
infile=plot_dist_all_TA_line_T.bin key=offset > eq12.ta.line_T.a1.0.scale.su3

suaddhead < eq13.ta.line_T.a1.0.scale ns=5501 | \
sushw key=dt a=20000 > eq13.ta.line_T.a1.0.scale.su1

sushw < eq13.ta.line_T.a1.0.scale.su1 \
```

```
key=delrt a=-20000 > eq13.ta.line_T.a1.0.scale.su2

sushw < eq13.ta.line_T.a1.0.scale.su2 \
infile=plot_dist_all_TA_line_T.bin key=offset > eq13.ta.line_T.a1.0.scale.su3
suaddhead < eq14.ta.line_T.a1.0.scale ns=5501 | \
sushw key=dt a=20000 > eq14.ta.line_T.a1.0.scale.su1

sushw < eq14.ta.line_T.a1.0.scale.su1 \
key=delrt a=-20000 > eq14.ta.line_T.a1.0.scale.su2

sushw < eq14.ta.line_T.a1.0.scale.su2 \
infile=plot_dist_all_TA_line_T.bin key=offset > eq14.ta.line_T.a1.0.scale.su3

suaddhead < eq15.ta.line_T.a1.0.scale ns=5501 | \
sushw key=dt a=20000 > eq15.ta.line_T.a1.0.scale.su1

sushw < eq15.ta.line_T.a1.0.scale.su1 \
key=delrt a=-20000 > eq15.ta.line_T.a1.0.scale.su2

sushw < eq15.ta.line_T.a1.0.scale.su2 \
infile=plot_dist_all_TA_line_T.bin key=offset > eq15.ta.line_T.a1.0.scale.su3

suaddhead < eq16.ta.line_T.a1.0.scale ns=5501 | \
sushw key=dt a=20000 > eq16.ta.line_T.a1.0.scale.su1

sushw < eq16.ta.line_T.a1.0.scale.su1 \
key=delrt a=-20000 > eq16.ta.line_T.a1.0.scale.su2
```

```
sushw < eq16.ta.line_T.a1.0.scale.su2 \
infile=plot_dist_all_TA_line_T.bin key=offset > eq16.ta.line_T.a1.0.scale.su3



# Plot
# use op=norm for normalizing each trace separately
# use op=neg to reverse polarity (otherwise same normalization as op=norm)
# For vertical scale: hbox=3.5 inches for 100 seconds,
# so use hbox=3.85 inches for 110 seconds
# First set of plots: same as plots generated by pkikp_step105

suop < eq1.ta.line_T.a1.0.scale.su3 op=norm | \
supswigp xcur=2.0 wbox=4 hbox=3.85 style=seismic \
nbpi=300 linewidth=0 \
title="eq1.ta.line_T.a1.0.scale.su3, 2/18/2022" \
label1="Time (s)" labelsize=9 n2tic=2 xbeg=-0.2 \
xend=1 interp=1 n1tic=5 titlesize=8 key=offset > \
eq1.ta.line_T.a1.0.scale.su3.ps

suop < eq2.ta.line_T.a1.0.scale.su3 op=norm | \
supswigp xcur=2.0 wbox=4 hbox=3.85 style=seismic \
nbpi=300 linewidth=0 \
title="eq2.ta.line_T.a1.0.scale.su3, 2/18/2022" \
label1="Time (s)" labelsize=9 n2tic=2 xbeg=-0.2 \
xend=1 interp=1 n1tic=5 titlesize=8 key=offset > \
eq2.ta.line_T.a1.0.scale.su3.ps
```

```
suop < eq3West.ta.line_T.a1.0.scale.su3 op=norm | \
supswigp xcur=2.0 wbox=4 hbox=3.85 style=seismic \
nbpi=300 linewidth=0 \
title="eq3West.ta.line_T.a1.0.scale.su3, 2/18/2022" \
label1="Time (s)" labelsize=9 n2tic=2 xbeg=-0.2 \
xend=1 interp=1 n1tic=5 titlesize=8 key=offset > \
eq3West.ta.line_T.a1.0.scale.su3.ps

suop < eq3East.ta.line_T.a1.0.scale.su3 op=norm | \
supswigp xcur=2.0 wbox=4 hbox=3.85 style=seismic \
nbpi=300 linewidth=0 \
title="eq3East.ta.line_T.a1.0.scale.su3, 2/18/2022" \
label1="Time (s)" labelsize=9 n2tic=2 xbeg=-0.2 \
xend=1 interp=1 n1tic=5 titlesize=8 key=offset > \
eq3East.ta.line_T.a1.0.scale.su3.ps

suop < eq4.ta.line_T.a1.0.scale.su3 op=norm | \
supswigp xcur=2.0 wbox=4 hbox=3.85 style=seismic \
nbpi=300 linewidth=0 \
title="eq4.ta.line_T.a1.0.scale.su3, 2/18/2022" \
label1="Time (s)" labelsize=9 n2tic=2 xbeg=-0.2 \
xend=1 interp=1 n1tic=5 titlesize=8 key=offset > \
eq4.ta.line_T.a1.0.scale.su3.ps

suop < eq5.ta.line_T.a1.0.scale.su3 op=norm | \
supswigp xcur=2.0 wbox=4 hbox=3.85 style=seismic \
nbpi=300 linewidth=0 \
title="eq5.ta.line_T.a1.0.scale.su3, 2/18/2022" \
```

```
label1="Time (s)" labelsize=9 n2tic=2 xbeg=-0.2 \
xend=1 interp=1 n1tic=5 titlesize=8 key=offset > \
eq5.ta.line_T.a1.0.scale.su3.ps


suop < eq6.ta.line_T.a1.0.scale.su3 op=norm | \
supswigp xcur=2.0 wbox=4 hbox=3.85 style=seismic \
nbpi=300 linewidth=0 \
title="eq6.ta.line_T.a1.0.scale.su3, 2/18/2022" \
label1="Time (s)" labelsize=9 n2tic=2 xbeg=-0.2 \
xend=1 interp=1 n1tic=5 titlesize=8 key=offset > \
eq6.ta.line_T.a1.0.scale.su3.ps

suop < eq7.ta.line_T.a1.0.scale.su3 op=norm | \
supswigp xcur=2.0 wbox=4 hbox=3.85 style=seismic \
nbpi=300 linewidth=0 \
title="eq7.ta.line_T.a1.0.scale.su3, 2/18/2022" \
label1="Time (s)" labelsize=9 n2tic=2 xbeg=-0.2 \
xend=1 interp=1 n1tic=5 titlesize=8 key=offset > \
eq7.ta.line_T.a1.0.scale.su3.ps

suop < eq8.ta.line_T.a1.0.scale.su3 op=norm | \
supswigp xcur=2.0 wbox=4 hbox=3.85 style=seismic \
nbpi=300 linewidth=0 \
title="eq8.ta.line_T.a1.0.scale.su3, 2/18/2022" \
label1="Time (s)" labelsize=9 n2tic=2 xbeg=-0.2 \
xend=1 interp=1 n1tic=5 titlesize=8 key=offset > \
eq8.ta.line_T.a1.0.scale.su3.ps
```

```
suop < eq9.ta.line_T.a1.0.scale.su3 op=norm | \
supswigp xcur=2.0 wbox=4 hbox=3.85 style=seismic \
nbpi=300 linewidth=0 \
title="eq9.ta.line_T.a1.0.scale.su3, 2/18/2022" \
label1="Time (s)" labelsize=9 n2tic=2 xbeg=-0.2 \
xend=1 interp=1 n1tic=5 titlesize=8 key=offset > \
eq9.ta.line_T.a1.0.scale.su3.ps

suop < eq10.ta.line_T.a1.0.scale.su3 op=norm | \
supswigp xcur=2.0 wbox=4 hbox=3.85 style=seismic \
nbpi=300 linewidth=0 \
title="eq10.ta.line_T.a1.0.scale.su3, 2/18/2022" \
label1="Time (s)" labelsize=9 n2tic=2 xbeg=-0.2 \
xend=1 interp=1 n1tic=5 titlesize=8 key=offset > \
eq10.ta.line_T.a1.0.scale.su3.ps

suop < eq11.ta.line_T.a1.0.scale.su3 op=norm | \
supswigp xcur=2.0 wbox=4 hbox=3.85 style=seismic \
nbpi=300 linewidth=0 \
title="eq11.ta.line_T.a1.0.scale.su3, 2/18/2022" \
label1="Time (s)" labelsize=9 n2tic=2 xbeg=-0.2 \
xend=1 interp=1 n1tic=5 titlesize=8 key=offset > \
eq11.ta.line_T.a1.0.scale.su3.ps

suop < eq12.ta.line_T.a1.0.scale.su3 op=norm | \
supswigp xcur=2.0 wbox=4 hbox=3.85 style=seismic \
nbpi=300 linewidth=0 \
```

```
title="eq12.ta.line_T.a1.0.scale.su3, 2/18/2022" \
label1="Time (s)" labelsize=9 n2tic=2 xbeg=-0.2 \
xend=1 interp=1 n1tic=5 titlesize=8 key=offset > \
eq12.ta.line_T.a1.0.scale.su3.ps

suop < eq13.ta.line_T.a1.0.scale.su3 op=norm | \
supswigp xcur=2.0 wbox=4 hbox=3.85 style=seismic \
nbpi=300 linewidth=0 \
title="eq13.ta.line_T.a1.0.scale.su3, 2/18/2022" \
label1="Time (s)" labelsize=9 n2tic=2 xbeg=-0.2 \
xend=1 interp=1 n1tic=5 titlesize=8 key=offset > \
eq13.ta.line_T.a1.0.scale.su3.ps

suop < eq14.ta.line_T.a1.0.scale.su3 op=norm | \
supswigp xcur=2.0 wbox=4 hbox=3.85 style=seismic \
nbpi=300 linewidth=0 \
title="eq14.ta.line_T.a1.0.scale.su3, 2/18/2022" \
label1="Time (s)" labelsize=9 n2tic=2 xbeg=-0.2 \
xend=1 interp=1 n1tic=5 titlesize=8 key=offset > \
eq14.ta.line_T.a1.0.scale.su3.ps

suop < eq15.ta.line_T.a1.0.scale.su3 op=norm | \
supswigp xcur=2.0 wbox=4 hbox=3.85 style=seismic \
nbpi=300 linewidth=0 \
title="eq15.ta.line_T.a1.0.scale.su3, 2/18/2022" \
label1="Time (s)" labelsize=9 n2tic=2 xbeg=-0.2 \
xend=1 interp=1 n1tic=5 titlesize=8 key=offset > \
eq15.ta.line_T.a1.0.scale.su3.ps
```

```
suop < eq16.ta.line_T.a1.0.scale.su3 op=norm | \
supswigp xcur=2.0 wbox=4 hbox=3.85 style=seismic \
nbpi=300 linewidth=0 \
title="eq16.ta.line_T.a1.0.scale.su3, 2/18/2022" \
label1="Time (s)" labelsize=9 n2tic=2 xbeg=-0.2 \
xend=1 interp=1 n1tic=5 titlesize=8 key=offset > \
eq16.ta.line_T.a1.0.scale.su3.ps

# Now replot with negative polarity (op=neg).  Then direct arrival will
# be negative and a positive impedance contrast (e.g. Moho if it's a
# first-order discontinuity) will be positive.
# This time, plot without normalizing each trace by its
# maximum amplitude.  So can see the effect of dividing
# each trace by its RMS noise level.  This will show up
# better in the negative-polarity plots.

suop < eq1.ta.line_T.a1.0.scale.su3 op=neg | \
supswigp xcur=2.0 wbox=4 hbox=3.85 style=seismic \
nbpi=300 linewidth=0 \
title="eq1.ta.line_T.a1.0.scale.su3, 2/18/2022" \
label1="Time (s)" labelsize=9 n2tic=2 xbeg=-0.2 \
xend=1 interp=1 n1tic=5 titlesize=8 key=offset > \
eq1.ta.line_T.a1.0.scale.su3.neg.nonorm.ps

suop < eq2.ta.line_T.a1.0.scale.su3 op=neg | \
supswigp xcur=2.0 wbox=4 hbox=3.85 style=seismic \
nbpi=300 linewidth=0 \
```

```
title="eq2.ta.line_T.a1.0.scale.su3, 2/18/2022" \
label1="Time (s)" labelsize=9 n2tic=2 xbeg=-0.2 \
xend=1 interp=1 n1tic=5 titlesize=8 key=offset > \
eq2.ta.line_T.a1.0.scale.su3.neg.nonorm.ps

suop < eq3West.ta.line_T.a1.0.scale.su3 op=neg | \
supswigp xcur=2.0 wbox=4 hbox=3.85 style=seismic \
nbpi=300 linewidth=0 \
title="eq3West.ta.line_T.a1.0.scale.su3, 2/18/2022" \
label1="Time (s)" labelsize=9 n2tic=2 xbeg=-0.2 \
xend=1 interp=1 n1tic=5 titlesize=8 key=offset > \
eq3West.ta.line_T.a1.0.scale.su3.neg.nonorm.ps

suop < eq3East.ta.line_T.a1.0.scale.su3 op=neg | \
supswigp xcur=2.0 wbox=4 hbox=3.85 style=seismic \
nbpi=300 linewidth=0 \
title="eq3East.ta.line_T.a1.0.scale.su3, 2/18/2022" \
label1="Time (s)" labelsize=9 n2tic=2 xbeg=-0.2 \
xend=1 interp=1 n1tic=5 titlesize=8 key=offset > \
eq3East.ta.line_T.a1.0.scale.su3.neg.nonorm.ps

suop < eq4.ta.line_T.a1.0.scale.su3 op=neg | \
supswigp xcur=2.0 wbox=4 hbox=3.85 style=seismic \
nbpi=300 linewidth=0 \
title="eq4.ta.line_T.a1.0.scale.su3, 2/18/2022" \
label1="Time (s)" labelsize=9 n2tic=2 xbeg=-0.2 \
xend=1 interp=1 n1tic=5 titlesize=8 key=offset > \
eq4.ta.line_T.a1.0.scale.su3.neg.nonorm.ps
```

```
suop < eq5.ta.line_T.a1.0.scale.su3 op=neg | \
supswigp xcur=2.0 wbox=4 hbox=3.85 style=seismic \
nbpi=300 linewidth=0 \
title="eq5.ta.line_T.a1.0.scale.su3, 2/18/2022" \
label1="Time (s)" labelsize=9 n2tic=2 xbeg=-0.2 \
xend=1 interp=1 n1tic=5 titlesize=8 key=offset > \
eq5.ta.line_T.a1.0.scale.su3.neg.nonorm.ps

suop < eq6.ta.line_T.a1.0.scale.su3 op=neg | \
supswigp xcur=2.0 wbox=4 hbox=3.85 style=seismic \
nbpi=300 linewidth=0 \
title="eq6.ta.line_T.a1.0.scale.su3, 2/18/2022" \
label1="Time (s)" labelsize=9 n2tic=2 xbeg=-0.2 \
xend=1 interp=1 n1tic=5 titlesize=8 key=offset > \
eq6.ta.line_T.a1.0.scale.su3.neg.nonorm.ps

suop < eq7.ta.line_T.a1.0.scale.su3 op=neg | \
supswigp xcur=2.0 wbox=4 hbox=3.85 style=seismic \
nbpi=300 linewidth=0 \
title="eq7.ta.line_T.a1.0.scale.su3, 2/18/2022" \
label1="Time (s)" labelsize=9 n2tic=2 xbeg=-0.2 \
xend=1 interp=1 n1tic=5 titlesize=8 key=offset > \
eq7.ta.line_T.a1.0.scale.su3.neg.nonorm.ps

suop < eq8.ta.line_T.a1.0.scale.su3 op=neg | \
supswigp xcur=2.0 wbox=4 hbox=3.85 style=seismic \
nbpi=300 linewidth=0 \
```

```
title="eq8.ta.line_T.a1.0.scale.su3, 2/18/2022" \
label1="Time (s)" labelsize=9 n2tic=2 xbeg=-0.2 \
xend=1 interp=1 n1tic=5 titlesize=8 key=offset > \
eq8.ta.line_T.a1.0.scale.su3.neg.nonorm.ps

suop < eq9.ta.line_T.a1.0.scale.su3 op=neg | \
supswigp xcur=2.0 wbox=4 hbox=3.85 style=seismic \
nbpi=300 linewidth=0 \
title="eq9.ta.line_T.a1.0.scale.su3, 2/18/2022" \
label1="Time (s)" labelsize=9 n2tic=2 xbeg=-0.2 \
xend=1 interp=1 n1tic=5 titlesize=8 key=offset > \
eq9.ta.line_T.a1.0.scale.su3.neg.nonorm.ps

suop < eq10.ta.line_T.a1.0.scale.su3 op=neg | \
supswigp xcur=2.0 wbox=4 hbox=3.85 style=seismic \
nbpi=300 linewidth=0 \
title="eq10.ta.line_T.a1.0.scale.su3, 2/18/2022" \
label1="Time (s)" labelsize=9 n2tic=2 xbeg=-0.2 \
xend=1 interp=1 n1tic=5 titlesize=8 key=offset > \
eq10.ta.line_T.a1.0.scale.su3.neg.nonorm.ps

suop < eq11.ta.line_T.a1.0.scale.su3 op=neg | \
supswigp xcur=2.0 wbox=4 hbox=3.85 style=seismic \
nbpi=300 linewidth=0 \
title="eq11.ta.line_T.a1.0.scale.su3, 2/18/2022" \
label1="Time (s)" labelsize=9 n2tic=2 xbeg=-0.2 \
xend=1 interp=1 n1tic=5 titlesize=8 key=offset > \
eq11.ta.line_T.a1.0.scale.su3.neg.nonorm.ps
```

```
suop < eq12.ta.line_T.a1.0.scale.su3 op=neg | \
supswigp xcur=2.0 wbox=4 hbox=3.85 style=seismic \
nbpi=300 linewidth=0 \
title="eq12.ta.line_T.a1.0.scale.su3, 2/18/2022" \
label1="Time (s)" labelsize=9 n2tic=2 xbeg=-0.2 \
xend=1 interp=1 n1tic=5 titlesize=8 key=offset > \
eq12.ta.line_T.a1.0.scale.su3.neg.nonorm.ps

suop < eq13.ta.line_T.a1.0.scale.su3 op=neg | \
supswigp xcur=2.0 wbox=4 hbox=3.85 style=seismic \
nbpi=300 linewidth=0 \
title="eq13.ta.line_T.a1.0.scale.su3, 2/18/2022" \
label1="Time (s)" labelsize=9 n2tic=2 xbeg=-0.2 \
xend=1 interp=1 n1tic=5 titlesize=8 key=offset > \
eq13.ta.line_T.a1.0.scale.su3.neg.nonorm.ps

suop < eq14.ta.line_T.a1.0.scale.su3 op=neg | \
supswigp xcur=2.0 wbox=4 hbox=3.85 style=seismic \
nbpi=300 linewidth=0 \
title="eq14.ta.line_T.a1.0.scale.su3, 2/18/2022" \
label1="Time (s)" labelsize=9 n2tic=2 xbeg=-0.2 \
xend=1 interp=1 n1tic=5 titlesize=8 key=offset > \
eq14.ta.line_T.a1.0.scale.su3.neg.nonorm.ps

suop < eq15.ta.line_T.a1.0.scale.su3 op=neg | \
supswigp xcur=2.0 wbox=4 hbox=3.85 style=seismic \
nbpi=300 linewidth=0 \
```

```
title="eq15.ta.line_T.a1.0.scale.su3, 2/18/2022" \
label1="Time (s)" labelsize=9 n2tic=2 xbeg=-0.2 \
xend=1 interp=1 n1tic=5 titlesize=8 key=offset > \
eq15.ta.line_T.a1.0.scale.su3.neg.nonorm.ps

suop < eq16.ta.line_T.a1.0.scale.su3 op=neg | \
supswigp xcur=2.0 wbox=4 hbox=3.85 style=seismic \
nbpi=300 linewidth=0 \
title="eq16.ta.line_T.a1.0.scale.su3, 2/18/2022" \
label1="Time (s)" labelsize=9 n2tic=2 xbeg=-0.2 \
xend=1 interp=1 n1tic=5 titlesize=8 key=offset > \
eq16.ta.line_T.a1.0.scale.su3.neg.nonorm.ps
```

STEP 201 MUTE

This step works on all earthquakes that had a bandpass filter applied for a particular line and Gaussian parameter. In this example I show Line T and α=1.

```
# pkikp_ta_step201mute_working_ta_line_T_a1.txt
#
# July 6, 2017; May 17, 2018; May 23, 2018; Sept. 15, 2018;
# Sept. 19, 2018; Jan. 11, 2019; Jan. 26, 2019; July 19, 2019
# Aug. 3, 2019; Aug. 8, 2019; August 10, 2019;
# Dec. 10, 2020; Feb. 1, 2021; March 27, 2021; March 29, 2021
# Feb. 23, 2022

# Run this "step201mute" job right after the "step201" job, for
# deconvolution output that shows significant sidelobes centered
# around T=0 (e.g., for traces that were bandpass filtered after
# deconvolution, or where deconvolution was done with a bandpass-
# filtered source wavelet and bandpass-filtered field traces.
# This jobs mutes input traces over a time window centered about
# T=0 (20 seconds after the beginning of each trace).  The mute
# is tapered to avoid sharp cutoffs.

# This job is run prior to vertically stacking deconvolved
# records for several earthquakes.  It operates on earthquakes
```

recorded by stations of the Transportable Array (TA).

These traces were resampled (from dt=0.025 s to dt=0.020 s)

in Step102 and Step103 and then deconvolved in Step104

using estimates of the earthquake source wavelets derived

from analysis of data recorded by the SESAME array

(as described in Verellen et al., 2020, GRL). For some

of the earthquakes, new source wavelets were estimated

by stacking traces recorded by TA stations (after aligning

first arrivals by cross-correlation with the SESAME wavelet

estimate).

#

The "step201" job works on the output file of job

pkikp_ta_step105_master_2013julyl07.m7.3.ta.line_T.txt,

etc., for other earthquakes.

#

The output time window for all the Step201 jobs (and

Step105 jobs) is -20 -> 90 seconds (nt=5501 samples).

#

Step201 renamed the output files of Step105 using the

following renaming scheme. Events are numbered by

date, starting with the most recent earthquake (recorded

by the westernmost stations of the TA array)

#

Depths are also listed. "dev" refers to events worked on

by Devon Verellen; "gus" refers to events worked on

by Gustavo Larramendi (a few events were worked on

by both):

Depth (km)

#

# eq.1	ph.2014.04.11.m7.1	dev.2	gus.2	61 km
# eq.2	ph.2013.10.15.m7.1	gus.7		23
# eq.3	ph.2013.07.07.m7.3	dev.1	gus.1	386
# eq.4	ph.2013.07.07.m6.6	dev.3		62
# eq.5	ph.2013.04.06.m7.0	dev.6	gus.8	66
# eq.6	ph.2012.10.17.m6.0	dev.7		338
# eq.7	ph.2012.08.31.m7.6	gus.5		44
# eq.8	ph.2012.08.26.m6.6	dev.e4	gus.10	91
# eq.9	ei.2012.04.21.m6.7	gus.9		24
# eq.10	ph.2012.04.17.m6.9	dev.4	gus.3	208
# eq.11	ph.2012.03.21.m6.6	dev.e3		118
# eq.12	ph.2012.02.06.m6.7	gus.6		18
# eq.13	ph.2011.12.14.m7.1	dev.5		129
# eq.14	ph.2011.12.13.m6.1	dev.8		167
# eq.15	ei.2011.07.31.m6.6	gus.4		20
# eq.16	ph.2011.06.13.m6.4	dev.e5		66
# ----	ph.2013.08.12.m6.0	dev.9		95

Set up distance files for TA "W" W-E array for

all the original stations (W32A-W61A). Note that

Station W55A was never deployed. Stations W37A and

W37B were deployed at different times at the same location

and so have been combined into a single station, "W37AB".

The same goes for stations W41A and W41B.

#

So: the total number of traces, including the first trace

```
# which is the deconvolved source wavelet ("WAVE"), is 30.
#
# NOTE: The distance for the first trace (source wavelet)
# will be a dummy distance.

# Convert distance files from ascii to binary format

a2b < plot_dist_all_TA_line_T.txt n1=1 > \
plot_dist_all_TA_line_T.bin

# NOTE: "nx" will be different for each W-E TA subarray.  It represents
# the number of stations for that array, plus one more for the
# source wavelet.
# NOTE: "nx1=2" means that the first trace (wavelet deconvolved by itself)
# will not be muted.  That will preserve the sidelobes so that these will
# contribute to the stacked waveform for the first trace.
# "t0=0" means that we're assigning a value of "zero" for time of the first sample.
# The mute trapezoid starts at t1=12 seconds and ends at t2=28 seconds
# nttap=200 samples = 200x0.02s/sample = 4 seconds
# So the weighting of the "trapezoid" tapers down from "one" at 12 seconds to
# zero at 12+4 = 16 seconds.  It's then zero from 16 seconds to 24 seconds,
# then climbs back up to 1 at 24+4 = 28 seconds. It's then "1" to the end
# of the trace.
# Each trace is multiplied by this mute.
mutestacktaper in=eq3West.ta.line_T.a1.0.scale out=eq3West.ta.line_T.a1.0.mute \
nx=30 nt=5501 dt=0.02 nx1=2 nx2=30 nxtap=0 t0=0 nttap=200 t1=12 t2=28

mutestacktaper in=eq4.ta.line_T.a1.0.scale out=eq4.ta.line_T.a1.0.mute \
```

```
nx=30 nt=5501 dt=0.02 nx1=2 nx2=30 nxtap=0 t0=0 nttap=200 t1=12 t2=28

mutestacktaper in=eq7.ta.line_T.a1.0.scale out=eq7.ta.line_T.a1.0.mute \
nx=30 nt=5501 dt=0.02 nx1=2 nx2=30 nxtap=0 t0=0 nttap=200 t1=12 t2=28

mutestacktaper in=eq10.ta.line_T.a1.0.scale out=eq10.ta.line_T.a1.0.mute \
nx=30 nt=5501 dt=0.02 nx1=2 nx2=30 nxtap=0 t0=0 nttap=200 t1=12 t2=28

mutestacktaper in=eq12.ta.line_T.a1.0.scale out=eq12.ta.line_T.a1.0.mute \
nx=30 nt=5501 dt=0.02 nx1=2 nx2=30 nxtap=0 t0=0 nttap=200 t1=12 t2=28

mutestacktaper in=eq13.ta.line_T.a1.0.scale out=eq13.ta.line_T.a1.0.mute \
nx=30 nt=5501 dt=0.02 nx1=2 nx2=30 nxtap=0 t0=0 nttap=200 t1=12 t2=28

mutestacktaper in=eq14.ta.line_T.a1.0.scale out=eq14.ta.line_T.a1.0.mute \
nx=30 nt=5501 dt=0.02 nx1=2 nx2=30 nxtap=0 t0=0 nttap=200 t1=12 t2=28

mutestacktaper in=eq15.ta.line_T.a1.0.scale out=eq15.ta.line_T.a1.0.mute \
nx=30 nt=5501 dt=0.02 nx1=2 nx2=30 nxtap=0 t0=0 nttap=200 t1=12 t2=28

# Add headers
# NOTE that dt is in microseconds and delrt is in milliseconds
# dt = 0.02 seconds = 20 milliseconds = 20,000 microseconds
# delrt = -20 seconds = -20,000 milliseconds (trace starts
# 20 seconds before first arrival)


suaddhead < eq3West.ta.line_T.a1.0.mute ns=5501 | \
```

```
sushw key=dt a=20000 > eq3West.ta.line_T.a1.0.mute.su1

sushw < eq3West.ta.line_T.a1.0.mute.su1 \
key=delrt a=-20000 > eq3West.ta.line_T.a1.0.mute.su2

sushw < eq3West.ta.line_T.a1.0.mute.su2 \
infile=plot_dist_all_TA_line_T.bin key=offset > eq3West.ta.line_T.a1.0.mute.su3

suaddhead < eq4.ta.line_T.a1.0.mute ns=5501 | \
sushw key=dt a=20000 > eq4.ta.line_T.a1.0.mute.su1

sushw < eq4.ta.line_T.a1.0.mute.su1 \
key=delrt a=-20000 > eq4.ta.line_T.a1.0.mute.su2

sushw < eq4.ta.line_T.a1.0.mute.su2 \
infile=plot_dist_all_TA_line_T.bin key=offset > eq4.ta.line_T.a1.0.mute.su3

suaddhead < eq7.ta.line_T.a1.0.mute ns=5501 | \
sushw key=dt a=20000 > eq7.ta.line_T.a1.0.mute.su1

sushw < eq7.ta.line_T.a1.0.mute.su1 \
key=delrt a=-20000 > eq7.ta.line_T.a1.0.mute.su2

sushw < eq7.ta.line_T.a1.0.mute.su2 \
infile=plot_dist_all_TA_line_T.bin key=offset > eq7.ta.line_T.a1.0.mute.su3

suaddhead < eq10.ta.line_T.a1.0.mute ns=5501 | \
sushw key=dt a=20000 > eq10.ta.line_T.a1.0.mute.su1
```

```
sushw < eq10.ta.line_T.a1.0.mute.su1 \
key=delrt a=-20000 > eq10.ta.line_T.a1.0.mute.su2

sushw < eq10.ta.line_T.a1.0.mute.su2 \
infile=plot_dist_all_TA_line_T.bin key=offset > eq10.ta.line_T.a1.0.mute.su3

suaddhead < eq12.ta.line_T.a1.0.mute ns=5501 | \
sushw key=dt a=20000 > eq12.ta.line_T.a1.0.mute.su1

sushw < eq12.ta.line_T.a1.0.mute.su1 \
key=delrt a=-20000 > eq12.ta.line_T.a1.0.mute.su2

sushw < eq12.ta.line_T.a1.0.mute.su2 \
infile=plot_dist_all_TA_line_T.bin key=offset > eq12.ta.line_T.a1.0.mute.su3

suaddhead < eq13.ta.line_T.a1.0.mute ns=5501 | \
sushw key=dt a=20000 > eq13.ta.line_T.a1.0.mute.su1

sushw < eq13.ta.line_T.a1.0.mute.su1 \
key=delrt a=-20000 > eq13.ta.line_T.a1.0.mute.su2

sushw < eq13.ta.line_T.a1.0.mute.su2 \
infile=plot_dist_all_TA_line_T.bin key=offset > eq13.ta.line_T.a1.0.mute.su3

suaddhead < eq14.ta.line_T.a1.0.mute ns=5501 | \
sushw key=dt a=20000 > eq14.ta.line_T.a1.0.mute.su1
```

```
sushw < eq14.ta.line_T.a1.0.mute.su1 \
key=delrt a=-20000 > eq14.ta.line_T.a1.0.mute.su2

sushw < eq14.ta.line_T.a1.0.mute.su2 \
infile=plot_dist_all_TA_line_T.bin key=offset > eq14.ta.line_T.a1.0.mute.su3

suaddhead < eq15.ta.line_T.a1.0.mute ns=5501 | \
sushw key=dt a=20000 > eq15.ta.line_T.a1.0.mute.su1

sushw < eq15.ta.line_T.a1.0.mute.su1 \
key=delrt a=-20000 > eq15.ta.line_T.a1.0.mute.su2

sushw < eq15.ta.line_T.a1.0.mute.su2 \
infile=plot_dist_all_TA_line_T.bin key=offset > eq15.ta.line_T.a1.0.mute.su3

# Plot
# use op=norm for normalizing each trace separately
# use op=neg to reverse polarity (otherwise same normalization as op=norm)
# For vertical.mute: hbox=3.5 inches for 100 seconds,
# so use hbox=3.85 inches for 110 seconds
# First set of plots: same as plots generated by pkikp_step105

suop < eq3West.ta.line_T.a1.0.mute.su3 op=norm | \
supswigp xcur=2.0 wbox=4 hbox=3.85 style=seismic \
nbpi=300 linewidth=0 \
title="eq3West.ta.line_T.a1.0.mute.su3, 2/23/2022" \
label1="Time (s)" labelsize=9 n2tic=2 xbeg=-0.2 \
xend=1 interp=1 n1tic=5 titlesize=8 key=offset > \
```

```
eq3West.ta.line_T.a1.0.mute.su3.ps



suop < eq4.ta.line_T.a1.0.mute.su3 op=norm | \
supswigp xcur=2.0 wbox=4 hbox=3.85 style=seismic \
nbpi=300 linewidth=0 \
title="eq4.ta.line_T.a1.0.mute.su3, 2/23/2022" \
label1="Time (s)" labelsize=9 n2tic=2 xbeg=-0.2 \
xend=1 interp=1 n1tic=5 titlesize=8 key=offset > \
eq4.ta.line_T.a1.0.mute.su3.ps

suop < eq7.ta.line_T.a1.0.mute.su3 op=norm | \
supswigp xcur=2.0 wbox=4 hbox=3.85 style=seismic \
nbpi=300 linewidth=0 \
title="eq7.ta.line_T.a1.0.mute.su3, 2/23/2022" \
label1="Time (s)" labelsize=9 n2tic=2 xbeg=-0.2 \
xend=1 interp=1 n1tic=5 titlesize=8 key=offset > \
eq7.ta.line_T.a1.0.mute.su3.ps

suop < eq10.ta.line_T.a1.0.mute.su3 op=norm | \
supswigp xcur=2.0 wbox=4 hbox=3.85 style=seismic \
nbpi=300 linewidth=0 \
title="eq10.ta.line_T.a1.0.mute.su3, 2/23/2022" \
label1="Time (s)" labelsize=9 n2tic=2 xbeg=-0.2 \
xend=1 interp=1 n1tic=5 titlesize=8 key=offset > \
eq10.ta.line_T.a1.0.mute.su3.ps

suop < eq12.ta.line_T.a1.0.mute.su3 op=norm | \
```

```
supswigp xcur=2.0 wbox=4 hbox=3.85 style=seismic \
nbpi=300 linewidth=0 \
title="eq12.ta.line_T.a1.0.mute.su3, 2/23/2022" \
label1="Time (s)" labelsize=9 n2tic=2 xbeg=-0.2 \
xend=1 interp=1 n1tic=5 titlesize=8 key=offset > \
eq12.ta.line_T.a1.0.mute.su3.ps

suop < eq13.ta.line_T.a1.0.mute.su3 op=norm | \
supswigp xcur=2.0 wbox=4 hbox=3.85 style=seismic \
nbpi=300 linewidth=0 \
title="eq13.ta.line_T.a1.0.mute.su3, 2/23/2022" \
label1="Time (s)" labelsize=9 n2tic=2 xbeg=-0.2 \
xend=1 interp=1 n1tic=5 titlesize=8 key=offset > \
eq13.ta.line_T.a1.0.mute.su3.ps

suop < eq14.ta.line_T.a1.0.mute.su3 op=norm | \
supswigp xcur=2.0 wbox=4 hbox=3.85 style=seismic \
nbpi=300 linewidth=0 \
title="eq14.ta.line_T.a1.0.mute.su3, 2/23/2022" \
label1="Time (s)" labelsize=9 n2tic=2 xbeg=-0.2 \
xend=1 interp=1 n1tic=5 titlesize=8 key=offset > \
eq14.ta.line_T.a1.0.mute.su3.ps

suop < eq15.ta.line_T.a1.0.mute.su3 op=norm | \
supswigp xcur=2.0 wbox=4 hbox=3.85 style=seismic \
nbpi=300 linewidth=0 \
title="eq15.ta.line_T.a1.0.mute.su3, 2/23/2022" \
label1="Time (s)" labelsize=9 n2tic=2 xbeg=-0.2 \
```

```
xend=1 interp=1 n1tic=5 titlesize=8 key=offset > \
eq15.ta.line_T.a1.0.mute.su3.ps
```

STEP 202

This step works on all earthquakes that you wish to stack together for a particular line and Gaussian parameter. In this example I show Line T and α=1. This particular example shows all earthquakes (1-16) being stacked, but other stacking jobs involve stacking the best and least noisy earthquakes for the best results.

```
# pkikp_ta_step202_eq.1.2.3.4.5.6.7.8.9.10.11.12.13.14.15.16_ta_line_T_a1.txt
#
# (Original job name, for SESAME lines:
# pkikp_stack_tpow.5_dev.1.2.3.4.5.6.7.8.e3.e4.e5_gus.4.5.6.7.9_line_W_a1.txt)
#
# July 6, 2017; May 17, 2018; May 23, 2018; Sept. 15, 2018;
# Sept. 19, 2018; Jan. 11, 2019; Jan. 26, 2019; July 19, 2019
# Aug. 3, 2019; Aug. 15, 2019; 8/21/19; 9/9/19; Sept. 22, 2021

# Feb. 1, 2020: additional scaling to correct for
# spherical spreading.
#
# 12/10/2020; 2/3/2021; 9/22/2021; 8/18/2021; 9/22/2021; Sept. 22, 2021

# Vertically stacks traces.  Works on output of jobs
# "pkikp_ta_step201_.....a1.txt"
```

#

The Step201 jobs first normalized each trace by its maximum value

(generally this was the sample at "zero time",

corresponding to the peak of the deconvolved direct

PKIKP arrival). Then each trace was normalized by the

RMS value of noise in a window preceding the direct

PKIKP arrival. The Step201 jobs, in turn, worked on the

output of jobs "pkikp_step105_.....txt",

etc., which inserted blank traces for unoccupied

stations, and padded, as necessary, the ends of traces

with zeroes to give output traces of nt=5501 samples

(-20 to 90 seconds).

#

Step201 renamed the output files of Step105 using the

following renaming scheme. Events are numbered by

date, starting with the most recent earthquake (recorded

by the westernmost stations of the TA array)

#

Depths are also listed. "dev" refers to events worked on

by Devon Verellen; "gus" refers to events worked on

by Gustavo Larramendi (a few events were worked on

by both):

#				Depth (km)
#				
# eq.1	ph.2014.04.11.m7.1	dev.2	gus.2	61 km
# eq.2	ph.2013.10.15.m7.1	gus.7		23
# eq.3	ph.2013.07.07.m7.3	dev.1	gus.1	386
# eq.4	ph.2013.07.07.m6.6	dev.3		62

```
# eq.5    ph.2013.04.06.m7.0      dev.6    gus.8    66
# eq.6    ph.2012.10.17.m6.0      dev.7             338
# eq.7    ph.2012.08.31.m7.6      gus.5             44
# eq.8    ph.2012.08.26.m6.6      dev.e4   gus.10   91
# eq.9    ei.2012.04.21.m6.7      gus.9             24
# eq.10   ph.2012.04.17.m6.9      dev.4    gus.3    208
# eq.11   ph.2012.03.21.m6.6      dev.e3            118
# eq.12   ph.2012.02.06.m6.7      gus.6             18
# eq.13   ph.2011.12.14.m7.1      dev.5             129
# eq.14   ph.2011.12.13.m6.1      dev.8             167
# eq.15   ei.2011.07.31.m6.6      gus.4             20
# eq.16   ph.2011.06.13.m6.4      dev.e5            66
# ----    ph.2013.08.12.m6.0      dev.9             95


# Set up distance file for TA "R" W-E array for
# all the deployed stations (W31A-W65A, including W41B).
# Note: The distance for the first trace (source wavelet)
# will be a dummy distance.

a2b < plot_dist_all_TA_line_T.txt n1=1 > \
plot_dist_all_TA_line_T.bin


# NOTE: "ntr" will be different for each W-E TA subarray.
# It represents the total number of stations for that subarray,
# plus one more for the source wavelet.
```

```
# add sections together
#
# for now, do not include eq.4 (high noise) or eq.16 (large artifacts)

traceadd2019 in1=eq1.ta.line_T.a1.0.90s.scale in2=eq2.ta.line_T.a1.0.scale \
out=temp1 ntr=30 nt=5501

traceadd2019 in1=temp1 in2=eq3.ta.line_T.a1.0.80s.scale \
out=temp2 ntr=30 nt=5501

traceadd2019 in1=temp2 in2=eq4.ta.line_T.a1.0.scale \
out=temp3 ntr=30 nt=5501

traceadd2019 in1=temp3 in2=eq5.ta.line_T.a1.0.scale \
out=temp4 ntr=30 nt=5501

traceadd2019 in1=temp4 in2=eq6.ta.line_T.a1.0.scale \
out=temp5 ntr=30 nt=5501

traceadd2019 in1=temp5 in2=eq7.ta.line_T.a1.0.scale \
out=temp6 ntr=30 nt=5501

traceadd2019 in1=temp6 in2=eq8.ta.line_T.a1.0.scale \
out=temp7 ntr=30 nt=5501

traceadd2019 in1=temp7 in2=eq9.ta.line_T.a1.0.scale \
out=temp8 ntr=30 nt=5501
```

```
traceadd2019 in1=temp8 in2=eq10.ta.line_T.a1.0.90s.scale \
out=temp9 ntr=30 nt=5501

traceadd2019 in1=temp9 in2=eq11.ta.line_T.a1.0.90s.scale \
out=temp10 ntr=30 nt=5501

traceadd2019 in1=temp10 in2=eq12.ta.line_T.a1.0.scale \
out=temp11 ntr=30 nt=5501

traceadd2019 in1=temp11 in2=eq13.ta.line_T.a1.0.scale \
out=temp12 ntr=30 nt=5501

traceadd2019 in1=temp12 in2=eq14.ta.line_T.a1.0.scale \
out=temp13 ntr=30 nt=5501

traceadd2019 in1=temp13 in2=eq15.ta.line_T.a1.0.scale \
out=temp14 ntr=30 nt=5501

traceadd2019 in1=temp14 in2=eq16.ta.line_T.a1.0.scale \
out=temp15 ntr=30 nt=5501

cp temp15 eq.1.2.3.4.5.6.7.8.9.10.11.12.13.14.15.16_ta.line_T.a1.0.stack

# Add headers
# NOTE that dt is in microseconds and delrt is in milliseconds
# dt = 0.02 seconds = 20 milliseconds = 20,000 microseconds
# delrt = -20 seconds = -20,000 milliseconds (trace starts
# 20 seconds before first arrival)
```

```
suaddhead < eq.1.2.3.4.5.6.7.8.9.10.11.12.13.14.15.16_ta.line_T.a1.0.stack ns=5501 | \
sushw key=dt a=20000 > \
eq.1.2.3.4.5.6.7.8.9.10.11.12.13.14.15.16_ta.line_T.a1.0.stack.su1

sugain < eq.1.2.3.4.5.6.7.8.9.10.11.12.13.14.15.16_ta.line_T.a1.0.stack.su1 \
tpow=0.5 \
> eq.1.2.3.4.5.6.7.8.9.10.11.12.13.14.15.16_ta.line_T.a1.0.stack.tpow.5.su1

sushw < eq.1.2.3.4.5.6.7.8.9.10.11.12.13.14.15.16_ta.line_T.a1.0.stack.tpow.5.su1 \
key=delrt a=-20000 > \
eq.1.2.3.4.5.6.7.8.9.10.11.12.13.14.15.16_ta.line_T.a1.0.stack.tpow.5.su2

sushw < eq.1.2.3.4.5.6.7.8.9.10.11.12.13.14.15.16_ta.line_T.a1.0.stack.tpow.5.su2 \
infile=plot_dist_all_TA_line_T.bin key=offset > \
eq.1.2.3.4.5.6.7.8.9.10.11.12.13.14.15.16_ta.line_T.a1.0.stack.tpow.5.su3

# Plot
# use op=norm for normalizing each trace separately
# use op=neg to reversepolarity (otherwise same normalization as op=norm)

# For vertical scale: hbox=3.5 inches for 100 seconds,
# so use hbox=3.85 inches for 110 seconds

suop < eq.1.2.3.4.5.6.7.8.9.10.11.12.13.14.15.16_ta.line_T.a1.0.stack.tpow.5.su3 op=norm | \
supswigp xcur=2.0 wbox=4 hbox=3.85 style=seismic \
nbpi=300 linewidth=0 \
title="eq.1.2.3.4.5.6.7.8.9.10.11.12.13.14.15.16_ta.line_T.a1.0.stack.tpow.5.su3, 9/22/2021" \
```

```
label1="Time (s)" labelsize=9 n2tic=2 xbeg=-0.2 \
xend=1 interp=1 n1tic=5 titlesize=8 key=offset > \
eq.1.2.3.4.5.6.7.8.9.10.11.12.13.14.15.16_ta.line_T.a1.0.stack.tpow.5.su3.ps


# Now replot with negative polarity (op=neg).  Then direct arrival will
# be negative and a positive impedance contrast (e.g. Moho if it's a
# first-order discontinuity) will be positive.

suop < eq.1.2.3.4.5.6.7.8.9.10.11.12.13.14.15.16_ta.line_T.a1.0.stack.tpow.5.su3 op=norm > tempnorm

suop < tempnorm op=neg | \
supswigp xcur=2.0 wbox=4 hbox=3.85 style=seismic \
nbpi=300 linewidth=0 \
title="eq.1.2.3.4.5.6.7.8.9.10.11.12.13.14.15.16_ta.line_T.a1.0.stack.tpow.5.su3, 9/22/2021" \
label1="Time (s)" labelsize=9 n2tic=2 xbeg=-0.2 \
xend=1 interp=1 n1tic=5 titlesize=8 key=offset > \
eq.1.2.3.4.5.6.7.8.9.10.11.12.13.14.15.16_ta.line_T.a1.0.stack.tpow.5.su3.neg.ps
```

SIGNFILTER

This example signfilter code is for Line V.

```
# pkikp_ta_step202_taper04.10.18.24s_eq.1.2.3.4.5.7.8.10.12.14.15.16_ta_line_V_a2_signfilter_w5.txt
#
# May 4, 2022; July 20, 2022; August 10, 2022
# Convert distance file from ascii to binary format

a2b < plot_dist_all_TA_line_V.txt n1=1 > \
plot_dist_all_TA_line_V.bin

cp eq.1.2.3.4.5.7.8.10.12.14.15.16_ta.line_V.a2.0.stack temp.stack

tracezero2019 in=temp.stack out=temp.stack.trace1zero ntr=32 nt=5501 \
 para=zap_stack_trace1zero_ta_line_V.txt

# length of taper = 300x0.02 = 6 seconds

mutestacktaper in=temp.stack.trace1zero \
 out=eq.1.2.3.4.5.7.8.10.12.14.15.16_ta.line_V.a2.0.taper04.10.18.24s \
nx=32 nt=5501 dt=0.02 nx1=1 nx2=32 nxtap=0 t0=0 nttap=300 t1=4 t2=24

cp eq.1.2.3.4.5.7.8.10.12.14.15.16_ta.line_V.a2.0.taper04.10.18.24s \
```

```
temptrace

# apply sign filter

signfiltermac_v4 in=temptrace \
out=temptrace_signfilter_w5 \
nx=32 nt=5501 nwtr=5 nxthresh=5

tracemultmac in1=temptrace \
in2=temptrace_signfilter_w5 \
out=temptrace_filteroutput_w5 \
ntr=32 nt=5501

cp temptrace_filteroutput_w5 \
eq.1.2.3.4.5.7.8.10.12.14.15.16_ta.line_V.a2.0.taper04.10.18.24s_w5

# Add headers
# NOTE that dt is in microseconds and delrt is in milliseconds
# dt = 0.02 seconds = 20 milliseconds = 20,000 microseconds
# delrt = -20 seconds = -20,000 milliseconds (trace starts
# 20 seconds before first arrival)

suaddhead < eq.1.2.3.4.5.7.8.10.12.14.15.16_ta.line_V.a2.0.taper04.10.18.24s_w5 ns=5501 | \
sushw key=dt a=20000 > \
eq.1.2.3.4.5.7.8.10.12.14.15.16_ta.line_V.a2.0.taper04.10.18.24s_w5.su1

sugain < eq.1.2.3.4.5.7.8.10.12.14.15.16_ta.line_V.a2.0.taper04.10.18.24s_w5.su1 \
tpow=0.5 \
```

```
> eq.1.2.3.4.5.7.8.10.12.14.15.16_ta.line_V.a2.0.taper04.10.18.24s_w5.tpow.5.su1

sushw < eq.1.2.3.4.5.7.8.10.12.14.15.16_ta.line_V.a2.0.taper04.10.18.24s_w5.tpow.5.su1 \
key=delrt a=-20000 > \
eq.1.2.3.4.5.7.8.10.12.14.15.16_ta.line_V.a2.0.taper04.10.18.24s_w5.tpow.5.su2

sushw < eq.1.2.3.4.5.7.8.10.12.14.15.16_ta.line_V.a2.0.taper04.10.18.24s_w5.tpow.5.su2 \
infile=plot_dist_all_TA_line_V.bin key=offset > \
eq.1.2.3.4.5.7.8.10.12.14.15.16_ta.line_V.a2.0.taper04.10.18.24s_w5.tpow.5.su3

# Plot
# use op=norm for normalizing each trace separately
# use op=neg to reversepolarity (otherwise same normalization as op=norm)

# For vertical scale: hbox=3.5 inches for 100 seconds,
# so use hbox=3.85 inches for 110 seconds

suop < eq.1.2.3.4.5.7.8.10.12.14.15.16_ta.line_V.a2.0.taper04.10.18.24s_w5.tpow.5.su3 op=norm | \
supswigp xcur=2.0 wbox=4 hbox=3.85 style=seismic \
nbpi=300 linewidth=0 \
title="eq.1.2.3.4.5.7.8.10.12.14.15.16_ta.line_V.a2.0.taper04.10.18.24s_w5.tpow.5.su3, 8/10/2022" \
label1="Time (s)" labelsize=9 n2tic=2 xbeg=-0.2 \
xend=1 interp=1 n1tic=5 titlesize=8 key=offset > \
eq.1.2.3.4.5.7.8.10.12.14.15.16_ta.line_V.a2.0.taper04.10.18.24s_w5.tpow.5.su3.ps

# Now replot with positive polarity, but
# WITHOUT normalizing
```

```
supswigp < eq.1.2.3.4.5.7.8.10.12.14.15.16_ta.line_V.a2.0.taper04.10.18.24s_w5.tpow.5.su3 \
xcur=2.0 wbox=4 hbox=3.85 \
style=seismic nbpi=300 linewidth=0 \
title="eq.1.2.3.4.5.7.8.10.12.14.15.16_ta.line_V.a2.0.taper04.10.18.24s_w5.tpow.5.su3, 8/10/2022" \
label1="Time (s)" labelsize=9 n2tic=2 xbeg=-0.2 \
xend=1 interp=1 n1tic=5 titlesize=8 key=offset > \
eq.1.2.3.4.5.7.8.10.12.14.15.16_ta.line_V.a2.0.taper04.10.18.24s_w5.tpow.5.su3.nonorm.ps

# Now replot with negative polarity (op=neg).  Then direct arrival will
# be negative and a positive impedance contrast (e.g. Moho if it's a
# first-order discontinuity) will be positive.

suop < eq.1.2.3.4.5.7.8.10.12.14.15.16_ta.line_V.a2.0.taper04.10.18.24s_w5.tpow.5.su3 op=norm >
tempnorm

suop < tempnorm op=neg | \
supswigp xcur=2.0 wbox=4 hbox=3.85 style=seismic \
nbpi=300 linewidth=0 \
title="eq.1.2.3.4.5.7.8.10.12.14.15.16_ta.line_V.a2.0.taper04.10.18.24s_w5.tpow.5.su3, 8/10/2022" \
label1="Time (s)" labelsize=9 n2tic=2 xbeg=-0.2 \
xend=1 interp=1 n1tic=5 titlesize=8 key=offset > \
eq.1.2.3.4.5.7.8.10.12.14.15.16_ta.line_V.a2.0.taper04.10.18.24s_w5.tpow.5.su3.neg.ps

# Now replot with negative polarity, but WITHOUT normalizing
# the traces.

suop < eq.1.2.3.4.5.7.8.10.12.14.15.16_ta.line_V.a2.0.taper04.10.18.24s_w5.tpow.5.su3 op=neg | \
supswigp xcur=2.0 wbox=4 hbox=3.85 style=seismic \
```

```
nbpi=300 linewidth=0 \
title="eq.1.2.3.4.5.7.8.10.12.14.15.16_ta.line_V.a2.0.taper04.10.18.24s_w5.tpow.5.su3, 8/10/2022" \
label1="Time (s)" labelsize=9 n2tic=2 xbeg=-0.2 \
xend=1 interp=1 n1tic=5 titlesize=8 key=offset > \
eq.1.2.3.4.5.7.8.10.12.14.15.16_ta.line_V.a2.0.taper04.10.18.24s_w5.tpow.5.su3.neg.nonorm.ps
# Now generate a color plot

suximage < eq.1.2.3.4.5.7.8.10.12.14.15.16_ta.line_V.a2.0.taper04.10.18.24s_w5.tpow.5.su2 \
 perc=99 wbox=1500 hbox=888 labelcolor=black blank=0.9 \
labelcolor=black titlecolor=black \
 legend=1 lwidth=16 label1="Time (s)" label2="Station" \
 title="eq.1.2.3.4.5.7.8.10.12.14.15.16_ta.line_V.a2.0.taper04.10.18.24s_w5.tpow.5.su2"

sustrip < eq.1.2.3.4.5.7.8.10.12.14.15.16_ta.line_V.a2.0.taper04.10.18.24s_w5.tpow.5.su2 \
> eq.1.2.3.4.5.7.8.10.12.14.15.16_ta.line_V.a2.0.taper04.10.18.24s_w5.tpow.5 \
outpar=line_V_a2_w5_nt_ntr_dt
```

TALLYRUN JOB

Example taken from Line V.

```
#pkikp_ta_step202_taper04.10.18.24s_eq.1.2.3.4.5.7.8.10.12.14.15.16_ta_line_V_a2_band_sign_w5_tallyr
unavg101.txt
#
# May 4, 2022; July 20, 2022; July 23, 2022; August 5, 2022; August 9, 2022;
# August 10, 2022; August 31, 2022
# Convert distance file from ascii to binary format

a2b < plot_dist_all_TA_line_V.txt n1=1 > \
plot_dist_all_TA_line_V.bin

cp eq.1.2.3.4.5.7.8.10.12.14.15.16_ta.line_V.a2.0.stack temp.stack

tracezero2019 in=temp.stack out=temp.stack.trace1zero ntr=32 nt=5501 \
 para=zap_stack_trace1zero_ta_line_V.txt

# length of taper = 300x0.02 = 6 seconds

mutestacktaper in=temp.stack.trace1zero \
 out=eq.1.2.3.4.5.7.8.10.12.14.15.16_ta.line_V.a2.0.taper04.10.18.24s \
nx=32 nt=5501 dt=0.02 nx1=1 nx2=32 nxtap=0 t0=0 nttap=300 t1=4 t2=24
```

```
cp eq.1.2.3.4.5.7.8.10.12.14.15.16_ta.line_V.a2.0.taper04.10.18.24s \
temptrace

# apply low-cut filter

tapernew2015 in=temptrace out=temptaper nx=32 nt=5501 nx1=0 nt1=500

bandnew2015 in=temptaper out=tempband nt=5501 dt=0.02 a=0.05 b=0.07 c=2.0 d=4.0

# apply sign filter

signfiltermac_v4 in=tempband \
out=temptrace_band_signfilter_w5 \
nx=32 nt=5501 nwtr=5 nxthresh=5

tracemultmac in1=tempband \
in2=temptrace_band_signfilter_w5 \
out=temptrace_band_filteroutput_w5 \
ntr=32 nt=5501

cp temptrace_band_filteroutput_w5 \
eq.1.2.3.4.5.7.8.10.12.14.15.16_ta.line_V.a2.0.taper04.10.18.24s_band_w5

# test run for program "tallyrunavg_v4.c"

tallyrunavg_v4 insign=temptrace_band_signfilter_w5 \
inamp=temptrace_band_filteroutput_w5 \
```

```
out1=test_line_V_a2.0_w5_tallyrunavg_nonzero \
out2=test_line_V_a2.0_w5_tallyrunavg_avgabs \
out3=test_line_V_a2.0_w5_tallyrunavg_avgsqr \
outavg1=test_line_V_a2.0_w5_nonzero_runavg101 \
outavg2=test_line_V_a2.0_w5_avgabs_runavg101 \
outavg3=test_line_V_a2.0_w5_avgsqr_runavg101 \
nx=32 nt=5501 ntavg=101

# Add headers
# NOTE that dt is in microseconds and delrt is in milliseconds
# dt = 0.02 seconds = 20 milliseconds = 20,000 microseconds
# delrt = -20 seconds = -20,000 milliseconds (trace starts
# 20 seconds before first arrival)

suaddhead < test_line_V_a2.0_w5_tallyrunavg_nonzero ns=5501 | \
sushw key=dt a=20000 > \
test_line_V_a2.0_w5_tallyrunavg_nonzero.su1

# sugain < eq.1.2.3.4.5.7.8.10.12.14.15.16_ta.line_V.a2.0.taper04.10.18.24s_band_w1.su1 \
# tpow=0.5 \
# > eq.1.2.3.4.5.7.8.10.12.14.15.16_ta.line_V.a2.0.taper04.10.18.24s_band_w1.tpow.5.su1

sushw < test_line_V_a2.0_w5_tallyrunavg_nonzero.su1 \
key=delrt a=-20000 > \
test_line_V_a2.0_w5_tallyrunavg_nonzero.su2

suaddhead < test_line_V_a2.0_w5_tallyrunavg_avgabs ns=5501 | \
sushw key=dt a=20000 > \
```

```
test_line_V_a2.0_w5_tallyrunavg_avgabs.su1

sushw < test_line_V_a2.0_w5_tallyrunavg_avgabs.su1 \
key=delrt a=-20000 > \
test_line_V_a2.0_w5_tallyrunavg_avgabs.su2

suaddhead < test_line_V_a2.0_w5_tallyrunavg_avgsqr ns=5501 | \
sushw key=dt a=20000 > \
test_line_V_a2.0_w5_tallyrunavg_avgsqr.su1

sushw < test_line_V_a2.0_w5_tallyrunavg_avgsqr.su1 \
key=delrt a=-20000 > \
test_line_V_a2.0_w5_tallyrunavg_avgsqr.su2

suaddhead < test_line_V_a2.0_w5_nonzero_runavg101 ns=5501 | \
sushw key=dt a=20000 > \
test_line_V_a2.0_w5_nonzero_runavg101.su1

sushw < test_line_V_a2.0_w5_nonzero_runavg101.su1 \
key=delrt a=-20000 > \
test_line_V_a2.0_w5_nonzero_runavg101.su2

suaddhead < test_line_V_a2.0_w5_avgabs_runavg101 ns=5501 | \
sushw key=dt a=20000 > \
test_line_V_a2.0_w5_avgabs_runavg101.su1

sushw < test_line_V_a2.0_w5_avgabs_runavg101.su1 \
key=delrt a=-20000 > \
```

```
test_line_V_a2.0_w5_avgabs_runavg101.su2

suaddhead < test_line_V_a2.0_w5_avgsqr_runavg101 ns=5501 | \
sushw key=dt a=20000 > \
test_line_V_a2.0_w5_avgsqr_runavg101.su1

sushw < test_line_V_a2.0_w5_avgsqr_runavg101.su1 \
key=delrt a=-20000 > \
test_line_V_a2.0_w5_avgsqr_runavg101.su2

# Plot
# use op=norm for normalizing each trace separately
# use op=neg to reversepolarity (otherwise same normalization as op=norm)
# For vertical scale: hbox=3.5 inches for 100 seconds,
# so use hbox=3.85 inches for 110 seconds
# Now replot with positive polarity, but
# WITHOUT normalizing

supswigp < test_line_V_a2.0_w5_tallyrunavg_nonzero.su2 \
xcur=2.0 wbox=1.5 hbox=3.85 \
style=seismic nbpi=300 linewidth=0 \
title="test_line_V_a2.0_w5_tallyrunavg_nonzero.su2, 8/31/2022" \
label1="Time (s)" labelsize=9 n2tic=2 xbeg=-0.2 \
xend=1 interp=1 n1tic=5 titlesize=8 key=offset > \
test_line_V_a2.0_w5_tallyrunavg_nonzero.su2.ps

supswigp < test_line_V_a2.0_w5_tallyrunavg_avgabs.su2 \
```

```
xcur=2.0 wbox=1.5 hbox=3.85 \
style=seismic nbpi=300 linewidth=0 \
title="test_line_V_a2.0_w5_tallyrunavg_avgabs.su2, 8/31/2022" \
label1="Time (s)" labelsize=9 n2tic=2 xbeg=-0.2 \
xend=1 interp=1 n1tic=5 titlesize=8 key=offset > \
test_line_V_a2.0_w5_tallyrunavg_avgabs.su2.ps

supswigp < test_line_V_a2.0_w5_tallyrunavg_avgsqr.su2 \
xcur=2.0 wbox=1.5 hbox=3.85 \
style=seismic nbpi=300 linewidth=0 \
title="test_line_V_a2.0_w5_tallyrunavg_avgsqr.su2, 8/31/2022" \
label1="Time (s)" labelsize=9 n2tic=2 xbeg=-0.2 \
xend=1 interp=1 n1tic=5 titlesize=8 key=offset > \
test_line_V_a2.0_w5_tallyrunavg_avgsqr.su2.ps

supswigp < test_line_V_a2.0_w5_nonzero_runavg101.su2 \
xcur=2.0 wbox=1.5 hbox=3.85 \
style=seismic nbpi=300 linewidth=0 \
title="test_line_V_a2.0_w5_nonzero_runavg101.su2, 8/31/2022" \
label1="Time (s)" labelsize=9 n2tic=2 xbeg=-0.2 \
xend=1 interp=1 n1tic=5 titlesize=8 key=offset > \
test_line_V_a2.0_w5_nonzero_runavg101.su2.ps

supswigp < test_line_V_a2.0_w5_avgabs_runavg101.su2 \
xcur=2.0 wbox=1.5 hbox=3.85 \
style=seismic nbpi=300 linewidth=0 \
title="test_line_V_a2.0_w5_avgabs_runavg101.su2, 8/31/2022" \
label1="Time (s)" labelsize=9 n2tic=2 xbeg=-0.2 \
```

```
xend=1 interp=1 n1tic=5 titlesize=8 key=offset > \
test_line_V_a2.0_w5_avgabs_runavg101.su2.ps

supswigp < test_line_V_a2.0_w5_avgsqr_runavg101.su2 \
xcur=2.0 wbox=1.5 hbox=3.85 \
style=seismic nbpi=300 linewidth=0 \
title="test_line_V_a2.0_w5_avgsqr_runavg101.su2, 8/31/2022" \
label1="Time (s)" labelsize=9 n2tic=2 xbeg=-0.2 \
xend=1 interp=1 n1tic=5 titlesize=8 key=offset > \
test_line_V_a2.0_w5_avgsqr_runavg101.su2.ps
```